Charles University in Prague
Faculty of Science
Institute of Hydrogeology, Engineering Geology and Applied Geophysics

MODELLING OF LUMPY CLAY FILLS

A dissertation submitted for the degree of
Doctor of Philosophy

JAN NAJSER

Prague, 2010

Declaration

The research presented in this Thesis is a result of my original scientific work undertaken during my Ph.D. study. I declare that it has not been submitted for any other academic degree at any other educational establishment.

Prague, March 2010

Jan Najser

Contents

List of Figures

List of Tables

List of symbols

A	parameter controlling the relative importance of volumetric $\dot{\epsilon}_v$ and shear $\dot{\epsilon}_s$ components on damage strain rate $\dot{\epsilon}^d$
C_c	slope of the normal compression line
C_s	slope of a swelling and recompression line
C_α	coefficient of secondary compression
c'	cohesion
D_s	weathering destructuration
d	diameter
E	Young modulus
e	void ratio
e_0	initial void ratio
e_e	intergranular void ratio
e_{fin}	final void ratio
e_i	intragranular void ratio
e_{s0}	void ratio of soil without double porosity structure
e_{s100}	void ratio of fully structured soil
e_t	total void ratio
Δe	difference between initial and final void ratios
G_s	specific gravity of soil grains
g	Earth's gravity
H, h	height
h_0	initial height
h_s	height of the soil
h_w	height of the water
Δh	difference between current and initial height
Δh_{unl}	swelling at the time of model height measurement
Δh_{fin}	final swelling of the model
Δh_{sw}	settlement during self-weight consolidation
Δh_e	settlement after construction of embankment
$\Delta h_{e\text{-}g}$	settlement after construction of embankment reinforced by geotextile
I_P	plasticity index
K_0	coefficient of earth pressure at rest

k	hydraulic conductivity
k_h	parameter describing rate of structure degradation
N	specific volume of normally consolidated soil at p' = 1 kPa.
n	porosity
n	multiple of Earth's gravity
n_e	intergranular porosity
n_i	intragranular porosity
n_t	total porosity
p'	mean effective stress
p_e'	equivalent pressure (value of p' at the point on the NCL at the same specific volume)
p_{iy}'	mean effective stress at yield in isotropic compression
p_{K0y}'	mean effective stress at yield in K_0 compression
p_y'	effective yield stress
q	deviator stress
r	radius
r_h	shear stifness parameter
S_r	saturation ratio
s	sensitivity
s_0	initial sensitivity
s_f	final sensitivity
u	pore water pressure
u_e	current excess pore pressure
$u_{e\text{-}max}$	maximum possible excess pore pressure calculated from the vertical stress increment with an assumption of impermeable soil
u_{max}	maximum pore pressure
v	specific volume
w_L	liquid limit
w_P	plastic limit
z_m	model depth
z_p	prototype depth
γ	unit weight
Δ_{max}	maximum strain difference
ε_a	axial strain

$\dot{\epsilon}^{d}$	damage strain rate
$\dot{\epsilon}_s$	shear component of damage strain rate
$\dot{\epsilon}_v$	volumetric component of damage strain rate
κ^*	slope of isotropic swelling line in ln v - ln p' space
λ^*	slope of isotropic normal compression line in ln v - ln p' space
ν	Poisson's ratio
$\rho_{d\text{-}0}$	initial dry density
σ_v'	vertical effective stress
$\sigma_{v\text{-}max}'$	maximum vertical effective stress
φ'	angle of friction (Mohr-Coulomb model parameter)
φ_c'	critical state friction angle
φ_p'	peak friction angle
ψ	angle of dilation
ω	angular velocity

Acknowledgements

I would like express my thanks to a number of people who contributed to the outcome of this thesis and supported me in various ways.

First, I want to thank my supervisor, Dr. Jan Boháč, who introduced me into soil mechanics and initiated the whole project. I am grateful for his assistance throughout the five years of my PhD study, helpful discussions and critical reading and commenting of several manuscripts.

I would like to thank Dr. David Mašín for supervising the numerical modelling part of the project.

The centrifuge modelling presented in this thesis was carried out in Institute for Geotechnical Engineering (IGT) at ETH Zürich. I am greatful to Prof. Sarah Springman for giving me the opportunity to spent a fascinating year in IGT group and for her support during that time. I would like to thank Dr. Jan Laue for his help with planning the centrifuge tests, for stimulating discussions and all the nights spent in the laboratory during running the centrifuge tests. These test would not be possible without the help of Markus Iten, Dr. Thomas Weber and IGT technicians Heinz Buschor and Ernst Bleiker. I also wish to thank to Dr. Michael Plötze for RTG diffraction analyses. The assistance of Marco Sperl and Dusan Bystricky during the laboratory experiments is appreciated. I would like to thank to Juliane, Phillipe, Bernd, Ralf, Matthias, Ivo, Erika and all the friends and colleagues who created the friendly and stimulating environment.

Special thank to Emma Pooley for her invaluable cooperation in all research activities related to centrifuge modelling, support and friendship.

I thank Dr. Karel Mach, Dr. Milan Větrovský and Dr. Jan Kurka for the valuable comments related to landfills.

I wish to thank to Jana, Vlaďka, Henrique, and all the colleagues and friends, which I met in Laboratory of Soil Mechanics at Charles University for their friendship and creating perfect conditions for research.

The financial support of the project was provided by research grants GAUK 74007 (Charles University in Prague), MSM0021620855 (Ministry of Education) and GACR 103/07/0678 (Czech Science Foundation).

The centrifuge modelling was carried out as part of a Marie Curie Research Training Network "Advanced Modelling of Ground Improvement on Soft Soils (AMGISS)". I would like to thank the coordinator of the AMGISS project, Dr. Mina Karstunen, who initiated the project and made my stay at ETH possible.

Very special thanks to my family, friends and my girlfriend Martina for their support and encouragement throughout this time.

Abstract

An extensive open cast mining of brown coal has been taking place in NW Bohemia since 1940's. During the mining process, overburden clay is placed in the form of irregularly shaped lumps of typical dimensions up to 500 mm into large spoil heaps. The total thickness of the lumpy clay layers is usually 20-50 m. The material of the landfill has a double porosity structure: porosity of clay lumps (intragranular porosity) and voids between clay lumps (intergranular porosity). The total porosity of fresh fill can be up to 70%. This soil presents special challenges for geotechnical design, primarily because of its high and non-uniform settlement. Further, the progressive transformation from the “granular“ to “fine-grained“ material makes the lumpy clay difficult to characterise and model.

The aim of the presented thesis is to describe the mechanical behaviour of the landfill by means of interpretation of field measurements, the centrifuge and numerical modelling. During site investigation for a motorway over a 20-30 years old landfill, two trial embankments were built and monitored over the period of 3 and 6 years respectively. The subsoil of the embankments was instrumented by hydrostatic levelling profiles, pore pressure transducers and depth reference points installed in boreholes. The interpretation of the field measurements revealed large settlements, which are attributed to the embankment surcharge, change of the groundwater level position during the monitoring and creep. A significant differential settlements were observed under both embankments.

Introductory modelling in a mini-centrifuge, combined with oedometer testing, demonstrated the key mechanisms in the double porosity fills: irreversible deformation at low stresses due to the rearrangement of the lumps, and reversible deformation (swelling) at higher stresses, similarly to the behaviour of the reconstituted material. Two different methods of landfilling were analysed. Placing fill under water resulted in high initial void ratios followed by large deformations while loading. Dry filling followed by fast natural saturation may be recommended with respect to further development of the landfills.

The centrifuge modelling of the field embankment was carried out at 150 g. Two tests with different techniques of embankment construction were performed. The results confirmed that hydraulic conductivity was controlled by the complex structure of the clayfills. Similarly to the field measurements, there were significant initial settlements during the self-weight consolidation due to compression of open macro voids. The double porosity structure in the fresh fill allowed the excess pore pressures to dissipate quickly, which accelerated the consolidation process initially. Thereafter, dissipation was controlled by the low permeability of the intragranular pores in the clay, once the intergranular pores had closed.

The rapid initial settlement was observed also after the embankment surcharge. In the centrifuge higher settlements were measured in the top 10 metres of the landfill than in the field. The major part of the difference can be attributed to the reduction of the porosity due to the climate effects *in situ*, which can cause a faster degradation of the soil structure close to the surface.

A hypoplastic model for clays with meta-stable structure was chosen for the numerical modelling of both the *in situ* trial embankments. The basic hypoplastic model for clays was calibrated using isotropic compression tests and triaxial compression tests on the reconstituted clay. Three additional model parameters describing the effects of double porosity structure were calibrated using oedometer tests on the specimens prepared from the scaled-down double porosity material (material with smaller size of clay lumps). The performance of the model was evaluated by a comparison with the results of the centrifuge model of self-weight consolidated landfill. Finally, the hypoplastic model was used for the simulation of both trial embankments and the results were compared with the *in situ* measurements. The *in situ* degradation of the double porosity structure due to weathering was back-analyzed from the numerical simulations of the settlements.

1 INTRODUCTION

1.1 Motivation, aims and methods

A large volume of clayey waste is produced as a by-product of the open cast mining of brown coal in North-Western Bohemia. Over 2 billions of tons of brown coal was excavated since 1945 with an average production of 3.6 m^3 of overburden clay per 1 m^3 of exploited brown coal (Vráblíková and Vráblík, 2000). The clayey overburden is placed in large landfills of the total area exceeding 100 km^2, which significantly change the landscape of NW Bohemia. In this thesis the term landfill is used for fills composed of clayey overburden of the coal seams and has no relation to domestic waste. The landfills have a typical double porosity structure. The term double porosity is used in the following text to describe the soil containing two systems of pores given by the porosity of the clay lumps and macro voids between them.

Due to the large area affected by mining, new constructions are often required on the top of the landfills. However, the complex behaviour of the landfills resulting in large and nonuniform settlement complicates the construction activities. The prediction of the landfill behaviour after the surcharge is extremely difficult due to inhomogeneity of the landfills, lack of information about the filling process and the change of the landfill structure depending on time, vertical stress and degree of saturation.

The aim of the thesis is to improve the knowledge about the deformation characteristics of the landfills and the changes of their structure. Two trial embankments had been constructed in 1998-2004 on an old landfill and monitored over 3-6 years. The results of the monitoring were analysed and the case histories were subjected to centrifuge and numerical modelling. The

main aim was a comparison of the field measurements with the results of the centrifuge and numerical modelling. The modelling provided additional information about the settlement and structure degradation during the self-weight consolidation, which was not analysed *in situ*. The results of modelling can be also related to particular initial conditions, which are unknown in the field.

A further task of the presented project was to discuss the relative importance of the main factors influencing the deformation behaviour of the landfills including vertical effective stress, position of the water level, influence of the non-uniform distribution of the macro voids and the destructuration of the top of the landfill due to the weathering.

There was no previous experience with either centrifuge modelling or advanced numerical modelling of clayey landfills of open cast mines. Therefore a set of mini-centrifuge tests was carried out to define optimum soil properties and to specify the technique for the modelling of the case history in the geotechnical centrifuge. The centrifuge models were instrumented similarly to the field embankments. Two tests with different techniques of embankmnent construction were carried out and compared.

A parallel between the behaviour of natural structured clays and clays with meta-stable structure was used for the numerical modelling of the landfills. A hypoplastic constitutive model for clays with meta-stable structure (Mašín, 2007) based on the hypoplastic model for clays (Mašín, 2005) was used for the simulation of the case histories.

1.2 Organisation of the thesis

A brief introduction to the behaviour of double porosity clays is presented in Chapters 2 and 3. Chapter 2 summarizes the range of geotechnical problems associated with double porosity clays and the most important aspects of their geotechnical behaviour. Chapter 3 is focused on the open cast mining landfills in NW Bohemia and describes the geology of the area, open cast mining, the filling process and the experience with construction on landfills.

The results of the project are presented in Chapters 4-7. Chapter 4 describes the locations and instrumentation of the trial embankments and discusses the results of the monitoring.

The preliminary modelling in the mini-centrifuge is presented in Chapter 5. It includes the preparation procedure of the soil for the scaled-down model, simple parametric studies in the mini-centrifuge, laboratory

investigations of the centrifuged samples (detemination of the water content and oedometer tests) and a study of different *in situ* filling techniques. The results of Chapter 5 can be also found in Najser et al. (2009b).

Chapter 6 describes a two-dimensional centrifuge modelling of the trial embankment 2. Two embankment construction techniques (“in-flight“ and “stationary“) are discussed. The results of the self-weight consolidation and of the behaviour after the application of the embankment surcharge are analysed. The results of the centrifuge modelling were also presented by Najser et al. (2008, 2010b), and Najser (2007a, 2007b, 2008).

Chapter 7 presents the numerical modelling. The first part describes the calibration of the hypoplastic model for clays and the calibration of the parameters describing the soil structure. The second part of Chapter 7 discusses the modelling of the case histories and of the centrifuge tests. The effects of the segregation of the lumps during filling and variations of water level are also analysed. The results of the numerical modelling can be found in Najser et al. (2009a, 2010a) and Najser (2009).

2 BEHAVIOUR OF DOUBLE POROSITY SOILS

2.1 Double porosity materials in geotechnical applications

Double porosity geomaterials comprise a wide range of soils and rocks ranging from the aggregated soils to fissured rocks. Their common feature is that they are composed of two distinct pore systems, differing in hydraulic conductivity. All such materials are characterized by a preferential flow and their hydraulic parameters can be generally described using the similar models (e.g. Gerke and van Genuchten, 1996 or Lewandowska et al., 2003).

This thesis deals with the double porosity clay composed of clay lumps. A major part of the research of the behaviour of lumpy clay carried out in the past years can be divided in two categories:

1. The behaviour of the fills composed of the clay lumps dredged out of the seabed.
2. The behaviour of the lumpy clay landfills originating as a by-product of open cast mining.

Dredging of the the clay from the sea was documented in various locations. In Sweden, the settlement of an instrumented embankment constructed on 6.4 m thick lumpy clay layer in Halmstadt harbour was described by Hartlen and Ingers (1981). The lumpy clay fill consisted of a 3 m thick barge-dumped bottom layer of stiff silty clay lumps of about 1 m^3 volume and a 3.4 m thick layer formed hydraulically (lumps of about 0.02 m^3). After 14

months, a 3 m high test embankment was constructed on the lumpy clay layer. The average settlement of 210 mm was observed over one year from the embankment construction, with the variable magnitude depending on the volume of macro voids between the lumps (significantly higher settlement was measured in the barge-dumped layer with bigger volume of the intergranular voids).

The capacity of disposal ponds for the clay dredged from the sea was studied by Ishihara et al. (2006). A filter-press technique was used to preconsolidate the dredged clay to increase its strength. The preconsolidated clay lumps were used to increase the height of the disposal pond dam.

An extensive study was carried out in Singapore, where the clay lumps dredged during an underground construction activities are used for land reclamation. The research was focused on deformation behaviour of the clay lumps, especially closing of the interlump voids. The site investigation of a 12 years old man-made island, which was reclaimed using large dredged clay lumps, was reported by Karthikeyan et al. (2004). The island was made of 0.5-2 m lumps, reaching the height of 8 m. A 10 m thick sand layer was placed on the top of the fill to accelerate the consolidation of the lumpy clay. After 12 years of consolidation, the density of the clayfill was still found to be variable as well as the strength and deformation characteristics. Yielding at the edges of the clay lumps and squeezing of the disintegrated material into interlump voids was detected. In the ultimate state the fill consisted of overconsolidated zones (part of the original lumps) and normally consolidated zones (disintegrated material in initial interlump voids). The creep deformation of the lumpy clay layer was also detected with the C_α in the range of 0.002-0.012.

Leung et al. (2001) presented the experimental investigation of the consolidation behaviour of clay lumps using a large one-dimensional compression apparatus and the centrifuge modelling. The clay lumps were prepared from the remoulded and recompressed original soil, from which 50-mm diameter clay balls were prepared using a cylindrical scoop. The behaviour typical for the double porosity soils was observed with significantly faster consolidation compared to the homogeneous clay. As the preferential flow paths through the interlump voids closed up, a rate of consolidation similar to the reconstituted soil was observed. Two pore pressure dissipation patterns were observed: fast dissipation of the pore pressure at the interlump voids and a much slower rate of dissipation of the pore pressure inside the lumps. It was therefore stated that the initial settlement of the fill is controlled by consolidation at the interlump voids and the long term settlement is controlled by the consolidation of the lumps (Manivannan et al., 1998). A higher settlement was observed as the size of the lumps increased. A comparison of the centrifuge models with the clay lumps of different shapes revealed that the spherical lumps settle less than cubic and irregular lumps.

A laboratory study of the double porosity clay formed by cubic lumps

was presented by Robinson et al. (2005). The lumps were cut from large clay lump (1 m^3) dredged from the sea with preconsolidation pressure of 200 kPa. It revealed that after consolidation to 100 kPa in a perspex cell (Fig. 2.1a), the permeability of the lumpy fill was significantly reduced to the order similar to that of the homogeneous clay (Fig. 2.1b). However, the shear strength profile indicated that the fill was still highly heterogeneous under the pressure of 100 kPa. When the preconsolidation pressure of the clay lumps was exceeded, the strength profile became uniform (Fig. 2.1c).

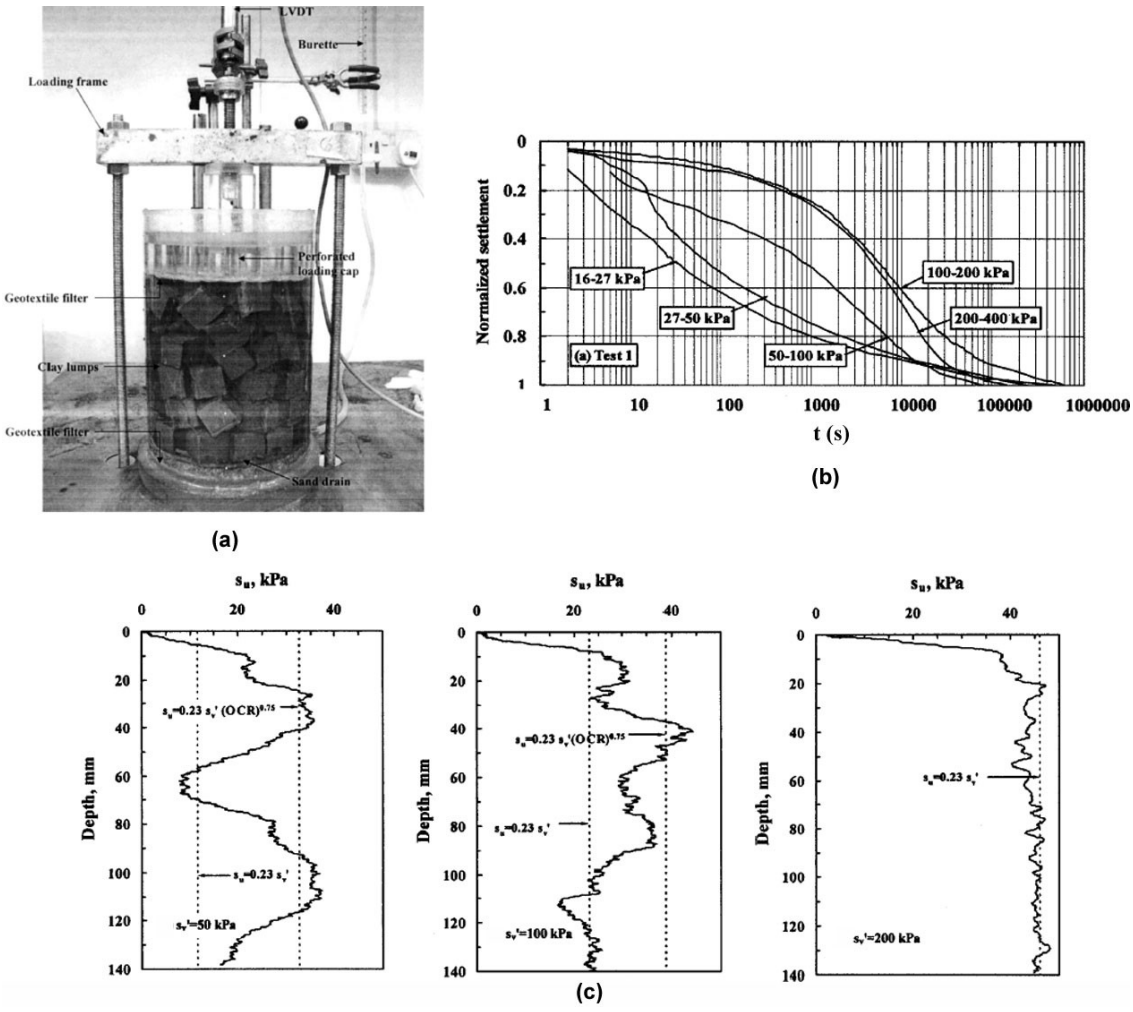

Fig. 2.1: Laboratory testing of lumpy clay: (a) - experimental setup; (b) - time-compression curves; (c) - shear strength profiles (Robinson et al., 2005).

Yang et al. (2002) described consolidation of a lumpy clay fill by the spring-box analogy (Fig. 2.2). It consists of a perforated piston, supported by columns of perforated boxes of springs interconnected by another set of springs. The springs connecting the perforated boxes represent the structure formed by the clay lumps and the spring inside a box represents the soil

skeleton within a lump. The perforations in each box of springs allow the exchange of fluid between the inside and the outside of the box, whenever there is a pressure difference. This analogy illustrates well the consolidation of the lumpy clay fill. It characterizes the lumpy clay as a two-system medium and follows the approach for fissured or fractured clay systems. In such a system, the permeability of the interlump system plays a key role. It directly affects the dissipation of pore pressure in the interlump voids, which in turn affects the pressure difference between the interlump and intralump voids and therefore has a significant influence on the fluid transfer between interlump and intralump voids.

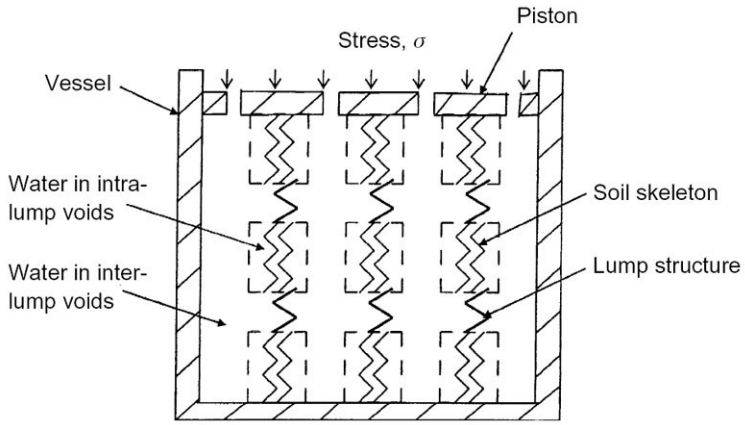

Fig. 2.2: Spring-box analogy presented by Yang et al. (2002).

Yang and Tan (2005) extended the results of Yang et al. (2002) by using FEM and taking into account non-linearity of the permeability (hydraulic conductivity in the interlump system changes significantly during consolidation). Swelling of the clay lumps and the variation of suction with time was studied by Robinson et al. (2004). The authors compared their experimental results with the FEM modelling by linear and non-linear elastic models. The study shows the importance of simulating continuous change in permeability for a realistic simulation of the three-dimensional swelling of the clay lumps.

A different geotechnical application of lumpy clay was reported by Cheuk et al. (2006). They described an investigation of the upheaval buckling of oil and gas offshore pipelines, which were covered by lumpy clay fill. The rate of the pipeline uplift, which depended on the degree of consolidation of the lumpy clay, was analysed by the centrifuge modelling. The different uplift velocities and two different consolidation time periods of the lumpy clay cover were simulated. The results showed that early commissioning of buried pipelines in an under-consolidated lumpy fill could lead to a reduction of the soil restraint, together with a decrease in the stiffness of the response. The “suction“ force generated underneath the pipe, which increased with the uplift

velocity, was found to be a significant contributor of the overall uplift resistance. Nevertheless, the quantitative analysis suggested that the beneficial effect from a higher degree of consolidation was much more significant than that achieved from a high suction force originating from a fast uplift.

In the past years, the behaviour of clayey landfills of open cast mines was studied widely. The most extensive research was carried out in the United Kingdom, further studies come from Germany, the Czech Republic, Canada and the USA. A summary of the research activities in the UK was given by Charles and Watts (2001). A detailed description of the mechanical behaviour of clayey landfills of open cast mines will be presented in the following section.

2.2 Behaviour of clayey landfills of open cast mines

During the open cast mining, the overburden soil is excavated and placed into spoil heaps. Following fundamental differences between the landfills of open cast mines and clay lumps dredged from the sea can be noted:

- The clay lumps dredged out of the seabed are usually of a similar shape and diameter, while the clay lumps excavated during open cast mining have highly variable shapes and the diameter ranging from millimetres up to blocks of >0.5 m.
- The lumps dredged from the sea are fully saturated, while the material from the open cast mining exhibits variable S_r.
- The overburden from the open cast mining exhibits usually significantly higher OCR compared to the clay dredged from the sea.

Spoil heaps can be divided into the inner landfills, backfilling the excavated space, and the outer landfills, which are filled outside of mine pits. These fills are usually dumped as non-engineered fills: fills, which have arisen as a by-product of human activity, and which have not been placed with a subsequent engineering application in view (Charles and Watts, 2001). The total porosity of the landfill (n_t, e_t) is given by the combination of the intragranular porosity (n_i, e_i), that is the porosity of clay lumps and the intergranular porosity (n_e, e_e), which characterizes the volume of macro voids between clay lumps. Both porosities are interrelated by Eqs. 2.1 and 2.2 (Feda, 1998).

$$n_t = n_i (1 - n_e) + n_e \tag{2.1}$$

$$e_t = e_i (1 + e_e) + e_e \tag{2.2}$$

A typical porosity of the fresh fill can reach up to 70% (Feda, 1998). The fresh landfill can be characterized by the behaviour typical for the granular soil with fast drainage of water through the open macro voids (Fig. 2.3a). Over time, the consolidation of the landfill takes place, the volume of the macro voids reduce due to the plastic straining at the contacts of the lumps and due to filling of the interlump voids with fine clay. The porosity and permeability of the landfill decreases and the behaviour resembles a fine grained material (Fig. 2.3b).

Fig. 2.3: Landfill during filling process (a) and after 10-15 years of self-weight consolidation (b).

Feda (1998) studied the complex mechanism of the transition of the landfills from the behaviour of a “granular“ soil to the behaviour of fine grained soil. The following structural mechanisms were described:

1. *Crushing of clay lumps*. It takes place more often with wet clay lumps as the clay is usually overconsolidated and wet lumps are weaker than dry lumps.
2. *Squashing of lumps*. Clay lumps are not disintegrated but compressed and deformed in a ductile manner. Wet lumps are predisposed to this type of deformation. Reduction of pore sizes accompanying squashing results in strain hardening.
3. *Rearrangement of lumps*. It comprises sliding and rotation of the lumps, which leads to densification of the soil.
4. *Contact bonding*. It is typical for wet clay lumps, which may mould one to another.

The first three mechanisms result in a reduction of intergranular voids. The rate of the structural degradation depends mostly on vertical stress, the

structure of the lumps and degree of saturation of the lumps. The most important factors influencing the structural degradation (σ_v', S_r) depend on the presence of water in the landfill. The water content can be therefore considered as a key factor influencing the behaviour of the fill.

The initial water content of the landfill is given by the original water content of the clay lumps, which can be partially changed during the transport by dessication or rainfall. After the filling, the lumps can absorb free water entering the landfill body through open macro voids. The increase of the water content in the outer part of the clay lumps reduces the shear strength at the contacts and accelerates the transition of the landfill from the “granular“ to “cohesive“ behaviour. Moreover, the increase of the groundwater level is a usual phenomenon especially in the inner spoil heaps, where water level was lowered by pumping during the mining process. Closing of interlump voids significantly reduces the permeability of the landfill and increases the degree of saturation. However, even 20-30 years after filling, the soil is not fully homogeneous and its double porosity structure remains, especially at shallow depths in the landfill. Despite closing of the macro voids, a similar behaviour as described by Robinson et al. (2005) can be expected (Fig. 2.1c): the overconsolidated zones are represented by the original clay lumps and the normally consolidated zones are represented by the macro voids filled by the material from the outer part of the clay lumps, which squeezed into the interlump voids and closed them up.

The top layer of the landfill is exposed to the cyclic changes of water content due to rainfall and climate effects. It can lead to a faster degradation of the double porosity structure and formation of a surface crust (Charles and Watts, 2001). Dykast (1993) reports that the changes due to the climate effects can be observed down to the depths of approximately 5 metres.

2.2.1 Shear strength of landfill

Determination of the shear strength of the landfills is usually very difficult. Laboratory tests are complicated by the problematic preparation of the representative specimens and the interpretation of the *in situ* measurements can be complicated by the non-homogeneous behaviour of the landfill and the zones of reduced strength. The strength of the fill often changes with time. A higher strength is typical for the fresh landfills with the “granular“ behaviour of the lumps, and it drops as the moisture content increases and the clayey behaviour prevails.

A potential risk of slope instability can be documented on the case history from Aberfan in Wales, which is the worst disaster induced by a landfill. In 1966, a heavy rainfall caused 150 000 m^3 of waste from coal mining to slide down the valley and kill 144 people of which 116 were children (Alexander,

1993). The landslides of landfills are documented also from the Czech Republic: in 1980's four large landslides occured, each with the volume of moving mass exceeding 50 millions m^3 (Vaníček and Vaníček, 2008). The landslide of the inner spoil heap in Vršany affected mining activity there. Three others, which occured in the outer spoil heaps affected buildings (Vřesová) or transport infrastructures (Loket spoil heap).

In the Czech Republic, it is now recommended to dump landfills with general inclination roughly 1:6, to reduce the possibility of slip failures (Vaníček and Vaníček, 2008). Back analyses of the landfills dumped in the past years can be used in the design of new landfills (Fig. 2.4). The trend in Fig. 2.4 suggests a decrease of the friction angle with increasing the vertical effective stress in the landfill. A similar decrease of the friction angle was also observed in the triaxial and shear box tests on the granulated clay specimens presented by Feda (1998) (Fig. 2.5). Large shear box (300x300 mm) tests on the landfill clay with the original grading curve and water content carried out by Herbstová and Herle (2009) also confirmed the reduction of friction angle with increasing vertical stress (Fig 2.6). The parametric studies of the slope failures indicate the friction angle of 13-16°, which decreases to approximately 7° after the failure (Vaníček and Vaníček, 2008). However, the shear tests on clay with reduced granulometry presented by Feda (1998) gave the friction angle above 20° (Fig. 2.5).

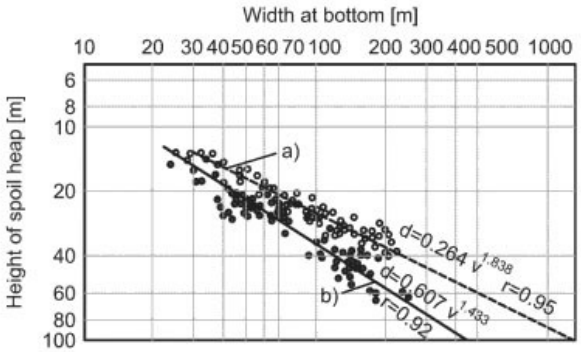

Fig. 2.4: Back analysis of the slopes of spoil heaps containing a) soils excavated from low depth and b) only limited amount of the soils excavated from the low depth (Vaníček and Vaníček, 2008).

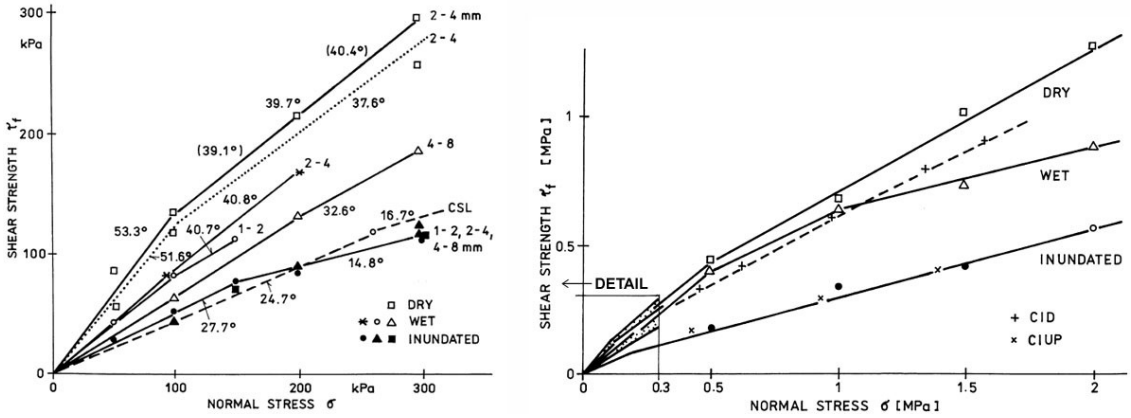

Fig. 2.5: Shear strength of granulated clay specimens (with ranges of granules 1-2, 2-4 and 4-8 mm) from the shear box and triaxial tests (Feda, 1998).The results include dry (oven dried), wet (natural water content) and inundated specimens.

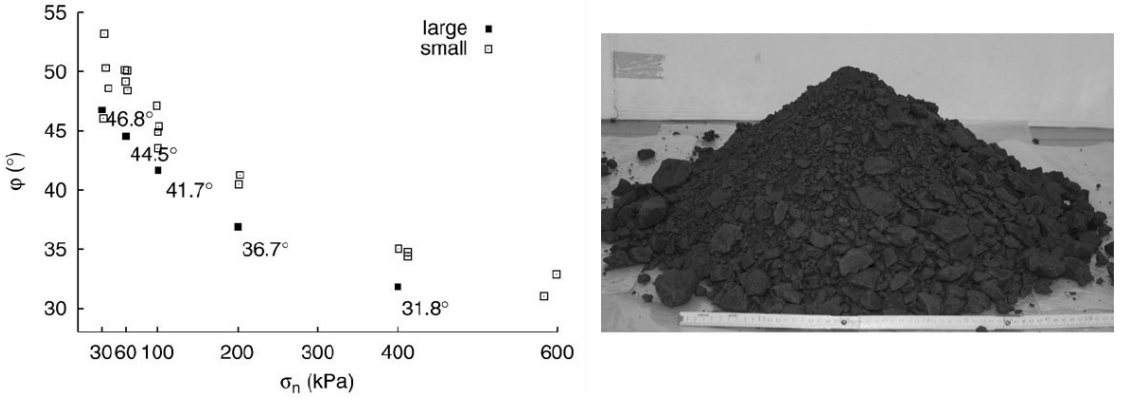

Fig. 2.6: Shear box tests of the landfill clay of natural water content carried out in the standard shear box (reduced dimensions of lumps) and large (300x300 mm) shear box with the original lump size distribution - photo (Herbstová and Herle, 2009).

2.2.2 Deformation of landfill

The primary compression of the landfill is associated with the transition mechanisms described in the previous section. A major part of the settlement during the self-weight compression is immediate and starts during the filling. Most of the fills is unsaturated during the filling, which increases the strength of the lumps and reduces the rate of transition from the “granular“ to “cohesive“ behaviour. On the other hand, in the saturated landfill the expulsion of water can increase the consolidation time. This is often the case, when after some time the groundwater level in the landfill increases and the surface is subjected to additional surcharge due to another layer of the fill or due to a construction.

A different compressibility of the saturated and unsaturated double porosity clay was studied by Feda (2003). Figure 2.7 shows oedometer compression curves of the specimens with reduced granulometry. The compression curve of the saturated specimen (1) exhibits the behaviour typical for the reconstituted soil, which is characterized by a linear shape in the semilogarithmic scale. The garlandlike compression curve is typical for unsaturated specimens (2). Its shape is influenced by the phases of strain softening (crushing of clay lumps) and phases of strain hardening (newly acquired structural stability due to the increased number of contacts).

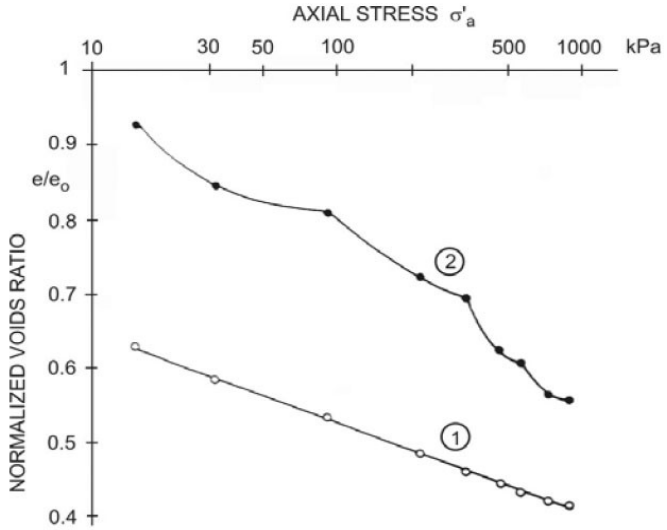

Fig. 2.7: Oedometer compression curves of fully (1) and partially (2) saturated specimens of granulated clay (Feda, 2003).

The secondary compression of the clayey landfills (the settlement under constant effective stress - creep) is widely reported (e.g. Charles, 2008; Charles and Watts, 2001; Boháč and Škopek, 2004). The coefficient of secondary compression C_α (= -Δ*e*/Δlog *t*) was found to be dependent on the compaction of the landfill with higher C_α typical for uncompacted fills (Charles, 2008). The linear relation between creep and logarithm of time was reported for most types of fill with average values of C_α = 0.5-1%. Laboratory experiments on granulated clay (Feda, 2004 and 2006) however revealed a multi-linear behaviour (Fig. 2.8). The multilinear behaviour was explained by various time-dependent intervening structural mechanisms (crushing of lumps, rearrangement etc.) with the collapsible stage (C_α = 7.52%) similar to a creep curve of the municipal solid waste (Feda, 2004).

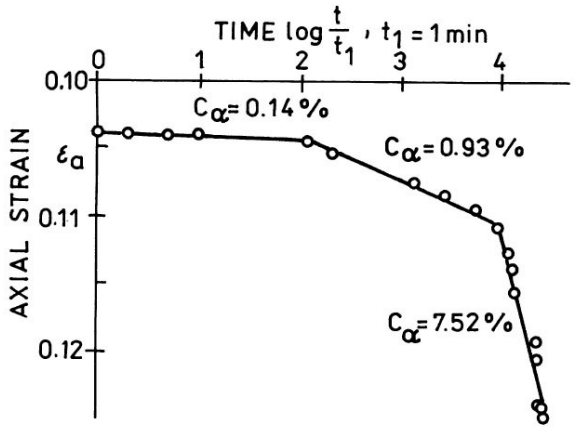

Fig. 2.8: Creep curve of landfill clay with reduced granulometry (Feda, 1998).

The clayey landfills of high porosity represent a typical example of a collapsible soil. The collapse settlement (sudden change of the structural configuration) is mostly associated with the increase of S_r (collapse on wetting, hydrocollapse). As presented by Charles and Watts (2001), most types of partially saturated fills are susceptible to collapse under a wide range of applied stress when first inundated, if they have been placed in sufficiently loose and dry condition. In the United Kingdom, hydrocollapses of clayey landfills associated both with rise of groundwater level (Corby, Ilkeston) and downward infiltration of surface water (Tamworth, Corby) were reported (Charles and Watts, 2001). An example of the collapse settlement due to the rising groundwater level in the opencast mining backfill at Horsley is presented in Fig. 2.9a. The water level rose by 34 m in three years and the collapse settlement in various depths was measured by magnet extensometers. The hydrocollapse in the saturated zone (bottom picture in Fig. 2.9a) is documented by the settlement of markers located in different depths below the surface (top picture in Fig. 2.9a). Another case history from Blindwells is presented in Fig. 2.9b.

Laboratory studies demonstrating the collapsible behaviour of the lumpy clay after inundation were presented for example by Feda (1998) and Záleský et al. (2001).

The compressibility of the landfill varies both in space (differential settlement) and in time (seasonal effects, average precipitation). The differential settlement is caused by the local inhomogeneities in the landfill structure. One possible reason can be the segregation of the lumps during filling, which leads to the variations of intergranular porosity in both horizontal and vertical direction. Another reason can be associated with an increase in water content in the landfill, which can cause local collapses of the structure during the consolidation. Variations in water content can be associated with higher infiltration of water from atmospheric precipitation in depressions where surface waters are collected (Vaníček and Vaníček, 2008). The rate of the

settlement often varies with time and it can be a function of the average precipitation as reported by Dykast (1993). Charles and Watts (2001) showed that the differential settlement can be also caused by abrupt changes in landfill depth (Fig. 2.10).

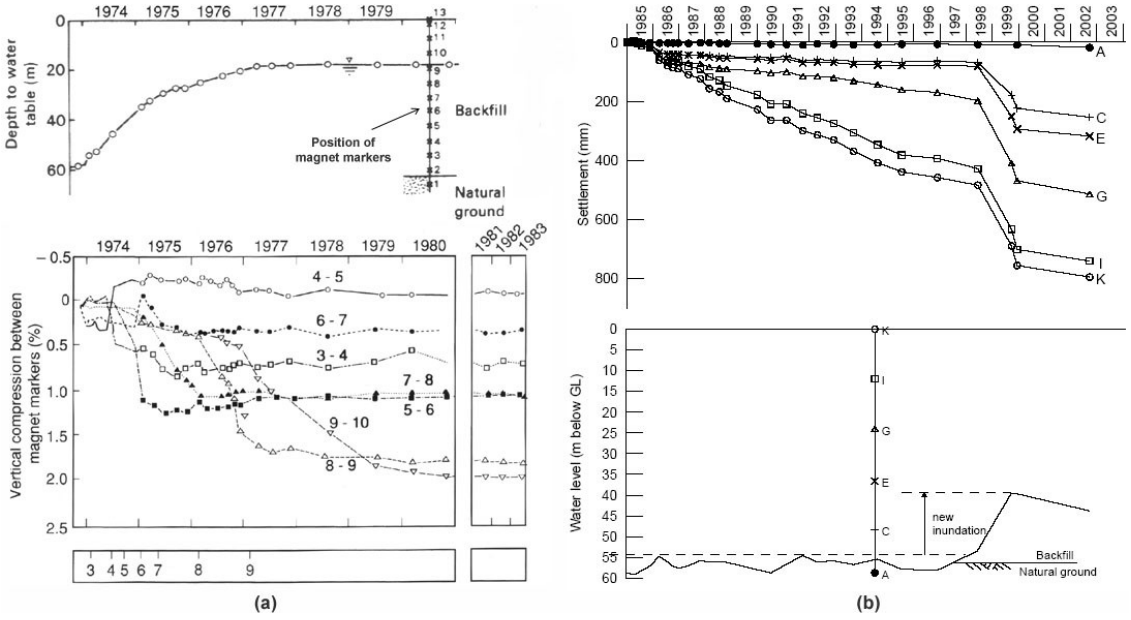

Fig. 2.9: In situ monitoring of hydrocollapse of landfills: (a) - landfill in Horsley (Charles and Watts, 2001); (b) - landfill in Blindwells (Watts and Charles, 2003).

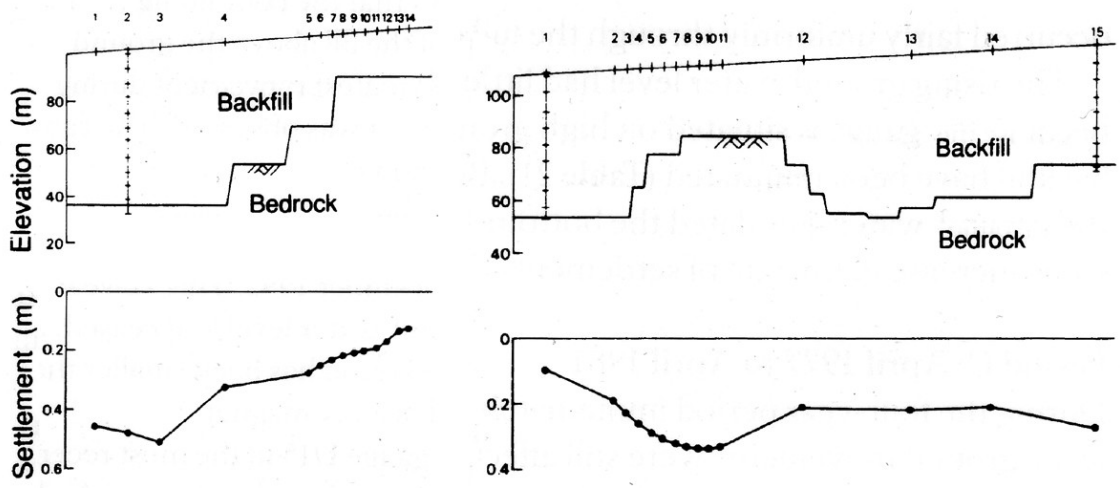

Fig. 2.10: Influence of variable depth of landfill in Horsley to magnitude of settlement (Charles and Watts, 2001).

3 LANDFILLS IN NORTH-WESTERN BOHEMIA

3.1 Geology of Most Basin

There are four Tertiary sedimentary basins with a brown coal seam in NW Bohemia: the Cheb Basin, the Sokolov Basin, the Most Basin and the Zittau Basin. In this section, the geological history of the Most Basin is described in detail as the case histories, which are analysed and modelled in this thesis, are located in the NE part of the Most Basin.

The Most Basin is the largest preserved sedimentary basin within Eger Graben - the easternmost part of the European Cenozoic Rift system, which extends from the coast of the North Sea to the Mediterranean. The area of the basin is cca 1400 km^2 and the preserved basin fill thickness reaches over 500 m. The basin is interpreted as a part of an incipient rift system that underwent two distinct phases of extension (Rajchl et al., 2008). The first phase was characterized by a N-S extension with E-W oriented faults, which were later overprinted by a NE-SW fault system resulting from the second extension phase in the NW-SE direction (Fig. 3.1).

The onset of the formation of the Most Basin is associated with the onset of the main phase of volcanic activity in NW Bohemia during the latest Eocene (Rajchl et al., 2008). The earliest part of the basin fill is the volcanogenic Střezov Formation, followed by clastics and carbonaceous deposits of the Most Formation (Fig. 3.2a). The Most Formation is subdivided into the Duchcov (“Underlying“) Member, overlain by the Holešice (“Main Seam“), Libkovice (“Overlying“) and Lom (“Lom Seam“) Members (Kvaček et al., 2004).

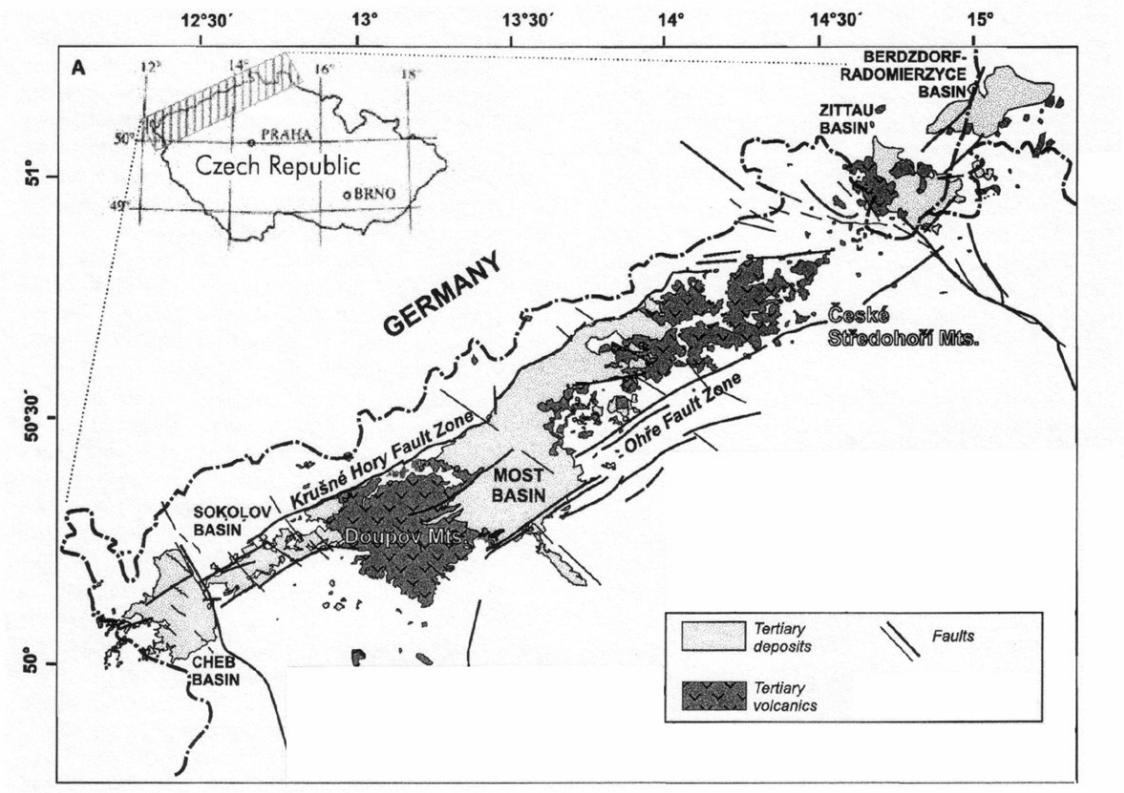

Fig. 3.1: Simplified geological map of Tertiary sedimentary basins in NW Bohemia (after Rajchl et al., 2008).

There were following environments during the deposition of the Most Formation (Kvaček et al., 2004). The early stages of the basin are characterized by flat land with stagnant-water lakes in the NW part filled by neovolcanics, lakes in the central part with clay deposition and fluvial and deltaic facies near the mouth of the stream coming from central Bohemia. These conditions enabled the coal seam to develop (Fig. 3.2a - deltaic clay and sand sediments are marked by "Ž" - Žatec delta and "B" - Bílina delta). The average thickness of the coal seam is 10-30 m, exceptionally it can reach up to 50 m. During the sudden subsidence of the basin, the landscape changed into a large lake of about 1-7 m in depth filled with clays of the Libkovice Member. The renewed shallowing of the lake resulted in the accumulation of the Lom Seam in the uppermost part of the basin fill. The intervals of the sedimentation in the Most Basin, their predominant character and times of deposition are summarized in Fig. 3.2b.

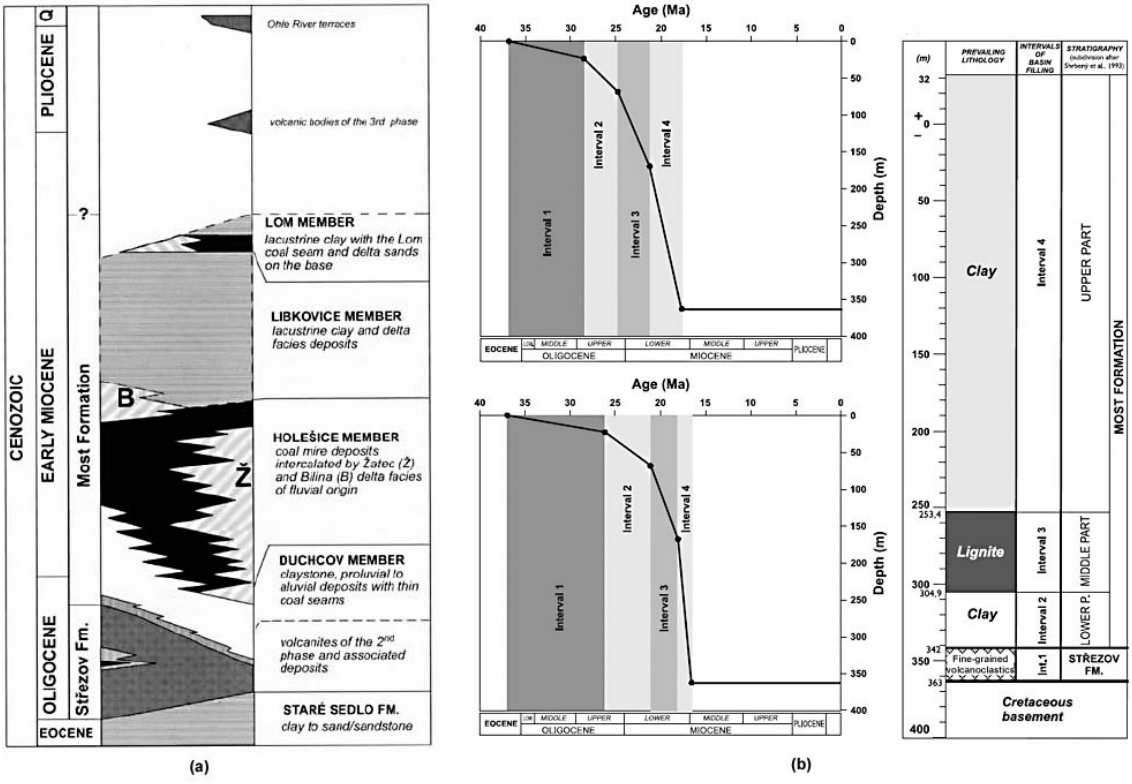

Fig. 3.2: (a) - lithostratigraphic column of the Most Basin (Kvaček et al., 2004); (b) - simplified vertical profile of the Most Basin (right) and depth-to-basement curves based on magnetostratigraphic data (top left) and paleontological and radiometric data (bottom left) illustrating the subsidence history of the deepest part of the Most Basin (Rajchl et al, 2008). The coal seam is represented by sedimentation interval 3 and overburden clay is represented by sedimentation interval 4.

3.2 Process of filling

The history of the coal mining in the NW Bohemian region dates from the 15th century, when the first mining activities of the local inhabitants are documented. In the 19th century, the significance of the mining increased due to the possibility of railway and water transport of the coal. In the first decades of the 19th century, deep mining still prevailed, but the significance of the surface mining gradually rose. The surface mining has been dominating since 1940's, when the first large open cast mines were opened. Since the second half of the 20th century, the Czech Republic is one of the most important producers of brown coal in the world (Fig. 3.3). Nowadays, about 78% of the total volume of the brown coal mined in the Czech Republic comes from the Most Basin and approximately 21% from the Sokolov Basin. The brown coal

reserves in the Most and Sokolov Basins are approximately 800-900 millions of tons and the mining activity is currently planned until 2040.

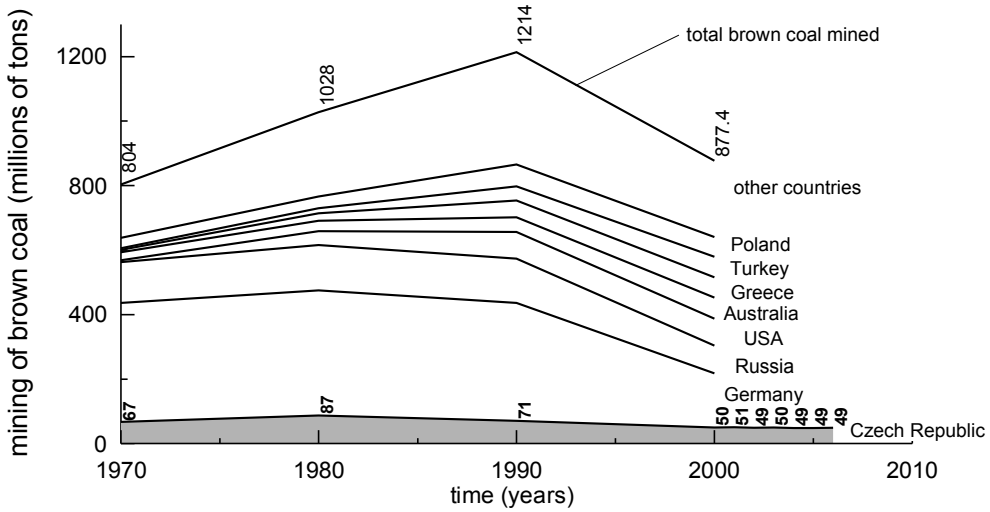

Fig. 3.3: Production of brown coal.

Approximately 200 milllion m^3 of clayey overburden is produced each year and deposited into landfills. The overburden clay is excavated, transported by belt conveyors and filled with stowing machines with a rotating boom (Fig. 3.4). Because the range of outer landfills is limited due to strong pressure to limit other annexation of agricultural land a percentage of inner landfills is increasing. In the last phase of the open pit mining in NW Bohemia the inner landfills will prevail (Vaníček and Vaníček, 2008).

Fig. 3.4: Filling the landfill (www.mapy.cz).

The clay overburden exhibits the average porosity of 40%, a liquid limit 70-92% and plasticity index of 35-60% (Feda 1998; Vaníček and Vaníček, 2008). From the clay minerals mainly the kaolinite and illite are presented with variable amounts of montmorillonite. The proportion of the clay-size particles ranges from 10 to 40% and silt from 20 to 60% (Vaníček and Vaníček, 2008). Generally, the clays have the character of overconsolidated fissured soils with stiff to very stiff consistency.

The description of the fresh fill can be found in Vaníček and Vaníček (2008). At the end of the transport, the individual lumps are partly compacted by free fall (from the height up to 20 m). The bulk density of the filled material is approximately 1500-1600 kg*m^{-3} with the intergranular porosity 30-45%. The macro voids between the lumps are interconnected and the permeability of soil for air is relatively high (Fig. 2.3a).

The process of the transition of the fill from the behaviour of “granular” soil to the behaviour of clayey soil was described in Section 2.2. One of the most important characteristics of an old landfill is the depth at which the macro pores are closed by surcharge of the overlaying clay. The landfill with open macro voids is collapsible with preferential paths for water infiltration through interconnected voids. There is also a greater risk of the differential settlement due to the variable intergranular porosity. It can be caused by different shapes and sizes of the lumps, segregation during filling, uneven free-fall “compaction” or variations in the water content. However, different depths of the closing of macro voids can be found in the literature. Herštus and Šťastný (1998) report the depth of 10 m based on the results of a field loading test. According to Vaníček and Vaníček (2008), the macro voids close in 10-40 m depending on the initial water content of the lumps. Větrovský (2006) in Vaníček and Vaníček (2008) stated, that the macro voids close in the range of σ_v' = 0.6-1.1 MPa, which corresponds to the depths of 40-70 m. The actual depth of closing of macro voids probably depends on the specific conditions at each site and it is a function of S_r and of the overconsolidation of the lumps.

3.3 Experience with building on landfill

Any building activity on the landfills presents a challenge for the geotechnical design due to the large and variable compressibility and difficult prediction of the mechanical behaviour. Spread foundations are usually preferred. The piles are usually used only for the foundations, where strict limits for differential settlement are requried (e.g. foundations of bridge piers). For practical reasons the length of piles is usually lower than the height of the landfill and their bearing capacity is likely to be reduced by negative skin

friction (Vaníček and Vaníček, 2008).

An example of the landfill settlement after filling can be seen in Fig. 3.5, which shows the settlement of “Ervěnice corridor“ in NW Bohemian mining region. The “corridor“ is the part of a large inner landfill and its average height is 130 m. The settlement varying from 0.15 to 1.5 m was measured over 2 km distance in 12 years after filling (Dykast, 1993).

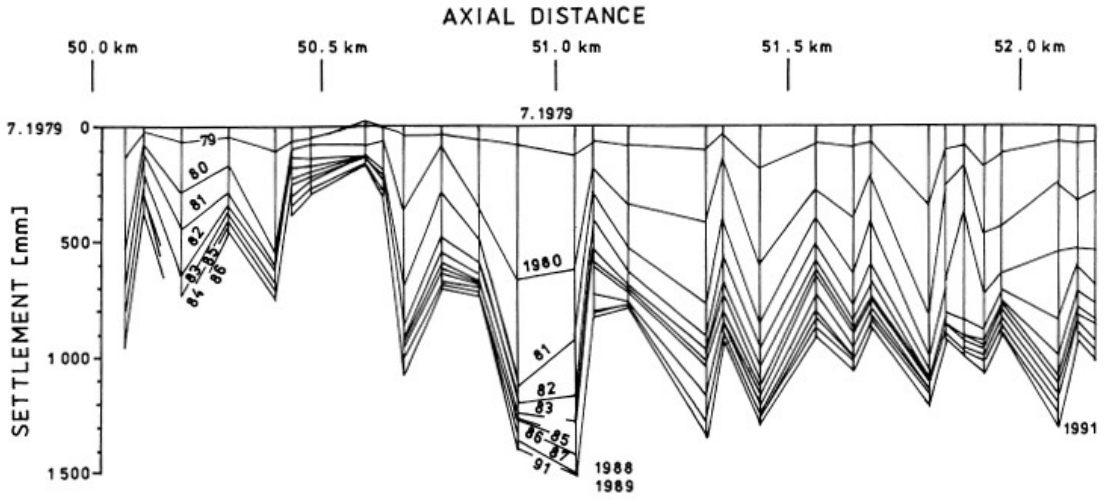

Fig. 3.5: Settlement of Ervěnice corridor in NW Bohemia (Dykast, 1993).

Ground improvement methods are often required before the construction to reduce large differential settlements. The following methods can be used:

Preloading of the surface

The construction of the temporary embankment on the landfill surface is probably the most effective method of ground improvement of the landfills. Because of the rapid initial settlement due to closing of the interlump voids, the effect of the preloading is fast and almost irreversible. The method was succesfully used in various locations in NW Bohemia and a good experience with the preloading was reported also from the United Kingdom (Charles, 2002). In saturated fills, the consolidation can be accelerated by installation of the vertical drains.

Dynamic compaction

This method is effected by repeated impacts of a heavy weight, which is dropped onto the ground surface. An experiment with dynamic compaction was carried out NW Bohemia in 1979-1980 (Barvínek, 1986). A 10 tons plate (1.4 x 1.4 m) was released from the height of 8 m with a 2.8 m distance between the impact places. The compressibility and hydraulic conductivity of the landfill was reduced in the top 5 m. The effect of dynamic compaction on

the NW Bohemian landfills was also studied in the geotechnical centrifuge (Pooley et al., 2008) However, this technique was never used in large scale in practice in the Czech Republic. In United Kingdom, the dynamic compaction was succesfully used for example in clayey landfill in Corby (Charles and Watts, 2001). Figure 3.6 compares settlements of the treated ground without any surcharge with the ground subjected to the construction of houses. Comparable settlement in both cases indicates, that the settlement of the houses was unrelated to the load by the buildings and that the ground movements were attributable to other causes (Charles, 2002).

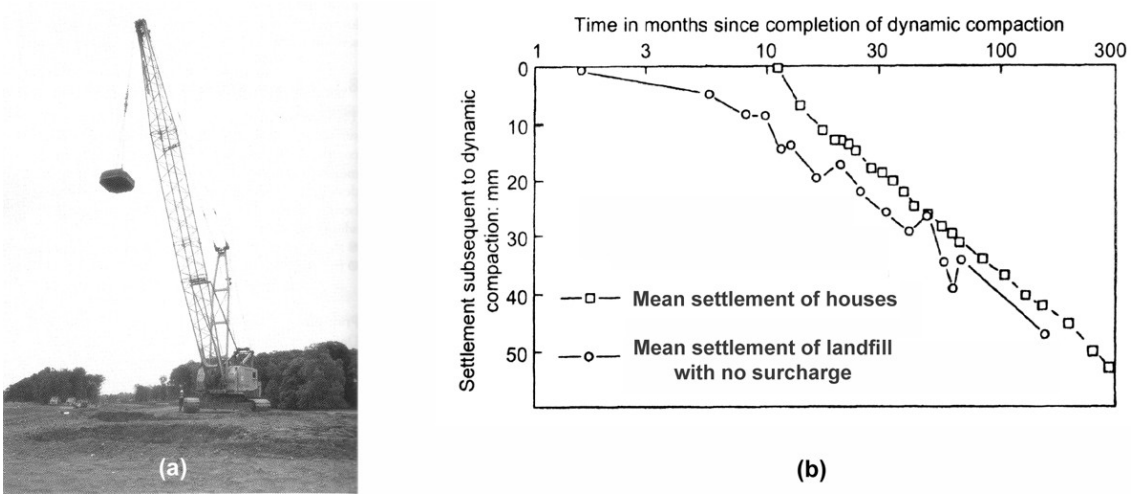

Fig. 3.6: (a) - dynamic compaction (Charles and Watts, 2001); (b) - comparison of settlement of loaded and not loaded landfill at Corby treated by dynamic compaction (Charles and Watts, 2001).

Deep vibration

This method can be used closer to existing structures than dynamic compaction. The reduction of the intergranular porosity in the active zone can be allegedly achieved with the help of “clay piles“, when a pre-driven profile is backfilled by clay of similar properties as is the surrounding material and subsequently compacted (Fig. 3.7, Vaníček and Vaníček, 2008). More efficient can be vibro stone columns, which can also increase the strength of the landfill and accelerate the consolidation.

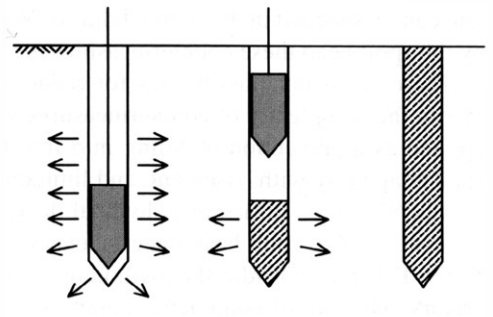

Fig. 3.7: Compaction using “clay piles“ (Vaníček and Vaníček, 2008).

Further ground improvement methods including vacuum preloading, explosive compaction, grouting methods or reinforcement by geosynthetics can

be found in the literature (e.g. Dykast, 1993; Vaníček and Vaníček, 2008; Charles, 2002) but their practical application is rare.

4 TRIAL EMBANKMENTS

4.1 Location of embankments

A new motorway from Prague (Czech Republic) to Dresden (Germany) crosses the area influenced by open pit mining of brown coal. Figure 4.1 shows part of the motorway route and the geological map of the NW part of the Czech Republic. The cross-section in Fig. 4.1 is localized in the place, where the motorway crosses the clayey landfills of open cast mines in the Most Basin. The motorway is divided into 7 parts (801-807) and the part 807 is separated into two sections (801/I, 801/II). The section 801/I between Trmice and Knínice is 12 km long and it crosses clayey landfills, a municipal waste landfill and a fly ash lagoon. The total length of the motorway route crossing the landfill areas is 5.9 km (Fig. 4.2), which represents almost 50% of the 801/I section (Kurka and Novotná, 2003).

Before the motorway construction, two trial embankments were built on its route at a site where a nearly completely backfilled mine pit had been used as a fly ash lagoon (Fig. 4.3). The thickness of the clayey fill under the embankments was 25-30 m. The subsoil under the clayfill consists of Tertiary overconsolidated clays and claystones (Škopek and Boháč, 2004). The age of the landfill was about 30 years at the time of embankments construction. Both embankments were instrumented and monitored for 3 and 6 years respectively. The groundwater level varied during the period of monitoring as a result of pumping of water from nearby fly ash lagoon. The groundwater level position in the period 1997-2004 is shown in Fig. 4.4. In 1999, pumping of water was interrupted and water level rose above the landfill surface. After the restoring of pumping, the water level dropped again (readings from 2004). The

measurements until 2001 were carried out in boreholes, while the last two measurements in Fig. 4.4 after the decrease of the water level in 2004 show the position of the water level in the fly ash lagoon further from the embankments. Therefore the decrease of the water level in 2004 directly below the embankments is expected to be smaller than shown in Fig. 4.4 due to the cone of depression. This is confirmed by the measurements of pore water pressures (Section 4.4.3).

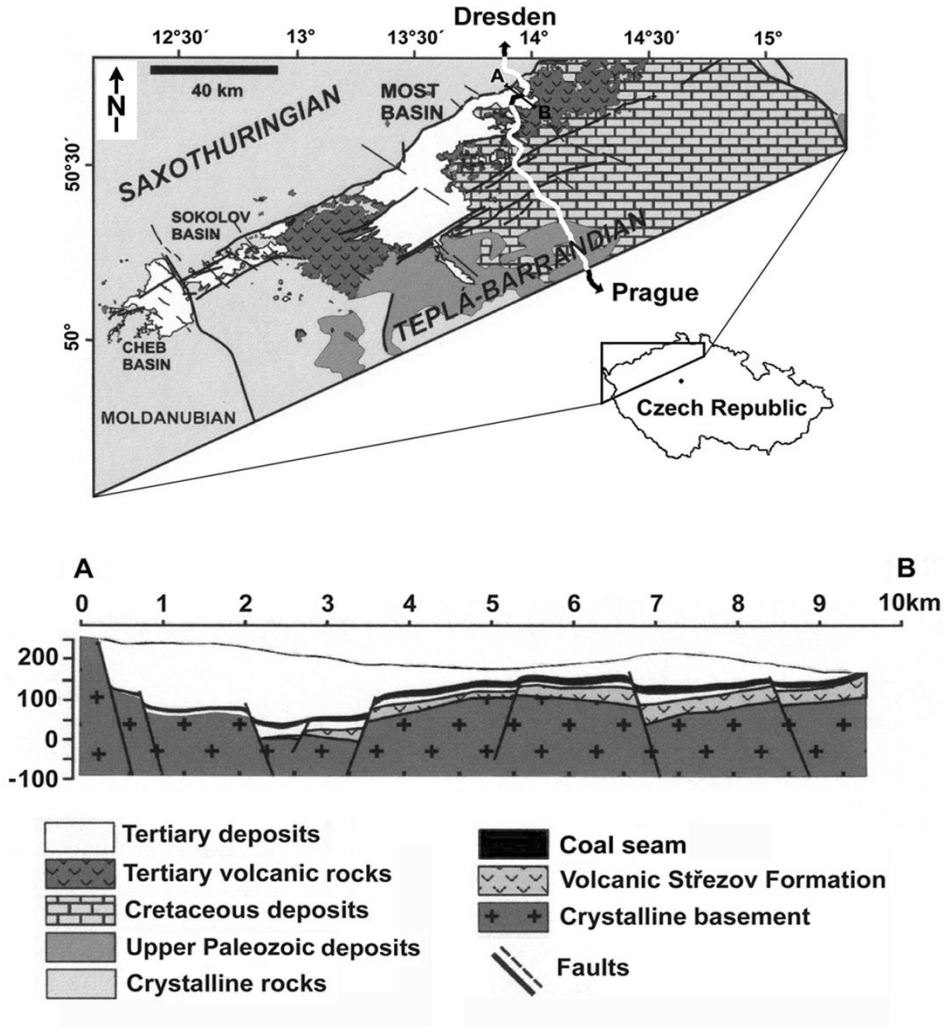

Fig. 4.1: Schematic geological map of Tertiary sedimentary basins in N-W Bohemia and cross-section of N-E part of Most Basin. (modified after Rajchl, 2006).

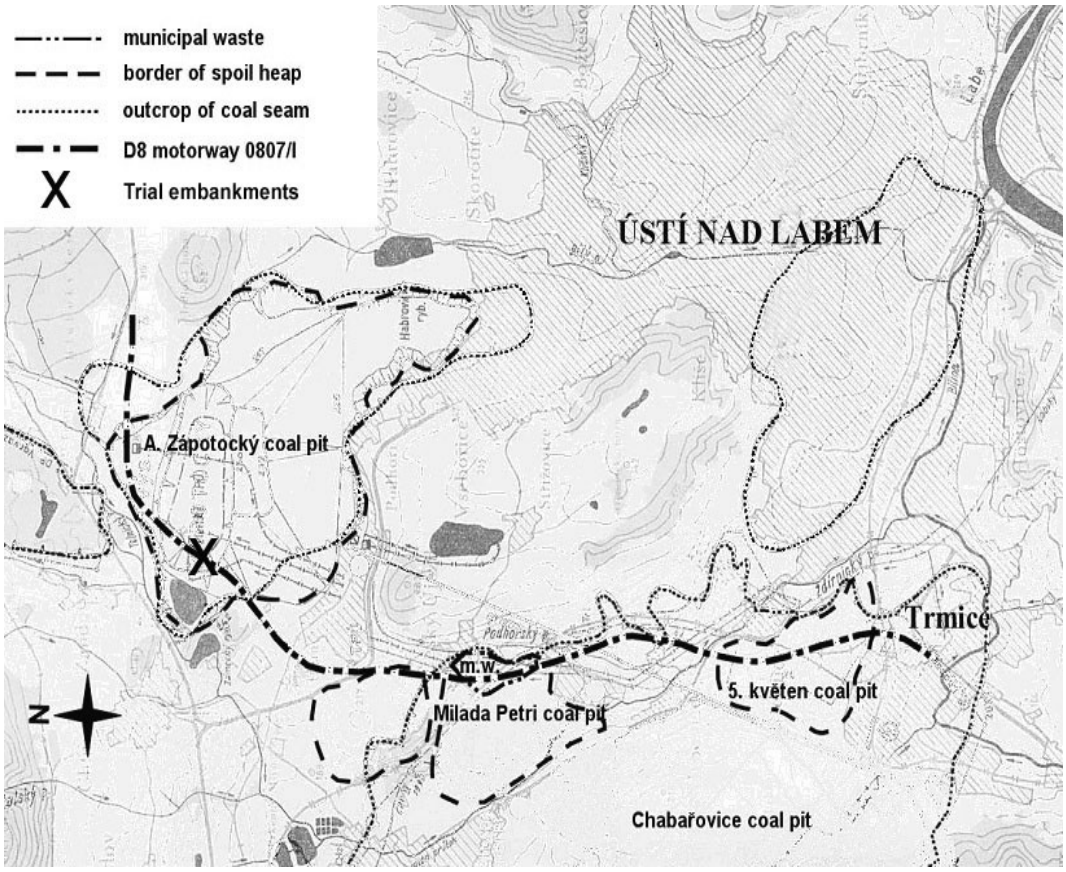

Fig. 4.2: Route of D8 motorway (part 0807/I) with neighbouring spoil heaps (after Kurka and Novotná, 2003).

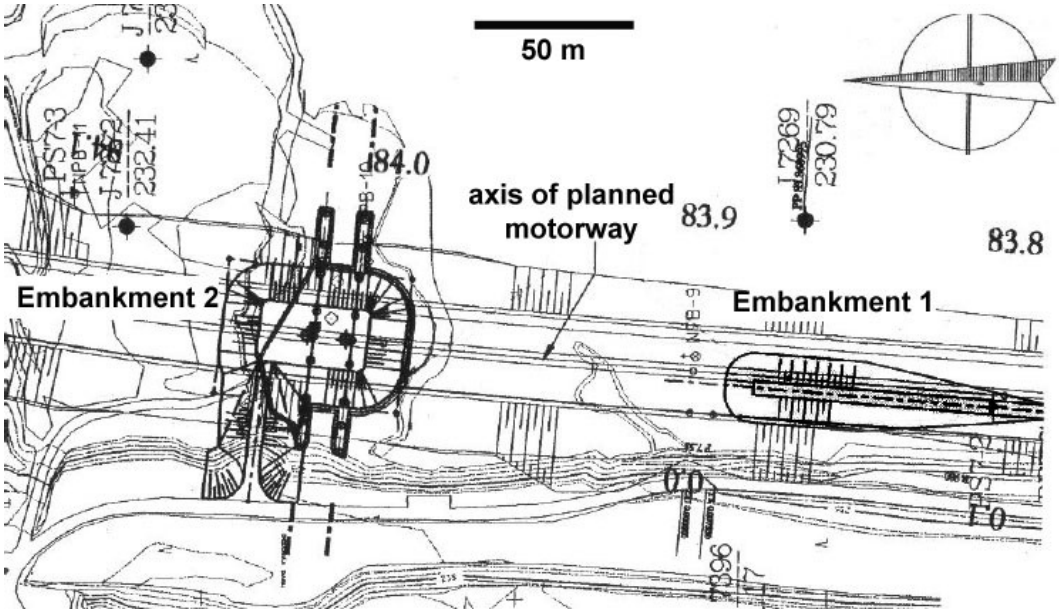

Fig. 4.3: Locations of trial embankments.

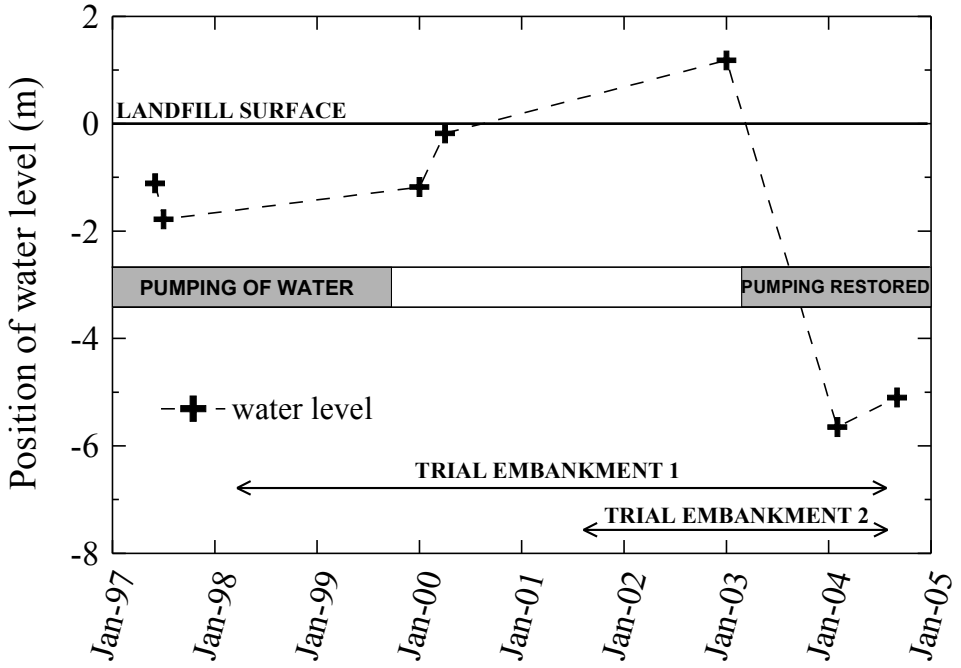

Fig. 4.4: Groundwater level variations during monitoring of embankments.

4.2 Embankment 1

Embankment 1 was constructed in April 1998 in a location where a 3.5 m thick permeable layer (fly ash and rubble) had been deposited on the top of the landfill. The groundwater level was about 2 m below the surface at the time of construction. The embankment was 6 m high with a 35 m long and 4.5 m wide crest and the slopes graded at 1 (vertical) : 1.5 (horizontal). The volume of the embankment was 5000 m^3. Figure 4.5 shows the embankment after its completion. The embankment was constructed from clayey soils. The soil was spreaded in 0.3-0.4 m layers and compacted to a minimum of 95% of maximum dry density according to Proctor Standard. The density of naturally moist clay ranged from 1820 to 1950 $kg*m^{-3}$ with an average of 1835 $kg*m^{-3}$ (Škopek, 2001).

The instrumentation of the embankment consisted of 18 surveying reference points on the landfill surface and at the top of the embankment, hydrostatic levelling profiles at the base of the embankment and depth reference points, inclinometers and pore pressure gauges in the embankment subsoil. Flexible plastic tubes for the hydrostatic levelling were installed in three

profiles perpendicular to the axis of the embankment. The position of the depth reference points (15 in total) was measured in two boreholes instrumented by plastic tubes (76 mm in diameter) with eight externally mounted free moving magnetic rings. The vertical movements of the rings were monitored by a reading unit manufactured by Glötzl, which was lowered into the plastic tube. The deepest reference point was installed 28.5 m below the landfill surface. The pore water pressure gauges were installed 6 m and 7.5 m below ground surface. A detailed description of the monitoring and discussion of the results can be found in Boháč and Škopek (2002) and Škopek and Boháč (2004).

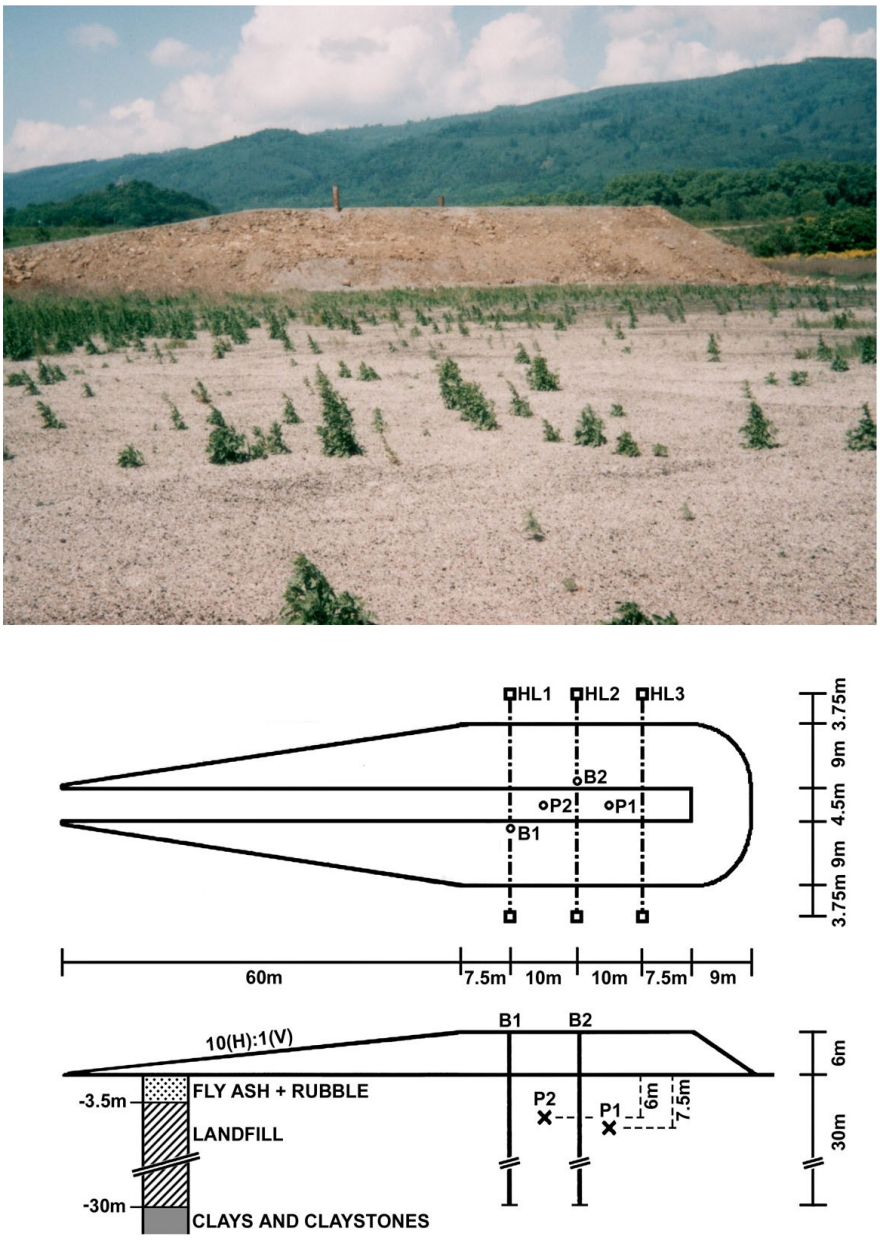

Fig. 4.5: Embankment 1, its instrumentation and geology of subsoil. (HL – hydrostatic levelling profiles, P – pore pressure gauges, B – boreholes with depth reference points).

4.3 Embankment 2

Embankment 2 was constructed 100 m from the first embankment, in August 2001. No fly ash was present under the embankment. The site was flooded during embankment construction (Fig. 4.6) and therefore a 1.4 m layer of rubble was placed on the surface of the landfill before constructing the

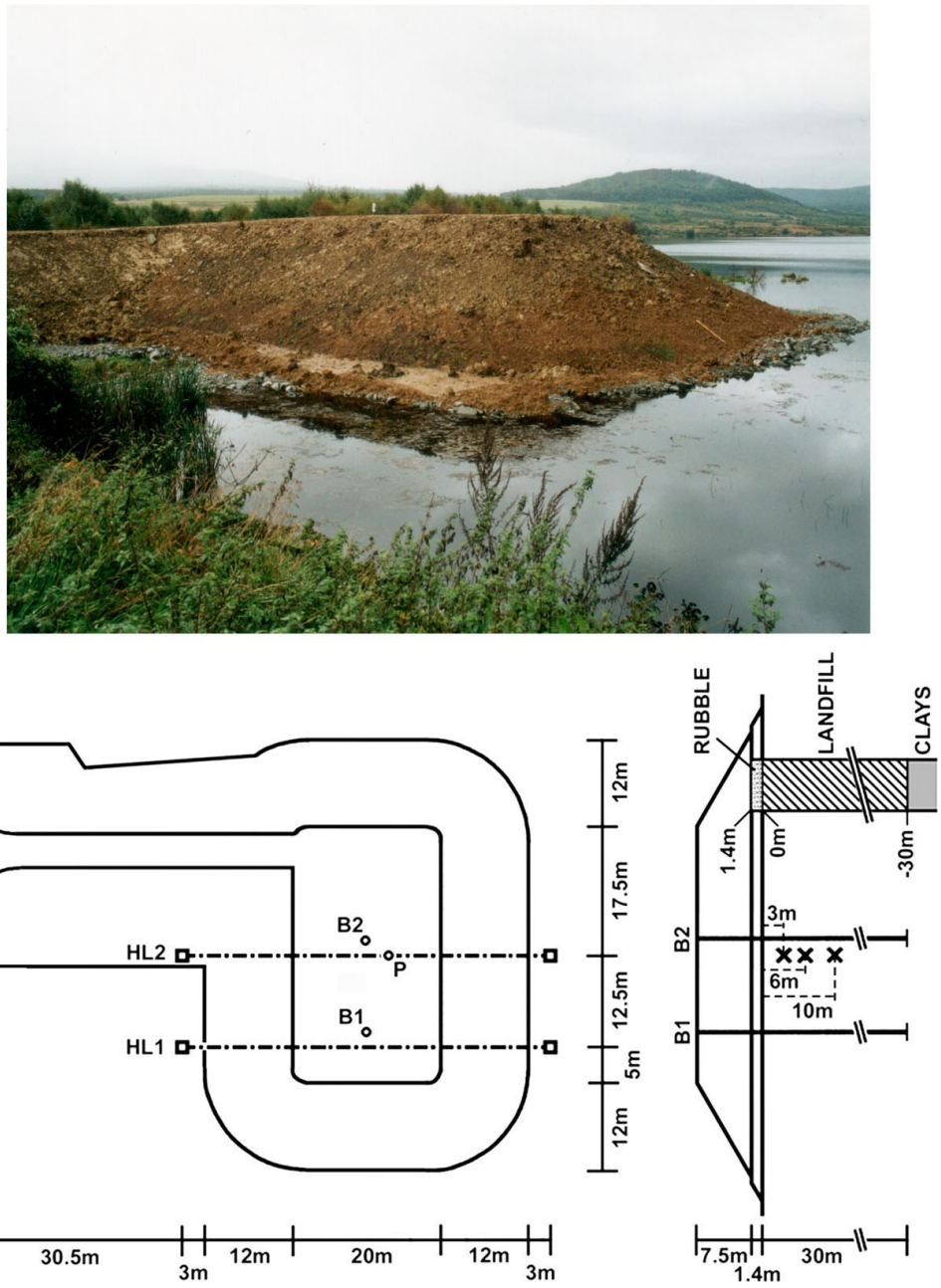

Fig. 4.6: Embankment 2, its instrumentation and geology of subsoil. (HL – hydrostatic levelling profiles, P – pore pressure gauges, B – boreholes with depth reference points).

embankment. This embankment was 7.5 m high with crest dimensions of 20 by 35 m. The volume of the embankment was 13586 m^3. The soil was compacted in 0.4 m thick layers similarly to Embankment 1. The average bulk density after the compaction was 1795 $kg*m^{-3}$. Embankment 2 was instrumented similarly to the first embankment, with surveying reference points, two hydrostatic levelling profiles at the base of the embankment, inclinometers, depth reference points in two boreholes (11 in total) and pore pressure transducers installed at three different depths (3, 6 and 10 m below the original surface).

4.4 Results of monitoring

The following section describes the results of monitoring of both trial embankments. Embankment 1 was instrumented and monitored by AZ Consult company and measurements of Embankment 2 were carried out by SG Geotechnika company. *In situ* measurement reports from both companies were used as a source of data presented in Section 4.4.

4.4.1 Hydrostatic levelling profiles

Figures 4.7a-c show the results from three hydrostatic levelling profiles located under Embankment 1. All graphs show rapid settlement developing immediately after the embankment construction. The fast initial settlement (Fig. 4.8) is typical for double porosity soil structure: it is associated with closing of interlump spaces and subsequent slower settlement rate is caused by consolidation of the clay lumps. The scatter of data in Fig. 4.7 can be explained by the combined effect of the accuracy of the measurements (±10 mm) and by the change of effective stresses due to the fluctuation of the water level. Clear evidence of increase in effective stresses was observed in 2004 by the increase in settlement, when pumping from the fly ash lagoon was restored and the groundwater table dropped to almost 6 m below the original ground surface (Figs. 4.4, 4.7, and 4.8). Data presented in Fig. 4.7a-c show the total settlement including the settlement of the free landfill surface, which was influenced by the variation in groundwater level and creep processes during the period of monitoring. Surveying of the cells located at the end of each profile indicated that the embankment surcharge did not influence the settlement at the ends of the hydrostatic levelling profiles. The net settlement caused only by the embankment surcharge (with data corrected for the settlement at the end of the profiles) is plotted in Fig. 4.7d-f. The net settlement curves for all the profiles are also presented by dashed lines in Fig. 4.8. The

figure shows that consolidation after embankment construction was finished in approximately 100 days and the major part of the deformation from the following measurements was caused by creep and the change of effective stress in the landfill due to the variation in the water level (this is discussed in detail in Section 4.5).

No measurements were carried out from 2000 until July 2004. The hydrostatic levelling gauges were not accessible during this period due to the rise of the water level above the surface. The heave of Embankment 1 measured on 1/12/1999 can be explained by the drop of effective stresses due to the rising water level. The opposite effect was observed in 2004, when pumping of water from the fly ash lagoon was restored and the water level dropped below the surface (Fig. 4.4).

A significant differential settlement was observed, reaching 90 mm, when all three hydrostatic levelling profiles are compared (Fig. 4.8). Similar observations were reported from different landfills based on surveying data (e.g. Dykast, 1993). The differential settlement could be caused by variations in intergranular porosity in the horizontal direction due to the segregation of the lumps during landfilling. The resulting landfills are not homogeneous and differential settlements should be expected. Generally there is a lack of information on the method of filling and on the initial conditions, for example about the existence of an effective drainage at the bottom of the landfill. The effect of the lump segregation during the filling is studied in detail in Section 7.4.1.

The results of the monitoring of Embankment 2 are presented in Figs. 4.9 and 4.10. The average settlement of the landfill under Embankment 2 is almost two times bigger because of the different heights of both embankments - Embankment 1 generated vertical effective stress 108 kPa, while vertical effective stress under Embankment 2 was 132 kPa (another 19 kPa was generated by rubble stone layer). The magnitude of the settlement could be also influenced by the shape of both embankments: width of the crown of Embankment 1 was 4.5 m compared to 20 m in the case of Embankment 2.

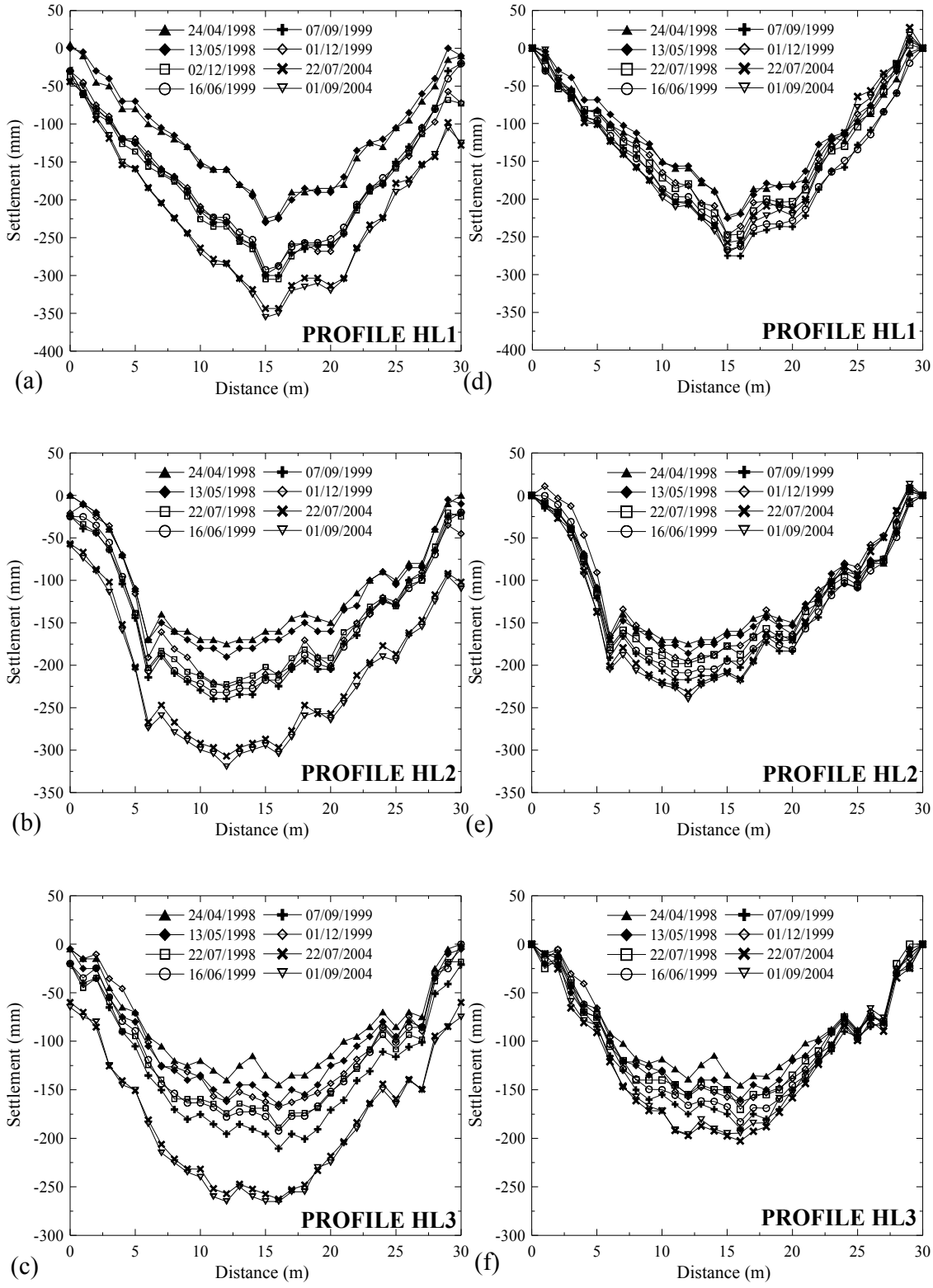

Fig. 4.7: Settlement under Embankment 1 (location of profiles can be seen in Fig. 4.5). Embankment was completed 23/04/1998.

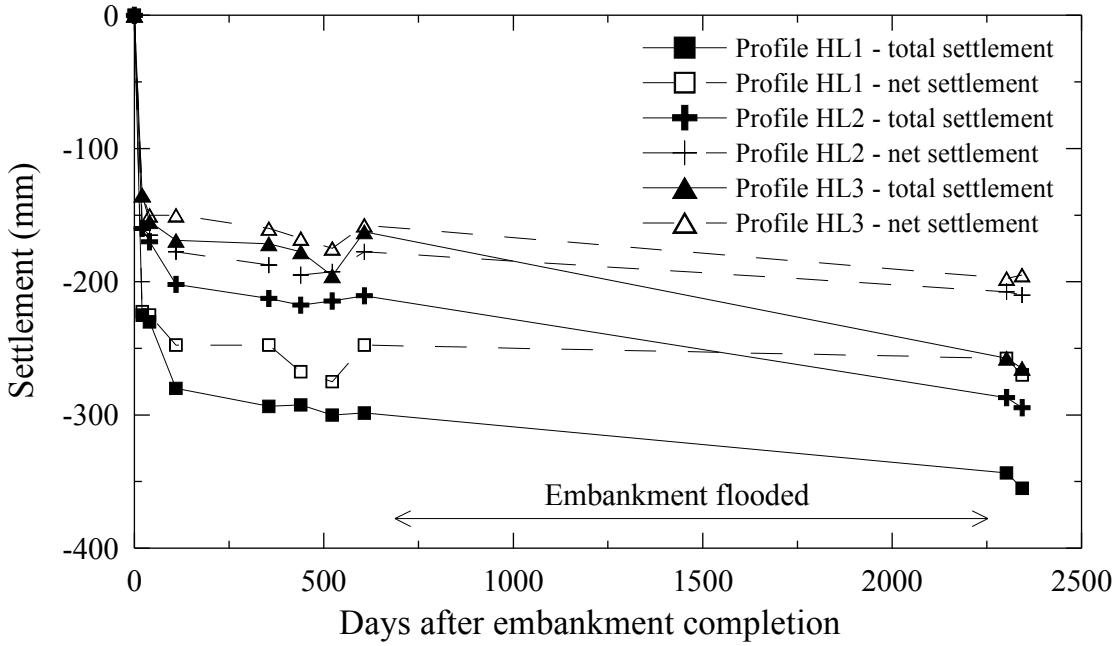

Fig. 4.8: Settlement at the centre of all hydrostatic levelling profiles.

The settlement curve has a similar shape compared to Embankment 1 with fast initial settlement, which took place mostly during the time of embankment construction (end of construction is marked by vertical line in Fig. 4.10. The settlement under Embankment 2 was measured also during the construction of the embankment and therefore the settlement in Fig. 4.9 seems to be more gradual compared to Embankment 1. Two hundred days after its construction, base of the embankment was flooded by rising water level and no measurements were carried out for following 900 days. After a decrease of the water level in 2004, the last measurement of the hydrostatic levelling profile 1 was carried out (measuring cell of profile 2 was not accessible due to a small landslide on the slope of the ramp). Similarly to Embankment 1, the 2004 measurement shows only a very small net settlement, which suggests that the consolidation under the embankment was finished. The total settlement of 97 mm from the previous measurement is caused partly by increasing vertical effective stress due to the drop of water level and partly by creep. A differential settlement of a similar magnitude (88 mm) compared to Embankment 1 was observed.

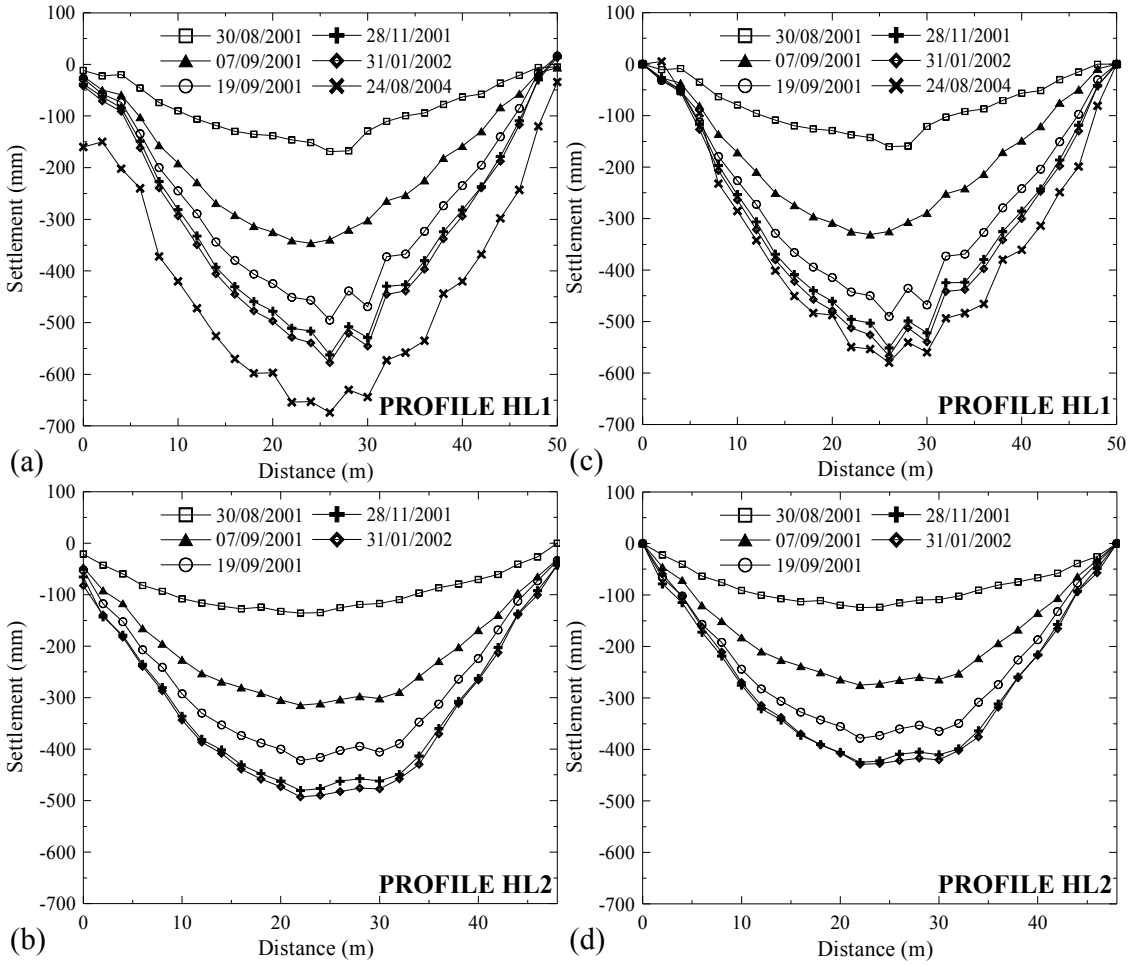

Fig. 4.9: Settlement under Embankment 2 (HL1 and HL2 profile in Fig. 4.6). Embankment was completed 11/09/2001.

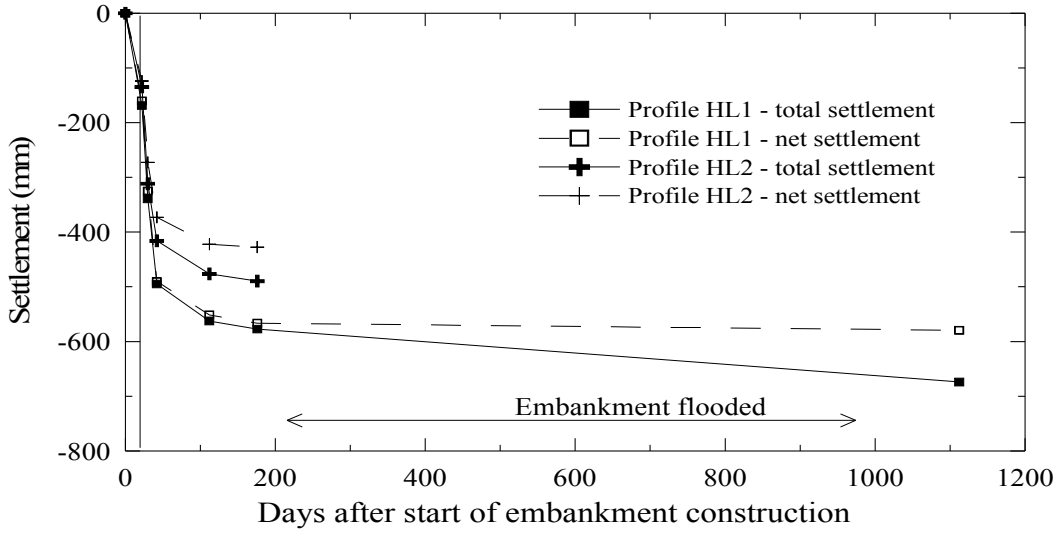

Fig. 4.10: Maximum settlement under the centre of Embankment 2.

4.4.2 Depth reference points

The results of the measurement of depth reference points coincide with the data from the hydrostatic levelling profiles. The data from Embankment 1 are plotted in Fig. 4.11 and the data from Embankment 2 in Fig. 4.12. All the profiles are influenced by the variations in the water level in a similar way as the hydrostatic levelling profiles. The readings from Embankment 1 exhibit a bigger scatter compared to Embankment 2. This can be caused by errors made during the installation of the magnetic rings (Boháč and Škopek, 2000). The measurements under Embankment 1 were carried out after its completion (23/04/1998) while Embankment 2 was monitored also during its construction. Tab. 4.1 shows the height of the embankment when the positions of depth reference points were measured. Data presented in Figs 4.11 and 4.12 indicate that the active zone is confined to the upper 17-20 metres of the landfill for Embankment 1 and approximately 22 metres for Embankment 2.

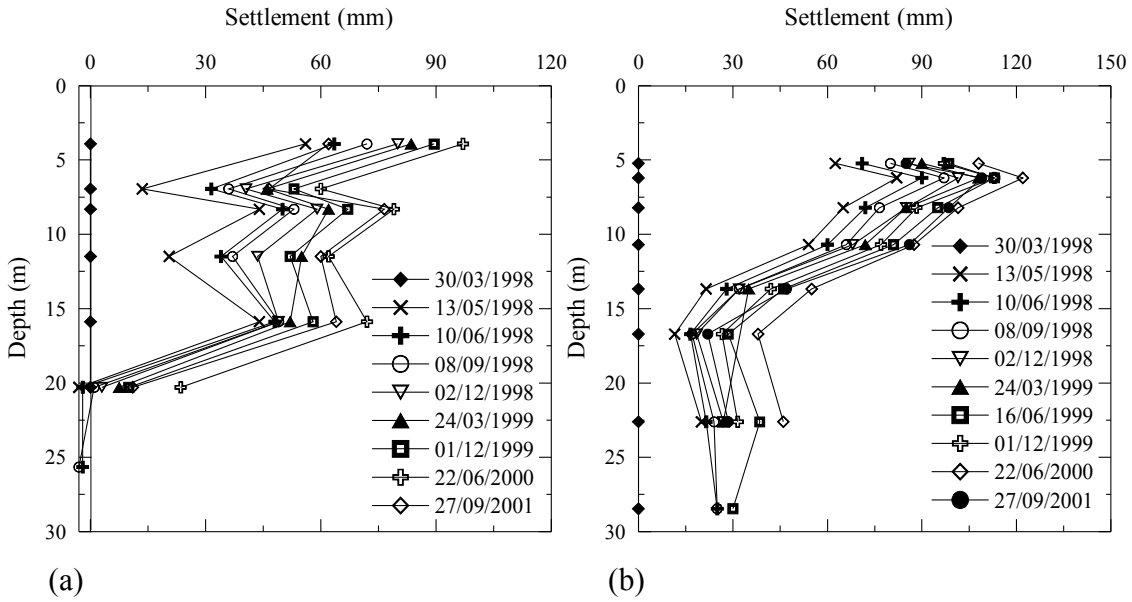

Fig. 4.11: Settlement of depth reference points under Embankment 1 ((a) - profile B1 in Fig. 4.5; (b) - profile B2 in Fig. 4.5).

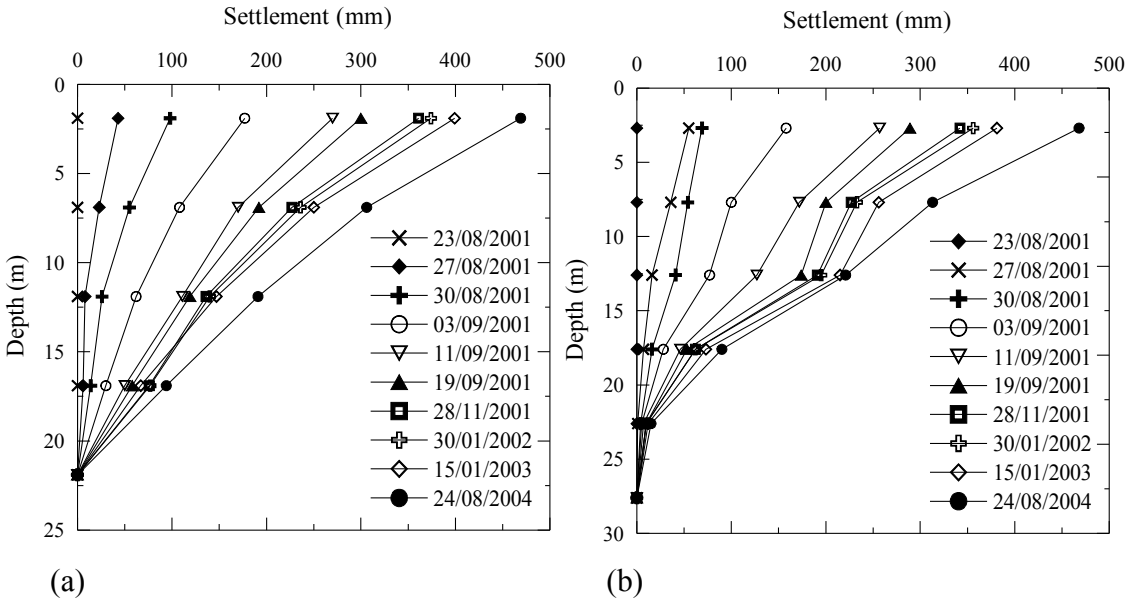

Fig. 4.12: Settlement of depth reference points under Embankment 2 ((a) - profile B1 in Fig. 4.6; (b) - profile B2 in Fig. 4.6).

	23/08/01	*27/08/01*	*30/08/01*	*03/09/01*	*11/09/01*	*19/09/01*	*28/11/01*	*30/01/02*	*15/01/03*	*24/08/04*
Profile B1	0.7 m	1.8 m	4.2 m	5.7 m	7.5 m	7.5 m	7.5 m	7.5 m	7.5 m	7.5 m
Profile B2	1.4 m	2.5 m	4.5 m	5.9 m	7.5 m	7.5m	7.5 m	7.5 m	7.5 m	7.5 m

Tab. 4.1: Height of the Embankment 2 during the measurement of of depth reference points.

4.4.3 Pore pressure gauges

The dissipation of excess pore water pressures under both embankments is shown in Figs. 4.13 and 4.14. The maximum excess pore pressures were measured a few days after the completion of the embankments.

Under Embankment 2, the maximum values are about 40 kPa higher than the surcharge caused by the embankment and rubble layer (151 kPa). This difference is attributed to difficulties in determining geostatic pore pressures due to the variations in water level. The decrease after 500 days from the embankment construction is presumably associated with the decrease in water level, while the excess pore pressures were probably equalized. Some error could be also attributed to the scatter in the measurements (±5 kPa). However, the maximum measured excess pore pressure was close to the

vertical stress generated by the embankment (in the case of Embankment 1, about 30% of excess pore pressure dissipated during embankment construction). The dissipation of excess pore pressure took about 150 days for Embankment 1. Under Embankment 2, excess pore pressure dissipation took about five times longer compared to Embankment 1, because of the longer drainage path in the clayfill (no fly ash on top). In the time range 45-520 days the dissipation was significantly faster for the gauge located 3 m below surface, while for deeper gauges the dissipation was more gradual. The maximum decrease of water pressure caused by pumping was 20 kPa, which indicates that the drop of the water level under both embankments was lower (only about 1/3) compared to drop of water level in the fly ash lagoon presented in Fig 4.4.

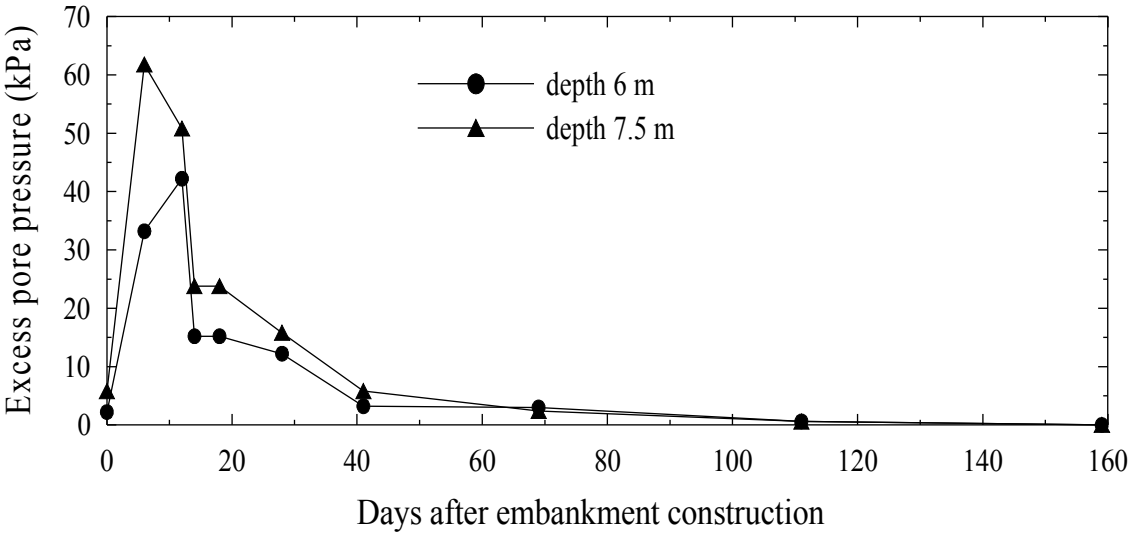

Fig. 4.13: Dissipation of excess pore pressures under Embankment 1 (P1, P2 in Fig. 4.5).

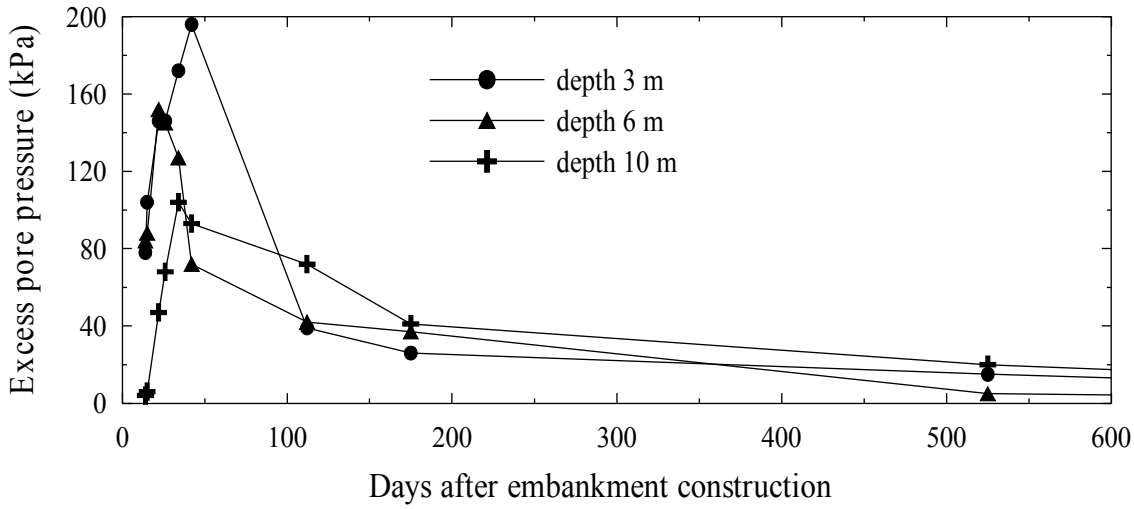

Fig. 4.14: Dissipation of excess pore pressures under Embankment 2 (P1, P2 in Fig. 4.6).

4.5 Creep of landfill

The effect of creep of the clayfill can be assessed from the comparison of settlement of hydrostatic levelling profiles (Figs. 4.8 and 4.10) and dissipation of excess pore pressures (Figs. 4.13 and 4.14). While the consolidation (and hence the primary settlements) finished 150 days after construction of Embankment 1, secondary settlement of 100 mm, 86 mm and 84 mm was measured in profiles 1, 2 and 3 in the time range 600-2300 days after embankment construction. Similarly under Embankment 2, deformation of 95 mm was measured in the range 200-1100 days after its construction.

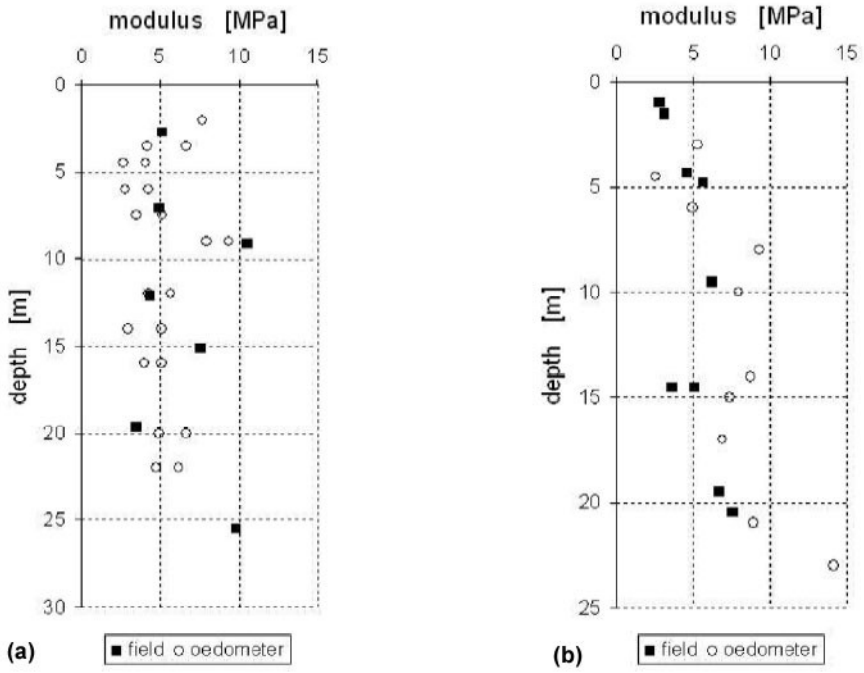

Fig. 4.15: Deformation moduli determined from the movement of reference points below embankments compared with oedometer moduli of undisturbed samples: (a) - Embankment 1; (b) - Embankment 2 (Škopek and Boháč, 2004).

A simple calculation of the landfill settlement from $s = h*\Delta\sigma_v'/E_{oed}$ indicates, that settlement due to the change in water level can be 10-20 mm (the assumed height of the landfill is h = 25 m, increase of σ_v' of 20 kPa and E_{oed} for reloading is 25-50 MPa, which is 5-10 times higher than that for primary loading (Fig. 4.15). A major part of the settlement after stabilizing of pore pressures (up to 80 mm) can be therefore attributed to creep of the landfill.

4.6 Summary

Field monitoring of two trial embankments revealed following mechanisms typical for the double porosity clay landfill:

- The landfill subjected to an embankment surcharge is highly compressible. A rapid initial settlement, caused by closing of interlump voids, was observed under both embankments.
- The total settlement under Embankment 1 reached 265-355 mm in the period of 6 years. The total settlement under Embankment 2 was 674 mm during 3 years of measurement.
- The net settlement (settlement caused only by embankment surcharge) was 195-270 mm under Embankment 1 and 580 mm under Embankment 2. An average difference between the total and net settlements was 78 mm for Embankment 1 and 94 mm for Embankment 2. This difference was partly caused by the variation in water level and partly by creep.
- A significant differential settlement was observed under both embankments, reaching 90 mm for Embankment 1 and 139 mm for Embankment 2 (measured 176 days after embankment construction). It demonstrates the large horizontal variability of the intergranular porosity in the particular landfill even after 30 years of the self-weight consolidation.
- The measurement of depth reference points specified the depth of active zone below both embankments. The active zone below Embankment 1 was limited to 17-20 m and below Embankment 2 it was 22-25 m.
- The rate of dissipation of pore pressures under both embankments corresponded to the length of drainage path in the clay. The dissipation under Embankment 1 was faster due to the more permeable fly ash layer on top of the landfill.
- The analysis of the pore pressures under both the embankments reveal that a part of the settlement is caused by creep.

5 PRELIMINARY TESTS IN MINI-CENTRIFUGE

5.1 Introduction to centrifuge modelling

The basic principle of centrifuge modelling is to increase Earth's gravity in the model by the rotation of the model around the central axis of the centrifuge (Fig. 5.1). Earth's gravity g is increased by scale factor n, which depends on angular velocity ω and the distance of the model from the centrifuge central axis r (Eq. 5.1).

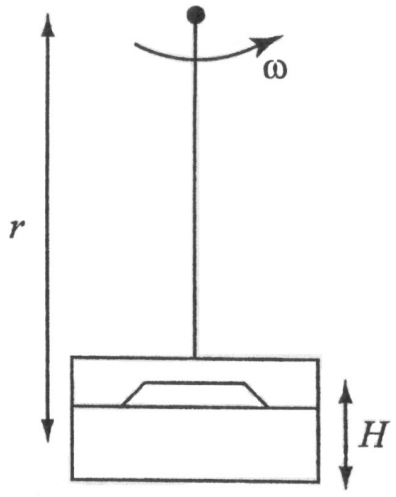

Fig. 5.1: Principle of the centrifuge modelling (Muir Wood, 2004).

$$n \cdot g = r \cdot \omega^2 \tag{5.1}$$

An increase of the vertical stress through the model is presented in Fig. 5.2. It demonstrates that by increasing the Earth's gravity *g* by factor *n*, the *in situ* vertical stress profile is simulated using an *n* times smaller model.

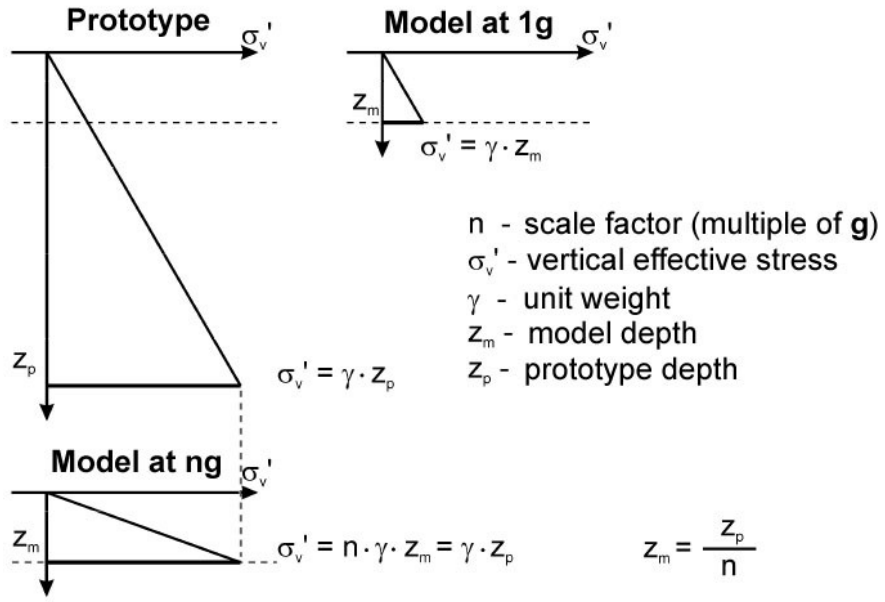

*Fig. 5.2: Comparison of vertical stress profiles in prototype, centrifuge model under n*g (g = 9.81 m/s^2) and stationary centrifuge model at 1 g (Laue, 2002).*

The value of *n* in the centrifuge model varies in both horizontal and vertical direction. The field of the same gravity level is slightly curved (it is defined by the same distance from the axis of rotation). This is mostly neglected and centrifuge models are constructed with a flat surface, which represents a slightly curved prototype as the g-level at the surface varies. More important is the variation of g-level in vertical direction. It implies that the vertical stress profile inside the model under *n*g* is slightly curved. In order to minimize the effect of this non-linearity, the nominal scaling factor *n* for the centrifuge test should be calculated at 1/3 of the model depth (the distance from the axis of rotation to 1/3 of the model depth is called *effective radius*). Then the vertical stresses in the model and prototype are equivalent at 2/3 depth (Schofield, 1980; Taylor, 1995) and a maximum under-stress occurs at the location of the effective radius, with a maximum over-stress occuring at the base (Fig. 5.3). Scaling factor *n* for all centrifuge tests in this thesis was

calculated at the effective radius position at the end of the test (this was necessary due to the large settlement of double porosity model during the test). Errors caused by the maximum under-stress and over-stress will be discussed separately for each centrifuge used.

Similar scaling laws as discussed above for scaling of linear dimensions can be derived also for other quantities. A physical derivation and discussion of these scaling laws is beyond the scope of this thesis and can be found for example in Taylor (1995). Table 5.1 shows the list of most frequently used scaling laws. One of the most important scaling laws is that for diffusion processes governing consolidation. In the centrifuge, consolidation can be simulated n^2 faster than in the field due to the reduction of linear dimensions (drainage path) by factor n. This allows long-term diffusion processes to be simulated in a relatively short time. A different time scaling law (1:1) is valid for creep (Tab. 5.1). Therefore the centrifuge environment is not useful in representing creep.

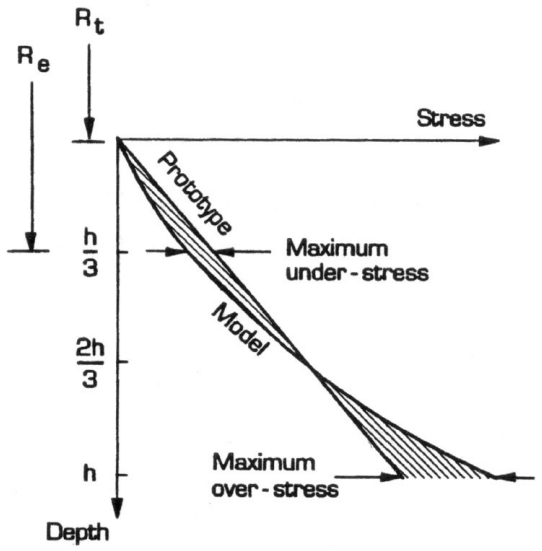

Fig. 5.3: Comparison of stress variation with depth in centrifuge model and its corresponding prototype (Taylor, 1995).

The prototype properties referred to in this thesis were calculated from the model parameters using the appropriate scaling law and they can sometimes differ slightly from the field parameters of the simulated problem.

quantity	scale factors: general	1g (laboratory)	ng (centrifuge)
length	n_ℓ	$1/n$	$1/n$
mass density	n_ρ	1	1
acceleration	n_g	1	n
stiffness	n_G	$1/n^\alpha$	1
stress	$n_\rho n_g n_\ell$	$1/n$	1
force	$n_\rho n_g n_\ell^3$	$1/n^3$	$1/n^2$
force/unit length	$n_\rho n_g n_\ell^2$	$1/n^2$	$1/n$
strain	$n_\rho n_g n_\ell / n_G$	$1/n^{1-\alpha}$	1
displacement	$n_\rho n_g {n_\ell}^2 / n_G$	$1/n^{2-\alpha}$	$1/n$
pore fluid viscosity	n_μ	1 or* $n^{1-\alpha/2}$	1 or* n
pore fluid density	$n_{\rho f}$	1	1
permeability (Darcy's Law)	$n_{\rho f} n_g / n_\mu$	1 or* $1/n^{1-\alpha/2}$	n or* 1
hydraulic gradient	$n_\rho / n_{\rho f}$	1	1
time (diffusion)	$n_\mu n_\ell^2 / n_G$	$1/n^{2-\alpha}$ or* $1/n^{1-\alpha/2}$	$1/n^2$ or* $1/n$
time (creep)	1	1	1
time (dynamic)	$n_\ell \left(n_\rho / n_G\right)^{1/2}$	$1/n^{1-\alpha/2}$	$1/n$
velocity	$n_g n_\ell \left(n_\rho / n_G\right)^{1/2}$	$1/n^{1-\alpha/2}$	1
frequency	$\left(n_G / n_\rho\right)^{1/2} / n_\ell$	$n^{1-\alpha/2}$	n
shear wave velocity	$\left(n_G / n_\rho\right)^{1/2}$	$1/n^{\alpha/2}$	1

*scaling of pore fluid viscosity introduced in order to force identity of scale factors for diffusion time and dynamic time

Tab. 5.1: Centrifuge scaling laws (Muir Wood, 2004).

5.2 Description of centrifuge MSE – GF 8

The tests were carried out in the mini-centrifuge MSE GF-8 at ETH Zürich in Switzerland (Fig. 5.4). The models were constructed in cylindrical containers with diameter of 80 mm and depth of 140 mm. The effective radius from the axis of rotation was 150 mm and 4 models could be spun at the same time. Before the construction of the models, a porous stone was placed at the bottom of the containers, so the models were drained both at the top and the bottom. A perspex tube was installed in each container before the model preparation. Its aim was to prevent difficulties with the removal of the model from the container after the test due to suction.

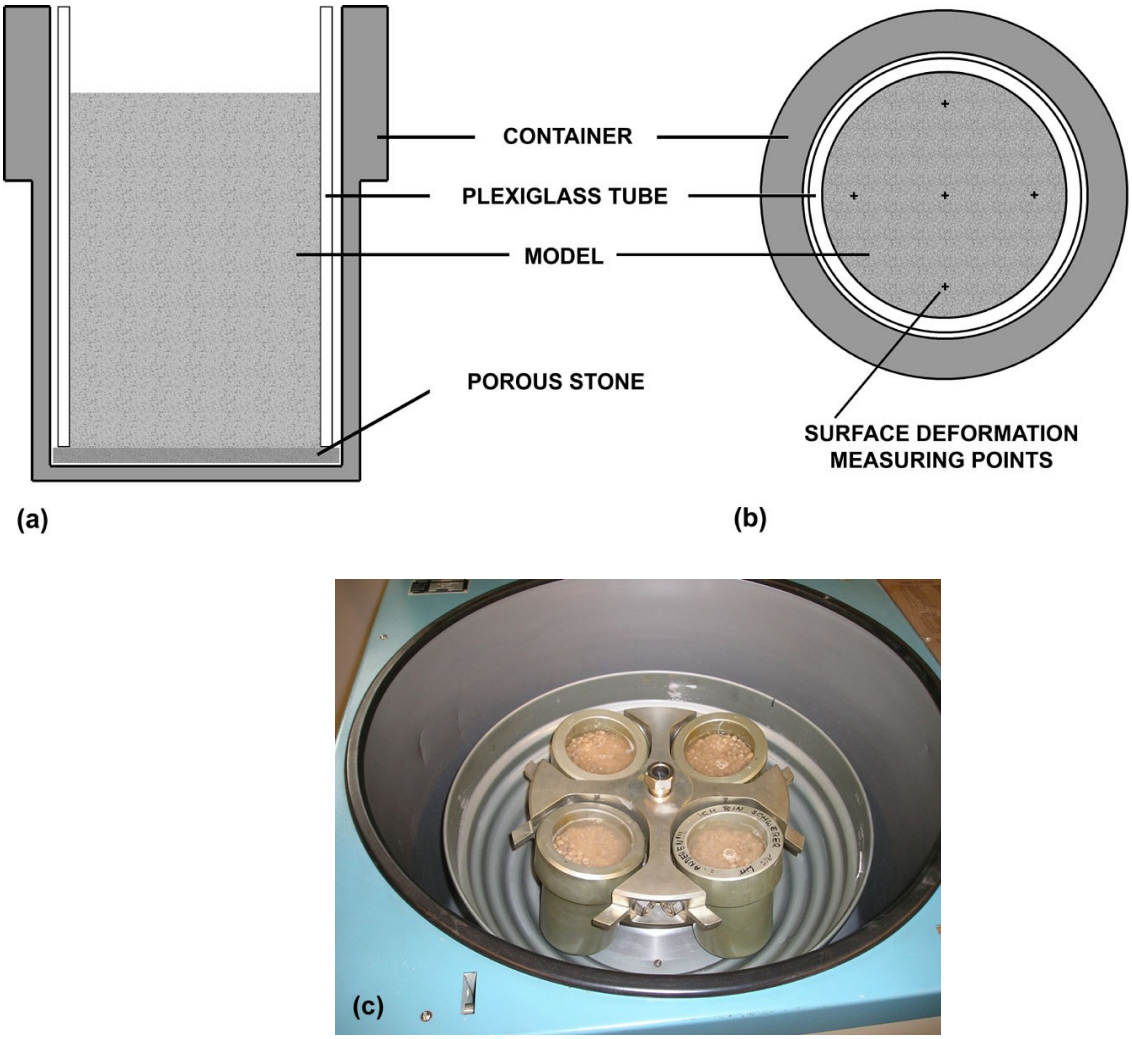

Fig. 5.4: Mini-centrifuge MSE GF-8: (a) - section of the model; (b) - plan view; (c) - containers inside the centrifuge.

Some difficulty arises in assuring a uniform gravity field inside the test container, due to the high ratio of soil depth to effective radius in the mini-centrifuge. If angular velocity, ω = 1000 r.p.m. and Earth's gravity is g = 9.81 m/s^2, n = 177, the maximum under-stress and over-stress for a typical height of the model (85 mm measured at the end of the test) at 1/3 of depth and the base are -9% and +9% respectively (after Taylor, 1995). Consequently, the value of n will differ with radius, increasing from 145 at the soil surface to 240 at the base, and in the elements at constant depth in the container at the centre and the side, by 1.7% at the base increasing to 4.7% at the soil surface. In clarifying the extent of possible errors, it is submitted that these were scoping tests and therefore absolute 'quality' of the numerical data was not important in relation to any specific field problem, as long as comparability between similar tests was assured. Fig. 5.5 compares the vertical stress profile *in situ* and in the mini-centrifuge for the maximum model height at the end of the test (96 mm). Here the maximum under-stress and over-stress

reached ±10%.

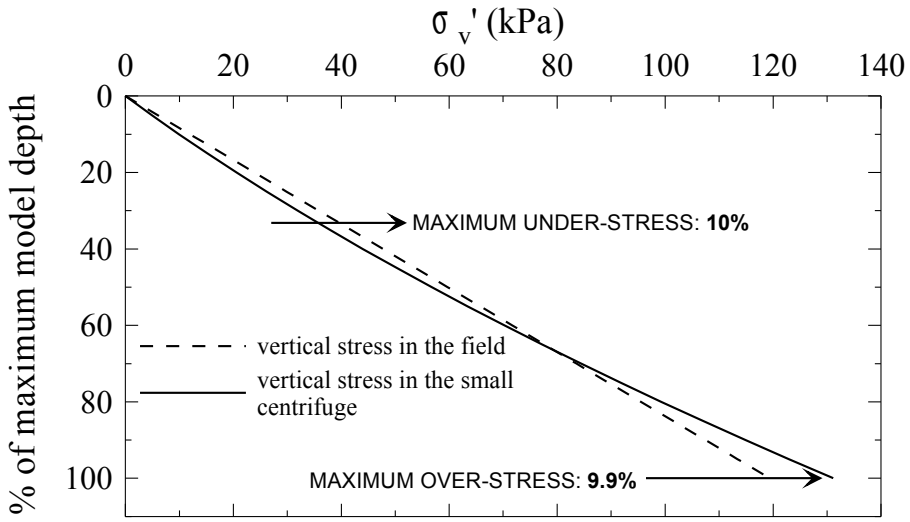

Fig. 5.5: Vertical stress variation with depth in the mini-centrifuge.

5.3 Classification of landfill clay

Classification tests on the clay from “5. květen” landfill were carried out at ETH Zürich. The sampling site was located approximately 5 km from the place of the trial embankments (relative position of the trial embankments and “5. květen“ landfill can be seen in Fig. 4.2. The clay from the same sampling site was used in all centrifuge tests described in Chapters 5 and 6.

The grading curve presented in Fig. 5.6 shows that the clay contains 33% of clay particles, 56% of silt and 11% of sand sized particles. The limits of consistency were determined to be w_L = 72% and w_P = 27% giving plasticity index of I_P = 45. The plasticity chart is presented in Fig. 5.7. Specific gravity of G_s = 2.71 was measured.

The mineralogical composition of the clay, determined by X-Ray diffraction is 36% kaolinite, 25% smectite, 11% illite and 25% quartz. Less than 3% of siderite, plagioklas feldspar and anatase were detected.

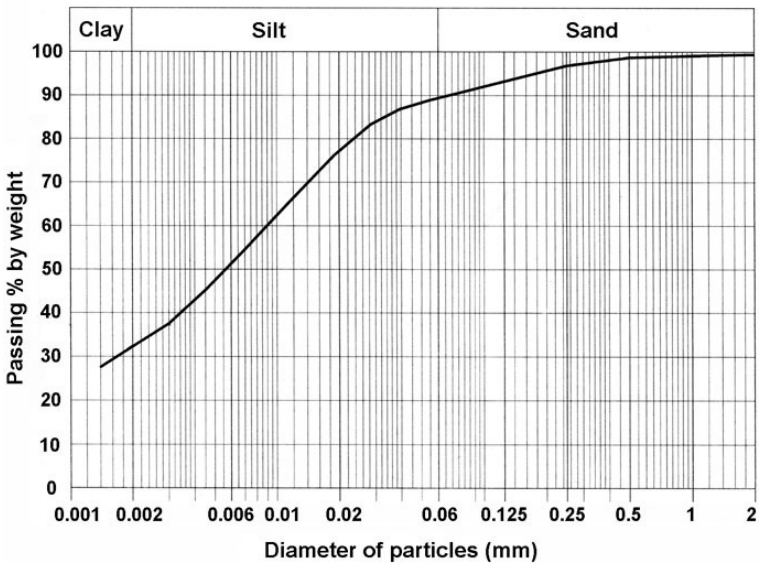

Fig. 5.6: Particle size distribution curve of landfill clay.

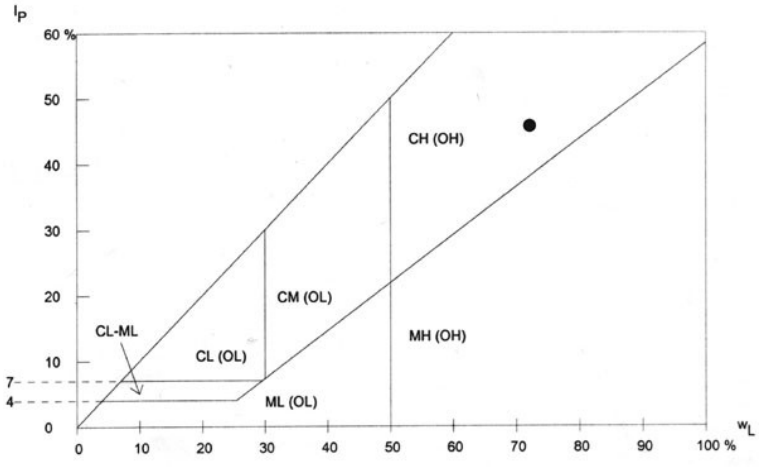

Fig. 5.7: Plasticity chart with position of tested material.

5.4 Soil preparation

The soil from “5. květen” landfill was air-dried at 50°C and crushed between two metal platens. The size distribution of the lumps required for the tests was obtained by sieving. No information on lump size distribution of the landfill at the site of the trial embankments was available. Therefore data from

neighbouring landfills (presented by Dykast, 1993) were considered for the centrifuge model. Lines marked as LSD (lump size distribution) curve 1 and LSD curve 2 in Fig. 5.8 show prototype lump size distributions used for the mini-centrifuge tests. Dashed lines represent the field data.

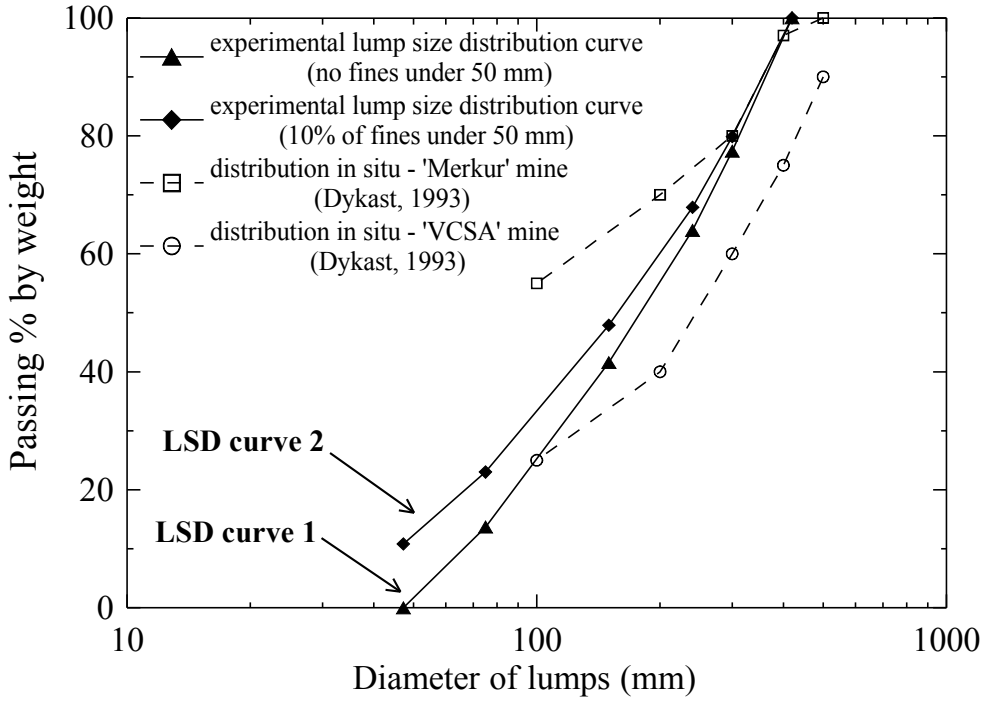

Fig. 5.8: Comparison of centrifuge lump size distribution curves in prototype scale with field data.

An alternative technique of the preparation of clay lumps for laboratory and centrifuge testing of double porosity clay is presented by Leung et al. (2001). The remoulded soil is recompressed one-dimensionally to its *in situ* strength. By using a cylindrical scoop, clay balls are taken from the recompressed soil and placed by hand in the container for further testing. This technique of *wet lump preparation* was found to be inappropriate from the following reasons resulting from different properties of clay lumps dredged from the seabed (Leung et al., 2001) and lumps from the landfills:

- All lumps prepared in wet state have similar and regular shape. The shape of the lumps in the Czech landfills is random and irregular. The shape of lumps is a crucial parameter as it influences intergranular porosity and consequently also compressibility of the soil.
- Remoulded soil looses its original structure. The clay lumps prepared from the remoulded soil looses its original fabric. The strength and hydraulic conductivity of the lumps (influencing the rate of the structure degradation of the soil), would be therefore different from the field.

- From practical and time reasons, it would not be possible to prepare small lumps to simulate the field lump size distribution (Fig. 5.8).

Dry lump preparation eliminates all these problems and it allows to keep the properties of the lumps as close as possible to the real landfill. However, a model prepared from dry lumps needs to be flooded before the test and there is no evidence that the full saturation was reached. During the saturation, both swelling and self-weight consolidation of the model starts, which complicates the determination of the initial model height. This problem will be discussed in the following section.

5.5 Test procedure

Before flooding, clay lumps were poured to the containers fitted with porous stones and perspex tubes and the height of the model was measured. This *initial height* was used for the calculation of the deformation during the tests. After flooding, the models were left for 24 hour to allow their full saturation. In this period, swelling took place and the height of the models increased. The effect of swelling was partly reduced due to the start of the self-weight consolidation in the bottom part, which occured as a result of reduced shear strength on the contacts of the clay lumps after the flooding of the model. The height of the model after its flooding could not be used in deformation calculations as the 'initial height', because the height changes due to the swelling and consolidation varied with the total height of the model. A different approach was used in the tests in the geotechnical centrifuge where the model heights were identical and *initial height* was measured after the swelling (it also corresponds to the initial state for numerical modelling discussed in Chapter 7). When the results of mini-centrifuge and geotechnical centrifuge tests are compared in this section, the same method of deformation calculation (with *initial height* measured before swelling) was used.

As shown in Fig. 5.4, the models were drained both from top and bottom. The mini-centrifuge does not allow any in-flight measurements during the test. The centrifuge was stopped on each occasion to measure the distance between the container top and the model surface at five points, and then the averaged value was taken to be representative. The rate of centrifuge acceleration and deceleration was measured and equivalent time at maximum g-level was calculated as indicated in Fig. 5.9. This equivalent time was included in calculation of prototype time of the test. However, the different stress history, especially in the initial stage of the mini-centrifuge tests with the high frequency of surface settlement measurements, influenced the rate of consolidation of the mini-centrifuge models. The first measurements of the

surface settlement therefore exhibit slower consolidation due to the relatively long time spent in unloading and reloading stages compared to time under maximum g-level (Fig. 5.10; the effect of this phenomenon will be seen in Section 5.6.2). In the later part of the test, when the frequency of measurements decreased, the settlement should not be significantly influenced.

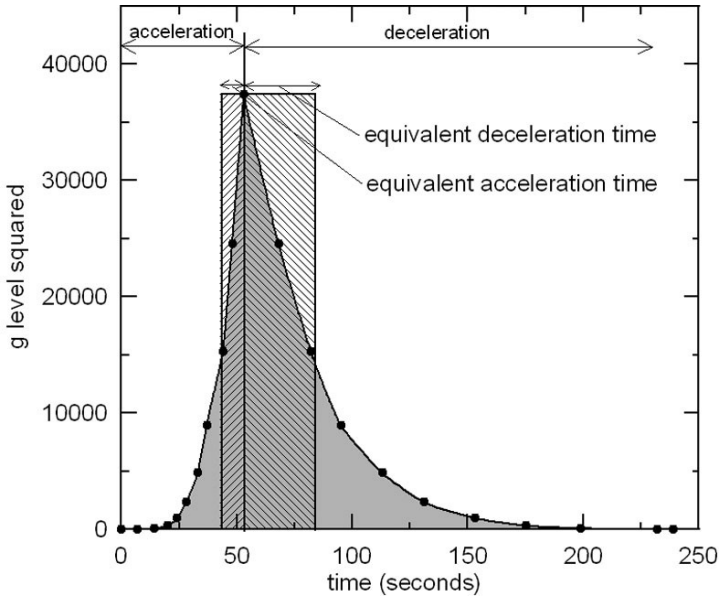

Fig. 5.9: Calculation of equivalent acceleration and deceleration time.

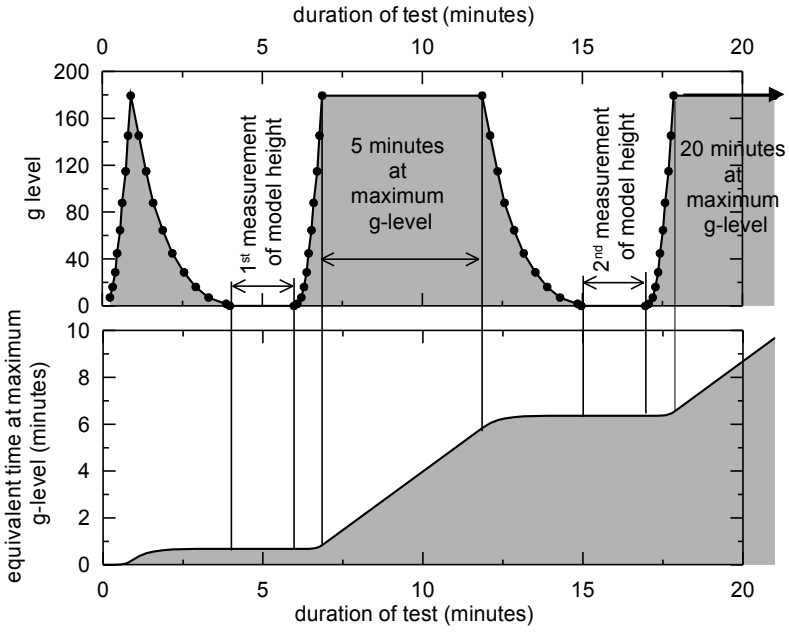

Fig. 5.10: Unloading and reloading stages during initial phase of mini-centrifuge test.

The effect of the measurement of the model height at 1 g is demonstrated at *e-log* σ'_v space in Fig. 5.11. Line 1 represents real normal compression line and line 2 the compression line obtained from the unloaded model on the assumption that all pore pressures equalized after unloading. For all the mini-centrifuge tests the swelling during unloading is included in the measurements of the settlement, but this inaccuracy should be of small importance from following reasons:

- The effect of swelling is relatively small in proportion to the large vertical deformation typical for the double porosity soil. The deformation associated with the degradation of the double porosity structure is mostly irrecoverable, with a very small elastic component (the slope of the swelling line BC is small in comparison with the slope of the compression line AB in Fig. 5.11). The small elastic deformation at the vertical stresses up to 100 kPa is confirmed in the following sections (e.g. Fig. 5.24).
- Due to the short time of unloading and low hydraulic conductivity of the clay, the pore pressures could not fully equalize (effective stress state during the height measurement lies somewhere on the swelling line BC in Fig. 5.11). The compression lines corresponding to the partially equalized pore pressures are represented by full lines between lines 1 and 2 in Fig. 5.11.

Therefore the results presented in the further text correspond to the NCL positioned between points D and B in Fig. 5.11.

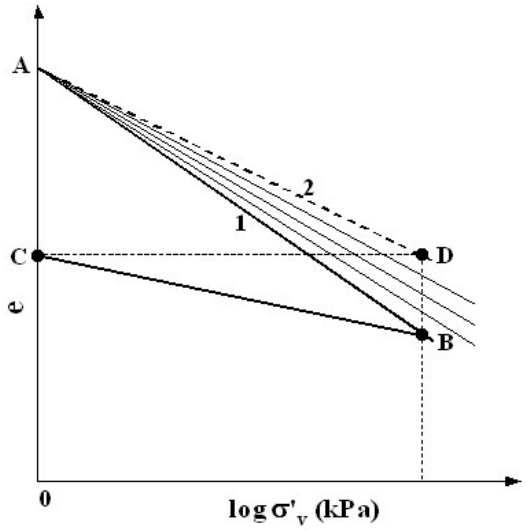

Fig. 5.11: Difference between the actual compression line (1) and the compression line measured on the unloaded model (2). Measurements of the surface settlement in the mini-centrifuge correspond to partially unloaded model (indicated by full lines between lines 1 and 2).

It was experimentally confirmed, that friction between the model and the perspex tube did not affect the results. The same settlement was reached, when the walls of the container were lubricated with silicon grease.

5.6 Test results

5.6.1 Parametric studies

The influence of lump size on vertical deformation was studied through the self-weight consolidation of four models at 180 g. Different ranges of the lump diameter (<45 mm, 45-450 mm, 450-720 mm and 720-1440 mm in the prototype scale) were tested, giving the ratios of the diameter of the container to the lump diameter decreasing from 360 (no particle size effect expected, after Ovesen, 1979) to 10 (with particle size effect anticipated). The initial soil depth in the containers was 103-105 mm. The equivalent prototype heights are presented in Tab. 5.2 (tests 1-4). Figure 5.12 shows similar vertical deformation curves for the larger lump size ranges 450-720 mm and 720-1440 mm, with a final vertical strain of 19% compared to only 15% for the smaller lump size range. This was due to different grading curves: a steeper grading curve (tests 3 and 4) causes higher intergranular porosity and higher settlement. This was also observed by Leung et al. (2001). The rate in the first 2 years of the consolidation curves indicates that the hydraulic conductivity of the two models with smaller lump size was reduced more than in the models with larger lump sizes, due to smaller intergranular voids and more fines in the voids. Figure 5.13 shows the change of vertical effective stress and the scaling factor *n* with the model depth at the end of the mini-centrifuge test 2.

Test No.	1	2	3	4	5-8*	9-11*	12	13
Nominal g-level	180	180	180	180	180	330	330	150
Initial prototype depth of clay° (m)	19.0	18.8	18.8	18.5	17.9	35.6	24.2	24.9
Prototype size distribution (mm)	<45	45-450^{+}	450-720	720-1440	45-450^{+}	45-450^{+} 10%<45$^{!}$	45-450^{+} 10%<45$^{!}$	45-450^{+} 10%<45$^{!}$
e_0°	2.19	1.84	1.93	1.88	1.88	1.48	1.45	1.43
e_{fin}	1.71	1.43	1.37	1.34	1.46	1.21	1.19	1.12
$\Delta e = e_{fin} - e_0$	0.48	0.41	0.56	0.54	0.42	0.27	0.26	0.31

*Tab. 5.2: Properties of mini-centrifuge tests (1-12) and geotechnical centrifuge test (13). Legend: *average values from identical models - the same mass of the soil was used, °measured before flooding of the models, $^{+}$LSD curve 1 in Fig. 5.8, $^{!}$LSD curve 2 in Fig. 5.8.*

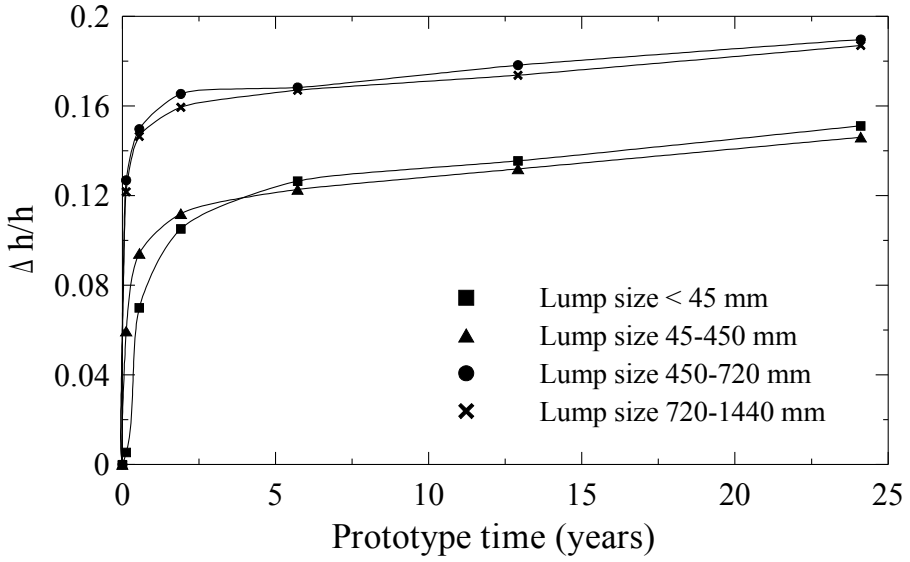

Fig. 5.12: Influence of size of clay lumps on magnitude of normalised settlement due to self-weight consolidation.

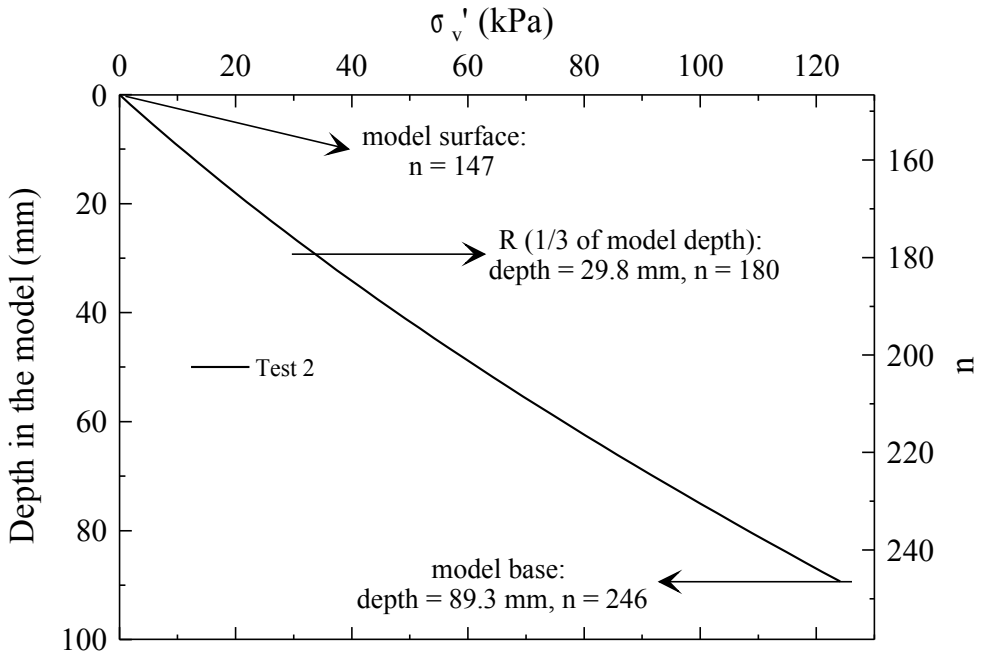

Fig. 5.13: Vertical profile of σ_v' in mini-centrifuge test 2.

After each test, the models were dissected and water content was measured at different depths to calculate the void ratios assuming full saturation. These values were plotted against the maximum vertical effective stress imposed during the centrifuge test (Fig. 5.14). The scatter of the data points for the models with larger lumps was caused by relatively small samples for the determination of water content compared to the size of the lumps.

Water content sampling was not possible for the model with the largest lumps. The data in Fig. 5.14 do not correspond to normal compression curves, because the void ratios were determined after unloading (Fig. 5.11). Since all of the plots are relatively straight, closing of intergranular voids through destruction of the double porosity structure takes place throughout the depth of the model rather than at any single stress point.

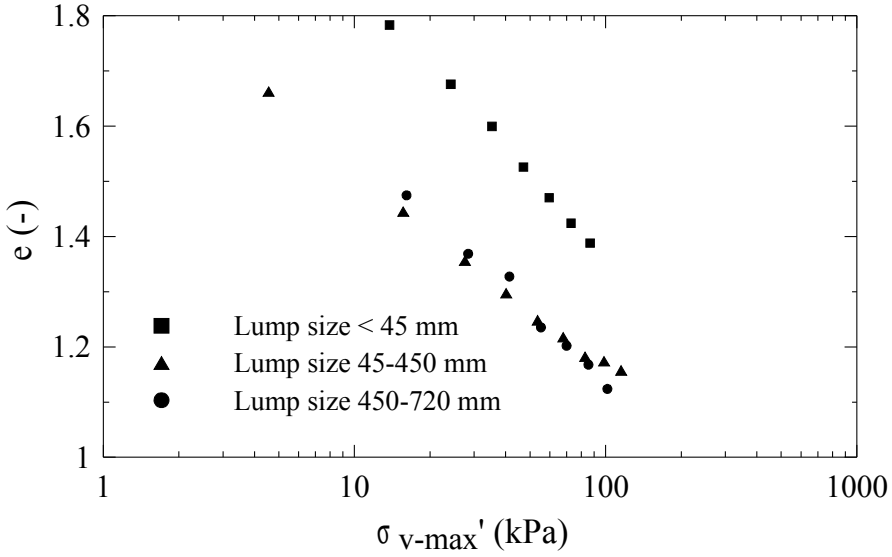

Fig. 5.14: Void ratio after unloading from previous maximum stress (calculated from water content).

Further tests were carried out to examine the influence of filling partly the intergranular voids on the magnitude of vertical strain. A set of 4 tests (tests 5-8 in Tab. 5.2) was performed at 180 g with the lump size corresponding to prototype dimensions of 45-450 mm and the landfill height of 17.9 m. The line "without fines" in Fig. 5.15 (LSD curve 1 in Fig. 5.8) shows the average vertical strains calculated from these tests. The averaging minimized the effect of some small and unavoidable variation in the initial intergranular porosity of models, due to the random arrangement of lumps. The line "with fines" in Fig. 5.15 (LSD curve 2 in Fig. 5.8) represents 3 tests that were carried out with a mixture including 10% of particles finer than 45 mm (scaled to prototype dimensions) on the landfills 35.6 m high (tests 9-11 in Tab. 5.2). Both sets of tests started with different initial void ratios (Tab. 5.2), which indicates that fine lumps partially filled intergranular voids in the case of LSD 2. Despite the higher vertical effective stresses by a factor of almost 2 in tests 9-11, after 23 years the average vertical strain is over 3% less than without fines. The comparison shows that different initial void ratios (caused by different intergranular porosities) have a major influence on the compressibility of the models. Similar results were obtained by Leung et al. (2001). The initial rate of

settlement “with fines” is lower than that “without fines”. This reduced consolidation rate in the “with fines” case indicates a lower total hydraulic conductivity when the intergranular voids are partially filled.

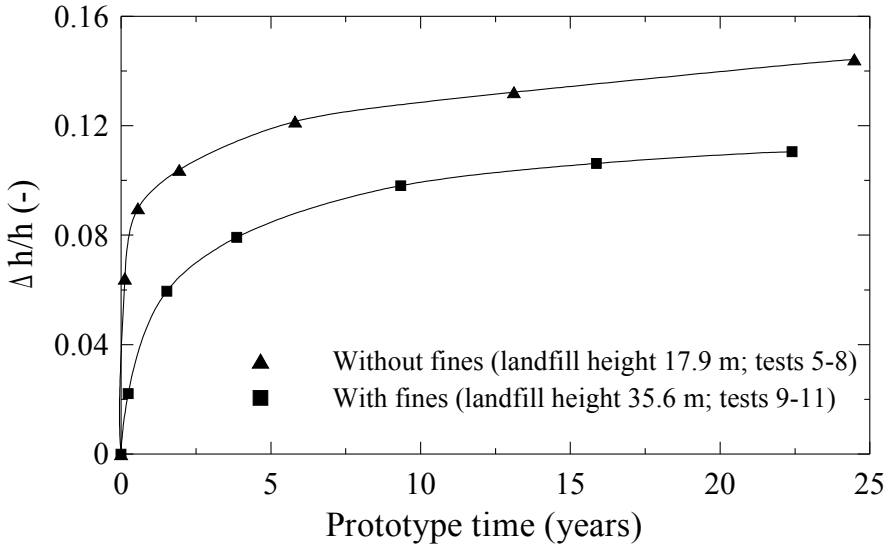

Fig. 5.15: Influence of fine particles on vertical strain of the landfill.

The consolidation curves of all data from both test series (with lump size distribution curves 1 and 2) are plotted in Fig. 5.16. The difference in the strain in both sets of tests is rather high, although the shape of all curves is similar. The maximum difference Δ_{max} between the data points was calculated for each measuring step and the dispersion is more or less constant from the first measurement (40 to 80 prototype days from the beginning of the consolidation) until the end of the test. This indicates that the difference is probably caused by different initial intergranular porosities, as the interlump voids reduce immediately after the centrifuge acceleration. The difference can influence the results of centrifuge modelling significantly. Therefore, it is necessary to achieve comparable initial densities when preparing the centrifuge model (pouring the lumps into the container). Furthermore, the results confirmed the hypothesis that the procedure of filling used *in situ* influences the compressibility of the fresh landfill.

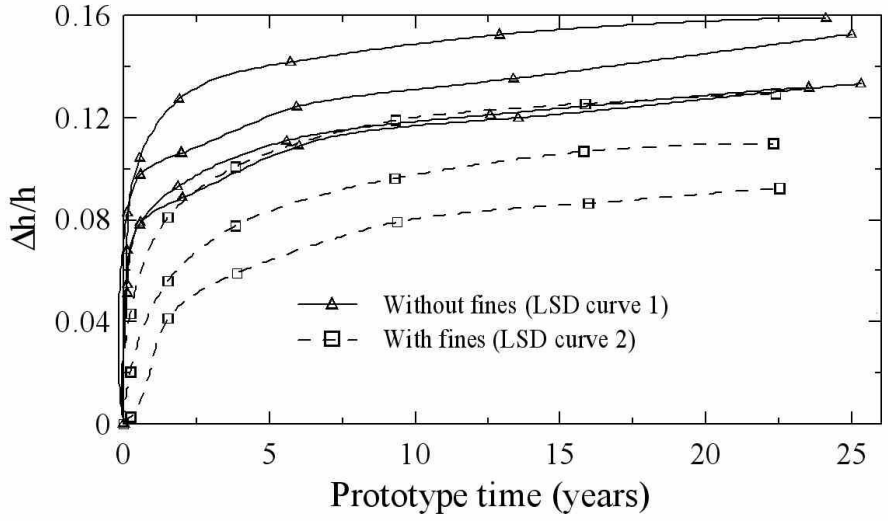

Measurement No.		1	2	3	4	5	6
LSD curve 1:	time (years)	0.12	0.56	1.94	5.81	13.11	24.48
	Δ_{max}	**0.0312**	**0.0261**	**0.0387**	**0.0328**	**0.0327**	**0.0273**
LSD curve 2:	time (years)	0.24	1.52	3.86	9.34	15.87	22.40
	Δ_{max}	**0.0405**	**0.0415**	**0.0419**	**0.0398**	**0.0391**	**0.0371**

Fig. 5.16: Comparison of four equivalent tests with lump size distribution curve 1 and three equivalent tests with lump size distribution curve 2.

5.6.2 Prediction of the self-weight consolidation behaviour

To choose the correct dimensions for the model in the geotechnical centrifuge, it is necessary to predict the vertical strain in advance. There are two technical reasons why a good estimation is necessary:

- The water table should be level with the surface of the consolidated landfill, to mimic the test embankment situation (the variations of water level due to pumping during embankment monitoring were neglected in the centrifuge test). In the geotechnical centrifuge standpipes controlling the position of the water table can not be altered without stopping the centrifuge, so the eventual consolidated soil height must be known before the test, to within ±2 mm.
- The height of the consolidated landfill was pre-determined by the test case conditions, so the dry model height required to achieve this had to be known in advance.

Fig. 5.17 shows the results of the mini-centrifuge test (test 12 in Tab. 5.2) that were used in estimating the vertical deformation for the geotechnical

centrifuge tests. The data from the mini-centrifuge could not be used as an exact prediction for the geotechnical centrifuge tests, because heights were measured when the mini-centrifuge was stationary and thus the soil had been unloaded, and swelling had occurred. Therefore the predicted strains of 10.5% after 15 years of the self-weight consolidation in the mini-centrifuge were smaller than the values in the geotechnical centrifuge (test 13 in Tab. 5.2) of 11.1% (Fig 5.17), but these were still very close to the predicted value.

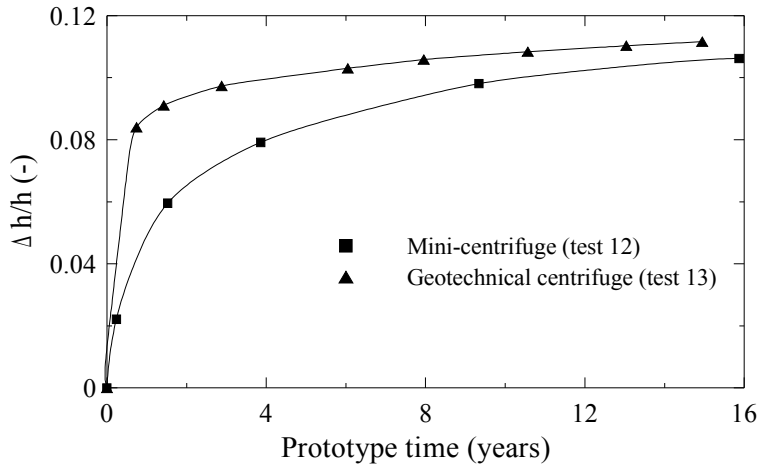

Fig. 5.17: Comparison of vertical strain in the landfill model in mini-centrifuge and geotechnical centrifuge.

The initial sections of the deformation curves can not be compared directly because both the length of the drainage paths and the stress histories are different, the latter due to the relatively long acceleration and deceleration time of the mini-centrifuge compared to the time at a maximum of *n*g*. The measurement of the surface settlement took approximately 2 minutes and each unloading/reloading cycle took approximately 200 seconds, while time at maximum *g* before the first three measurements was 0, 5, and 20 minutes respectively as shown in Fig. 5.10.

5.6.3 Study of different filling techniques

The preferred landfilling method adopted in the Czech mines to date is to prevent groundwater from rising in the fill and to protect the landfill from infiltration of the free water at any stage (Vaníček and Vaníček, 2008). If the clay lumps remain unsaturated with suction in their core, the strength and stiffness of the landfill is higher than when the lumps are saturated. However, an unsaturated clayfill might collapse on wetting (Feda, 1998; Charles, 2008), which could cause problems in the case of developed landfills. For civil

engineering practice, fully saturated material is more predictable and easier to deal with.

A set of mini-centrifuge tests was carried out to investigate different techniques for placing the clay lumps in the container. Two models were prepared using lump size distribution curve 2, with a prototype landfill depth of 32 m, each with a slightly different preparation technique. In the first model, the lumps were poured into an empty container (dry pluviation) and saturated after first acceleration, while in the second case, the soil was pluviated through water.

The same mass of soil was used for both of these tests, with no mechanical compaction applied after pluviation. The height of both models was measured immediately after filling and void ratios were calculated (marked by “A” in Fig. 5.18). The initial volume of the model poured through water was about 40% greater than that of the dry model. This difference can be explained by the higher effective stresses in the dry model and the buoyancy of the lumps, which fell with lower velocity through the water and impacted the surface with less compactive energy than the dry lumps (Laue et al., 2005). This lead to increased initial intergranular porosity in comparison with the dry placement method. Furthermore, in water clay lumps fail to slide past each other to form a denser packing, because they do not overcome the mobilised contact strength. Finally, small air bubbles could have attached to the dry lumps during entry into the water, although this was not thought to have been a significant mechanism.

In the field, higher vertical stress result in reduction of porosity during landfilling. Both mini-centrifuge models were therefore accelerated for a prototype time increment of 1 year to replicate the *in situ* stresses and the surface deformation was measured again (“B” in Fig. 5.18). The height of the dry pluviated model (still dry) was reduced under the increased gravity as a result of rearrangement and crushing of some clay lumps. However, settlements in the model pluviated through water (flooded) were considerably greater due to plastic strains at the contacts of the lumps and consequent closing of the intergranular voids. Nevertheless, the total porosity of the flooded model was still higher than in the dry sample, probably due to lower vertical effective stresses, lower impact stresses during pluviation (Laue et al., 2005) and ongoing swelling of the clay lumps. After this stage, the dry pluviated model was also filled with water and both models were left for 24 hours at rest until no additional swelling was measured. It was assumed that full saturation was achieved and model height was measured to calculate the void ratio (“C” in Fig. 5.18). Swelling was higher in the model that was originally dry.

Both models were then accelerated for the prototype time of 23 years. The dry pluviated model exhibited larger and more rapid settlement (equivalent to delayed collapse on wetting), which resulted in a denser structure at the end of consolidation. Based on the results and direct observation of the models,

four typical states of the soil were identified (Fig. 5.19).

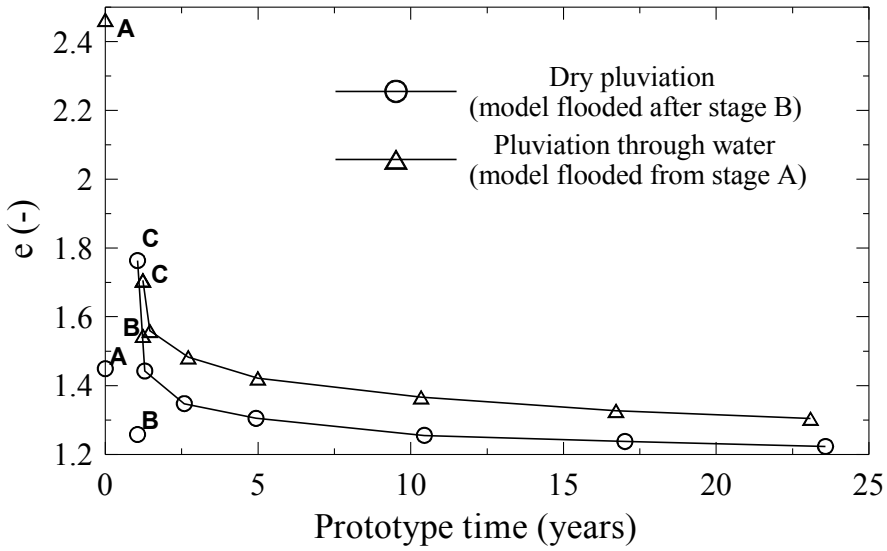

Fig. 5.18: Comparison of two methods of landfilling.

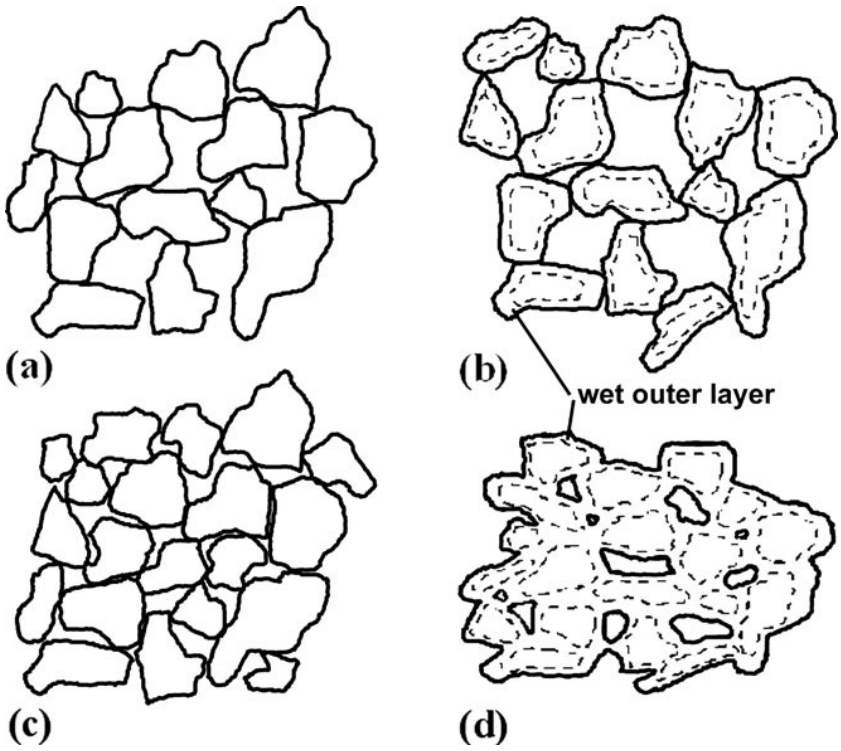

Fig. 5.19: Different states of double porosity structure: (a) initial stage - dry lumps with no compaction; (b) initial stage - lumps with wet outer layer with no compaction (intergranular porosity is even higher due to apparent contact bonding); (c) dry lumps after compaction - breaking and rearrangement of lumps leads to decrease in total porosity, interlump voids still linked; (d) wet lumps after compaction - plastic straining at contacts, densest state with occluded remaining interlump voids.

The major disparity between the two models is the difference in intergranular porosity at shallow depths. The loose structure in the model poured into water (Fig. 5.19b) still remained in the top part of the model, where low vertical stress could not change the original structure. The clay lumps in the dry pluviated model were packed more densely (similar to 5.19a). When subjected to additional surcharge, the soil with loose structure (poured into water) exhibited more settlement because of the higher original intergranular porosity. This confirms that the practice of filling into water is not advisable for landfill placement. Dry filling followed by fast natural saturation (transition from 5.19a to 5.19d) may be recommended to create more consistent ground conditions for further development (giving a more homogeneous and predictable landfill material).

5.6.4 Preliminary modelling of test embankment

The final stage of mini-centrifuge testing was a 1D simulation of the test embankment. After the self-weight consolidation of 3 models (tests 9-11 in Tab. 5.2) with lumpy clay fill to prototype depths of 31.7 m at 330 g, the final vertical settlement was measured and a surcharge corresponding to 100 kPa was applied to two models. The third pot was left as a reference without any surcharge, in order to separate the surface deformation induced by creep and unloading/reloading cycles from that caused by the surcharge.

Fig. 5.20 shows a comparison of surface settlement for all models for the duration of the test. It is plotted in absolute values and prototype scale (metres) because of small variations in model height. Zero deformation corresponds to the initial situation in the prototype test case, of a consolidated landfill (after 23 years of the self-weight consolidation) before surcharge application. The centrifuge was stopped for 30 minutes while the surcharge was applied, resulting in significant swelling, which influenced the next few measurements of settlement. This was observed in the model height measurements in the reference pot, where the first data point (A) after surcharge application indicated up to 0.5 m heave. However, the next height measurement (B) is consistent with data before the application of the surcharge, so it is assumed that the reference model had reconsolidated. Swelling probably also influenced the shape of the consolidation curves of the two models with applied surcharge, but the higher stress level under the surcharge probably reversed the swelling more rapidly than in the reference pot. The results of both models with applied surcharge are similar and indicate ongoing surface deformation, continuing even 15 years after embankment construction, as also observed in the reference model. This is significant for comparison with field measurements of the trial embankments, since hydrostatic levelling data under the field embankments were calculated as net settlements: a difference in height between the landfill surface under the centre

of the embankment (“C“ in Fig. 5.21) and a reference point on the landfill surface (“B“ in Fig. 5.21). Reasons for continuing deformation in the mini-centrifuge tests may be similar as *in situ* (creep) but they are probably also affected by unloading/reloading cycles. To eliminate all these factors, net settlements of the embankment should be compared. The mini-centrifuge tests therefore confirmed the need for a reference model without embankment surcharge, since the self-weight deformation continues to be significant even after 23 years of consolidation. Measurement of net settlement as a difference in deformation of free landfill surface and total deformation under the embankment (C and B in Fig. 5.21) was therefore used in further tests in the geotechnical centrifuge, where continuous surface settlement of the reference model after embankment construction was also observed.

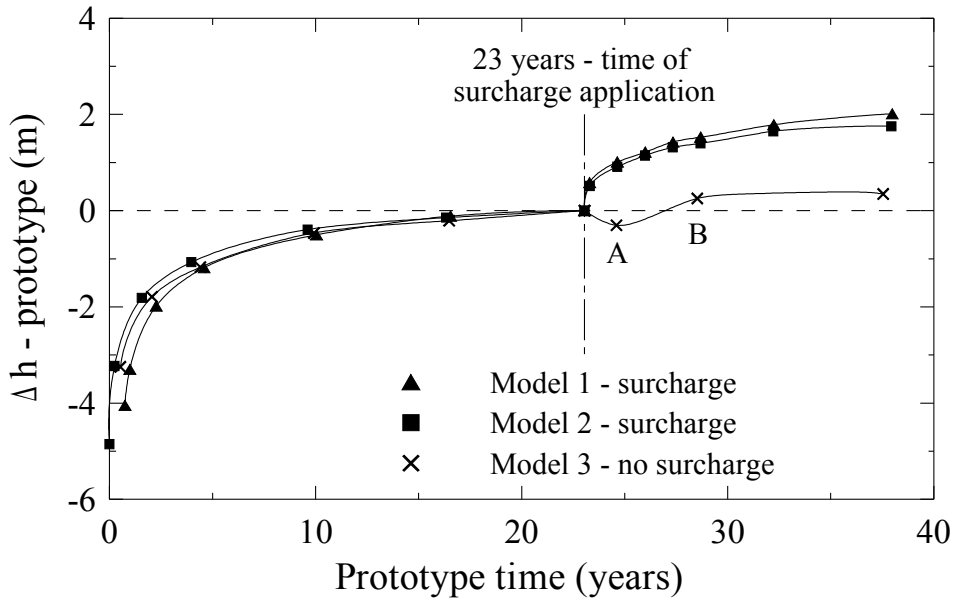

Fig. 5.20: Simple 1D simulation of test embankment.

Figure 5.22 shows a detailed plot of the settlement after surcharge application in both the 1D mini-centrifuge test (Test 12) and a 2D model (Test 13) in the geotechnical centrifuge (results from the geotechnical centrifuge will be described in detail in Chapter 6). The solid lines show the total settlements of the landfill, measured for both 1D and 2D models. Dashed lines show net settlements. The net settlement curves show a better correlation between the mini-centrifuge and geotechnical centrifuge models, especially after a few years of consolidation. A very similar shape of the settlement curves was measured also *in situ* (Figs. 4.8 and 4.10). The greater deformation in the mini-centrifuge could be due to the large number of unloading/reloading cycles.

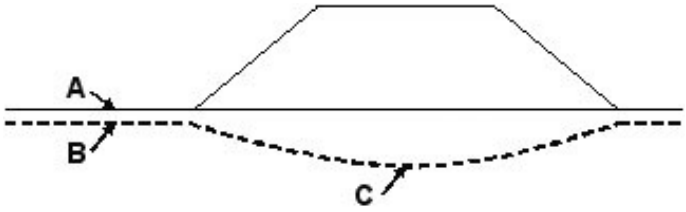

Fig. 5.21: Settlements associated with 2D embankment construction: A - landfill surface before embankment construction; B - surface of landfill caused by self-weight consolidation after construction of adjacent embankment; C - settlement profile under the centre of the embankment.

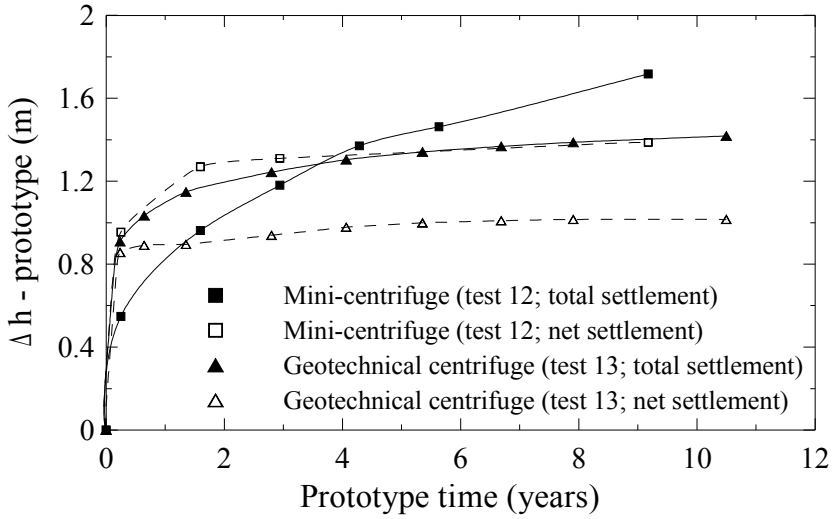

Fig. 5.22: Vertical settlement after embankment surcharge in both centrifuges.

5.6.5 Compressibility tests on mini-centrifuge models

The aim of the tests was to determine the compressibility of the lumpy clay landfill in a partially consolidated state, under self-weight loading. Four models with clay lumps, 45-450 mm in diameter in prototype scale (LSD curve 1), were consolidated at 180 g for 25 years (tests 5-8 in Tab. 5.2). After consolidation, the models were taken out of the centrifuge and removed from the model containers. Oedometer rings (d = 71.5 mm, h = 20 mm) were pressed into the samples from different heights and oedometer specimens were trimmed with extreme care to preserve the original structure of the landfill (Fig. 5.23). Table 5.3 shows the maximum vertical stress experienced by the specimens during consolidation in the mini-centrifuge at the corresponding prototype depth, calculated at the centre of each oedometer specimen.

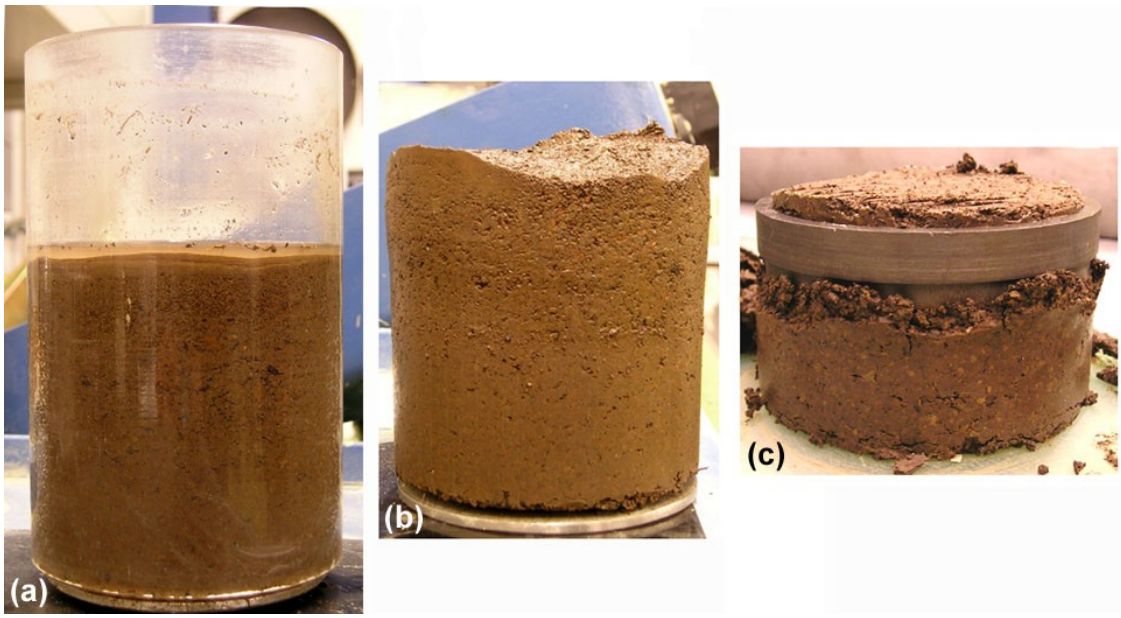

Fig. 5.23: Preparation of oedometer specimen from mini-centrifuge model: (a) - model after the centrifuge test; (b) - model removed from the plexiglass tube; (c) - cutting of oedometer sample.

The compression curves of all specimens are shown in Fig. 5.24. The initial total porosity corresponds to the maximum vertical stress reached during consolidation in the mini-centrifuge. After reloading (up to about 100 kPa), all reconsolidation lines had rejoined the normal compression line.

Oedometer test No.	*1*	*2*	*3*	*4*	*5*	*6*	*7*
Maximum σ_v' during consolidation in centrifuge (kPa)	20	55	94	18	33	69	80
Initial e_0 (measured at 0.5 kPa)	1.77	1.52	1.38	1.68	1.60	1.41	1.42
Average prototype depth (m)	3.5	8.3	12.9	3.2	5.4	10.1	11.3

Tab. 5.3: Data from oedometer specimens.

The normal compression lines were linear, with a similar gradient in the *e-log* σ_v' space (average C_c = 0.46). Figure 5.24 also shows the two unloading cycles followed on the centrifuge samples from 100 kPa to 12 kPa and from 1570 kPa to 4.5 kPa. A significant difference was observed: the average value of C_s for the first unloading cycle was 0.05 and 0.1 for the second stage. This difference is a distinctive characteristic of double porosity soil, with less elastic recovery from lower maximum vertical effective stress.

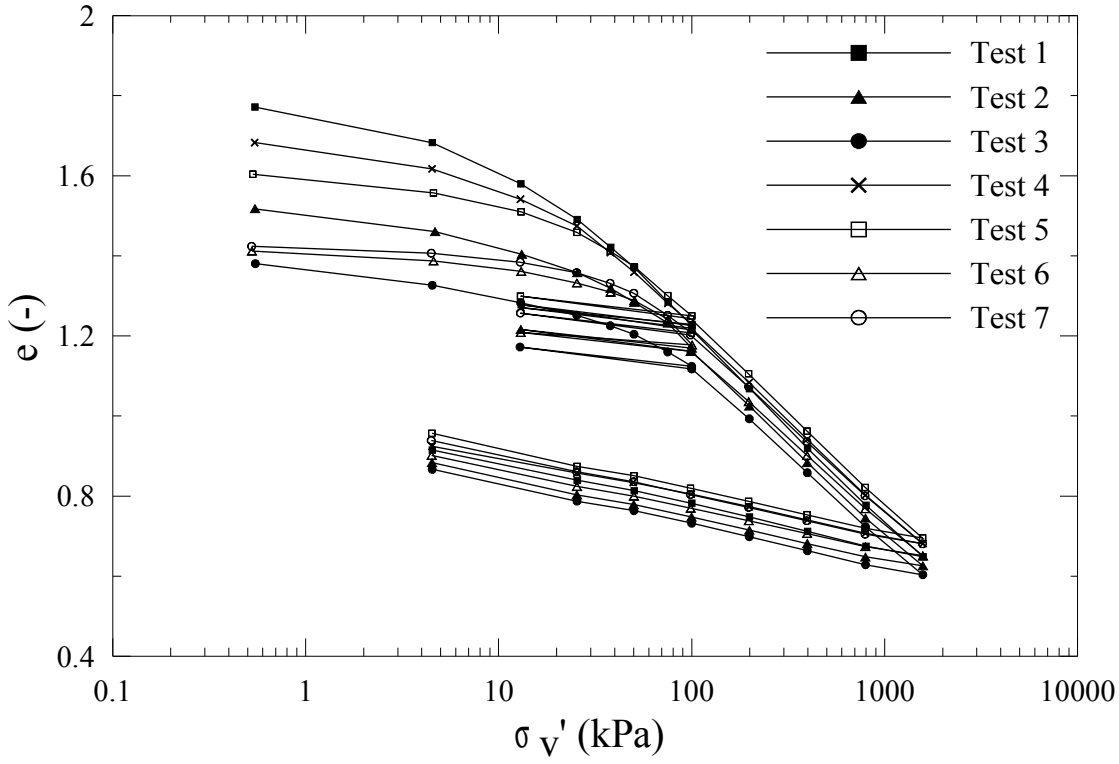

Fig. 5.24: One dimensional compressibility of models extracted from the mini-centrifuge and tested in an oedometer.

Clearly, the dominant mechanism on virgin loading is destruction of the double porosity structure through plastic deformation (or fractal crushing) of the clay lumps and closing the intergranular voids. This type of deformation is mostly irreversible, as suggested by the lower value of C_s, and leads to homogenisation of the soil as the double porosity structure is lost. As the intergranular porosity reduces, there is less scope for consolidation through this mechanism and subsequent deformation is achieved mainly through consolidation within the clay lumps, which will be stiff since they are still overconsolidated due to the depth of the original coal seam. However, the landfill behaves more like a composite normally consolidated soil and therefore the elastic component of compression becomes more significant, and C_s increases. This is supported by the similarity of the double porosity soil response under higher loading stages to that of reconstituted soil. Enriquez (2006) presented C_s = 0.12 on reconstituted oedometric specimen, which matches well with the normal consolidation line of the double porosity specimens under high load. Smooth oedometer curves (with no kinks) in the loading stage up to 100 kPa, and the linear shape of water content variation line in Fig. 5.14, indicate that degradation of the double porosity structure and consequent variation in C_s is gradual with no collapse on loading.

Figure 5.25 shows normalized settlement curves from oedometer test 1. A significant change in the rate of consolidation was observed in the range

of 4 to 50 kPa, while the settlement curves during loading to 50 and 100 kPa have a similar shape. It indicates closing of the preferential drainage paths through the open macro voids up to 50 kPa. At higher stresses, the rate of consolidation was influenced predominantly by the hydraulic conductivity of the clay. The macro voids could remain partially open even above 50 kPa, but they were occluded and did not allow fast drainage (see Fig. 5.19d). The vertical effective stress of 50 kPa corresponds to prototype depth of approximately 6.5 m.

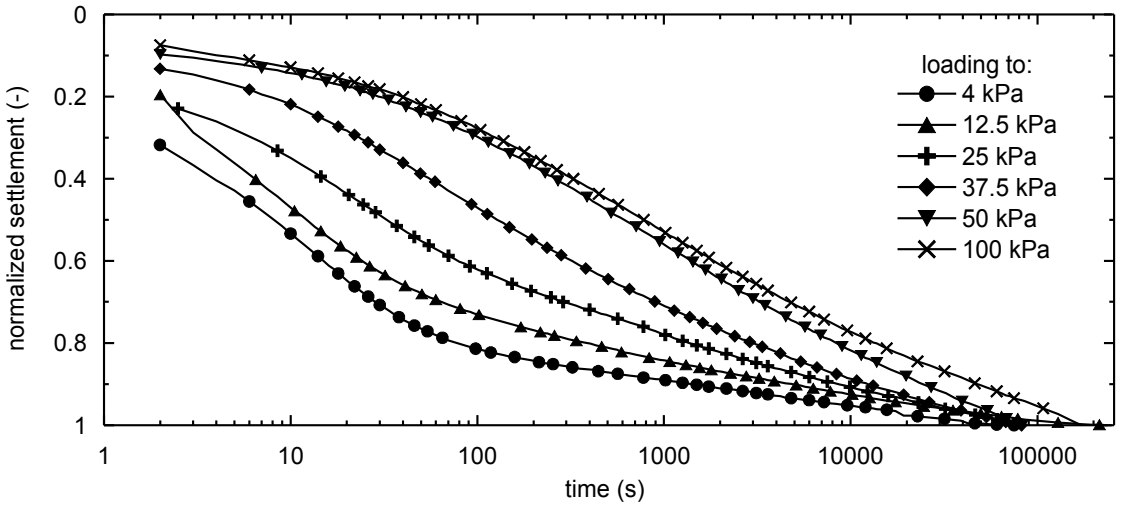

Fig. 5.25: Selected time-compression curves from oedometer test 1.

5.7 Summary

The mini-centrifuge was used to model double porosity clay landfills. The tests were aimed at determining soil parameters (lump size distribution and fines content) for subsequent tests in the geotechnical centrifuge, and estimating the magnitude of the settlement during consolidation of a scaled-down model after a prototype timespan of 23 years. The results of the mini-centrifuge tests were used successfully to plan the geotechnical centrifuge tests and to modify technical details, based on a reference model.

The parametric studies revealed important effect of intergranular porosity to the settlement of the landfill. Partial filling of interlump spaces with fine soil can significantly reduce the compressibility of the soil. The models for centrifuge tests should be prepared with extreme care to ensure a uniform grading of clay lumps within the model and to ensure comparability of the tests.

Further tests on mini-centrifuge models, including variation of water

content in the model and oedometer tests on specimens of centrifuged soil, were carried out to examine the degradation of double porosity structure in the vertical profile. These tests indicate a gradual reduction in the volume of intergranular voids up to stress levels of approximately 100 kPa, when most of these macro voids seem to have closed.

Oedometer tests on the model material tested in the centrifuge showed two different processes of deformation of the double porosity soil. When low vertical effective stress was applied, vertical deformations resulted from plastic straining at contacts between the clay lumps, their rearrangement and closing of interlump voids. The elastic component in this stress range is therefore very small. When subjected to larger vertical effective stress, interlump voids are mostly closed and the behaviour of the soil is similar to that of reconstituted clay.

The comparison of different filling methods indicates, that filling in water results in higher compressibility in the top part of the landfill due to the reduced shear resistance at the contacts between the wet lumps. Dry filling followed by fast natural saturation may be recommended for engineering practice as a best method.

The most serious drawback of the mini-centrifuge tests was swelling of the soil during stopping the centrifuge. However, the suction in the 100 mm high model could not dissipate fully during the short period of unloading, so the effect of swelling is believed small. Moreover, the error caused by swelling is assumed insignificant due to the small elastic component of total deformation, especially in proportion to the large vertical deformation typical in the double porosity soil. Finally, the mini-centrifuge tests were carried out only as a preliminary study before the geotechnical centrifuge tests and the conclusions are valid despite this problem.

6 MODELLING IN GEOTECHNICAL CENTRIFUGE

6.1 ETH geotechnical drum centrifuge

The ETH geotechnical centrifuge is the centrifuge of drum type with diameter of the drum of 2.2 m and maximum acceleration of 440 g (Springman et al., 2001). The models were prepared in square containers (400 x 400 mm in plan, 200 mm height), which were rotated through 90° and then mounted into the drum before the test. Figure 6.1 shows a sketch of the centrifuge with instrumentation for the test and two containers mounted on the opposite sides of the centrifuge drum. The second container was acting as a counterweight during the tests. In the central part of the centrifuge, a pair of multipurpose actuators is mounted on the tool platform, which can be clutched to rotate with the drum at the same speed. It can be also accelerated and decelerated independently of the drum. Additionally, radial and vertical motion of each actuator can be controlled in-flight. As shown in Fig. 6.2, a laser measuring device was mounted on the actuator to measure vertical settlement of the model surface during the tests. The laser could be moved vertically and tangentially, to allow the surface of the model to be scanned in several profiles. The change of the laser position in all directions is marked by arrows in Fig. 6.2.

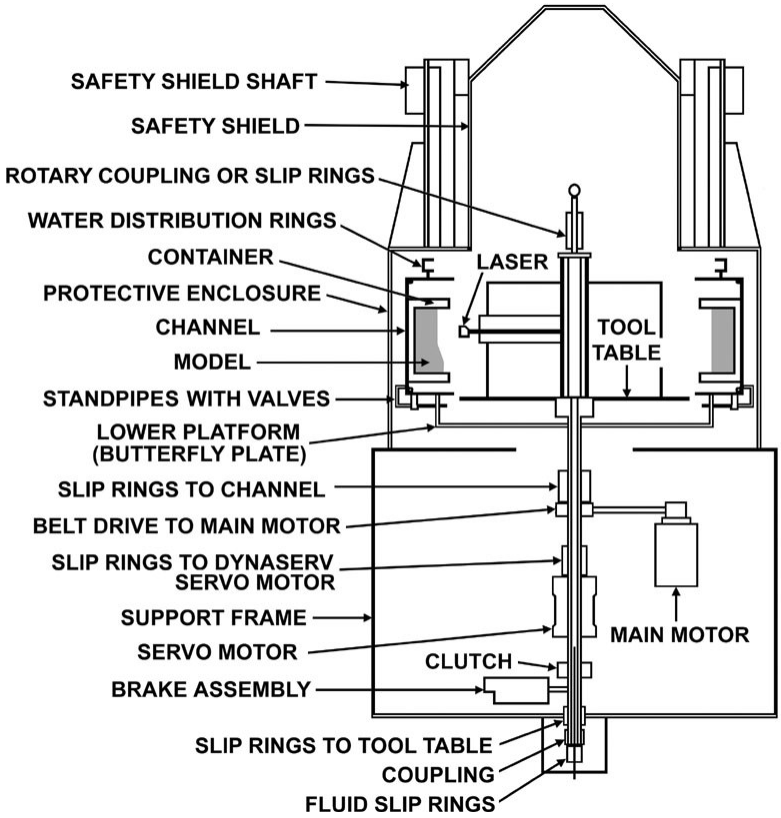

Fig. 6.1: Sketch of drum centrifuge at ETH Zürich (modified after Springman et al., 2001).

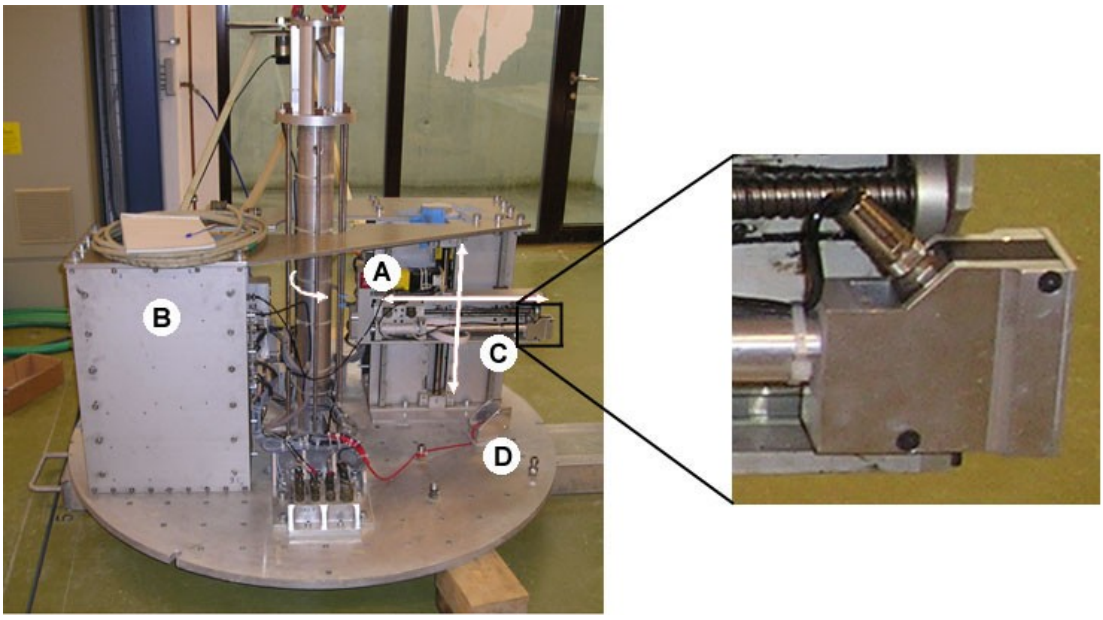

Fig. 6.2: Tool platform before mounting in the centrifuge: A - actuator A; B - actuator B, C - laser scanning device; D - camera mounted on the tool table.

Similarly to the mini-centrifuge, a variation of vertical stress with depth in the centrifuge model can be calculated. Due to the bigger centrifuge radius, the resulting error in vertical stress distribution is only ±2.7% (Fig. 6.3) compared to the error of ±10% calculated for the mini-centrifuge models (Fig. 5.5). This calculation assumes the final height of the model of 145 mm and g-level of 150, which corresponds to the centrifuge tests presented in this chapter.

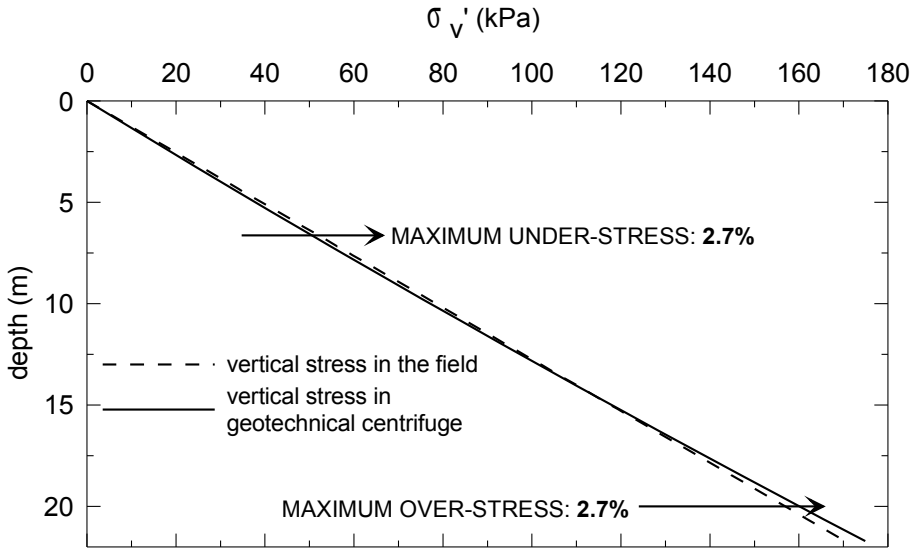

Fig. 6.3: Variation of vertical stress with depth in geotechnical centrifuge.

6.2 Preparation and intrumentation of the model

The soil preparation technique used for the geotechnical drum centrifuge models was the same as in the mini-centrifuge tests (Section 5.4). The alternative technique of preparing wet clay lumps from the slurry (details are presented in Section 5.4) described by Leung et al. (2001) was not suitable, due to the targeted lump size distribution and the requirement of irregularly shaped lumps. The grading corresponding to the prototype lump size distribution curve 2 (Fig. 5.8) was used for all tests. Before the test, a 2 mm thick sand layer was placed at the bottom of the container to allow a good connection to the bottom drainage channels. The sand layer was separated from the clay lumps by a filter paper. Dry lumps were poured into the container in four layers. Pore pressure transducers were installed between the layers at ¼, ½ and ¾ of the model depth (Fig. 6.4). A geotextile was placed at the

landfill surface in the area of embankment construction.

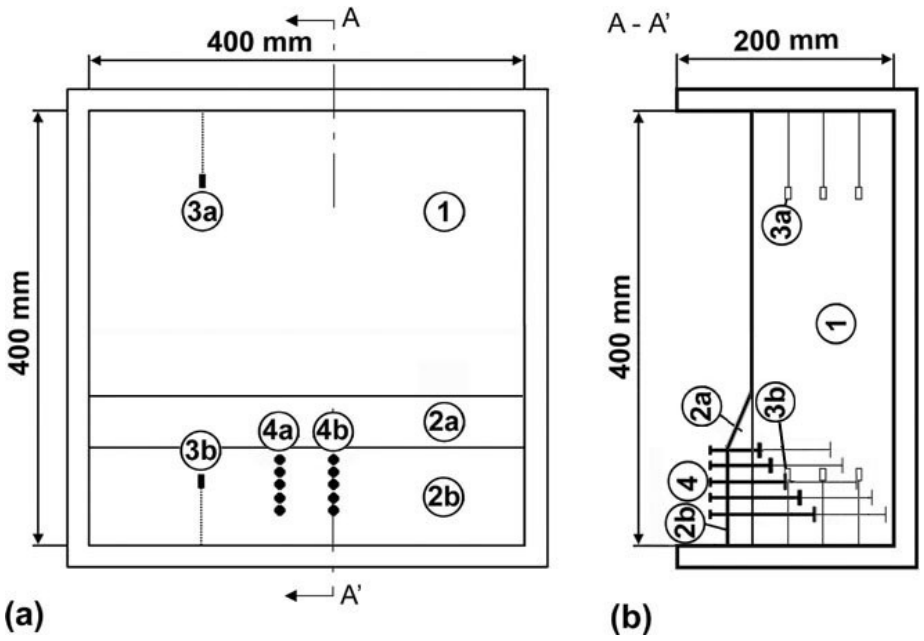

Fig. 6.4: Centrifuge model including instrumentation (Test 2Dc): (a) - plan view, (b) - cross section (1 – landfill, 2a – embankment slope, 2b – embankment crown, 3 – pore pressure profiles, 4a – straws with bottom discs in the top part of the landfill, 4b – straws in the bottom part of the model).

The main goal of the centrifuge modelling was to study the response of the double porosity material to loading under well defined laboratory conditions. To replicate the case history, the centrifuge model was instrumented similarly to the trial embankment subsoil. A laser mounted on the tool platform actuator measured the vertical settlement of the landfill. It scanned the model in three profiles in selected time intervals. After embankment construction, the surface settlement was measured in the same way. The pore pressure was measured with Druck PCDR81 pore pressure gauges (10 mm in length and 6 mm in diameter, Fig. 6.5) installed during the model construction. The gauges were not fixed and they could move with the soil. Equivalent to the field conditions, the pore pressure transducers measured the pore pressure between the lumps. Due to the similar dimensions of the lumps and transducers, no pore pressure gauges could be installed inside the lumps. In total, six transducers were placed at three horizontal levels and in two vertical profiles. The first profile was installed under the embankment (3b in Fig. 6.4) while the second one was under “far-field” conditions (3a).

A new method called “system of straws”, based on LVDT technology created by Laue (1996), was developed for measuring the deformations at different depths. The straw is composed of a 2 mm diameter solid aluminium

rod and two discs, one at the top and one at the bottom (Fig 6.6). In pouring the lumps into the container, the straws were built into the model to stand vertically with their bottom discs at different levels. The rods were lubricated with silicon grease to reduce friction between the surface and the soil. The straw could move freely during the test according to the position of the bottom disc, which moved with the surrounding soil. The top disc was above the model surface and the change of its position was measured by the laser mounted on the actuator (Fig 6.2).

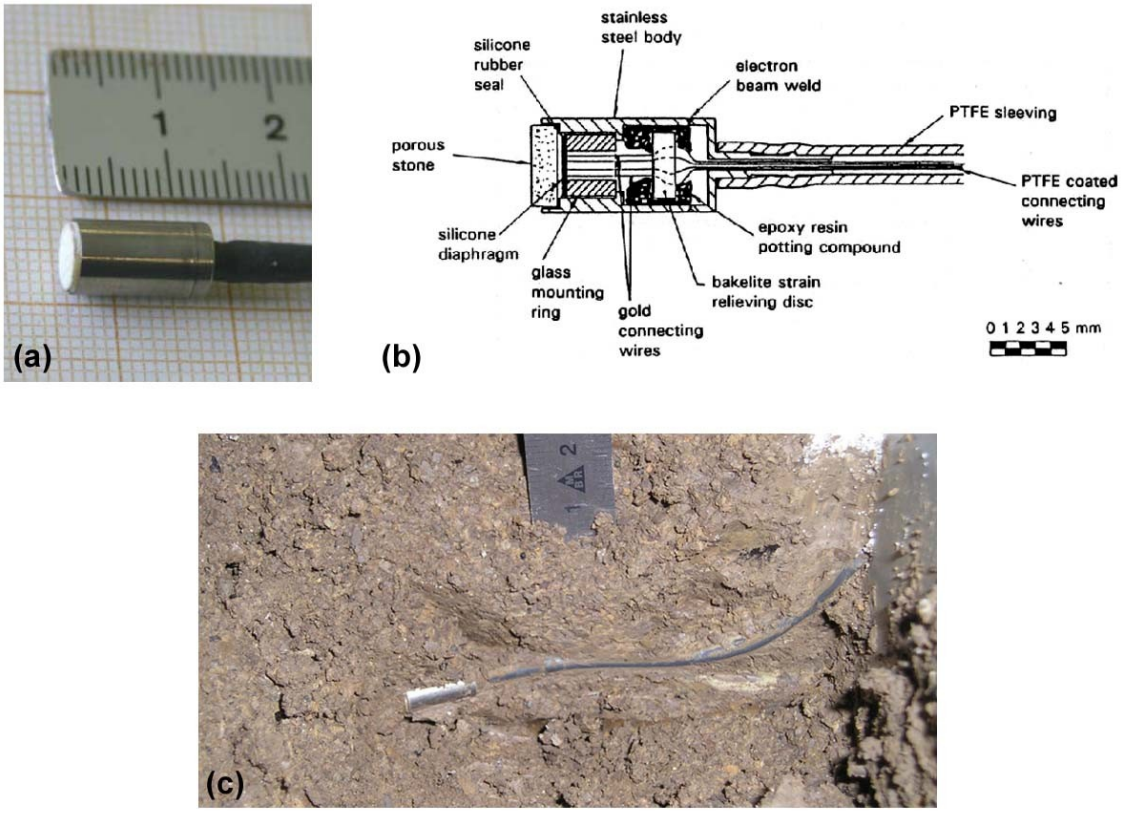

Fig. 6.5: (a) - Druck PDCR81 pore pressure transducer (Weber, 2007); (b) - cross-section (Taylor, 1995); (c) - pore pressure transducer in the model (excavation after centrifuge test).

In each test identical models with the same instrumentation were installed in both containers (Fig. 6.1). After the self-weight consolidation, the embankment was constructed in one container (referred to as an “embankment container“ throughout the text), while no embankment was constructed in the counterweight container.

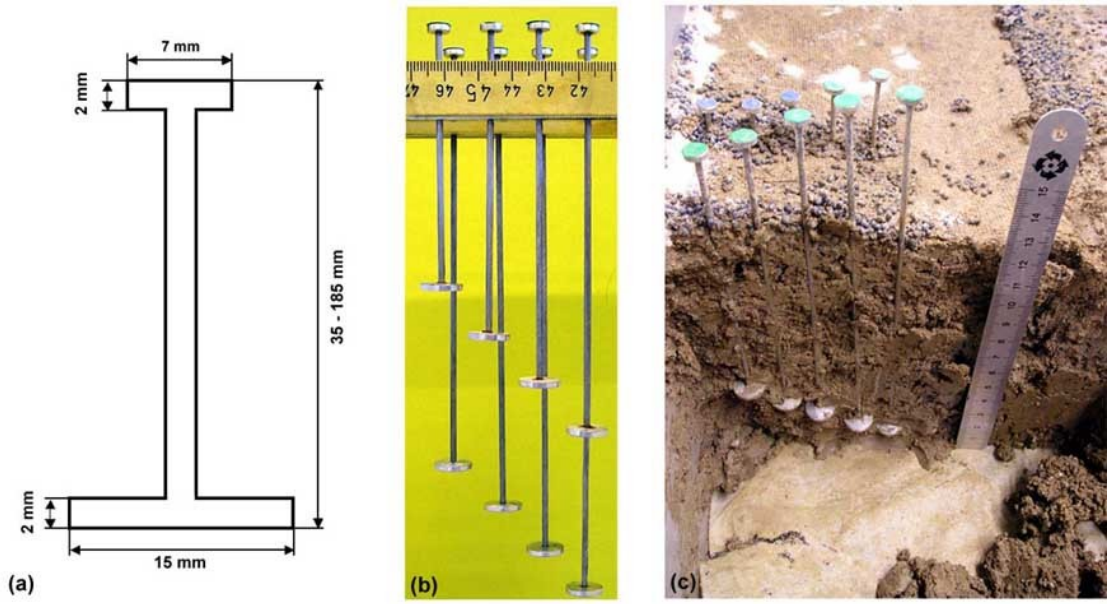

Fig. 6.6: Straws designed for measurement of vertical deformation: (a) - dimensions of straw; (b) - system of straws before installation to the model; (c) - straws during excavation after the test.

6.3 Position of water level

During the monitoring of the field embankments, a significant influence of the water level to the settlements was observed. As shown in Fig. 4.4, the water level below the embankments varied due to pumping. During the centrifuge test, the water level was kept constant. The level was chosen before the start of the test by the height of a standpipe located outside the container. Some technical limitations had to be respected. The water level was to be kept below the landfill surface for the whole test, because of the laser measurements of the landfill height. Water above the soil surface would not allow the laser to detect the soil surface correctly. Fig. 4.4 shows that *in situ* the water level was located close to the landfill surface and the water level during the centrifuge tests was therefore kept as close as possible to the surface of the fully consolidated landfill.

Before every test, the deformation of the model caused by self-weight consolidation was estimated based on the mini-centrifuge test results. The position of the standpipe was then adjusted to keep the water level just below the estimated surface of the self-weight consolidated model.

Certainly, the height of the water level was influenced slightly by the

curvature of the water level in the centrifuge model (a higher water level close to the container walls parallel with the axis of rotation) and by g-level (a higher water level close to the bottom wall compared to the top wall). The curved water level surface is inevitable in all centrifuge tests and the magnitude of the curvature depends on the centrifuge radius (Taylor, 1995). Figure 6.7 shows the plan view of the centrifuge model with an ideally flat surface after the self-weight consolidation and the water level position relatively to the model surface. The water level rose slightly above the soil surface close to the left and right edges of the model, but it did not interfere with the laser scanning (Figs. 6.12 and 6.13). The flooded areas were observed during the tests by cameras located at the tool table (Fig. 6.2) giving an evidence, that the water level is close to the soil surface.

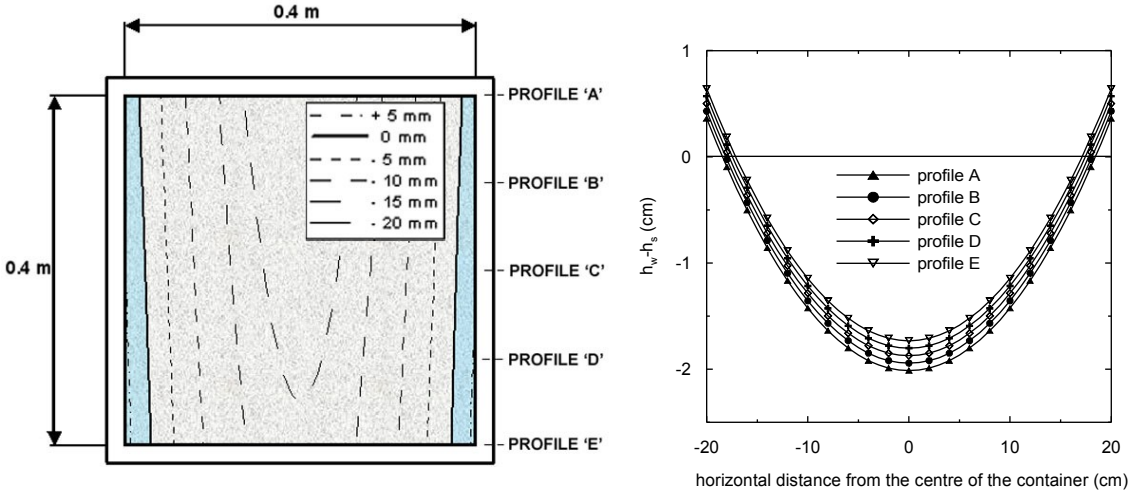

Fig. 6.7: Relative position of the water level and the soil surface for the self-weight consolidated model during centrifuge tests at 150 g: plan view (left) and five vertical sections (right) - position of sections is marked on the left figure.

The fixed position of the water level could influence the self-weight consolidation of the model. At the beginning of the consolidation, the top part of the soil was not flooded. It resulted in higher vertical effective stress, which could influence the rate of degradation of the soil structure during the self-weight consolidation. The significance of this effect is analysed by numerical modelling in Chapter 7.

6.4 Test procedure

The landfill models were prepared in the container outside the centrifuge. After finishing, the model was partially saturated, which created suction to keep the model stable during installation into the drum channel (Fig. 6.1). The stability of the model during its installation was also maintained by a wooden plate screwed to the top side of the container. This plate provided an additional support to the model before the start of the test and was removed shortly before the acceleration of the centrifuge. During its installation, the container was rotated through 90° and bolted onto the centrifuge drum in the position shown in Fig. 6.1. The centrifuge was accelerated to 20 g and the lumpy clay layer was flooded in-flight through the water supply system. The groundwater level was kept constant during the whole test, with the water table close to the surface of the consolidated landfill model.

After full saturation, the centrifuge was accelerated to 150 g. During consolidation, the model surface and the straws were scanned by the laser and the pore pressures were continuously monitored. After consolidation, an embankment was constructed at the model surface. Two different techniques of the construction were used. The process is described in Section 6.5. After the construction, laser scanning and monitoring of pore pressures was carried out until the surface settlement stabilised and at least 90% of the excess pore pressures dissipated.

6.5 Description of embankment construction techniques

The technique of embankment construction was identified to be a major problem of the geotechnical centrifuge testing. The realistic stress history of the model can be achieved only if the embankment is constructed in-flight without any change of the g-level. It will be discussed in Section 6.6 that the simulation of the *in situ* problem in question requires the g-level of 150 or higher to get the dimensions of the model that fit in the centrifuge. However, development of a suitable in-flight filling technique at 150 g was found to be difficult.

An in-flight filling system for the geotechnical drum centrifuge at ETH Zurich was developed by Weber et al. (2006) (Fig. 6.8a). The embankment material is poured through a filling tube mounted on the tool platform. This system was applied for g-levels up to 50 g. Various attempts have been made to adjust this system for higher g-levels and different filling materials were

tested. To use the in-flight filling system at 150 g succesfully, the following improvements were made (Fig. 6.8b):

1. For the whole test, the filling tube used by Weber was fixed by belts to the tool platform tower in a constant position to prevent any deflection due to the high centrifugal force at 150 g.
2. The outer end of the tube was fixed in place by a tripod screwed to the tool platform.
3. Another (more flexible) tube was used to join the tripod and the actuator. This tube could move with the actuator, so the filled material could be directed at the desired place at the model surface.
4. Lead balls with a low friction angle were used instead of sand as a filled material to prevent blocking of the filling tube.

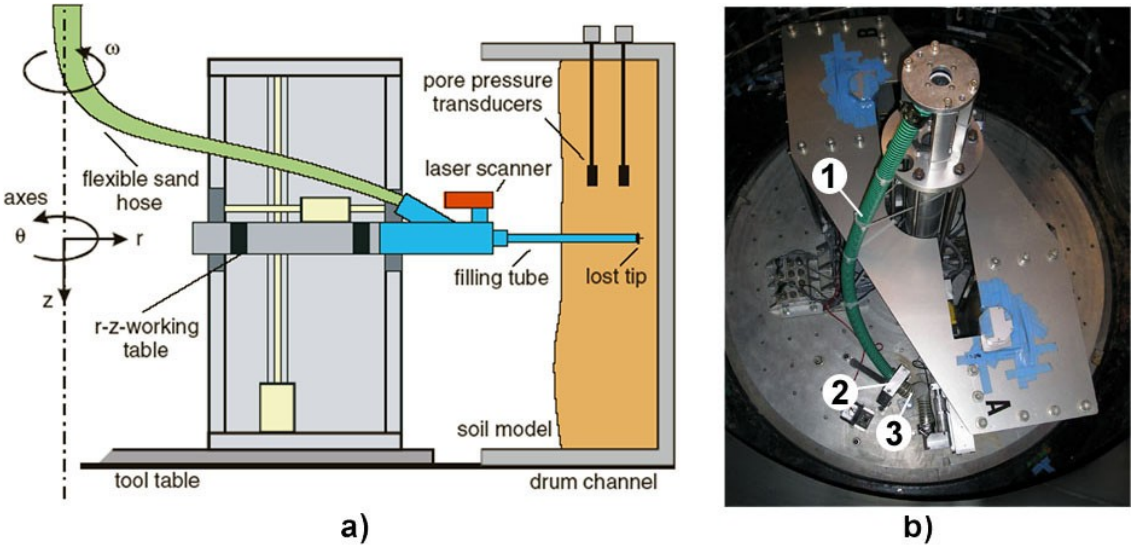

Fig. 6.8: (a) - in-flight filling system developed for installation of sand compaction piles (Weber et al., 2006); (b) - in-flight filling system for embankment construction at 150 g (test 2Dc): 1 - filling tube fixed to tool platform tower, 2 - tripod supporting filling tube, 3 - flexible tube fixed to actuator.

The following tests with different embankment construction techniques were carried out:

Test 2Da: After the self-weight consolidation of the landfill model at 150 g, the centrifuge was stopped and the embankment was constructed manually under stationary conditions. Afterwards the centrifuge was re-accelerated to 150 g.

Test 2Dc: The test was carried out at 150 g with modified in-flight filling system (Fig. 6.8b). After the self-weight consolidation, the tool platform was stopped and the filling tube installed (the centrifuge drum with the model was still rotating). The tool platform was then re-accelerated and the embankment was

constructed from the lead balls poured through the filling tube.

Further discussion of the filling techniques with respect to the modelled case study is in the following section.

6.6 Comparison of field embankment with centrifuge prototype

The case history of Embankment 2 was chosen for modelling in the geotechnical centrifuge. Ideally in prototype scale all dimesions and time intervals of the model should correspond to the case history (“prototype“ properties, e.g. time, dimensions etc. given in the text were calculated as the model properties multiplied by the appropriate scaling law). However, some parameters of the model had to be adjusted due to technical and time constraints or due to lack of information from the field.

The dimensions of the centrifuge container (400 x 400 mm) did not allow building a 3D embankment due to the extent of its active zone. Therefore a 2D axisymmetrical model was chosen. The two-dimensional geometry of the embankment could lead to a higher settlement of the landfill after the embankment construction compared to the field.

The limited 'headroom' in the centrifuge restricts the maximum height of the landfill layer. For the test carried out at 150 g, the maximum height of the self-weight consolidated landfill model in the prototype scale was 20 m. The depth of 20 m does not represent the real thickness of the landfill *in situ* (which was 25-30 m, Tab. 6.1), but it approximately corresponds to the depth of the active zone below the embankment in the field (Fig. 4.12).

Important factors influencing the behaviour of double porosity clays are dimensions and shape of the clay lumps. The lump preparation technique resulted in a random shape of clay lumps, which is believed to be similar as *in situ* (Fig. 6.9). The introductory tests not discussed in the thesis showed that at g-level over 150, the smaller lumps are predominantly of platy shape, which did not correspond to *in situ* conditions. The lump size distribution has a significant effect on intergranular porosity and hydraulic conductivity of the fill as discussed in Section 5.6.1 and therefore it is one of the key factors for the modelling of the landfill behaviour. Unfortunately no field data on the lump size distribution were available from the site of the trial embankments and therefore only rough estimation of the size distribution could be made based on the data from other landfills in the area (Fig. 5.8). Lump dimensions between 0.315-2.8 mm were used (the percentage of the fractions within this range was controlled by sieving) and 10% of fine particles (below 0.315 mm) was added (LSD curve

2 in Fig. 5.8).

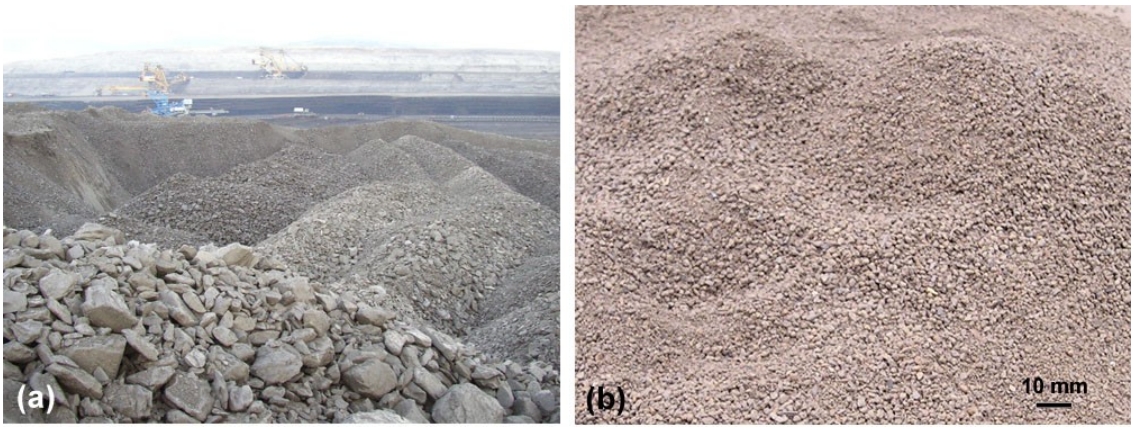

Fig. 6.9: (a) - fresh landfill in situ (photo by M. Větrovský); (b) scaled-down clay lumps for centrifuge tests - grading curve corresponds to LSD curve 2 (Fig. 5.8).

Unlike *in situ*, top and bottom drainage was used to reduce the total time required for the test. The prototype times of the various stages of the test did not correspond exactly to the *in situ* time: the self-weight consolidation period was finished when the pore pressures in the landfill equalized and no settlement of the model surface was observed (~16 years in prototype scale, Tab. 6.1). After the embankment construction, the test continued until 90% dissipation of the excess pore pressures was reached.

The embankment construction process was significantly different in the centrifuge tests 2Da, 2Dc and *in situ*. In the field, the rubble stone layer was placed in the embankment area and the hydrostatic levelling profiles were installed on the top of the fill. The embankment was then constructed gradually from compacted layers of fine graded soil. The whole process of construction took approximately 35 days.

In situ the underlying rubble stone layer increased the shear strength of the embankment subsoil. In the centrifuge, this effect was simulated by a geotextile, which was placed on top of the landfill before embankment construction.

In the test 2Da, the centrifuge was stopped and the embankment was constructed from wet sand under stationary conditions. The height and the shape of the embankment could be precisely controlled during the construction. However, the model was unloaded so the stress history did not reflect the field conditions. The period of reloading of the centrifuge corresponds to 45 days in the prototype time. It approximately correlates with the period needed for construction of the embankment of 35 days *in situ*.

	Landfill height after consolidation (m)	Lump dimensions (mm)	Time of landfill consolidation	Time of embankment surcharge application	Time of monitoring after embankment construction
Model 2Da	0.1475	0.315-2.8 (+10% < 0.315)	367 mins	2.88 mins	290 mins
Scaling law	1/n	1/n	$1/n^2$	$1/n^2$	$1/n^2$
Prototype 2Da	22.125	47.25-420 (+10% < 47.25)	15.7 yrs	45 days	12.4 yrs
Model 2Dc	0.1392	0.315-2.8 (+10% < 0.315)	379 mins	35 mins	460 mins
Prototype 2Dc	20.883	47.25-420 (+10% < 47.25)	16.2 yrs	547 days	19.7 yrs
Field embankment	cca 30 m*	no direct information	~25 yrs	~35 days	3 yrs
*prototype depth should be at least equal to the active zone in the field					

Tab. 6.1: Comparison of centrifuge models, corresponding prototypes and case history (Embankment 2).

The error caused by unloading and reloading of the model was believed not significant in comparison with the large deformations typical for virgin loading of the double porosity soil and the small elastic recovery during its unloading. The effect was shown by the one-dimensional unloading curve from the similar average stress level of 100 kPa (Fig. 5.24). Figure 6.10a shows the excess pore pressures from the transducers located in the model in the depths of 5.25 m and 15.75 m (prototype scale) in both containers. The excess pore pressures measured in the counterweight container are generated only by the unloading-reloading cycle. No excess pore pressures were measured by the upper transducer, the lower transducer shows a maximum value of 6 kPa (it is less than 5% of the total embankment surcharge and cca 10% of the excess pore pressures measured under the embankment). The comparison of surface settlements (Fig. 6.10b) shows a slightly higher influence of the unloading-reloading cycle. However, counterweight model was reloaded to the same stress level (path 1-2-3 in Fig 6.10c), while the model in the “embankment“ container was subjected to higher stress (path 1-2-3-4 in Fig. 6.10c), which approached the state of the soil closer to the virgin loading curve.

The in-flight construction of the embankment during the test 2Dc allowed the stress history to be kept similar to the field. The lead balls were poured through the filling tube in two cycles of 32 discrete charges in specified locations to ensure uniform spatial distribution of the surcharge. Calculated impact positions for these charges are shown in Fig. 6.11. However, the filling

took 35 minutes under 150 g, which corresponds to the prototype time of 547 days. It is 15 times longer than *in situ* and the construction process therefore did not reflect actual filling in the field.

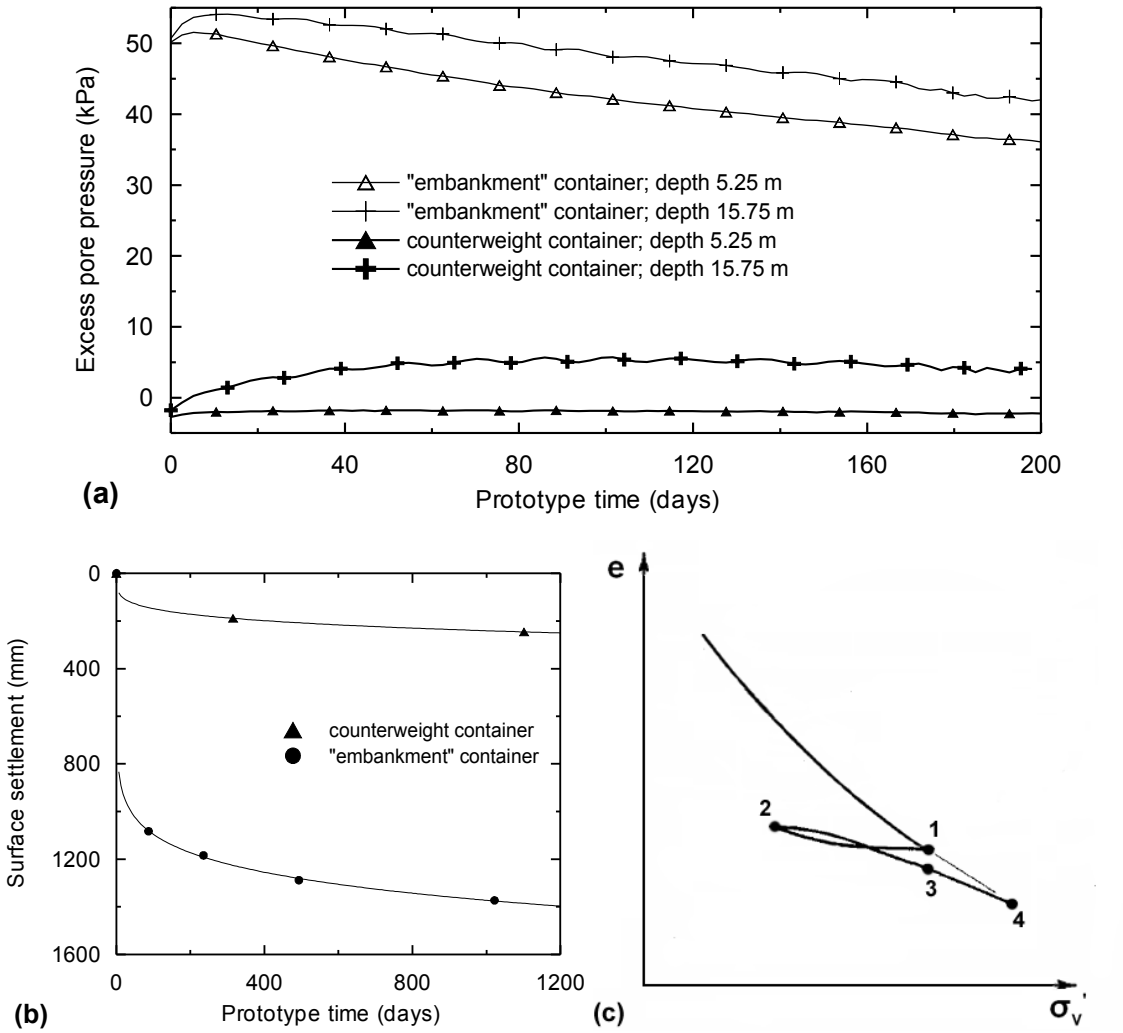

Fig. 6.10: Comparison of excess pore pressures (a) and surface settlements (b) in both containers after embankment construction and centrifuge re-aceleration in the test 2Da; (c): 1-dimensional simplification of the stress path in "embankment" container (1-2-3-4) and counterweight container (1-2-3) during unloading-reloading cycle.

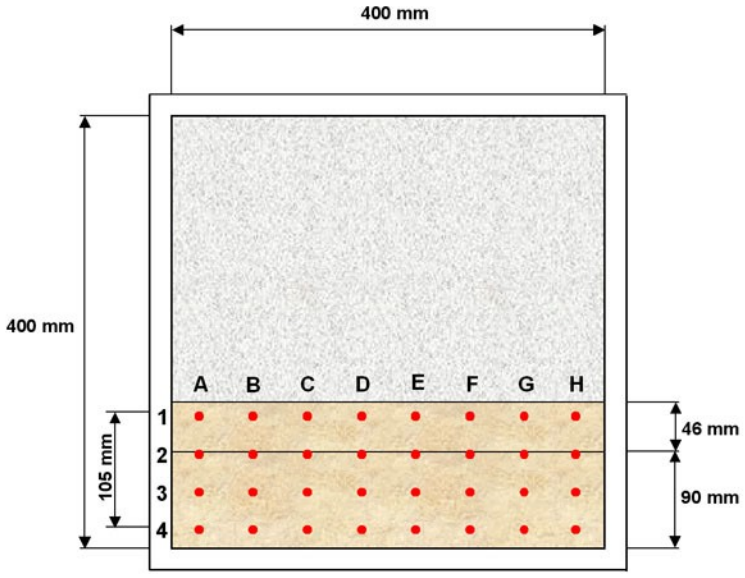

Fig. 6.11: Impact positions of the lead balls charges during in-flight construction in test 2Dc. A single charge was applied to positions A1-H1 (embankment slope) and two charges were applied to positions A2-H4 (embankment crest).

6.7 Setup of centrifuge tests

The centrifuge test setup for both test series (2Da and 2Dc) differs slightly due to the different embankment material and different instrumentation (system of straws). The differences are summarized in Tab. 6.2. Plan views and sections of both models are presented in Figs. 6.12 and 6.13.

		Embankment construction:		*Embankment properties:*			
Test:	Straw system:	Filling technique:	g-level:	Material:	Density:	Thickness:	σ_v' at the base:
2Da	no	stationary	1	sand	1847 kg/m^3	50 mm	123 kPa
2Dc	10 straws	in-flight	150	lead balls	6700 kg/m^3	15 mm	~130 kPa

Tab. 6.2: Summary of differences in centrifuge tests 2Da and 2Dc.

Test 2Da did not include the system of straws for the measurement of settlements inside the landfill. In test 2Dc caused that no results of the surface settlement were obtained after the embankment construction, since the laser did not detect lead balls surface correctly. Therefore no direct comparison of

the landfill settlement of both the models due to the embankment construction was possible. The results from both these test series (surface settlement from test 2Da and settlement of “straws“ from test 2Dc) were combined and used for comparison with field monitoring of Embankment 2 in Section 6.9. The results from the self-weight consolidation of both tests are presented in Section 6.8. The summary of the results from the centrifuge tests and the *in situ* monitoring of Embankment 2 is given in Tab. 6.3.

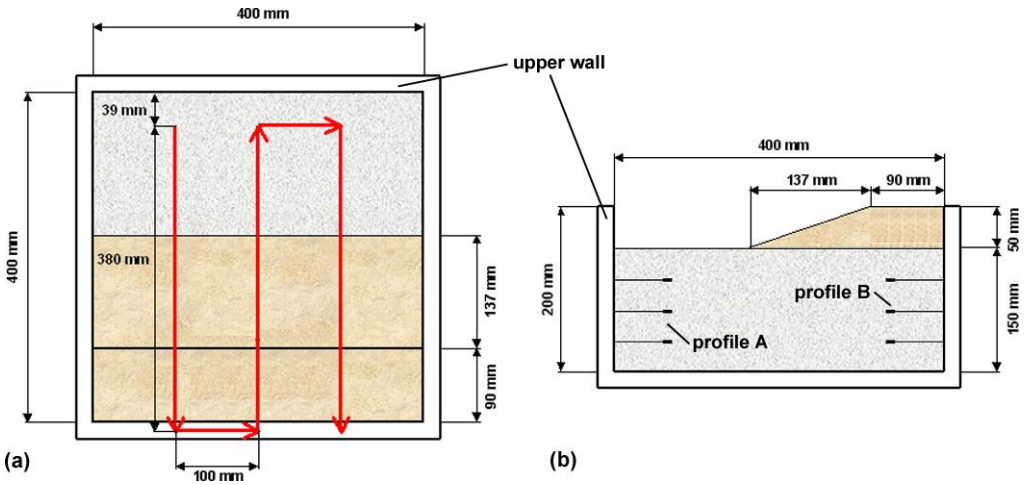

Fig. 6.12: Plan view and section of model in test 2Da. Red line shows laser scanning path.

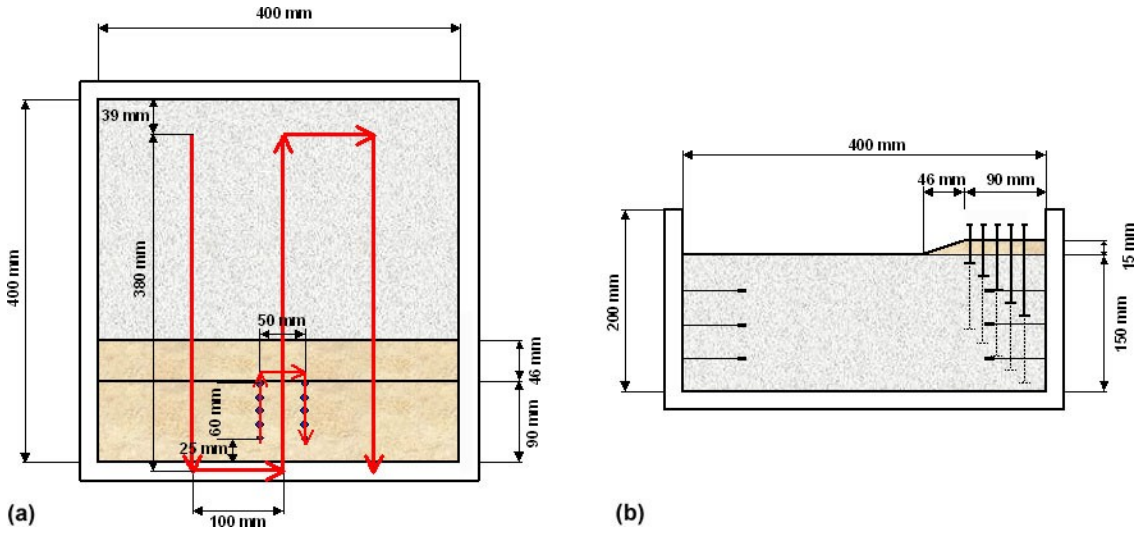

Fig. 6.13: Plan view and section of model in test 2Dc. Red line shows laser scanning path. Settlement in various depths was measured by scanning upper discs of “straws“ (dots in (a)).

The stress generated by the embankment surcharge was 132 kPa *in situ*, 123 kPa in test 2Da and 120-135 in test 2Dc, where the shape of the embankment slightly varied as its surface could not be exactly controlled and flattened.

	Type of measurement	*Results in section*	*Test 2Da*	*Test 2Dc*	*Embankment 2 (field)*
Self-weight consolidation	Pore pressures	6.8.1	yes	yes	no
	Surface settlement	6.8.2	yes	yes	no
	Depth reference points	6.8.3	no	yes	no
Embankment consolidation	Pore pressures	6.9.1	yes	yes	yes
	Surface settlement	6.9.2	yes	no	yes
	Depth reference points	6.9.3	no	yes	yes

Tab. 6.3: Summary of available results from centrifuge tests and field measurements.

6.8 Results of self-weight consolidation

The results of the self-weight consolidation could not be directly compared to any *in situ* measurements, because the real landfill was instrumented at the time of the trial embankment construction. However, contrary to the field observations, the centrifuge tests were carried out under well defined conditions (geometry, drainage, lump size distribution) and the interpretation of the results can improve knowledge about the behaviour of the landfills. The results have been also used for the evaluation of the used constitutive model and calibration of the hydraulic conductivity in Chapter 7.

Measuring the landfill settlement during the self-weight consolidation *in situ* would be rather difficult because of the problematic definition of the initial height of the landfill. *In situ*, filling takes usually a few years until the final height is reached and consolidation starts before the end of filling. The centrifuge models were prepared in a short time from air dried clay lumps, and their water content was increased before the acceleration of the centrifuge. It resulted in swelling of the models. Moreover, the centrifuge models are prepared at 1 g conditions and their vertical stress profiles therefore differ from the stress profile *in situ*. Contrary to the mini-centrifuge tests, the initial height h_0 of the

models was measured after swelling and all settlements were calculated as a difference between the initial and actual heights: $\Delta h = h_0 - h$. All the models in the geotechnical centrifuge tests were of the same geometries, and the magnitude of swelling could not be therefore influenced by different initial heights of the models. This definition of the initial height also coincides with the initial state of the soil in numerical modelling in Chapter 7.

6.8.1 Pore pressures

The measurement of pore pressures during the test 2Da is presented in Fig. 6.14. It shows the pore pressures from the three transducers of profile A and the three transducers in profile B (in the area of the planned embankment - see Fig. 6.4). The transducers in both profiles were located in ¼, ½ and ¾ of the depth of the landfill, which approximately corresponded to a depth of 5.25 m, 10.5 m and 15.75 m of the consolidated landfill (in prototype scale). Figure 6.14 reveals the same rate of pore pressure dissipation in both profiles and similar values of both maximum and final pore pressures at all levels. The maximum measured values correspond to the time of centrifuge acceleration to 150 g. After dissipation of 95% of excess pore pressures, the self-weight consolidation stage of the test was finished. The small differences between the two profiles are caused by a slightly different vertical positions of the transducers.

The results from profile B (under planned embankment) of centrifuge test 2Dc are presented in Fig. 6.15. Although the lump size distribution curves and the preparation process of the models 2Da and 2Dc were identical, Fig. 6.15 shows slower consolidation in the test 2Dc, especially in the deeper part of the model (maximum pore pressure 250 kPa for lower transducer compared to 225 kPa in the test 2Da). The rates of excess pore pressure dissipation for the transducers located in 10.5 m and 15.75 m from both the “embankment“ containers are compared in Fig. 6.16. The ratio $u_e/u_{e\text{-}max}$ was calculated from the current excess pore pressures (u_e) and the maximum possible excess pore pressures ($u_{e\text{-}max}$), which were derived from unit weight of the soil after acceleration. The value $u_e/u_{e\text{-}max}$ of 1 thus represents the situation after full loading at 150 g when no excess pore pressures dissipated and $u_e/u_{e\text{-}max} = 0$ means full dissipation of excess pore pressures. The different rate of consolidation could be caused by slightly different structure of the landfill caused during filling (a more dense arrangement in the test 2Dc) resulting in lower hydraulic conductivity, but it can be also attributed to a malfunction of the drainage of one of the models.

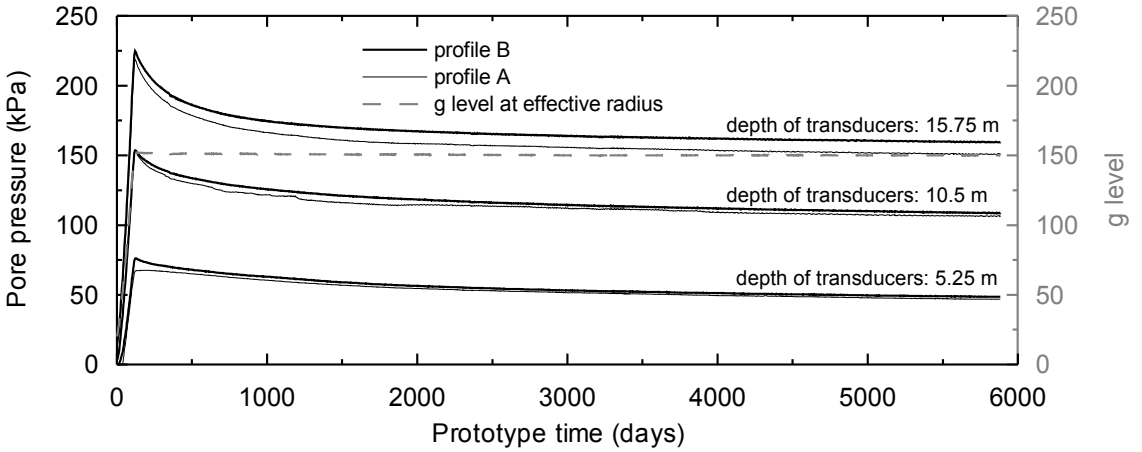

Fig. 6.14: Test 2Da - pore pressures during self-weight consolidation of centrifuge model.

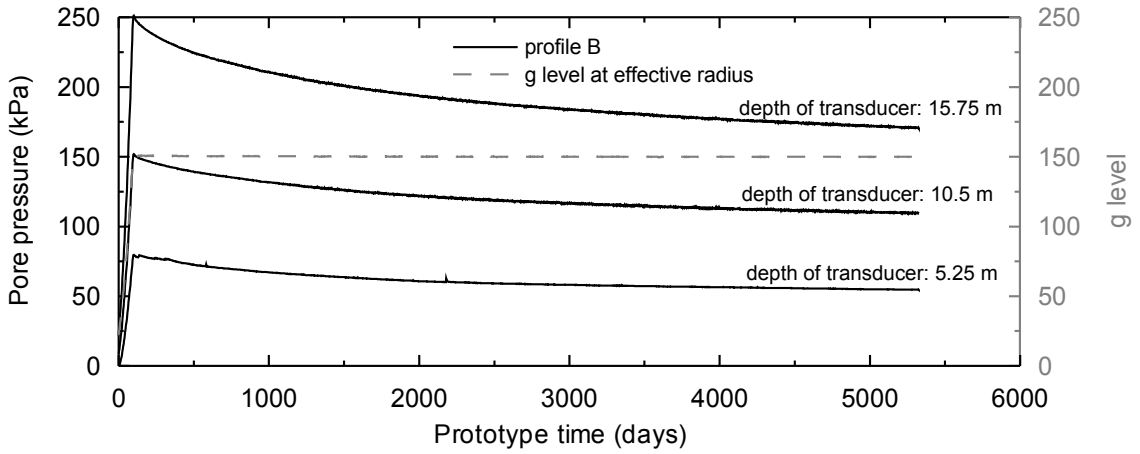

Fig. 6.15: Test 2Dc - pore pressures during self-weight consolidation of centrifuge model.

Fig. 6.16 also shows a similar rate of excess pore pressures dissipation from the transducers located in the centre and in ¾ of the model depth. Since the drainage path from 15.75 m was half of the drainage path from 10.5 m, the dissipation should be four times faster. The observed similar rates are explained by a lower hydraulic conductivity in the deeper part due to closed macro voids, while in the upper half of the model the preferential paths remained open and water from the central part of the model could drain faster upwards.

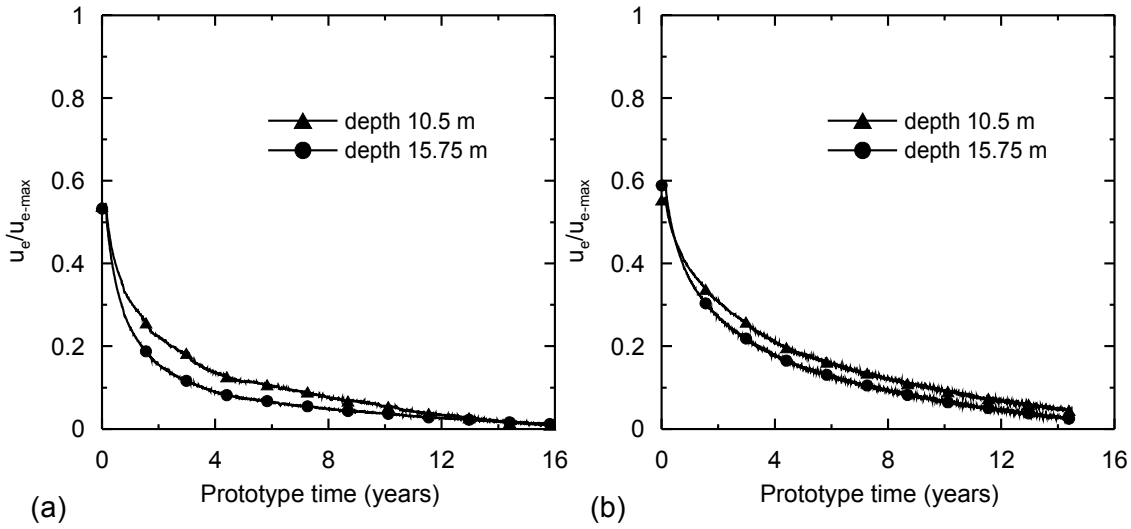

Fig. 6.16: Comparison of rate of dissipation of excess pore pressure in both embankment containers: (a) - 2Da; (b) - 2Dc.

6.8.2 Surface settlement

The settlement of the landfill during the self-weight consolidation reflects the dissipation of the pore pressures. The rapid initial settlement observed is associated with closing of interlump voids and fast drainage. About 90% of the total measured settlement took place before the first scanning of the landfill surface (after prototype time of half a year). The remaining 10% occured during following 15 years, when the hydraulic conductivity in the deeper part of the fill must have decreased significantly due to the closed macro voids.

Figure 6.17 presents the settlement curves from both containers of test 2Da (profiles 1 and 3 are presented for each container). Data from test 2Dc are presented in Fig. 6.18. The rates of settlement are similar for all curves with a slightly faster settlement in test 2Da. There are very small differences in the average settlement in profiles 1 and 3 within one container. Some differences can be observed when the settlements in the two containers are compared (especially in test 2Da). This is probably caused by a slight nonuniformity of the initial porosities despite the identical preparation procedures. However, the final settlement of 8 presented profiles is in the range 21.2-23.5%, which is a much better agreement than in the mini-centrifuge tests (see Fig. 5.16).

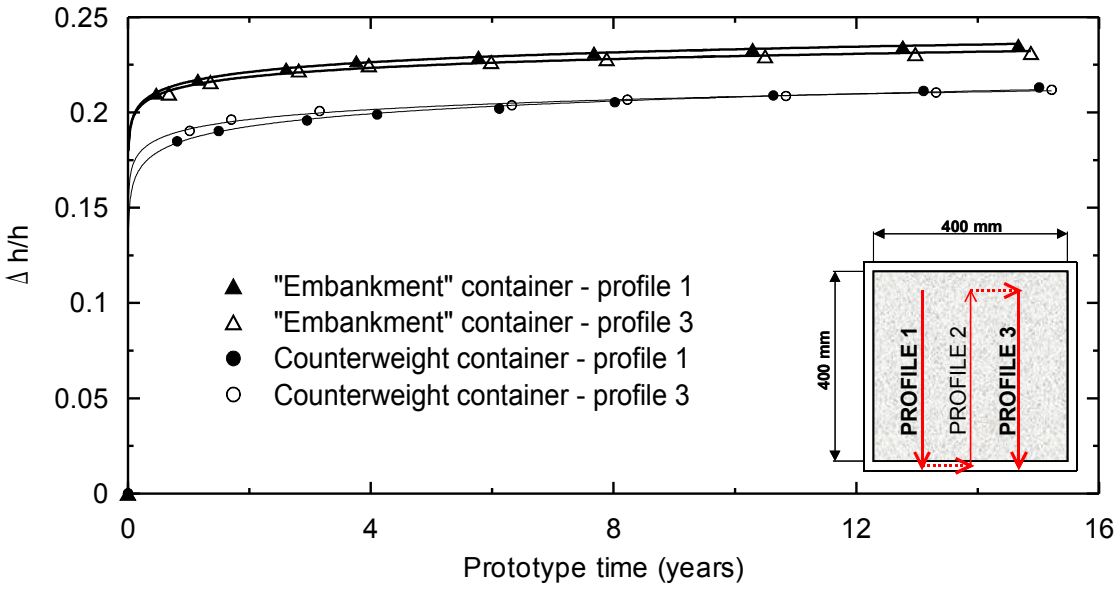

Fig. 6.17: Average settlement during test 2Da.

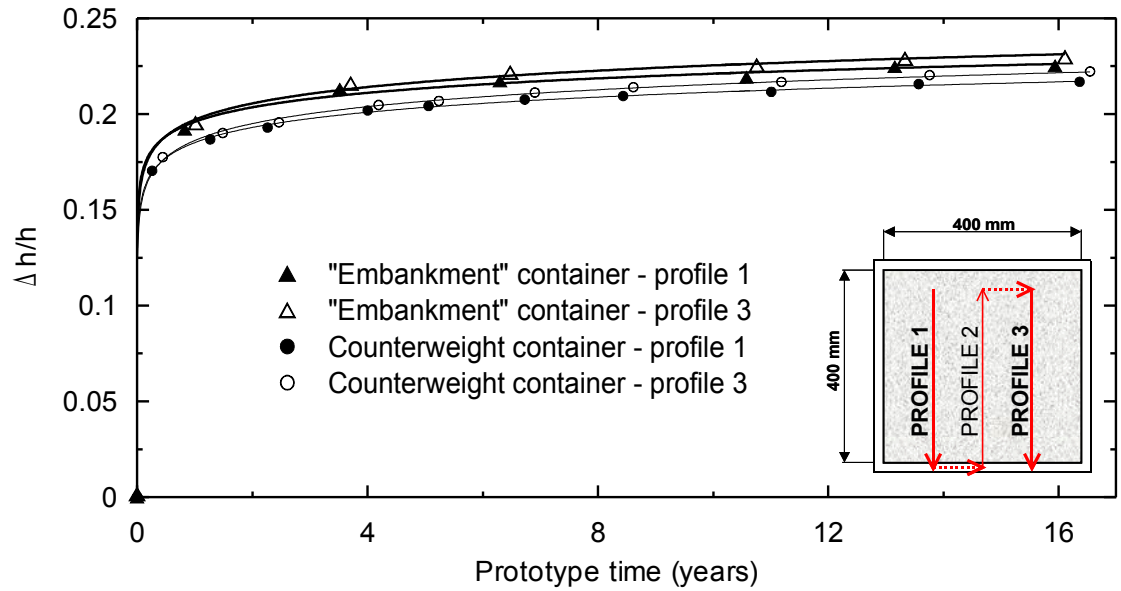

Fig. 6.18: Average settlement during test 2Dc.

Each data point in Figs. 6.17 and 6.18 represents the average settlement along the measured profile, neglecting observed differential settlement along the profile. Figure 6.19 shows all readings measured by the laser along one profile (profile 1 from “embankment“ container from test 2Da was chosen). It represents about 2600 readings as the laser speed along the profile during the scanning was 3 mm/s with reading every 0.05 sec. It

corresponds to one measurement carried out every 0.15 mm in the model scale and every 22.5 mm in the prototype scale. The first measurement in Fig. 6.19 (corresponding to the time of 0 years) was carried out after the installation of the model into the centrifuge, before the acceleration. This first line shows that the surface of the model was relatively flat before the start of the test. After acceleration, all measurements show differential settlement. The differential settlement was caused by segregation of the clay lumps during the model construction, which resulted in inhomogeneous intergranular porosity in the horizontal direction. All models were constructed with the effort to reach a uniform distribution of clay lumps, but despite this some segregation took place.

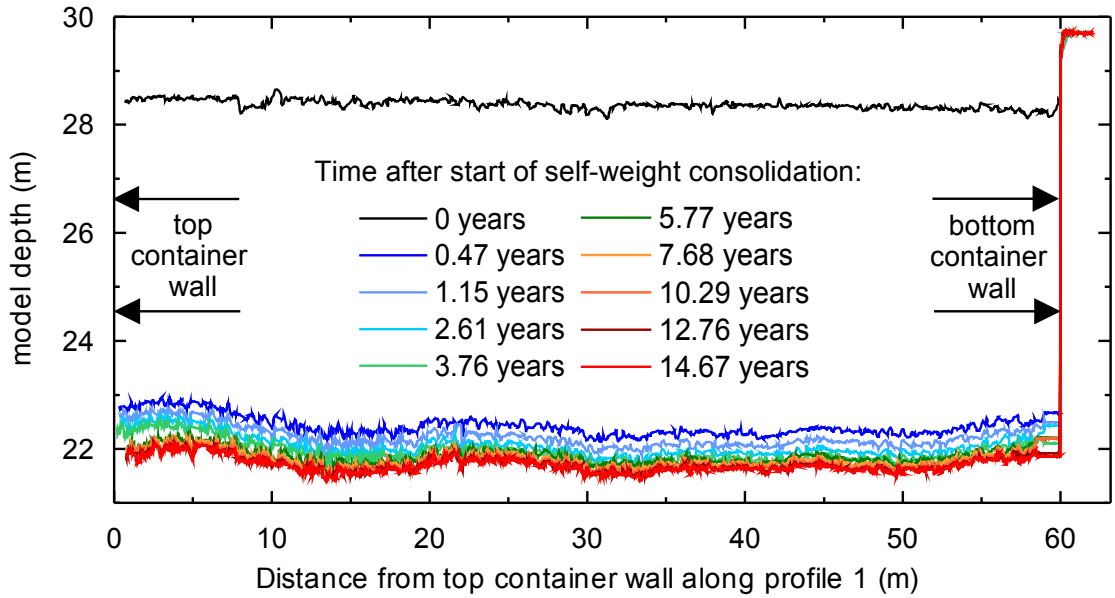

Fig. 6.19: Settlement along the profile (Profile 1, "Embankment" container, test 2Da).

Selected profiles of Fig. 6.19 were replotted in Fig. 6.20 to analyse the effect of differential settlement. Zero on the vertical axis corresponds to the average settlement at the selected time of measurement. The measurement at the prototype time of 0 years shows a maximum deviation of ±0.2 m from the average value. After acceleration, a differential settlement of 0.75 m over the distance of 11 m (3-14 m from top container wall) was measured. No major change in the rest of the self-weight consolidation suggests, that the differential settlement was driven by an initial closing of macro voids in the fill and it was associated with variations of intergranular porosity in the horizontal direction.

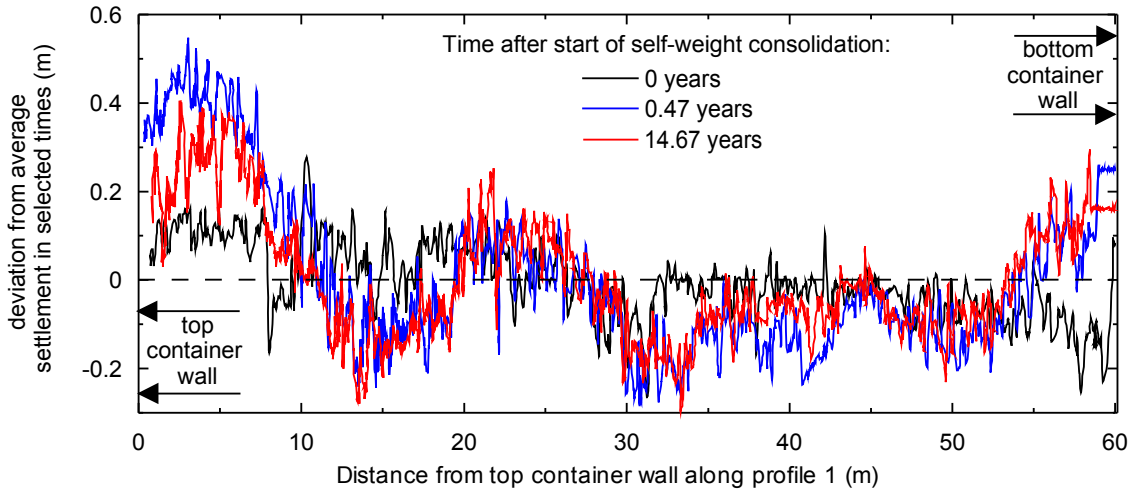

Fig. 6.20: Development of the differential settlement along the profile (Profile 1, "Embankment" container, test 2Da).

The described behaviour was observed in all measured profiles of all centrifuge models. Immediately after centrifuge acceleration the differential settlement differing in shape and magnitude took place. The final shape of the landfill surface could not be predicted before the start of the tests. A similar behaviour can be expected *in situ*. The differential settlement is further analysed by means of a simple laboratory experiment and the numerical modelling in Section 7.4. With respect to further development of the landfills, it may be suggested to use a ground improvement method before any construction to reduce the double porosity structure in the shallow depths and ensure more uniform settlement. A review of the ground improvement methods suitable for the double porosity landfills was given in Section 3.3.

6.8.3 Depth reference points

A system of straws was installed in both models in the test 2Dc. In each model, 10 straws were installed in two profiles. The plan view and section is presented in Fig. 6.13 and data are in Figs. 6.21 and 6.22. The apparent difference in the rate of settlement between both models is believed to be caused by different frequency of laser scanning and not to correspond to different permeabilities. The settlement of some of the straws was accompanied by a small deviation of the straw from the vertical, which caused the laser missing the position of the upper straw disc (some data in Figs. 6.21 and 6.22 are missing). From this reason the settlements of 2 straws from the "embankment" container and 3 straws from the counterweight container could not be presented at all. The problematic interpretation of the laser scanning could also cause the scatter in the presented results.

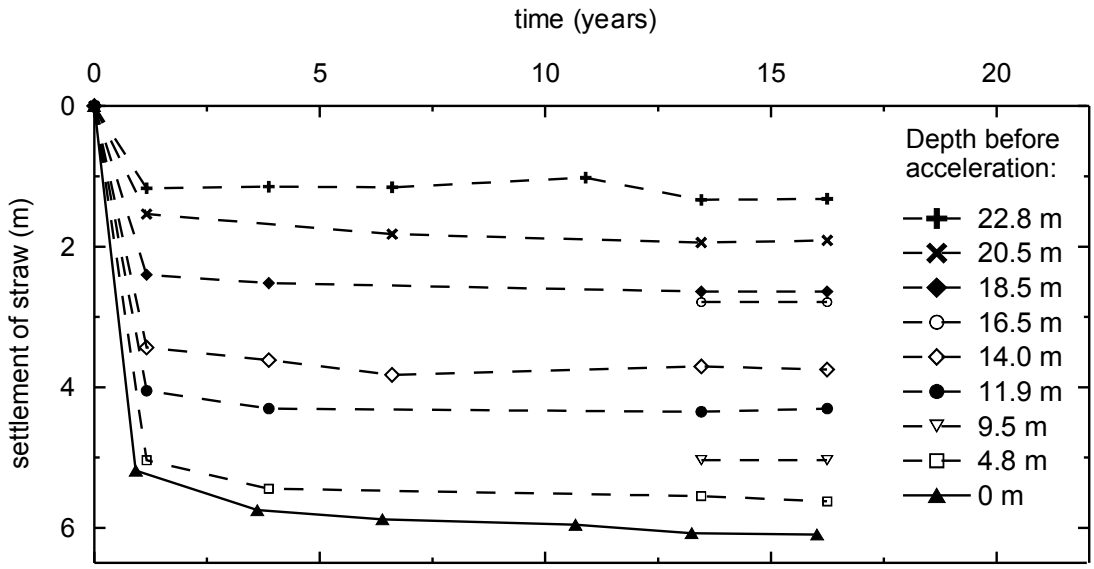

Fig. 6.21: Settlement of depth reference points ("embankment" container).

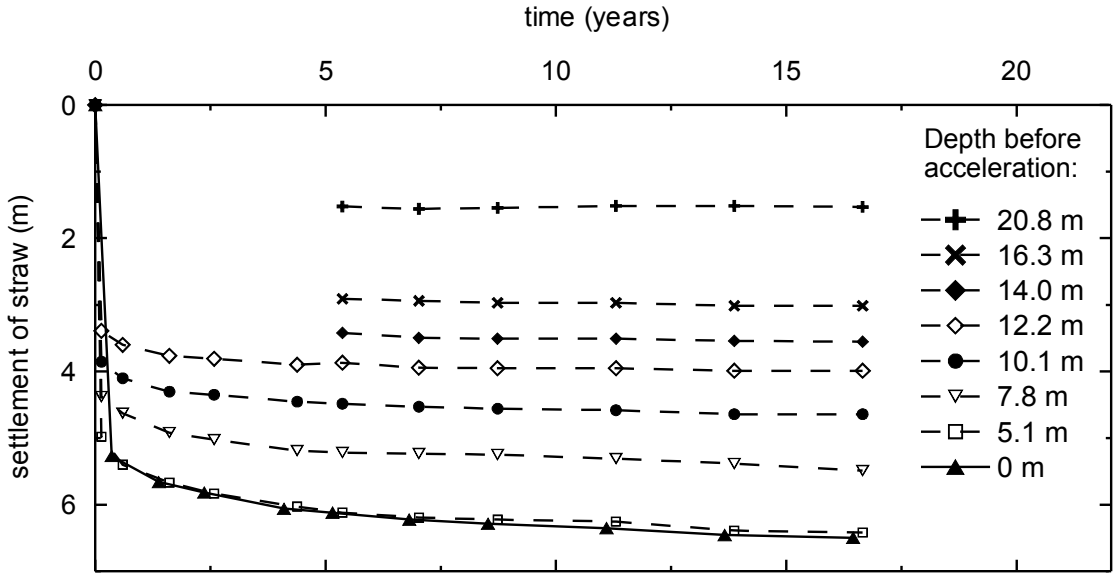

Fig. 6.22: Settlement of depth reference points (counterweight container).

The shape of the settlement curves corresponds to the surface settlements (the surface settlement curves are also presented for comparison in Figs 6.21 and 6.22 - depth of 0 m). The final settlements of both the models are shown in Fig. 6.23. It presents a good agreement between both models. Despite some scatter, it demonstrates a gradual settlement in the landfill

profile, so the process of structure degradation seems to be continuous and no particular depth (stress level), where structure of the soil would collapse could be defined (this is in line with the results of the mini-centrifuge tests). The comparison of straws in shallow depths with the surface settlement reveals a very small settlement in the top part of the fill. The thickness of this zone may be estimated to be in the range of 5-8 m. The thickness differs in both models probably due to the limited accuracy of the measurements caused by small absolute settlements of the straws and due to large intervals between the straws. However, this lower settlement indicates only limited structure degradation in the upper layer.

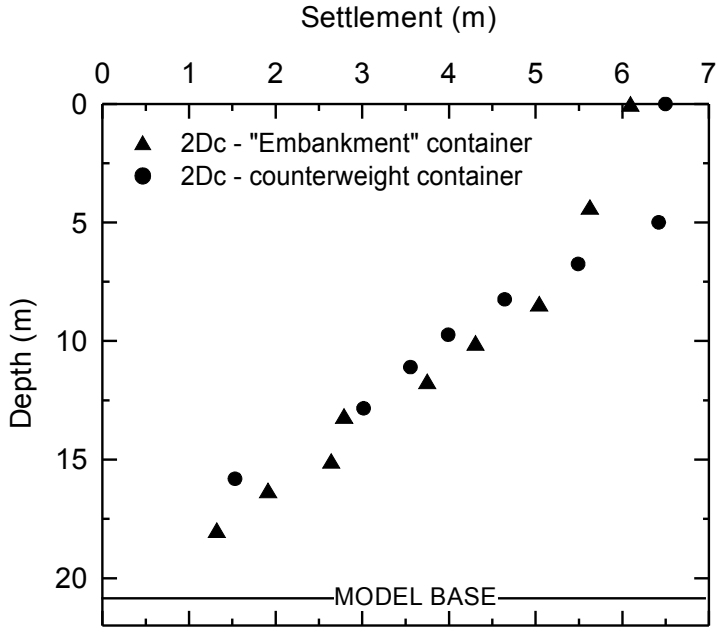

Fig. 6.23: Comparison of settlement in both containers.

6.9 Modelling of Embankment 2

6.9.1 Pore pressures

Figure 6.24 shows the distribution of pore pressures due to the embankment surcharge in both the centrifuge tests. The isochrones correspond to different times after the embankment construction (noted in legend). In test 2Da, the maximum values of excess pore pressures correspond to the time it took the centrifuge to accelerate after the embankment construction, while in test 2Dc, the maximum pore pressures were reached at the end of in-flight construction of the embankment. Both curves demonstrate the unusual behaviour of the double porosity soil. A similar rate of pore pressure dissipation was measured by the transducers located in the centre (10.5 m) and in the bottom (15.75 m) part of the model, although the drainage path for the deeper transducer was half that of the transducer located in the middle of the model. This can be explained by interlump voids closing in the bottom part of the model during the self-weight consolidation and by the faster drainage through the macro voids in top 5-6 m of the prototype, which remained interconnected after the self-weight consolidation. This hypothesis is supported by the rate of consolidation of the oedometer tests (Fig. 5.25), which indicated fast drainage through macrovoids up to 50 kPa (6.5 m).

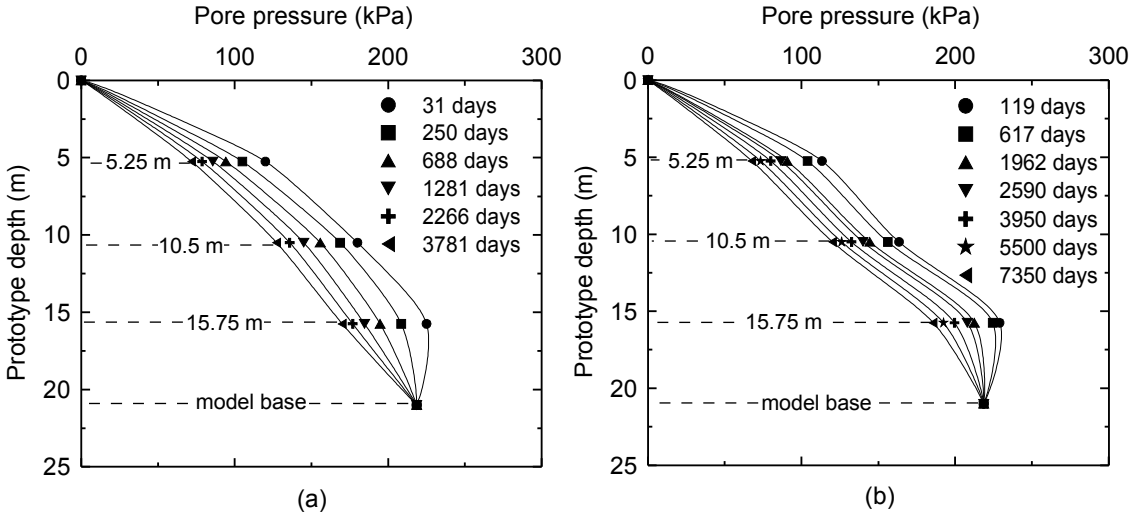

Fig. 6.24: Pore pressures under the embankment (profile 3b in Fig. 6.4), (a) - test 2Da; (b) - test 2Dc.

The excess pore pressure dissipation rate from both the tests can be compared also from Figs. 6.25 and 6.26 and from Tab. 6.4. It shows, similarly

to the self-weight consolidation results, a significantly faster consolidation in test 2Da. The maximum values are similar (Tab. 6.4), although the embankment in test 2Da was constructed much faster (45 days compared to 547 days for test 2Dc - Tab. 6.1). Tab. 6.4 presents the pore pressures before the construction of the embankment, the maximum measured pore pressures and the partially dissipated pore pressures after 3 years (end of *in situ* monitoring), 11 years (end of test 2Da) and 20 years (end of test 2Dc). Due to the settlement of the landfill after embankment surcharge, the position of all pore pressure transducers moved down relatively to the groundwater level. That means that even after full dissipation of excess pore pressures, the transducers would not reach the same pore pressures as before the embankment construction (the final pore pressures would be by about 4 (8, 12) kPa higher for the transducers located 15.75 (10.5, 5.25) m below the surface, respectively).

	Test 2Da			*Test 2Dc*		
Depth of transducer	5.25 m	10.5 m	15.75 m	5.25 m	10.5 m	15.75 m
u - after self-weight consolidation (kPa)	48.6	108.8	159.6	43.4	96.0	169.3
u_{max} (kPa)	122.9	179.9	223.6	116.6	165.2	229.2
$u_{3\ years}$ (kPa)	88.7	148.6	188.2	98.0	151.3	220.2
$u_{11\ years}$ (kPa)	71.7	127	169.7	79.4	132.5	199.6
$u_{20\ years}$ (kPa)	-	-	-	67.8	120.5	186.1

Tab. 6.4: Pore pressures in selected times after embankment construction.

Figure 6.25 shows also profile A of the pore pressure transducers located under “far field“ conditions and not influenced significantly by the embankment surcharge (Fig. 6.4a). The small increase of the pore pressures in this profile (up to 15 kPa) can be explained by the combined effect of the embankment surcharge and deceleration-acceleration cycle due to the embankment construction.

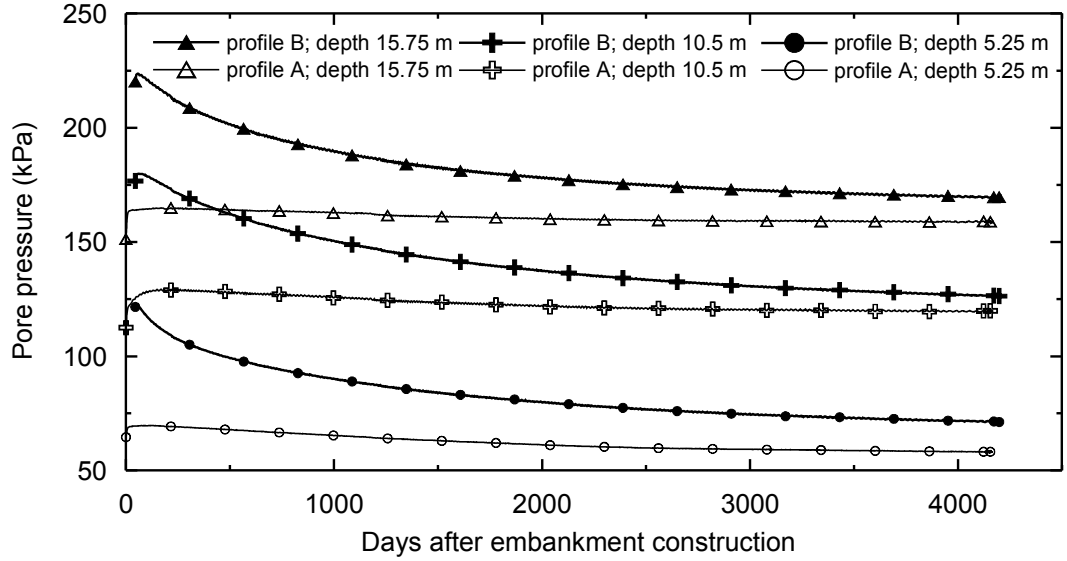

Fig. 6.25: Comparison of both pore pressure profiles in test 2Da (profile B located under the embankment, profile A under "far-field" conditions).

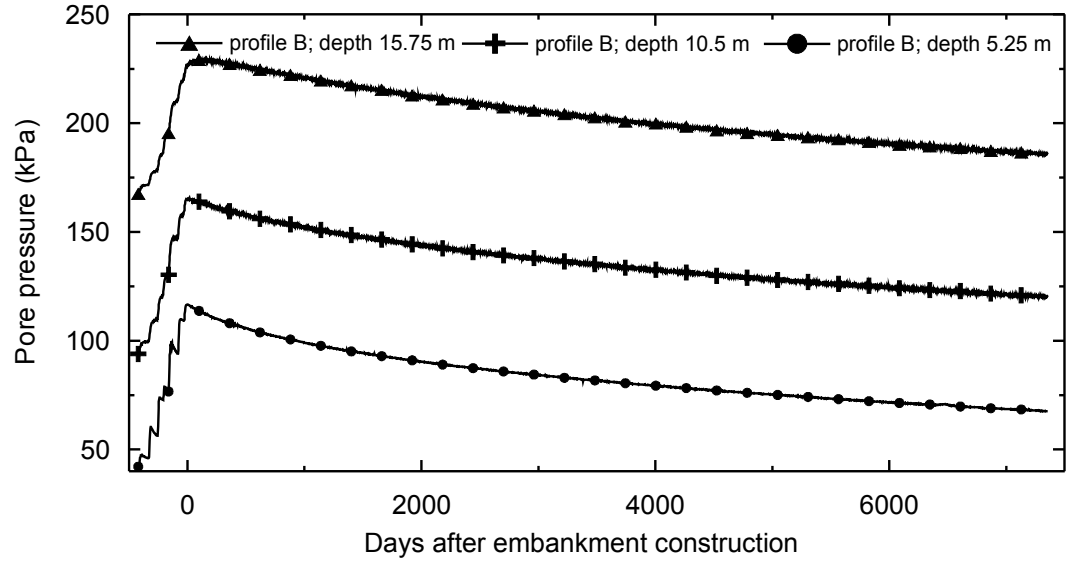

Fig. 6.26: Pore pressures under the embankment in test 2Dc.

A direct comparison of the pore pressures in the centrifuge and *in situ* is rather difficult because of the different drainage paths resulting from the different positions of the transducers and different drainage conditions in the centrifuge. Further, the 3D embankment *in situ* was modelled as 2D in the centrifuge. However, when plotted in the same time scale (Fig. 6.27), the *in situ* maximum excess pore pressures are significantly higher. It indicates lower hydraulic conductivity in shallow depths *in situ*. On the other hand, the rate of

consolidation *in situ* was significantly faster (the additional decrease in pore pressures measured 500-1000 days after the embankment construction was associated mostly with the renewal of water pumping from the fly ash lagoon as described in Section 4.4.3).

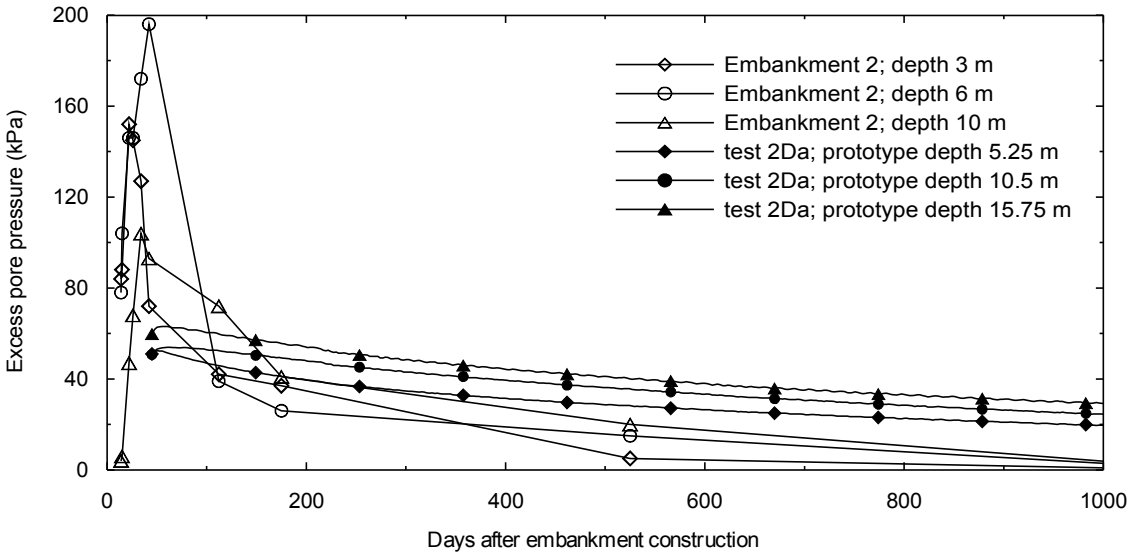

Fig. 6.27: Comparison of excess pore pressures after the embankment construction – data from field measurements and from test 2Da.

6.9.2 Surface settlement

The laser scanning profiles 1 and 3 (Fig. 6.28) measured in test 2Da were analysed to determine the settlement of the landfill. Contrary to *in situ* measurements, where the settlement of the landfill was directly measured by HL profiles, the laser scan in the centrifuge measured the position of the embankment surface. The thickness of the embankment was exactly measured after its construction so the position of the landfill below the embankment could be calculated by subtracting the embankment height with assumption of an incompressible embankment. An example of the laser scanning results from profile 1 is presented in Fig. 6.29. It shows an insignificant settlement in the upper part of the container, where no surcharge was applied, compared to the obvious settlement in the area subjected to the embankment surcharge.

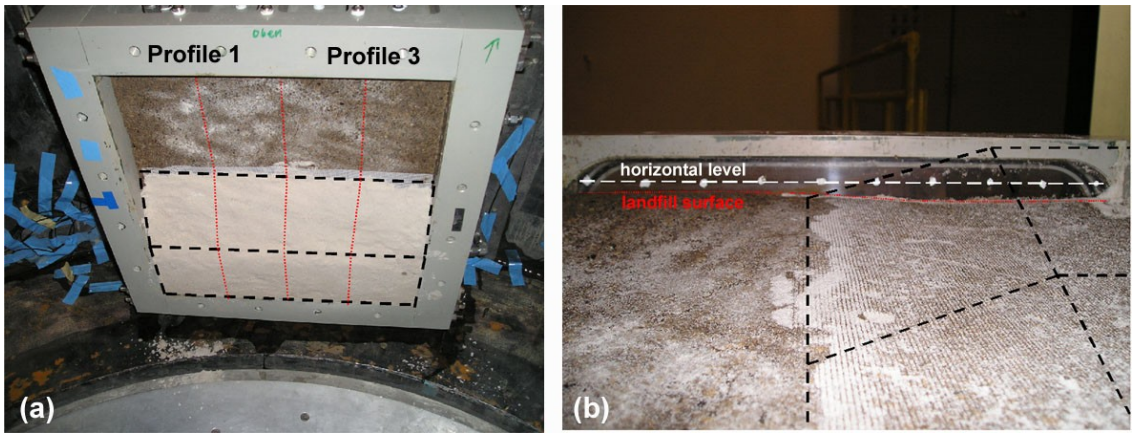

Fig. 6.28: (a) - test 2Da, model after construction of embankment with indication of laser profiles and the shape of embankment; (b) - "embankment" container at the end of the test after removing of embankment layer with significantly higher settlement in embankment area.

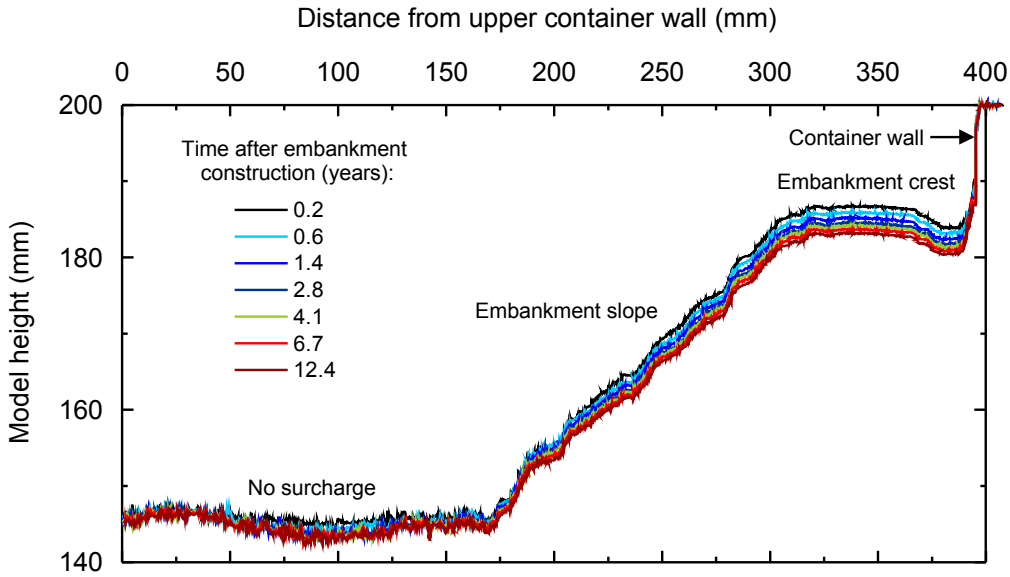

Fig. 6.29: Laser scan results from profile 1.

The average settlement along the profiles 1 and 3, is presented in Fig. 6.30. The centrifuge data are plotted from the beginning of the self-weight consolidation. The zero settlement refers to the end of the self-weight consolidation to allow a comparison with the field data from Embankment 2. The consolidation curve after the embankment construction had a similar shape when compared to the self-weight consolidation curve, with a rapid initial settlement measured after the application of the surcharge. It indicates that similar processes as described in Section 6.8.2 took place: the first part of the consolidation curve exhibits a rapid settlement associated with closing of macro voids due to the increase of vertical stress after the embankment construction. This is followed by a slow rate of consolidation in the following

years due to the reduced hydraulic conductivity and slow dissipation of excess pore pressures generated by the embankment. The comparison of both profiles shows the differential settlement reaching 0.27 m (which is 16% of the maximum settlement) at the end of the test (1.44 m in profile 1 and 1.71 m in profile 3). The settlement presented in Fig. 6.30 corresponds to “total“ settlements measured *in situ* as it includes the settlement of the free landfill surface during the time of monitoring. The settlement of the free landfill surface (without embankment surcharge) in the centrifuge is represented by an average settlement in the counterweight container where no embankment was constructed. The settlement in the counterweight container reached 0.41 m (0.25 m measured immediately after re-acceleration as a result of unloading-reloading cycle and an additional settlement of 0.16 m measured in the following 11 years).

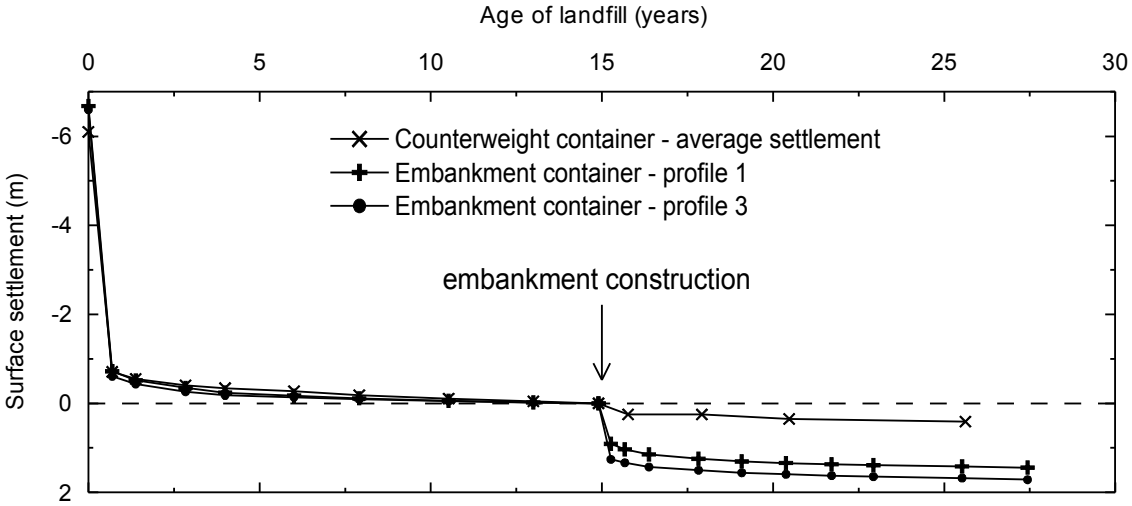

Fig. 6.30: Comparison of surface settlement in profiles 1 and 3 under the embankment and in counterweight container.

However, the comparison of the field and centrifuge results should be presented as net settlement (the settlement generated only by the embankment surcharge, neglecting the variations due to the change of water level *in situ* (Fig. 4.10) and the unloading-reloading cycle and subsequent settlement in the counterweight container in the centrifuge). The net settlements are presented in Fig. 6.31, where total settlements are also indicated by grey lines and empty symbols. The shapes of the centrifuge and field consolidation curves are similar, although the field settlements were lower by approximately 50% than those measured in the centrifuge. This significant difference arose in the initial phase of consolidation (during closing of macro voids), which indicates different intergranular porosities *in situ* and in the centrifuge model. This difference can be explained by the following reasons:

1) The top layer of the landfill *in situ* is exposed to the rainfall and

climate effects. It is likely that clay lumps are decomposed due to weathering and interlump spaces are partly filled with clay, which results in lower compressibility. However, the weathering can result in preferential drainage paths that develop due to cyclic swelling and shrinking in the weathered zone (e.g., Schofield, 1980), which can explain the fast dissipation of pore pressures measured in the field (Fig. 6.27). In the laboratory, weathering does not occur and the soil remains more compressible due to high porosity.

2) Another possible explanation can be associated with groundwater conditions during the self-weight consolidation. *In situ*, water level gradually increased over the years from the bottom of the fill, while in the centrifuge, the model was fully saturated from the beginning of the self-weight consolidation (except of top 7.5 m, which were only partially saturated in the initial part of the consolidation). It caused higher initial vertical effective stress *in situ*, more intensive structure degradation and lower compressibility of the landfill. This phenomenon will be analysed in Section 7.6.2.

3) *In situ* compressibility could have been also partially lowered by preloading of the surface by the rubble stone layer. However, the estimated vertical stress of 19 kPa generated by the rubble stone layer had probably only a minor influence compared to the other effects.

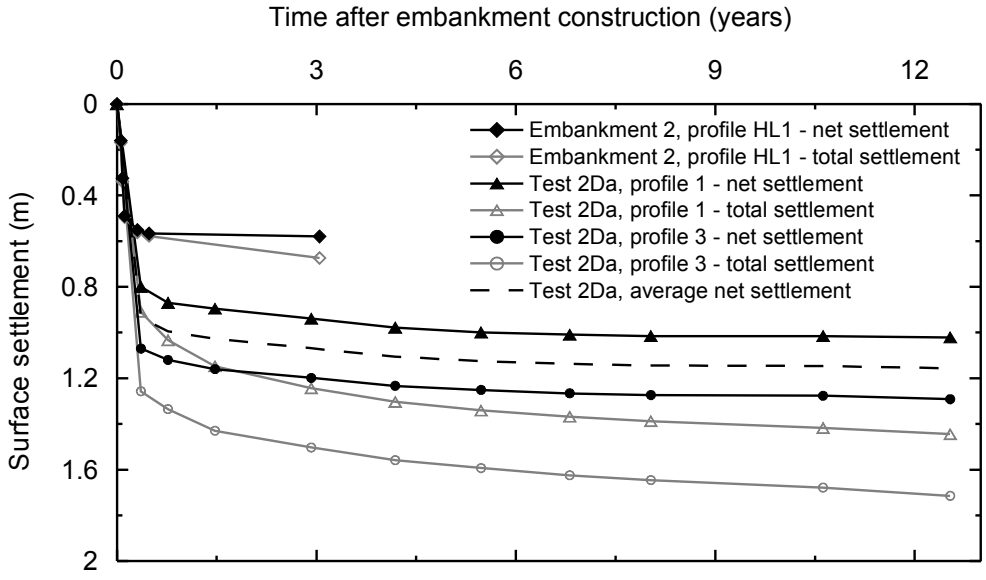

Fig. 6.31: Net settlements and total settlements in situ (Embankment 2, profile HL1) and in centrifuge.

6.9.3 Depth reference points

Pouring of lead balls during the in-flight construction of the embankment in test 2Dc caused the inclination of some straws and those could not be detected by the laser. The small absolute settlement of the straws caused higher inaccuracies and more difficult interpretation of the measured data. The only set of data suitable for processing was from the time of 656 days. The settlement is plotted in Fig. 6.32, together with the *in situ* data from profile B1 (Fig. 4.6). The surface settlements from the field and the centrifuge are also presented for comparison. All data are plotted as the total settlements, because net settlements of the depth reference points could not be calculated (Fig. 6.31 shows that the ratio of total and net surface settlements is similar *in situ* and in the centrifuge, so the relative comparison of total settlements of depth reference points could provide useful information). Significantly higher settlements were measured in the shallow depths in the centrifuge.

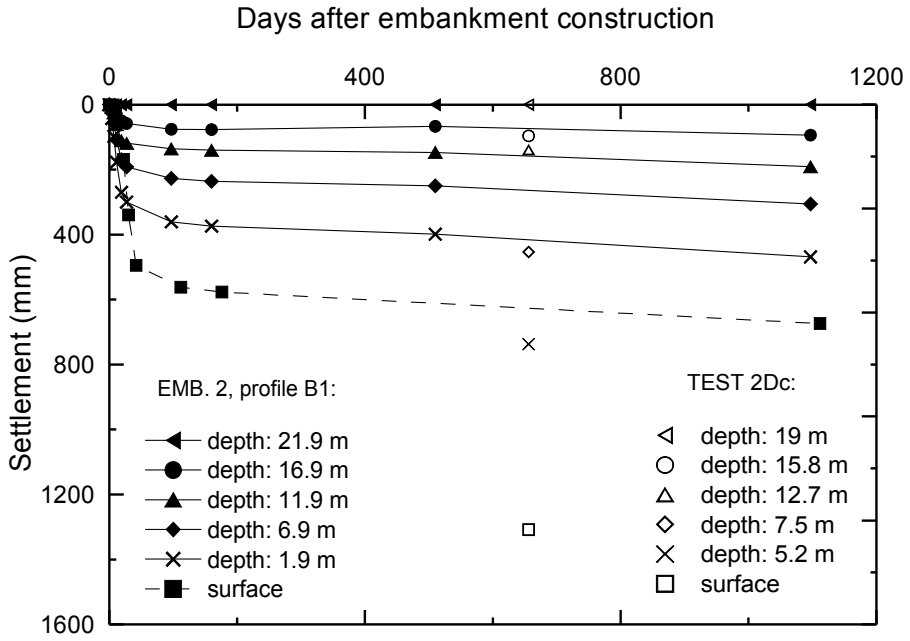

Fig. 6.32: Settlement of depth reference points in situ and in centrifuge. The depth of the reference points before the embankment construction is marked in legend.

The settlement of the centrifuge straws compared to both the *in situ* profiles is presented in Fig. 6.33. The *in situ* settlement at 656 days was interpolated from the measurements carried out 1.5 and 2.9 years after the embankment construction. The settlement in the lower part of the model is similar to the *in situ* data. The interlump voids are mostly closed at depth because of high vertical stress during the self-weight consolidation. In the upper part of the model (approximately top 10-12 m), the settlement is greater

due to the higher interlump porosity compared to the field. These findings are in line with the interpretation of surface deformation measurements. They also correspond with Fig. 6.23, where a very small settlement was observed during the self-weight consolidation in the upper 5-8 metres, indicating that the very soft structure was preserved in the shallow depths after the self-weight consolidation in the centrifuge. It shows that the weather conditions *in situ* and wetting and drying cycles can significantly reduce interlump voids and the compressibility in the shallow depths of the landfill.

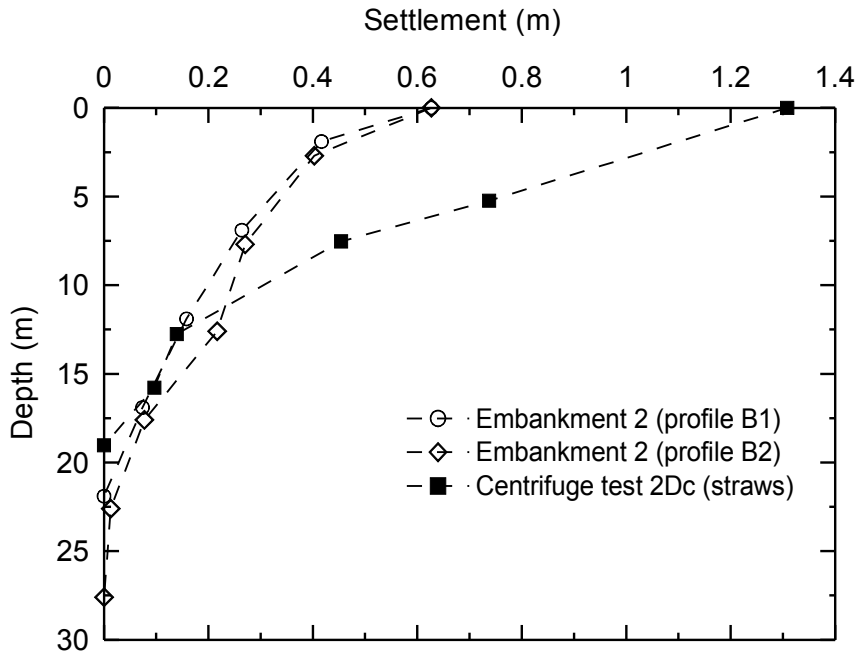

Fig. 6.33: Settlement of depth reference points 656 days after completion of embankment.

6.10 Summary

The results of the *self-weight consolidation* of the landfill models in the geotechnical centrifuge suggested that the hydraulic conductivity of the soil is controlled by its double porosity structure. The structure allows a speedy expulsion of water in the deeper part of the fill, driven by excess pore pressures, and leads to rapid consolidation of the soil. The dissipation of excess pore pressures is much slower after the intergranular voids have closed, being controlled by the permeability of the clay. This process is associated with a fast initial settlement of the landfill surface, which is followed by a slow subsequent settlement, when the porosity and hydraulic conductivity

of the soil decreased. The settlement of straws revealed, that in the top section (5-8 m) of the model the double porosity structure remains and high compressibility is preserved.

The behaviour of the models *after embankment surcharge* confirmed the observations during the self-weight consolidation. Closing of macro voids in the shallow depths produced large initial settlements associated with the high initial permeability of the soil. This was followed by slow consolidation and slow settlement rate after closing of macro voids.

Significantly higher settlements were observed in the centrifuge compared to the field (Embankment 2) due to the higher intergranular porosity in the top 10-12 metres. This difference is attributed to weathering effects *in situ*, which may have caused faster degradation of the soil structure. The soil in the weathered zone is less compressible, although surface cracks develop at shallow depths through cyclic swelling and shrinking *in situ*, permitting fast drainage. The higher settlement of the centrifuge model can be also attributed to different groundwater conditions compared to the field, which affected the initial vertical stress profile and the magnitude of destructuration before the embankment construction.

An unpredictable differential settlement of the landfill surface was observed reaching 0.7 m over the distance of 11 m during the self-weight consolidation. It was caused by horizontal variations in the intergranular porosity due to segregation of the lumps. It occured during the model construction despite the effort to reach a homogeneous lump distribution. The differential settlement was observed also after the embankment construction as a result of closing of macro voids in the shallow depths. It seems to be a serious problem for the construction on the landfills *in situ*, which can be reduced by an appropriate ground improvement technique reducing the volume of intergranular pores.

7 NUMERICAL MODELLING

7.1 Description of constitutive model

The double porosity landfill clay possesses two types of structure: the double porosity structure, which is given by the clay lumps and the macro voids, and the structure of the clay lump, which is given by the sedimentation fabric and the overconsolidation of the clay. The combined effect of both the structures must be considered in a numerical model.

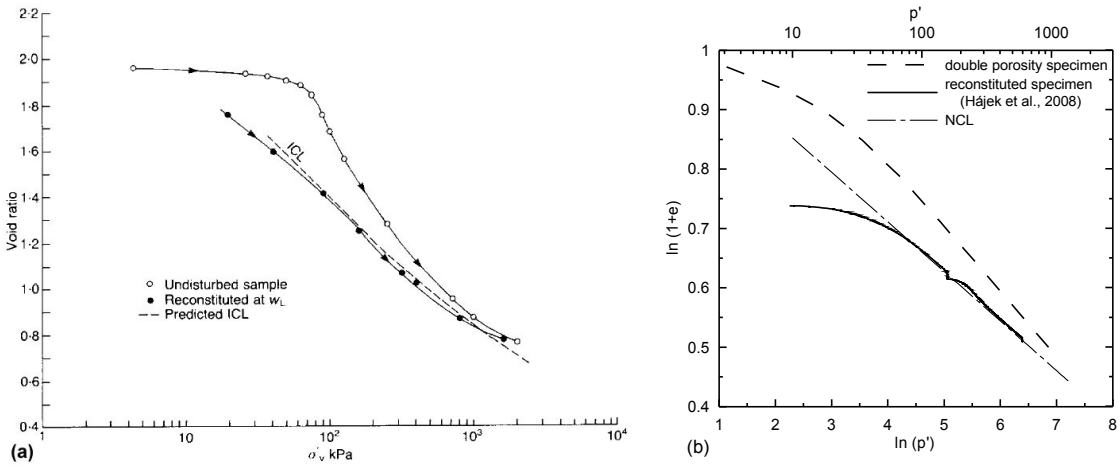

Fig. 7.1: Comparison of compression test on (a) natural structured clay (Bothkennar clay, Burland, 1990) and (b) granulated clay with double porosity structure from "5. květen" landfill.

Double porosity clays exhibit a similar mechanical behaviour as natural structured clays as demonstrated in Fig. 7.1. Therefore the same constitutive models can be used for modelling of the natural and double porosity structured clays. A parallel between the behaviour of the natural structured clays and the double porosity clays was used also by Koliji et al. (2008) for the modelling of aggregated soil with double porosity structure.

A number of advanced constitutive models for structured clays was developed in past years using different approaches including elastoplasticity framework (Kavvadas and Amorosi, 2000; Rouainia and Muir Wood, 2000; Wheeler et al, 2003; Baudet and Stallebrass, 2004, Callisto et al., 2002), viscoplasticity (Rocchi et al, 2003) and hypoplasticity (Mašín, 2007).

Some studies were focused on the behaviour of the double porosity materials, including a constitutive framework for aggregated soils with the double porosity structure (Koliji et al., 2008), development of the constitutive model for unsaturated double porosity soils (Koliji et al., 2008b), the application of the meshless method for consolidation of the lumpy clay (Nogami et al., 2004) or using of finite element method to solve the non-linear permeability of the double porosity clay fill (Yang and Tan, 2005; Wong et al., 2007).

For the purpose of this thesis, modelling of the soil structure and its degradation with plastic strain is the key aspect of the constitutive model. The hypoplastic constitutive model for clays with meta-stable structure developed by Mašín (2007) was chosen for the numerical modelling because of a small number of model parameters, simple calibration procedure and a good performance when compared to advanced elastoplastic models (Mašín, 2009). The model was developed by introducing a structure degradation law into the hypoplastic model for clays developed by Mašín (2005). The more accurate predictions of the hypoplastic model when compared with the elastoplastic models (Mašín, 2009) are due to the non-linear nature of the hypoplastic equation. It does not a priori distinguish between elastic and plastic deformations and it includes anelastic deformations from the beginning of the loading process (Kolymbas et al., 2000).

The basic hypoplastic model for clays (Mašín, 2005) requires five parameters, similar to the parameters of the Modified Cam Clay model: φ_c - critical state friction angle, λ^* - slope of isotropic normal compression line, κ^* - slope of isotropic swelling line, N - position of normal compression line, r_h - shear stiffness parameter. All these parameters can be easily calibrated from the isotropic compression test and triaxial shear test on a reconstituted soil.

In the hypoplastic model the structure is incorporated in a similar way as in the other recent models for structured clays (e.g. Baudet and Stallebrass, 2004; Callisto et al., 2002; Rocchi et al, 2003), namely by using the sensitivity framework developed by Cotecchia and Chandler (2000). They demonstrated the similar response to loading (both in compression and shear) shown by clays of different origins, histories and structure. Both reconstituted and natural

(structured) clays have the state boundary surface (SBS - the surface in the stress-porosity space, which bounds all accessible states of the soil) of the same shape. The differences in the mechanical behaviour of the natural and reconstituted soils are given by the different sizes of SBS, while other soil properties remain unchanged. Sensitivity is then defined as the ratio of the size of SBS of the natural clay to the corresponding size of SBS of the reconstituted clay at the same specific volume (Fig. 7.2). Clays with the stable structure can be defined by the constant sensitivity, while clays with meta-stable structure can be characterized by decreasing sensitivity due to the structure degradation during compression and shear.

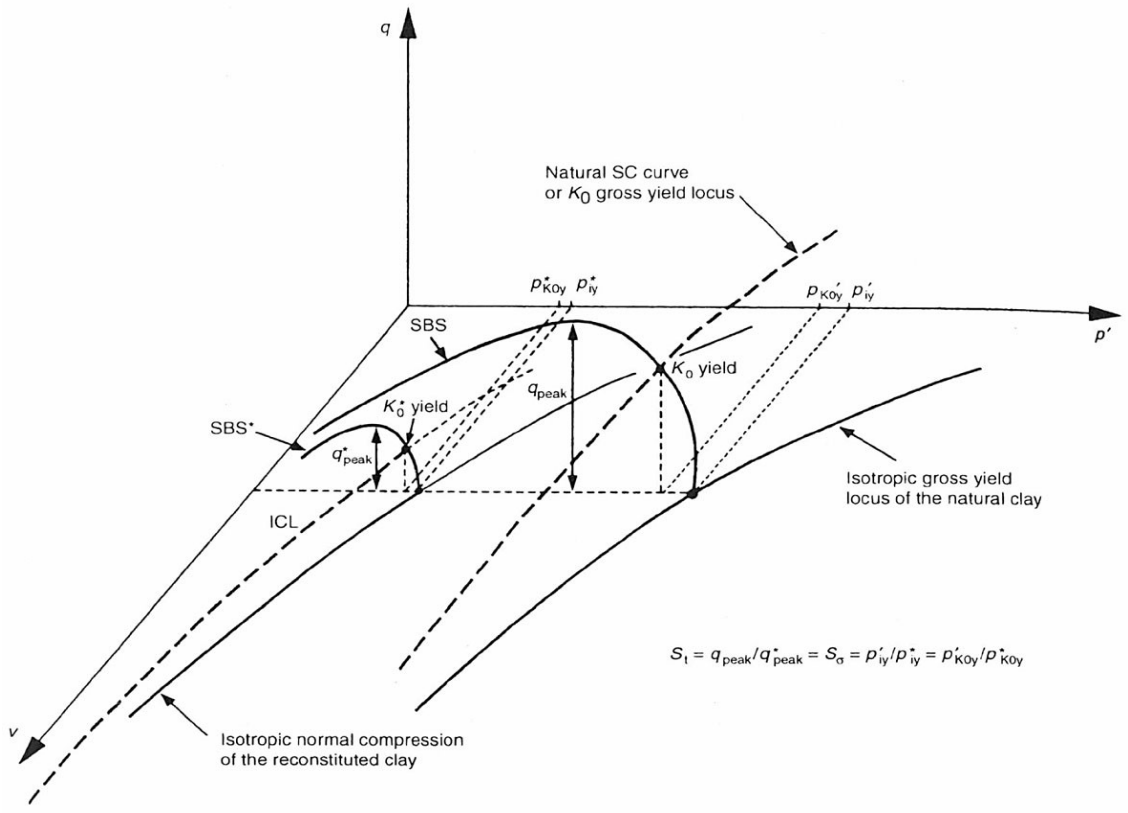

Fig. 7.2: Definition of sensitivity based on idealized behaviour of natural and reconstituted clay (Cotecchia and Chandler, 2000).

The incorporation of the structure into the hypoplastic constitutive model for clays requires one additional state variable *s* (*sensitivity*), defined as the ratio of the sizes of SBS of the structured and reference (reconstituted) materials. The rate formulation of sensitivity reads

$$\dot{s} = \frac{k_h}{\lambda^*} (s - s_f) \, \dot{\epsilon}^d \tag{7.1}$$

where k_h is a constitutive parameter that controls the rate of the structure degradation and s_f is the final sensitivity. The damage strain rate $\dot{\epsilon}^d$ is defined by

$$\dot{\epsilon}^d = \sqrt{(\dot{\epsilon}_v)^2 + \frac{A}{1-A}(\dot{\epsilon}_s)^2} \tag{7.2}$$

where A is a parameter that controls the relative importance of volumetric $\dot{\epsilon}_v$ and shear $\dot{\epsilon}_s$ components (Mašín, 2007).

The incorporation of the structure therefore requires three new model parameters (k_h, s_f and A) and the specification of the initial sensitivity s_0. The influence of the model parameters A and k_h on model predictions is demonstrated in terms of normalised incremental response envelopes (Mašín and Herle, 2005) in Fig. 7.3. The response envelopes were proposed as a graphical representation of the resulting stress rates imposed by different unit strain rates at one particular initial state. The influence of the parameter k_h and initial sensitivity s_0 in *ln v - ln p'* space can be seen in Fig. 7.4.

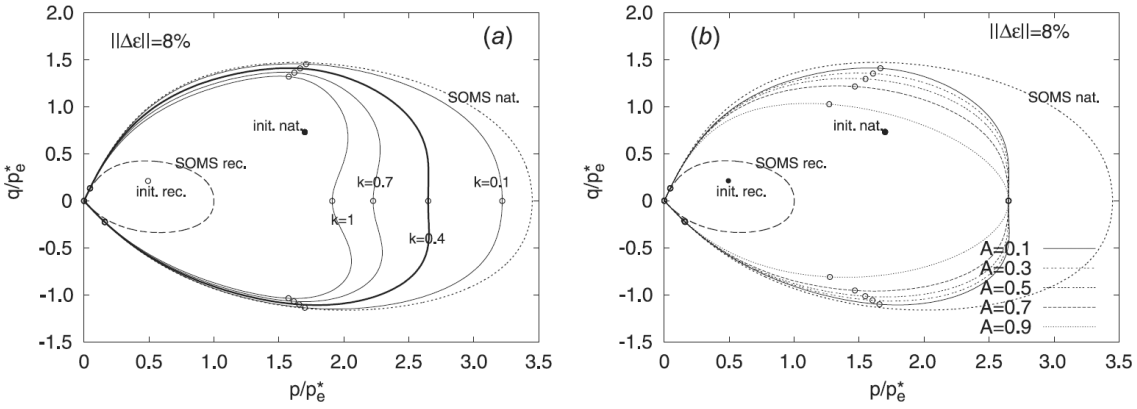

Fig. 7.3: Rate of the structure degradation measured by means of normalised incremental stress response envelopes (k is used for parameter k_h, Mašín, 2007).

The numerical modelling presented in this thesis was performed using finite element method with software package Tochnog Professional (Rodemann, 2008).

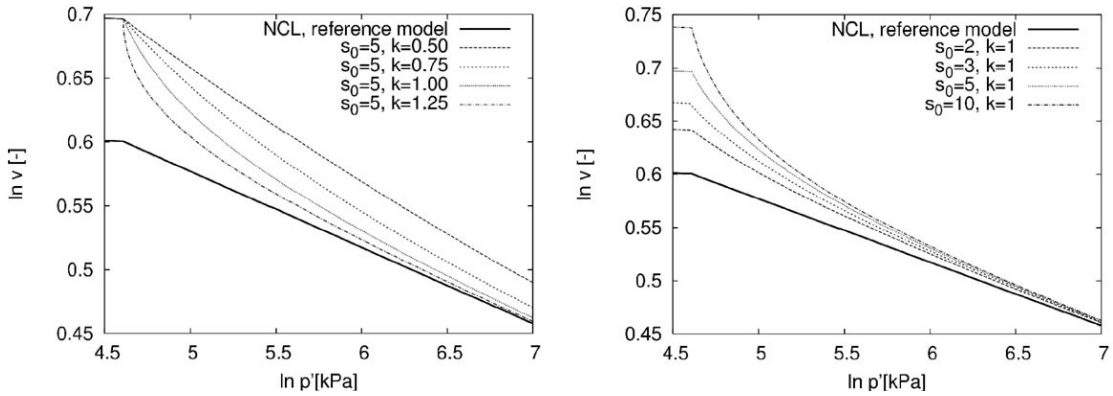

Fig. 7.4: Influence of parameter k_h (k is used for parameter k_h) and initial sensitivity s_0 in isotropic compression test (Mašín, 2009).

7.2 Determination of parameters for constitutive model

A number of laboratory tests on the landfill material has been carried out by various researchers at Charles University recently. Some of the experiments are discussed in this section and used for calibration of the constitutive model. Additional tests were carried out by the author to complete the available data and to assure that the behaviour of the subsoil of the trial embankments coincides with earlier results.

All presented laboratory tests were carried out on specimens from the former “5. květen“ mine (the same soil was used also for the centrifuge tests). The exceptions are the triaxial compression tests presented in Section 7.2.1.2, which were carried out on the specimens from the trial embankments subsoil and the tests of Enriquez (2006) carried out on the clay from the Marie mine in the Sokolov Basin located SW from the Most Basin (Fig. 3.1). The properties of the clay from the Most and Sokolov Basins are very similar as demonstrated in Tab. 7.1. The laboratory tests were carried out in triaxial and oedometer apparatuses in the laboratories at Charles University in Prague and ETH Zürich.

site		*Former mine "5. květen", Most Basin*	*Former mine Marie, Sokolov Basin (Enriquez, 2006)*
w_L		72	71
I_P		46	32
Density of solid particles		2.71 g/cm^3	2.66 g/cm^3
Grading	sand	11%	13%
	silt	56%	57%
	clay	33%	30%
Mineralogy		Kaolinite 36%, Smectite 25%, Illite/Muscovite 12%, Quartz 21%, < 3%: K-Feldspar, Siderite, Anatase	Kaolinite 36%, Smectite 20%, Illite/Muscovite 10%, K-Feldspar 14%, Siderite 7%, Quartz 5%, Chlorite 3%, < 3%: Calcite, Pyrite, Anatase

Tab. 7.1: Properties of clay samples from the Most and Sokolov Basins.

7.2.1 Calibration of basic hypoplastic model

7.2.1.1 Calibration of soil compressibility (parameters **N** *and* **λ*** *)*

Isotropic compression tests on reconstituted clay specimens from the "5. květen" landfill carried out by Hájek (2008) were used for calibration of the model parameters N and λ^*. The description of the laboratory experiments can be also found in Hájek et al. (2009).

From the five tests presented in Hájek et al. (2009), the three tests with the most similar slope of NCL were chosen for calibrating the parameters for the constitutive model (Fig. 7.5). The values of $N = 1.045$ and $\lambda^* = 0.0835$ were determined. The parameter κ^* for the particular tests was difficult to determine (Fig. 7.5). The parameter influences significantly the compression curve in the low stress range and therefore its value used in the numerical simulations was specified directly from the oedometer tests on double porosity specimens with reduced granulometry (Section 7.2.2). In calibrating the other parameters on the tests with reconstituted soil, however, the value of $\kappa^* = 0.014$ was used.

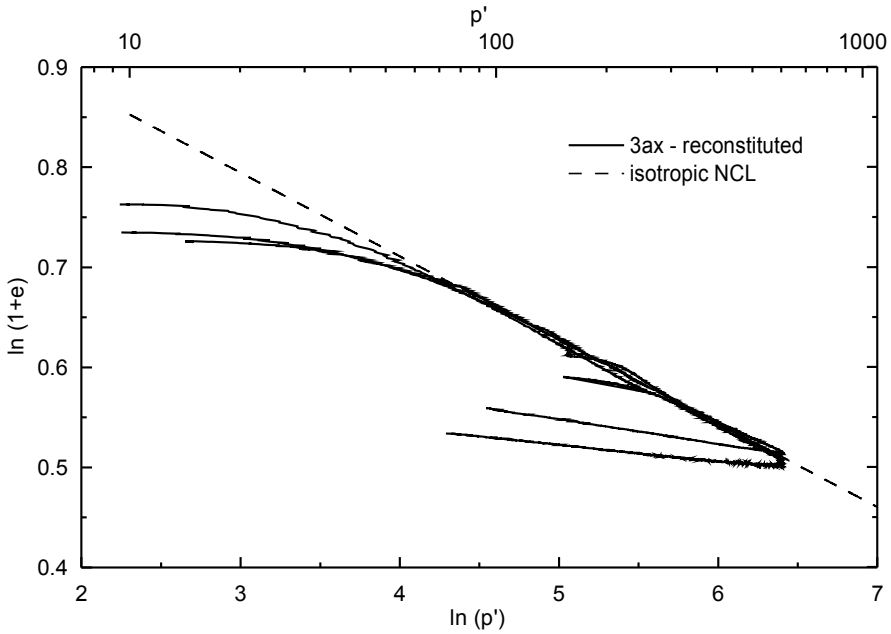

Fig. 7.5: Calibration of parameters N and λ on isotropically compressed triaxial specimens by Hájek et al (2008).*

7.2.1.2 Calibration of shear strength and stiffness (parameters φ_c and r_h)

A set of triaxial compression tests on the reconstituted specimens was carried out to determine the parameter φ_c'. The rotary drill core samples from the subsoil of Embankment 1 were reconstituted from a slurry of the water content of 1.5 w_L and K_0 compressed to 50 kPa in a high press. The triaxial specimens had a diameter of 38 mm and height of 76 mm. A radial drainage was used. The specimens were saturated and consolidated isotropically to the required mean effective stress (p' = 100, 200 and 300 kPa). Undrained shear tests with the measurement of pore pressures were carried out (the rate of axial deformation was 0.0015 mm/min).

The value of φ_c' = 22.4° was determined and used as the parameter of the constitutive model. The stress paths of the tests and the critical state stress envelope passing through the origin are plotted in Fig. 7.6. It shows also the results of two tests on undisturbed specimens. These tests represent a material of the partially decomposed clay lump. Estimated φ_p' is 30° (c' = 0 kPa). However, it is expected that the peak strength of the clay lump material will depend on the maximum depth of the soil before its excavation and can be variable due to the different overconsolidation.

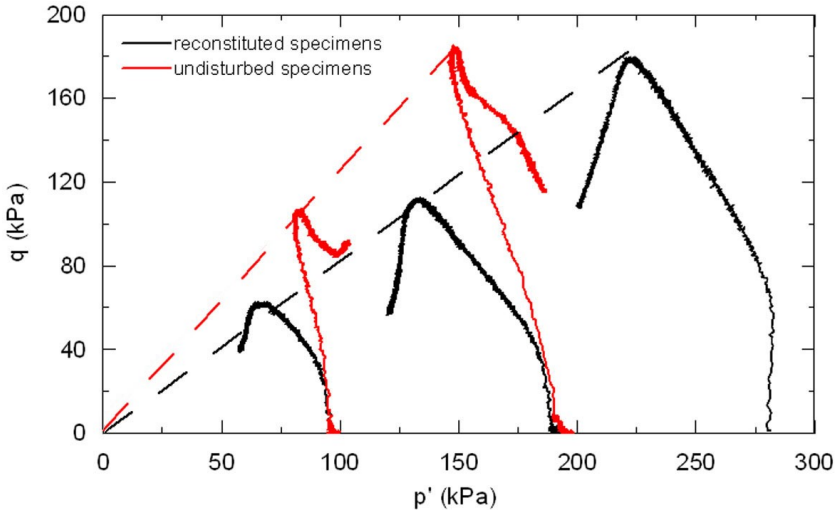

Fig. 7.6: Triaxial compression tests on reconstituted and undisturbed specimens.

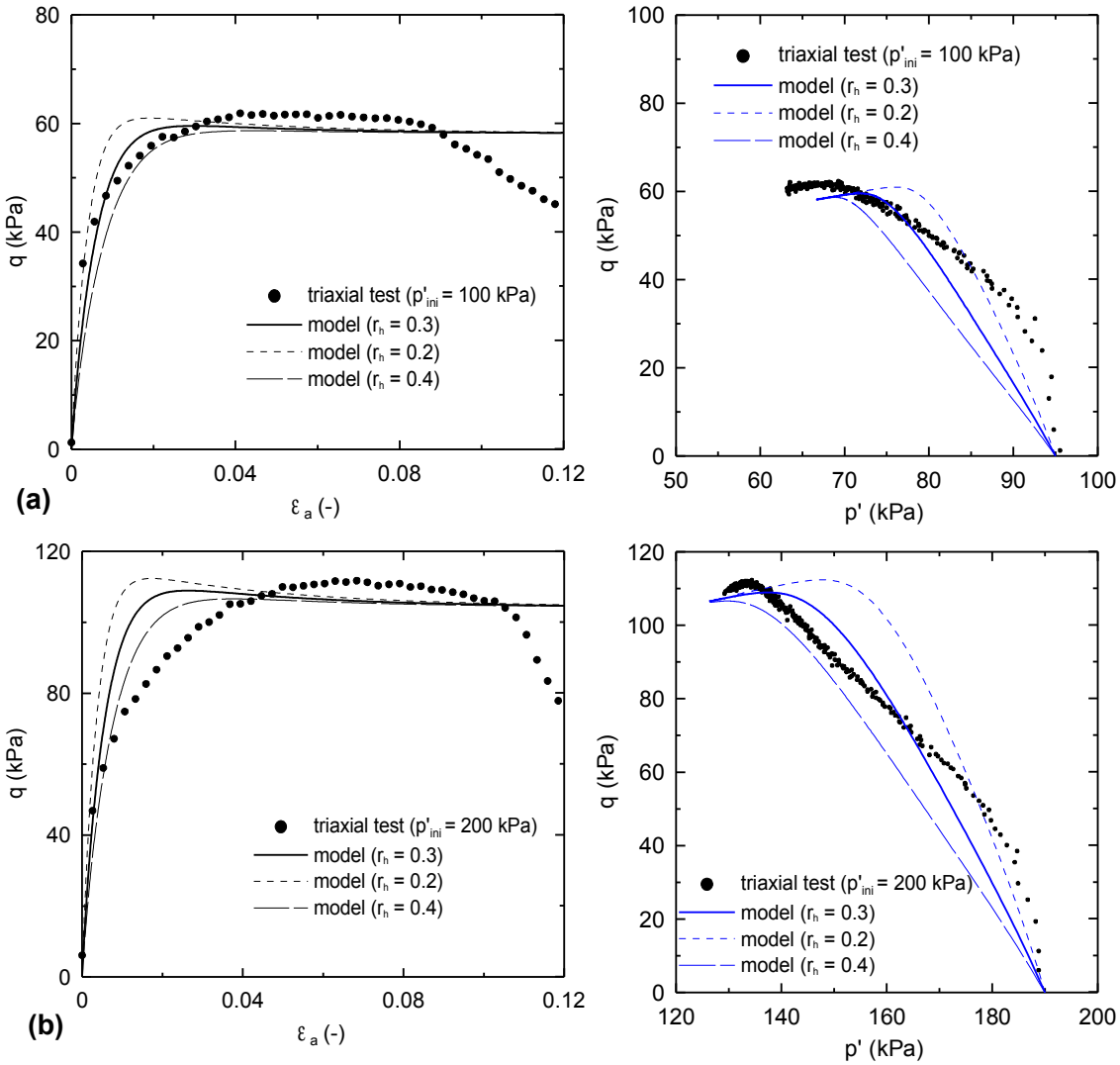

Fig. 7.7: Calibration of the parameter r_h using the results of triaxial compression tests on reconstituted clay: (a) - specimen consolidated to p' = 100 kPa; (b) - specimen consolidated to p' = 200 kPa. Stress path are plotted until the critical state was reached.

The parameter r_h was calibrated by a parametric study on stress-strain curves of the reconstituted triaxial specimens carried out at mean effective stress 100 and 200 kPa (Fig. 7.7). The best correlation was found for r_h = 0.3.

7.2.1.3 Evaluation of the basic hypoplastic model

Two different test series on the reconstituted specimens were used for the calibration of the basic hypoplastic model. Therefore the performance of the model was subsequently examined by simulating three triaxial compression tests on the material of the clay lump from the “5. květen“ landfill carried out by Herbstová et al. (2005). The evaluation demonstrates that the parameters based on the reconstituted clay are suitable for predictions of the behaviour of the clay lump material. Fig. 7.8 presents the predictions of the stress strain curves and stress paths of the three tests with different overconsolidation ratio (specimens were reconsolidated in the triaxial cell to the mean effective stresses 50, 140 and 800 kPa). The results confirmed a good agreement of the numerical simulation with the measured data. The post rupture strength of the triaxial specimens, which is expected to lie close to the critical state line (Burland, 1990) also closely correlates with the critical state friction angle of φ_c' = 22.4° used for the calibration of the model.

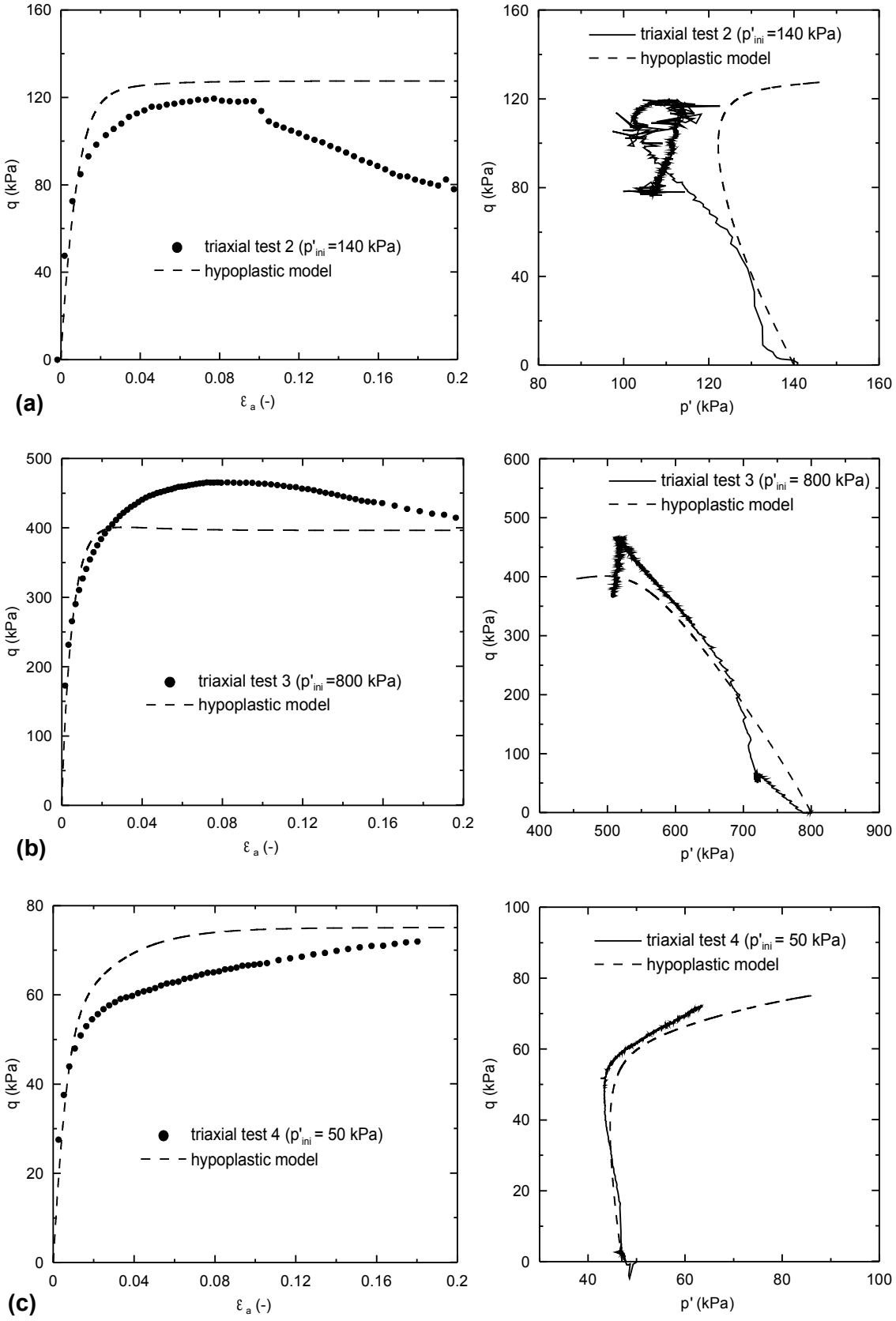

Fig. 7.8: Triaxial compression tests on material of clay lump and prediction of basic hypoplastic model for clays.

7.2.2 Calibration of parameters describing double porosity structure

The structure parameters k_h, A and s_f were calibrated, and the initial sensitivity of the soil s_0 was specified, from the oedometer tests on the double porosity clay specimens with scaled-down lump size distribution preconsolidated in the mini-centrifuge to different vertical effective stress (tests discussed in detail in Section 5.6.5, Fig. 5.24). The reference material was represented by the reconstituted clay (Section 7.2.1), since its properties were shown to be equivalent to the properties of the clay lump material. The different conditions during the isotropic compression tests (calibration of the basic hypoplastic model) and K_0 compression (calibration of the structure parameters) were respected as presented in Fig. 7.9. For oedometer tests the value of p' was calculated using $K_0 = 0.62$ obtained from Jaky's formula $K_0 = 1 - \sin\varphi_c'$.

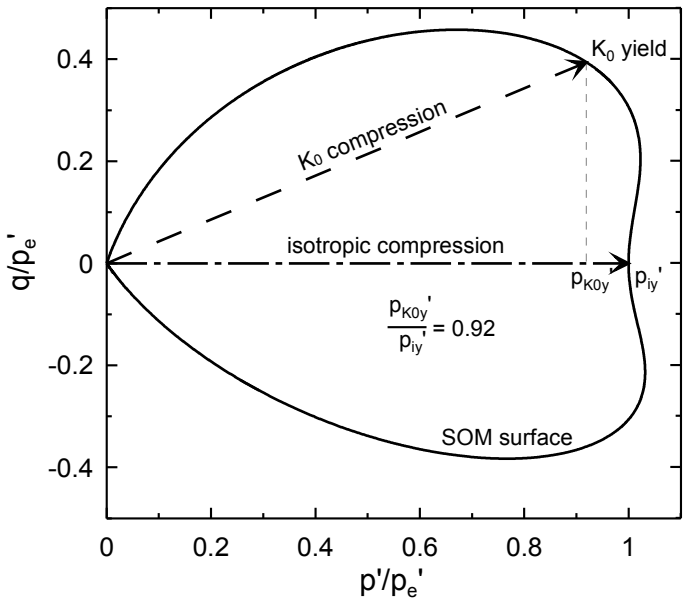

Fig. 7.9: Swept-out-memory (SOM) surface of basic hypoplastic model with isotropic and K_0 normal compression lines. The ratio of mean effective stresses at yield in isotropic and K_0 compression of 0.92 was respected during calibration.*

As no shear tests on the double porosity material were performed, a value of the parameter A was estimated based on the experience with the behaviour of natural structured clays, $A = 0.25$ (Mašín, 2007). The comparison of the compression lines of the undisturbed and reconstituted specimens in

* SOM surface is a close approximation of the state boundary surface (Mašín and Herle, 2005), which is not explicitly included in the formulation of the hypoplastic model.

Figs 7.10 indicates that the compression lines of the undisturbed specimens are influenced by the overconsolidation of the clay and no effect of the bonding inside the clay lumps can be observed. The structure of the double porosity specimen with reduced granulometry is controlled by the structure of the clay lumps (given by their overconsolidation) and the macro voids (the volume of macro voids in a particular stress level can be quantified as a difference in *ln (1+e)* between the undisturbed and double porosity specimen in Fig. 7.10). The required vertical stress for the complete removing of the soil structure (overconsolidation + macrovoids) was not reached before the end of the oedometer tests (Fig. 7.11). However, the results indicate that at higher stresses the compression line of the double porosity specimens will join the NCL of the reconstituted soil and the value of s_f = 1 was therefore used. The oedometer tests on undisturbed, reconstituted and double porosity clay specimens from the Sokolov Basin carried out up to σ_v' = 7000 kPa (Enriquez, 2006) proved a complete destructuration of the double porosity clay specimen.

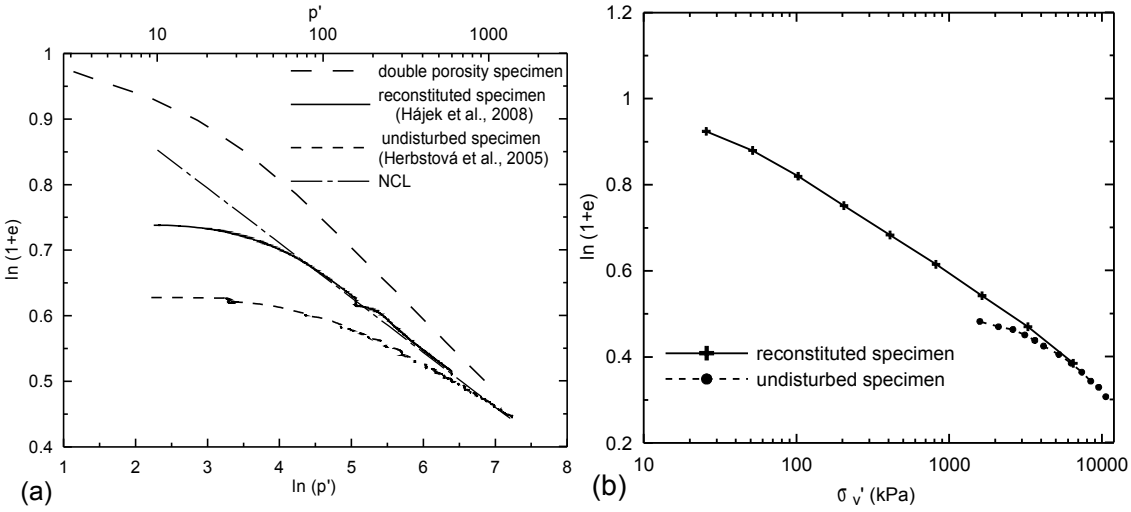

Fig. 7.10: (a) - comparison of compression tests on reconstituted clay, undisturbed specimen from landfill (partially decomposed) and double porosity specimen with reduced granulometry ("5. květen" landfill); (b) - compression tests on reconstituted and undisturbed clay from the Sokolov Basin (Enriquez, 2006).

The parameter k_h, the initial value of structure s_0 and the basic model parameter κ^*, which influence the slope of the compression curve before reaching NCL, were calibrated separately for each oedometer double porosity specimen (Section 5.6.5). Figure 7.11 shows the best-fit curves for all 7 oedometer specimens. Table 7.2 summarizes the corresponding values of k_h, κ^* and s_0 together with the maximum σ_v' reached during the pre-consolidation of the soil in the mini-centrifuge before the oedometer tests. When plotted against σ_v' reached in the centrifuge (Fig. 7.12a-c), it is evident that the parameter κ^* and the value of s_0 depend on the pre-consolidation vertical

stress and consequently on the initial void ratio of the oedometer specimens.

Oedometer test No.	σ'_v *in centrifuge (kPa)*	κ^*	k_h	s_0	e_0
1	20	0.023	0.35	7.2	1.73
2	55	0.016	0.35	4.2	1.48
3	94	0.0135	0.35	2.8	1.35
4	18	0.019	0.27	5.8	1.64
5	33	0.014	0.21	5.3	1.57
6	69	0.009	0.28	3.7	1.38
7	80	0.009	0.18	3.8	1.39

Tab. 7.2: Data from calibration of the soil structure parameters on oedometer specimens with reduced granulometry.

No stress dependency was found for the parameter k_h, so the average value from all tests (k_h = 0.28) was considered.

For the stress dependent parameter κ^* it was taken into account that the initial conditions for the centrifuge modelling should represent the loosest state of the landfill before the self-weight consolidation takes place. Therefore κ^* = 0.0187 was chosen as a mean value of the three loosest oedometer specimens.

A similar dependency on the vertical stress was found also for the initial sensitivity s_0. It is not surprising, since increasing the vertical stress in the mini-centrifuge causes a degradation of the soil structure. Even a small change in s_0 significantly influences the predictions of the landfill settlement, because it influences the yield stress, in which the soil stiffness decreases significantly due to structure degradation (Fig. 7.13). The importance of the initial sensitivity and its influence on the “apparent preconsolidation stress“ was discussed also by Koliji et al. (2008). The dependency of s_0 on e_0 was therefore considered in the present analyses. A linear relationship was found to represent appropriately the experimental data (Fig. 7.12d):

$$s_0 = 10.35 \cdot e_0 - 10.87 \tag{7.3}$$

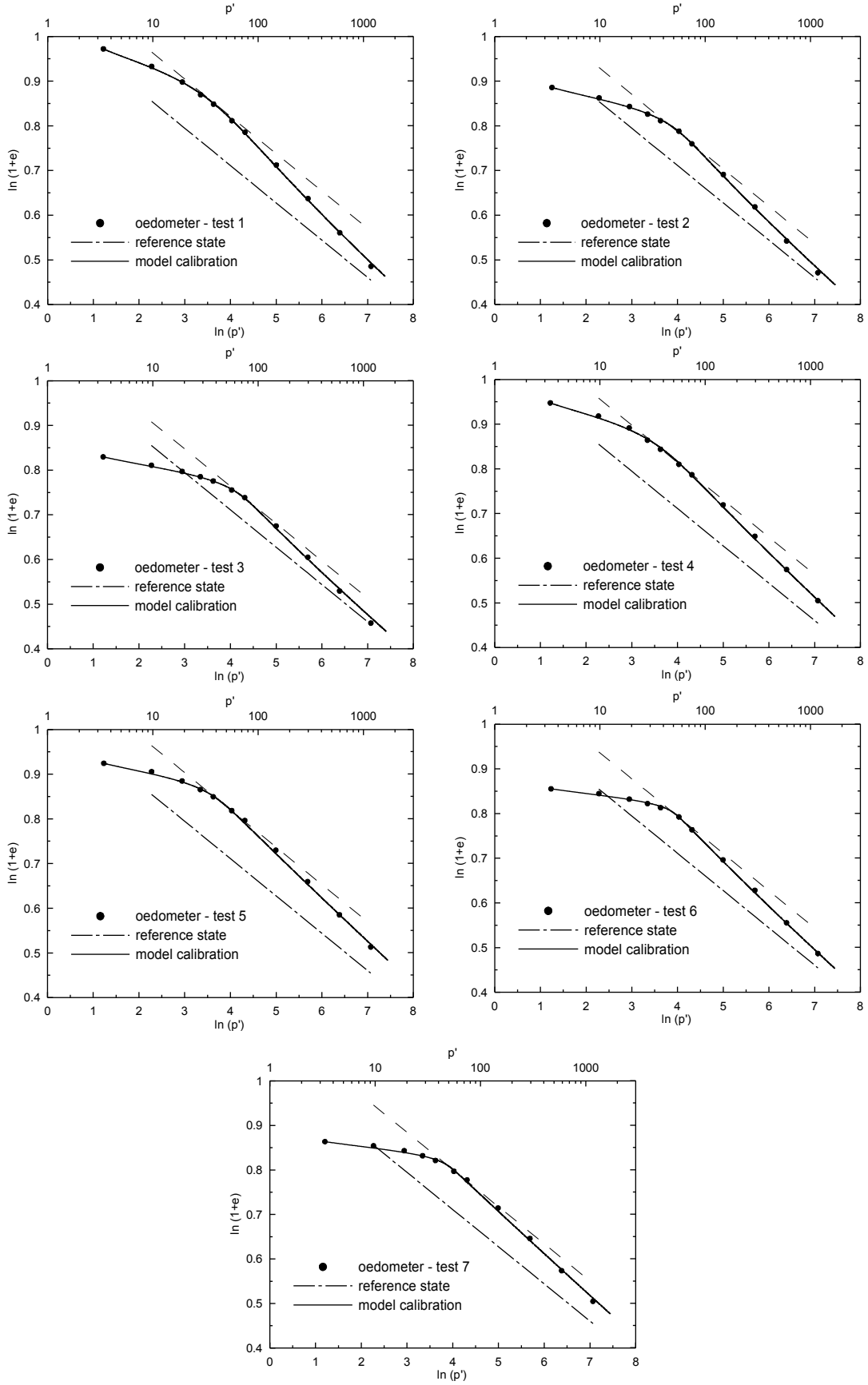

Fig. 7.11: Calibration of soil structure from oedometer tests on double porosity clay.

The initial void ratio was measured in the first step of the oedometer loading curve, which corresponded to the mean effective stress of 0.4 kPa. The initial value of e_0 was determined before the start of each centrifuge test and therefore e_0 and s_0 could be specified for the numerical modelling of each centrifuge test. The initial value of e_0 from the field was not available, so the average value of those measured before the centrifuge tests was used for the numerical modelling of the case histories.

A summary of the calibrated parameters of the hypoplastic model for structured clays is given in Tab. 7.3.

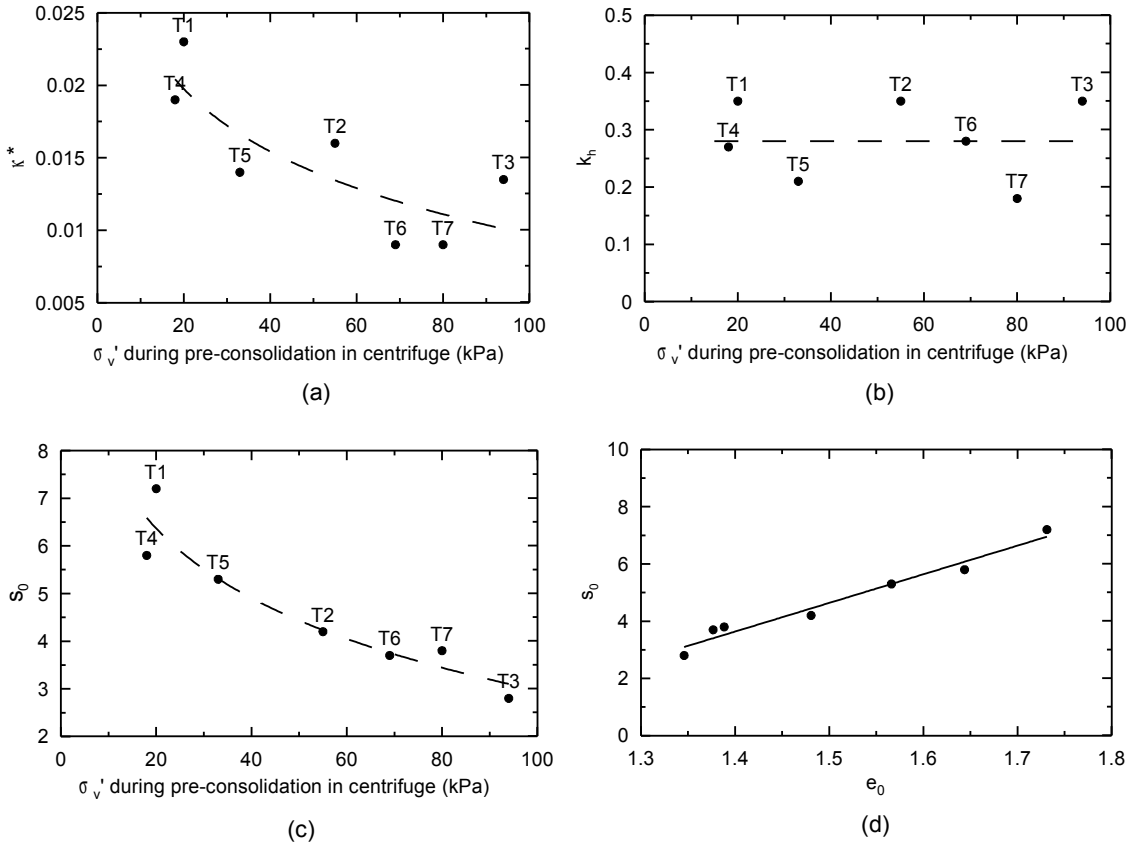

Fig. 7.12: The dependency between preconsolidation stress applied to the oedometer specimens in the mini-centrifuge and k_h, κ^* and s_0 (a, b, c). The dependency between e_0 and s_0 (d).

φ_c'	λ^*	κ^*	N	r_h	k_h	A	s_f
22.4	0.0835	0.0187	1.045	0.3	0.28	0.25	1

Tab. 7.3: Parameters of hypoplastic models for clays with meta-stable structure.

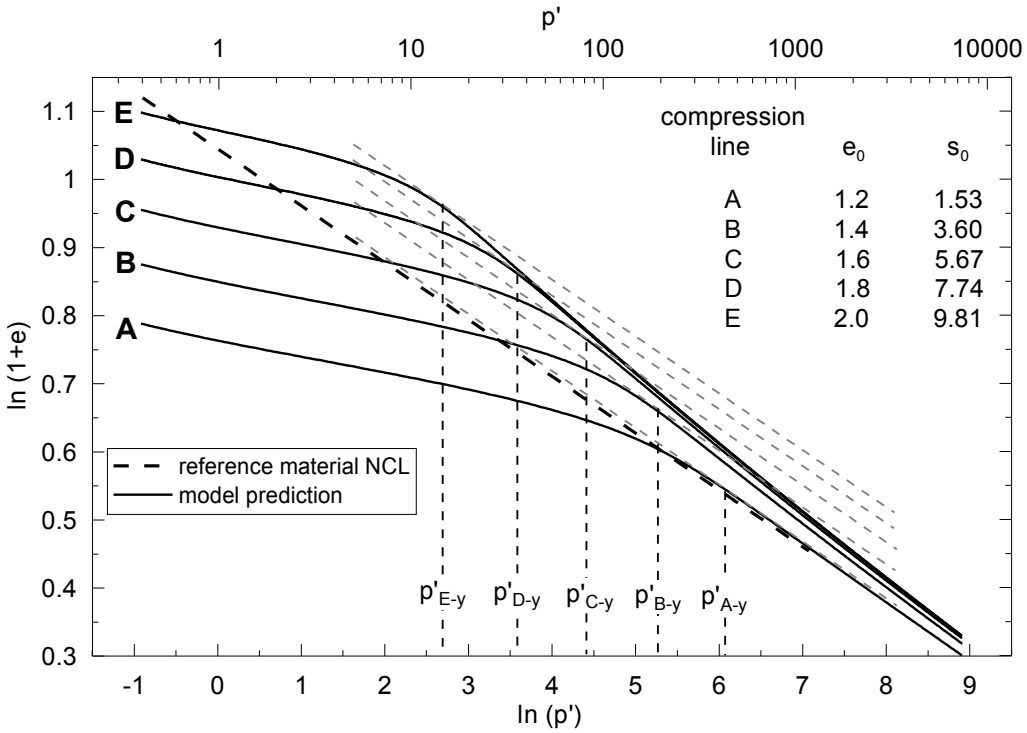

Fig. 7.13: Influence of initial void ratio on soil structure and yield stress p'_y in K_0 compression.

7.3 Modelling of mini-centrifuge tests

1D finite element consolidation analyses of two sets of mini-centrifuge tests were carried out. The aim was to compare the final settlement obtained from the mini-centrifuge with the numerical modelling results (Section 7.3.2) and to evaluate the effect of unloading on the measurements of the height taken during the tests (Section 7.3.3). The description of the mini-centrifuge and the test procedure were presented in Sections 5.2 and 5.5.

7.3.1 Initial conditions

The mini-centrifuge tests 5-8 (LSD curve 1) and 9-11 (LSD curve 2) (Section 5.6) were chosen for the numerical modelling (the average properties of the models before flooding are presented in Tab. 5.2). The initial properties for the numerical modelling had to be specified after the saturation and full swelling of the models.

For the modelling the parameters listed in Tab. 7.3 were used. The initial void ratio e_0 was calculated for each mini-centrifuge test from the dry mass of the soil and its volume (e_0 = 2.12; 2.03; 2.08; 2.07 for models 5-8 and e_0 = 1.8; 1.72; 1.85 for models 9-11). The average from the measured values for each set of tests was used: e_0 = 2.07 for tests 5-8 and e_0 =1.79 for tests 9-11. The initial sensitivity was calculated from Eq. 7.1, reaching s_0 = 10.54 for tests 5-8 and s_0 = 7.63 for tests 9-11. The height of the simulated landfill corresponded to the average prototype height of 19.2 m for tests 5-8 and 40.3 m for tests 9-11 (swelling during the saturation of the models was 7% in tests 5-8 and 13% in tests 9-11).

The hydraulic conductivity linearly dependent on the landfill depth was used ($k = 5*10^{-8}$ m/s at $\sigma_v' = 5$ kPa and $k = 1*10^{-10}$ m/s at $\sigma_v' = 150$ kPa). The values were based on a back analysis of the self-weight consolidation of the geotechnical centrifuge model 2Da (Section 7.5.4). The shape of the initial part of the consolidation curve in the mini-centrifuge was significantly influenced by unloading-reloading cycles and therefore it could not be used in determining the hydraulic conductivity. The grading curve of the geotechnical centrifuge models corresponded to the LSD curve 2, which could lead to an underestimation of the hydraulic conductivity in the numerical modelling of the mini-centrifuge tests 5-8 (no fines in macro voids).

Similarly to the mini-centrifuge models, the numerical modelling was carried out with an assumption of a fully saturated soil and both top and bottom drainage. The curvature of the vertical stress profile in the centrifuge (Fig. 5.5) was neglected and the linear increase of σ_v' with the model depth was assumed in all numerical models.

7.3.2 Modelling of self-weight consolidation of mini-centrifuge tests

The comparison of the mini-centrifuge and numerical modelling of both sets of tests is presented in Fig. 7.14. The settlement measured after 25 years of the self-weight consolidation in the mini-centrifuge reached 3.67-3.94 m for tests 5-8 with the average settlement of 3.8 m. The numerical model showed the settlement of 4.74 m. The mini-centrifuge models 9-11 reached the settlement 7.7-9.2 m with the average of 8.4 m, while the numerical modelling gave 9.8 m. The most of this difference is believed to be due to unloading before the measurement of the model height in the mini-centrifuge (this problem is analysed in Section 7.3.3).

The shape of the experimental consolidation curves was also influenced by the unloading-reloading cycles: the initial part of the settlement curve exhibits an apparently lower permeability as a result of the relatively long

time of the acceleration and deceleration stages compared to the time at maximum g-level (see Fig. 5.10). The continuous settlement measured in the later part of the mini-centrifuge tests could be partly associated with unloading-reloading cycles, which increased the settlement even after the full dissipation of the pore pressures.

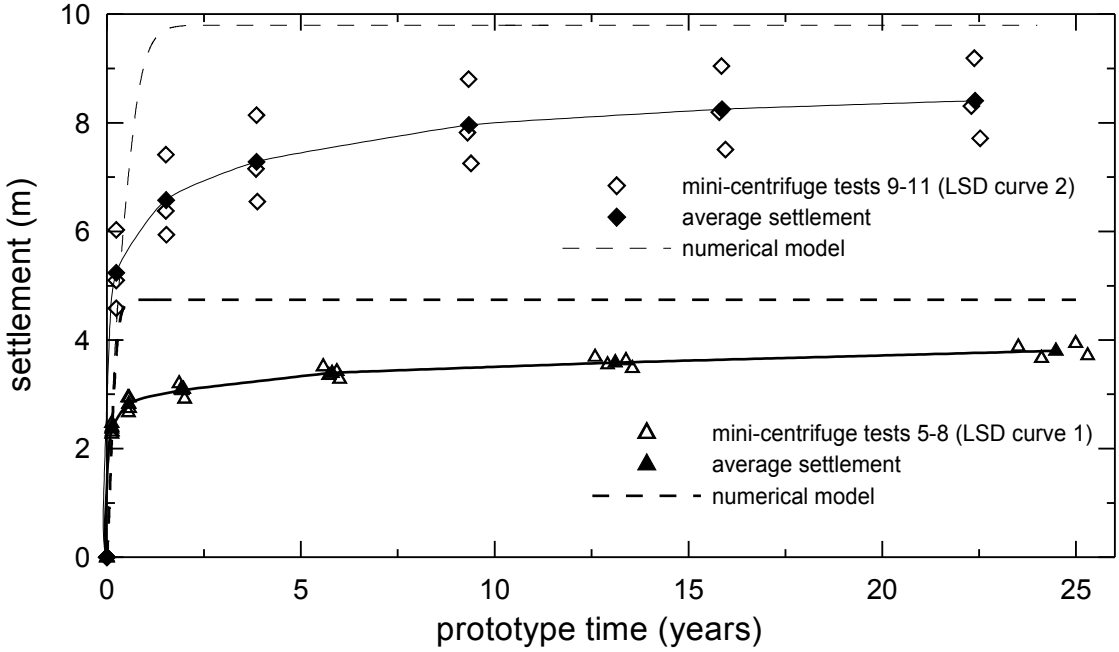

Fig. 7.14: Performance of numerical model compared to mini-centrifuge tests.

7.3.3 Effect of unloading-reloading cycles

The effect of unloading was analysed by the numerical modelling of the mini-centrifuge tests 5-8 using the same geometry and initial conditions as described in Section 7.3.1, with one modification. The model parameter κ^* presented in Tab. 7.3 was calibrated to simulate correctly the first part of the compression line before it reaches the NCL. Such a value of κ^* leads to an overestimation of the stiffness in unloading. The behaviour of the soil during unloading was not considered because no unloading takes place in the simulation of the case history. For the investigation of unloading in the mini-centrifuge, the parameter κ^* was changed from $\kappa^* = 0.0187$ to $\kappa^* = 0.022$ before the unloading started. The value of $\kappa^* = 0.022$ was an average of the slopes of the swelling lines in the oedometer tests of the double porosity specimens (Fig. 5.24). The unloading from $\sigma_v' = 100$ kPa was considered as it

corresponded better with the average σ_v' in the mini-centrifuge model.

Unfortunately, the numerical model did not converge while modelling full unloading, so the effect of unloading in the mini-centrifuge could not be directly evaluated. The most likely reason was the dependency of the soil stiffness on the stress level predicted by the hypoplastic model. At low stresses (high unloading) the stiffness was too low, which caused problems in the coupled consolidation analysis. The maximum unloading, which could be modelled corresponded to 31 g. A parametric study was carried out simulating the unloading from 180 g to 72 g, 63 g, 54 g, 45 g, 36 g and 31 g (it represents 60%, 65%, 70%, 75%, 80% and 83% unloading respectively) to investigate the general trends of the model behaviour during unloading.

The results are presented in Fig. 7.15, showing time vs. settlement curves with swelling after the unloading, which occured at the prototype time of 25 years. The magnitude of swelling is a function of the g-level after unloading. The unloading of all numerical models was gradual, based on the experimental measurements of the deceleration rate of the mini-centrifuge (Fig. 5.9). The crosses in Fig. 7.15 correspond to one minute after unloading to the final g-level in the particular test. It simulated the average time of measuring the settlement in the mini-centrifuge, which took place approximately one minute after centrifuge deceleration. Figure 7.16a shows the ratios of swelling at the time of measuring the model height (Δh_{unl}) to the final swelling, when all pore pressures in the model equalized (Δh_{fin}) for all numerical models (it presents percentage of the swelling, which occured before the measurement of the model height). This number decreases from 64% in the model unloaded to 72 g to 45% in the model unloaded to 31 g. The extrapolated trend observed in Fig. 7.16a indicates that in fully unloaded model only approximately 20% of the swelling took place before the measurement of the model height.

The part of swelling, which occured before the measurement of the model height is plotted in Fig. 7.16b as percentage of the total settlement of the model before unloading. The trend of the numerical simulations indicates that in unloading to 1 g, the measured settlement would be approximately 10.5% lower compared to the settlement under maximum g-level before the unloading started. Assuming the underestimation of the settlement due to the unloading by 10.5%, the final settlement in the mini-centrifuge tests 5-8 presented in Fig. 7.14 would be approximately 4.25 m, which is significantly closer to the numerical prediction of 4.75 m (the difference of 10%).

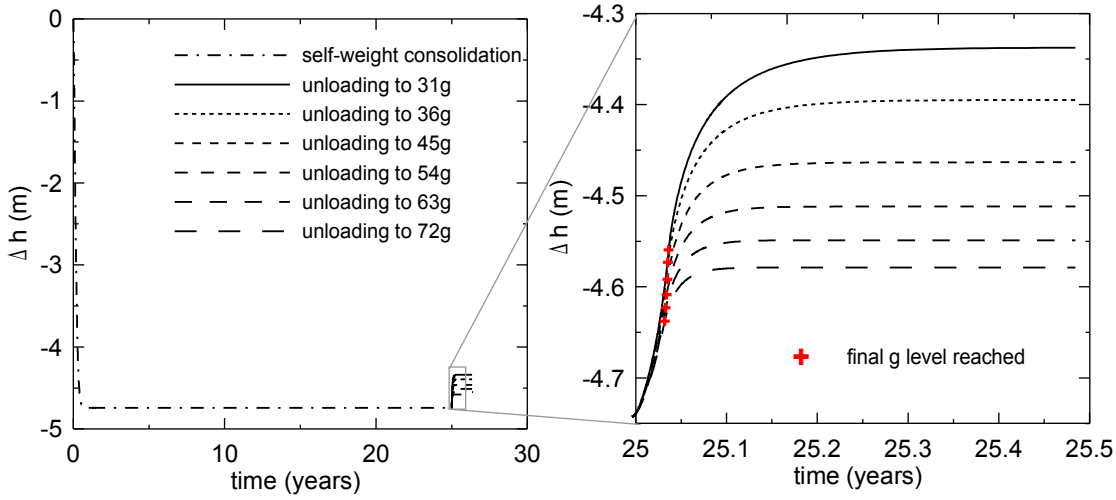

Fig. 7.15: Modelling of magnitude of swelling due to unloading to various g-levels.

In the case of the mini-centrifuge tests 9-11, 10.5% of swelling gives the settlement of 9.4 m before unloading, which is close to 9.8 m settlement predicted by the numerical model (the difference is only 4%).

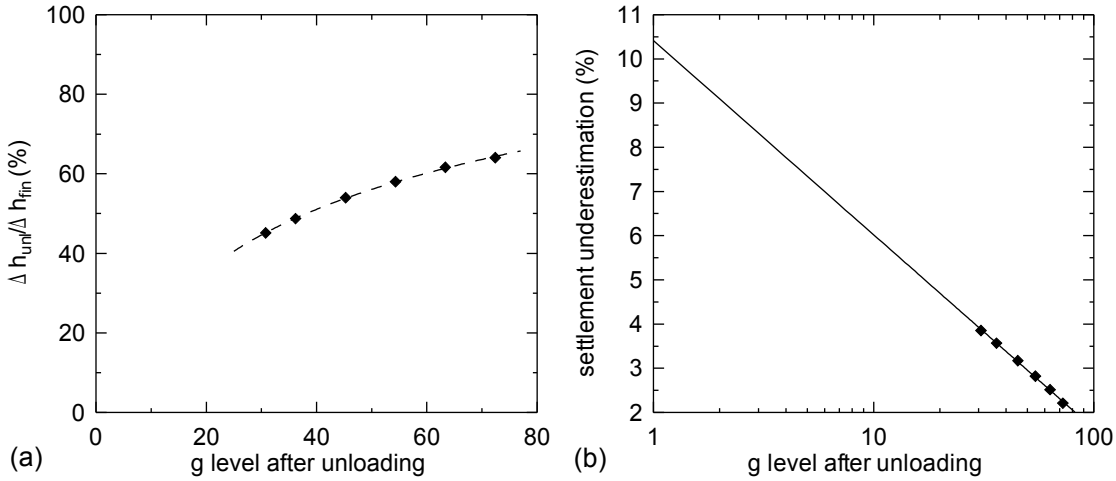

Fig. 7.16: (a) - percentage of swelling, which occured after unloading to different g-levels before model height measurement; (b) - percentage of swelling before model height measurement relatively to model height.

A better correlation of the numerical model prediction with tests 9-11 could be associated with a slightly different hydraulic conductivity of both sets of the mini-centrifuge tests. It can be assumed, that the effect of unloading can be even higher for tests 5-8: the hydraulic conductivity was calibrated on the centrifuge model with the LSD curve 2, while the grading of the mini-centrifuge models 5-8 corresponded to the slightly more permeable LSD curve 1 (no fines in the macro voids). Therefore a faster equalization of the pore pressure,

bigger swelling before the measurement of the settlement and a better correlation with the numerical model can be expected.

7.4 Modelling of lump segregation

A non-uniform settlement is the typical characteristic of mining landfills (Charles and Watts, 2001; Vaníček and Vaníček, 2008). One of the key mechanisms causing the non-uniform settlement is a segregation of the clay lumps during landfilling. Sliding of the larger lumps on the slopes of the fresh landfill causes a higher concentration of these lumps at the base of the slope, while the smaller lumps tend to remain at the top of the slope. This process leads to spatial variability in the lump size distribution and consequently differencies in the intergranular porosity of the landfill. The degradation of the double porosity structure therefore leads to the differential settlement of the landfill surface. A simple laboratory experiment was carried out to study the effect of lump segregation on the void ratio of the landfill and on its compressibility.

7.4.1 Determination of void ratio

The experiment was carried out with dried scaled-down lumps of the clay from the “5. květen“ landfill. The soil preparation was the same as for the centrifuge tests and the lump size distribution curve 2 was used. The clay lumps were scaled down by 150 compared to the assumed *in situ* grading. The soil was dry pluviated from the 0.1 m height into a 300 mm long and 35 mm wide plexiglass container. The clay was pluviated from two fillers located 75 mm and 225 mm from the container wall (¼ and ¾ of the total length of the container). After filling, the model was splitted into seven sections according to the horizontal distance from the fillers: sections with 0-20 mm from the locations of the fillers were marked *top 1* and *top 2*, respectively, sections 20-55 mm from the fillers were marked *slope 1*, *2* and *3* and sections 55-70 mm from the fillers were marked *bottom 1* and *2*. The model and the sections are shown in Fig. 7.17. The left-most section was not used for any analysis as it had to be excavated in accessing the soil.

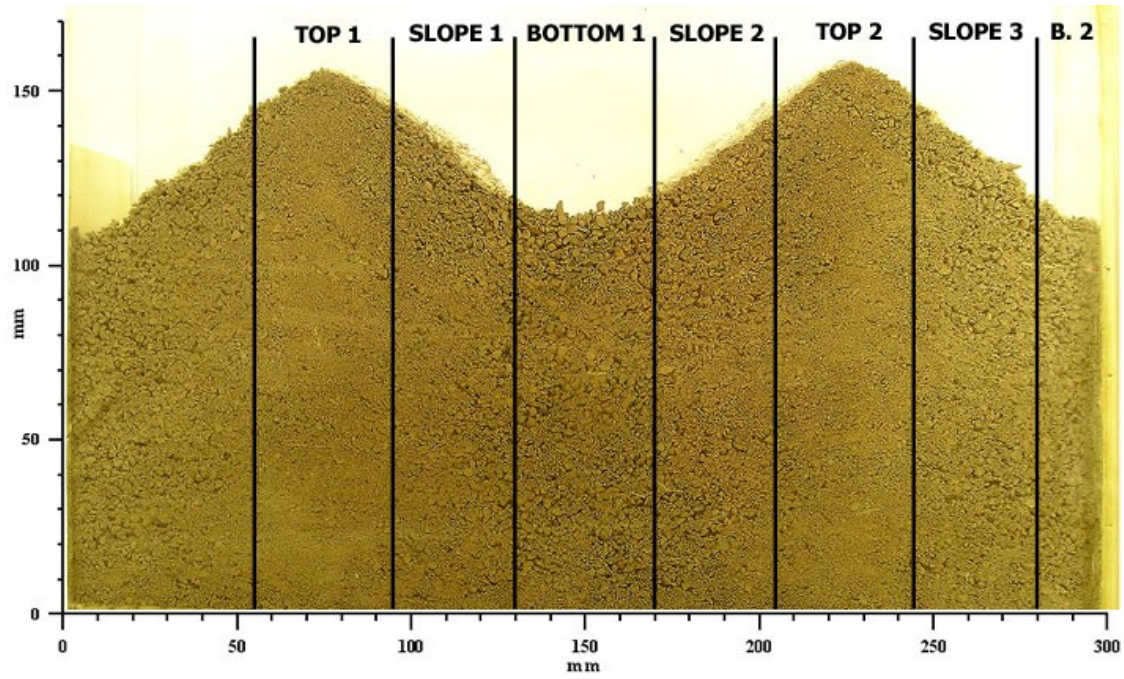

Fig. 7.17: Laboratory experiment for simulation of lump segregation during landfilling.

The laboratory experiment presented here does not fully reproduce landfill placement. *In situ* the position of the stowing machines is not fixed during filling, so the lump size distribution in the field varies in both the vertical and horizontal direction. However, the simplified model demonstrates the conical heaps, and the segregation process on their slopes, which takes place *in situ* (Figs. 2.3 and 3.4).

The lump size distribution curves for all seven sections were obtained by sieving. The results show significant differences between the sections. Figure 7.18 shows that both top sections exhibit significantly higher percentage of the lumps below 0.5 mm in diameter, which corresponds to the lumps up to 75 mm *in situ* (using scaling factor of 150). The soil from both bottom sections exhibits 2.5 times and 3-4 times higher amount of lumps above 2 mm (above 300 mm *in situ*) compared to the slope and bottom sections, respectively. The slope sections represent a transition between the top and bottom states. The accuracy of the measurement is demonstrated by the small difference between the top sections 1 and 2 and the slope sections 1, 2 and 3. Bigger differences can be seen when both bottom sections are compared. It can be explained by the lower overall amount of the soil in the section *bottom 2*, which could cause lower accuracy of the lump size distribution measurement. The original LSD curve of the soil before the experiment is plotted for the comparison. None of the grading curves reached 10% of lumps under 0.315 mm as the original LSD curve. It probably results from sieving after the experiment, when part of the finer lumps did not pass through the sieves due to electrostatic forces.

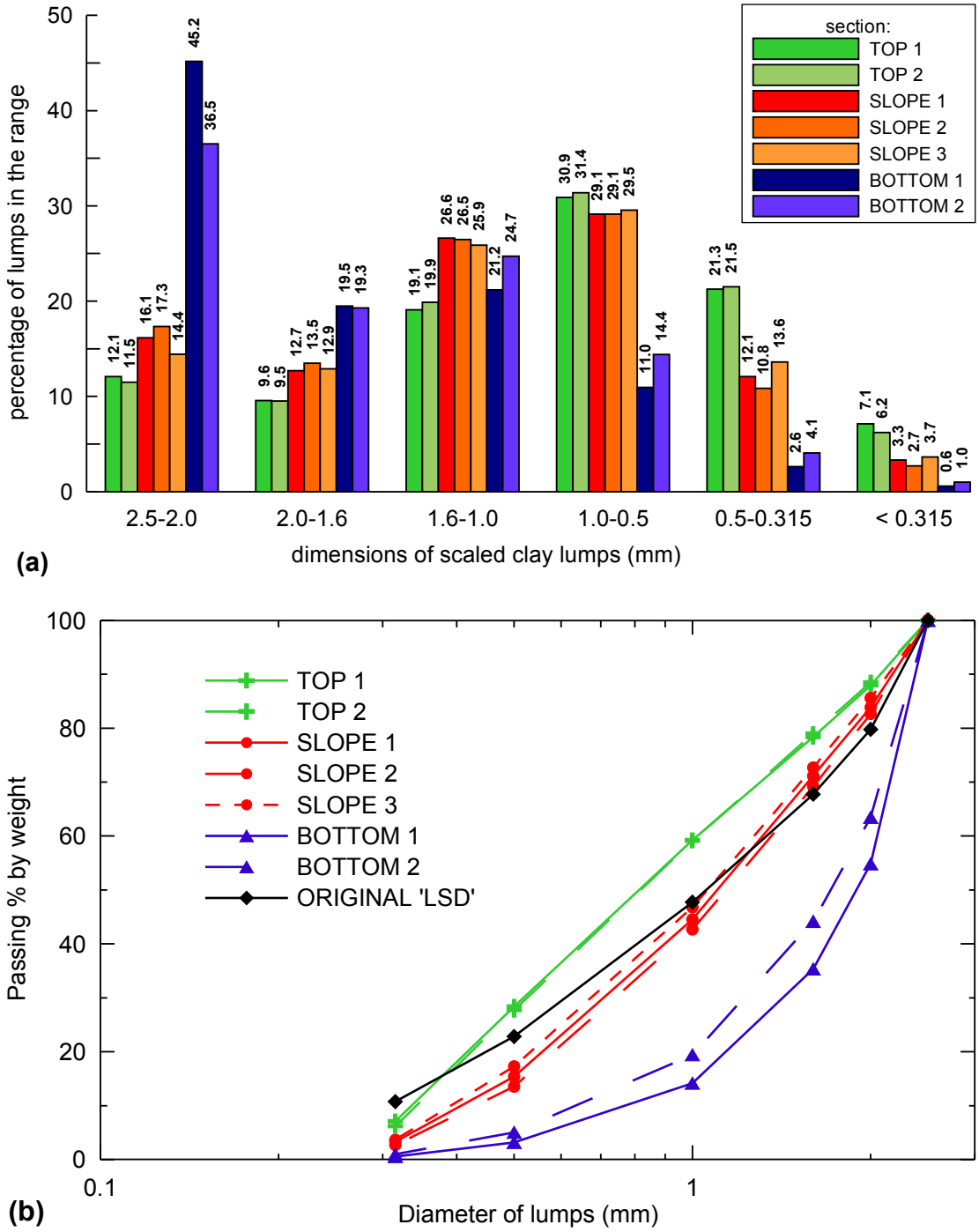

Fig. 7.18: Lump size distributions after segregation of clay lumps during filling.

The values of initial void ratio e_0 were calculated from the average void ratios in the top, slope and bottom sections (Fig. 7.19). The initial sensitivity s_0 was estimated from Eq. 7.3. The exact determination of s_0 would require compression tests using LSD corresponding to the top, slope and bottom sections and determination of e_0-s_0 relations for each section.

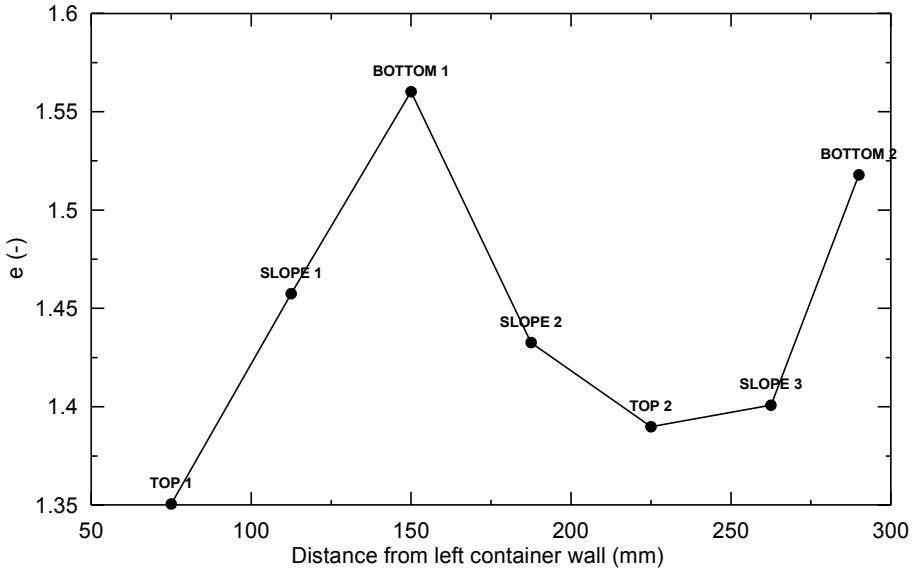

Fig. 7.19: Variation of void ratio in the measured sections.

7.4.2 Results of numerical modelling

The effect of the segregation of clay lumps in the landfill below a trial embankment was analysed by four numerical models with identical geometries but different initial properties. The geometry and finite element mesh of the centrifuge model are presented in Fig. 7.20. First, the self-weight consolidation of the 28.5 m high landfill was simulated. After 20 years of consolidation, 2D embankment was constructed on the landfill surface. The embankment did not represent exactly any of the case histories described in Chapter 4. Its geometry corresponded to the centrifuge model 2Da from Chapter 6. The embankment crest was 27 m long and the slopes were graded at 1 (vertical) : 3 (horizontal). The vertical effective stress generated by the embankment was 100 kPa.

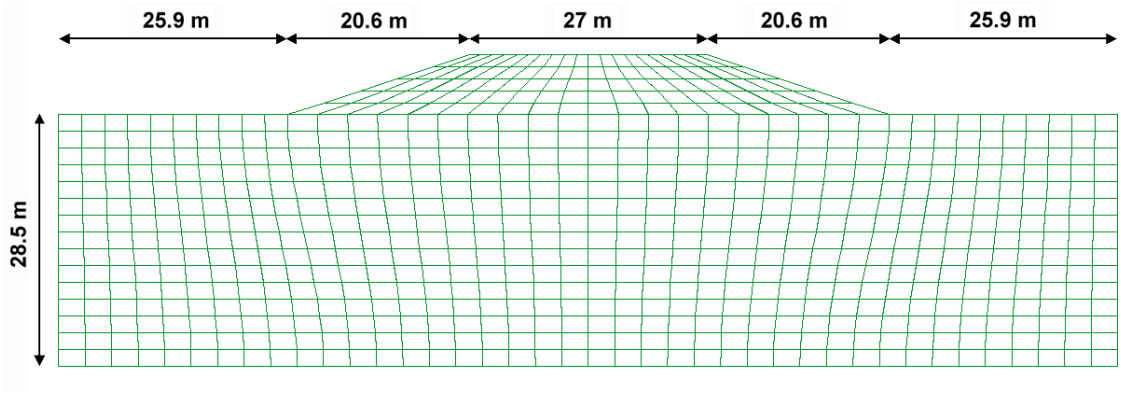

Fig. 7.20: Geometry and finite element mesh of numerical model.

Different values of e_0 and s_0 were used for the numerical models, according to the average void ratio for the top, slope and bottom sections measured in the laboratory (Fig. 7.19). The initial values of the fourth model corresponded to the void ratio of the unsorted clay lumps determined before the laboratory experiment (values of e_0, s_0 for all models are presented in Tab. 7.4).

	h_0 (m)	$\rho_{d\text{-}0}$ (kg/m^3)	e_0	s_0	Δh_{sw} (m)	Δh_e (m)	$\Delta h_{e\text{-}g}$ (m)
top	28.5	1642	1.66	6.33	5.07	3.56	2.87
slope	28.5	1627	1.73	7.01	5.50	-	3.14
bottom	28.5	1598	1.86	8.34	6.44	-	3.34
unsorted	28.5	1624	1.74	7.13	5.59	-	3.14

Tab. 7.4: Comparison of input data and resulting settlement of numerical models.

The comparison of the landfill settlement after the self-weight consolidation is presented in Tab. 7.4 (Δh_{sw}). It shows significantly different magnitudes of the settlement. The settlement of the “top section“ model (the model with the lump size distribution equivalent to the top section - Fig. 7.18) exhibited only 78% of the settlement of the “bottom“ graded model, which represents the differential settlement of 1.37 m. Differential settlement can be expected over the horizontal distance of approximately 11 m, as calculated using the dimensions from Fig. 7.17 and the scaling factor 150. It indicates that even a relatively small change in void ratio can significantly affect the settlement.

For the “top“ section model the settlement due to the embankment reached 3.56 m (measured under the centre of the embankment). Other sections could not be investigated, as the numerical analyses did not converge. The construction was simulated by the gradual increase of the unit weight of

the embankment over 45 days in the numerical model. In all four models the base of the embankment was therefore reinforced by the geotextile to prevent the collapse. The geotextile was modelled by truss elements without interface elements with the thickness of 0.1 m and the Young modulus of E = 25 GPa. The final settlements are presented in Tab. 7.4 ($\Delta h_{e\text{-}g}$) and the consolidation curves (including the self-weight consolidation of the landfill) are compared in Fig. 7.21. It shows the same shape when compared to the self-weight consolidation due to closing of the remaining macro voids in the upper part of the fill. The difference in the settlement between “top“ and “bottom“ section model after the embankment construction reaches 0.5 m. It can be observed from Fig. 7.21 that the difference between the models is reached in the initial part of the consolidation curves and is associated with the rapid closing of macro voids. A similar trend can be observed in the field measurements and the centrifuge tests, for example in Fig. 5.16.

Although the results do not represent exactly the process of filling *in situ*, they demonstrate that the significant differential settlement over a relatively short distance due to the segregation of the lumps may be expected. It can explain the variations in the settlement measured by the different hydrostatic levelling profiles *in situ* (Figs. 4.7-4.10). and the differential settlement observed over the laser scanning profiles in the geotechnical centrifuge models during the self-weight consolidation (Figs. 6.19 and 6.20).

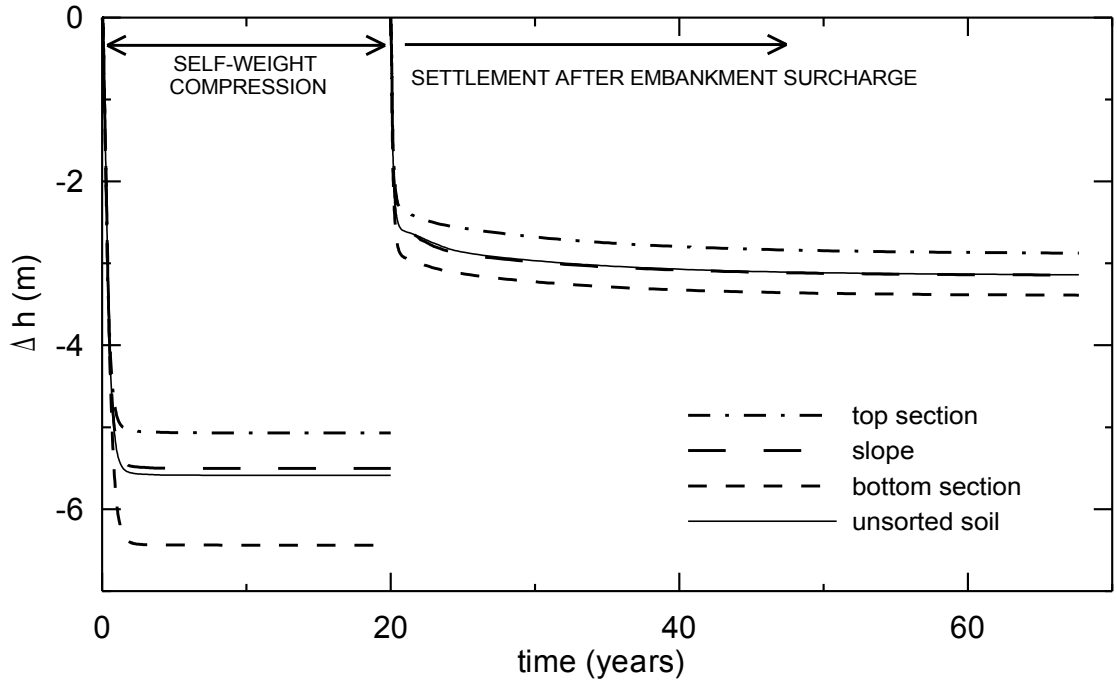

Fig. 7.21: Settlement of landfill models with different intergranular porosity.

7.5 Modelling of centrifuge tests 2Da and 2Dc

The aim of the numerical modelling of the geotechnical centrifuge tests 2Da and 2Dc was a direct comparison of the 2D centrifuge and the numerical model including the self-weight consolidation of the landfill. The geometry of both the centrifuge tests was similar until the end of the self-weight consolidation. The different embankment construction techniques and the materials in both the centrifuge tests (Tabs. 6.1 and 6.2) resulted in the different dimensions of the embankments and the different rates of surcharge application. However, the similar bearing pressure in both the centrifuge tests allowed the joint interpretation of the tests (Section 6.9), which is compared to the numerical modelling results in this chapter. The geometry and the rate of the surcharge application of the centrifuge test 2Da was used in the numerical model. The influence of the geotextile under the embankments in the centrifuge models and the influence of the rising groundwater level during the self-weight consolidation was also considered.

7.5.1 Description of the model and input data

The geometry and the finite element mesh of the model is presented in Fig. 7.20. The height of the embankment was 6.8 m with the unit weight of the embankment material of γ = 18.1 kN*m^{-3} giving σ_v' = 123 kPa. (Tab. 6.2). The embankment body (constructed from the wet sand in the centrifuge model) was modelled using the Mohr-Coulomb model (Tab. 7.5). The embankment surcharge was applied in 45 days similarly to the centrifuge test 2Da. A reinforcement simulating the geotextile used in the centrifuge was applied at the base of the embankment to prevent failure.

The parameters of the landfill presented in Tab. 7.3 were used. The initial sensitivity was determined from the measurement of the void ratio before the centrifuge test using Eq. 7.3 (e_0 = 1.78, s_0 = 7.54). The unit weight of the landfill γ = 16.1 kN*m^{-3} was estimated as the average density of the scaled-down double porosity clay before the centrifuge test. The hydraulic conductivity of the centrifuge model was chosen by a back-analysis of the self-weight consolidation of the centrifuge model (Section 7.5.4).

	E (kPa)	ν (-)	φ' (°)	c' (kPa)	ψ (°)
Embankment	25 000	0.25	40	1	20

Tab. 7.5: Mohr-Coulomb model parameters of the embankment.

In the centrifuge, the groundwater level was kept at the same distance from the container base (close to the surface of the consolidated model of the landfill) for the whole test. However, when the centrifuge test started with the unconsolidated landfill model, the water level was located approximately 7.5 m below the surface (Fig. 7.22). It resulted in a higher vertical effective stress in the initial part of the self-weight consolidation. In order to keep the numerical model as close as possible to the centrifuge tests, the same relative change of the groundwater level from the 7.5 m depth to the landfill surface was used in the initial part of the self-weight consolidation by performing a large-strain updated-mesh analysis.

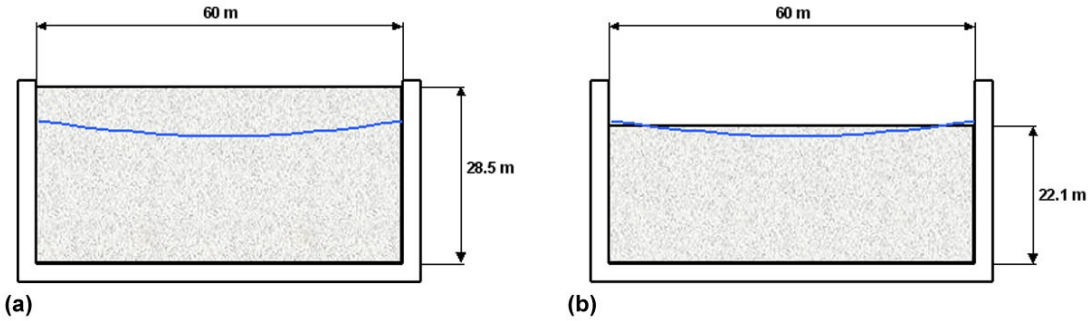

Fig. 7.22: Centrifuge model before (a) and after (b) the self-weight consolidation. The dimensions are shown in the prototype scale. See also Fig. 6.7.

7.5.2 Self-weight consolidation

A good agreement of the self-weight consolidation curves of the centrifuge and numerical models is shown in Fig. 7.23. It presents a direct evaluation of the hypoplastic model performance (the settlement of all mini-centrifuge tests was influenced by unloading-reloading cycles). The settlement measured in the centrifuge tests 2Da and 2Dc varied in all measured profiles (relative settlements are shown in Figs. 6.17 and 6.18) from 6 to 6.8 m with an average of 6.4 m. The settlement in the numerical model was 5.7 m. It can be slightly influenced by the hydraulic conductivity of the landfill as described in Section 7.5.4.

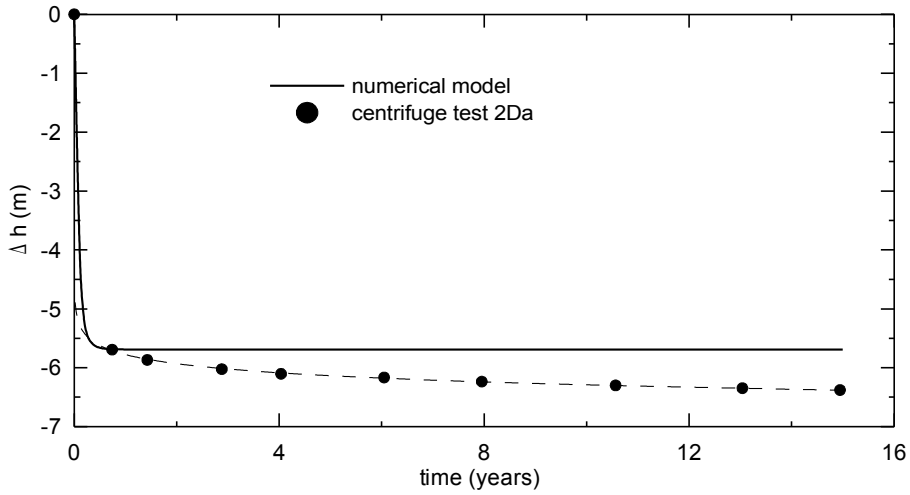

Fig. 7.23: Comparison of self-weight consolidation curves from centrifuge test 2Da and numerical model.

The change of the position of the water level during the self-weight consolidation (Fig. 7.22) can influence the structure in the upper part of the fill due to the change in σ_v'. Figure 7.24 shows lower void ratios in top 7.5 m (not fully flooded at the start of the test) than expected from the extrapolated data from the lower depth.

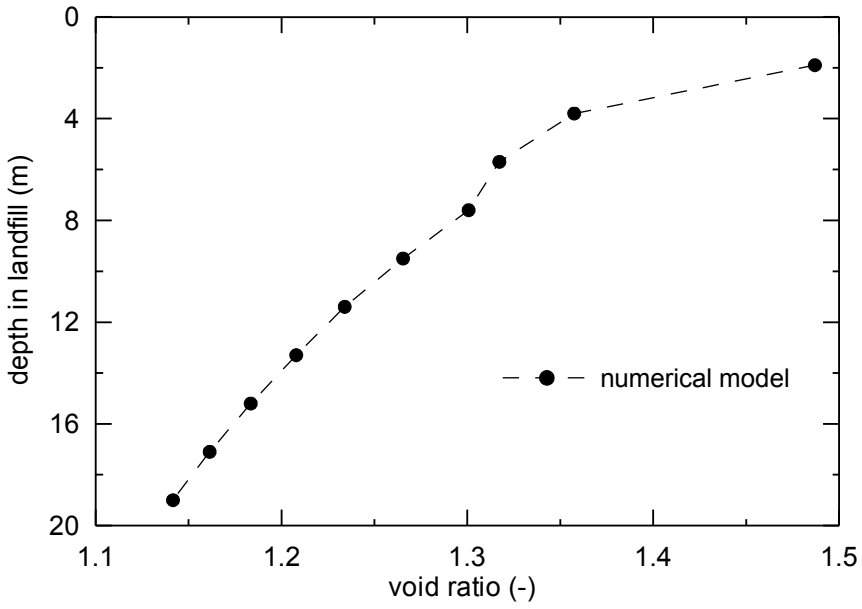

Fig. 7.24: Influence of the position of the groundwater level during the self-weight consolidation.

7.5.3 Settlement after embankment surcharge

The comparison of the settlement under the embankment is presented in Fig. 7.25. It shows the average settlement measured in the interval marked by dots in Fig. 7.26. This interval corresponds to the centrifuge tests, where the average settlement measured over the same distance from the central axis was calculated from the laser scanning data. Figure 7.25 shows 20% smaller settlement of the centrifuge model (the final settlement of 1.6 m in prototype scale) than in the numerical model (the final settlement of 2 m). The difference may be explained by the change in intergranular porosity during the preparation of the centrifuge model. To stabilize the model before the installation into the centrifuge, suction was created by adding water, which enabled the fines to enter the macro voids. The profile of the final settlement in the numerical model is presented in Fig. 7.26. The maximum settlement (2.12 m) was reached under the centre of the embankment, while under the edges of the crown the settlements were only 1.89 m.

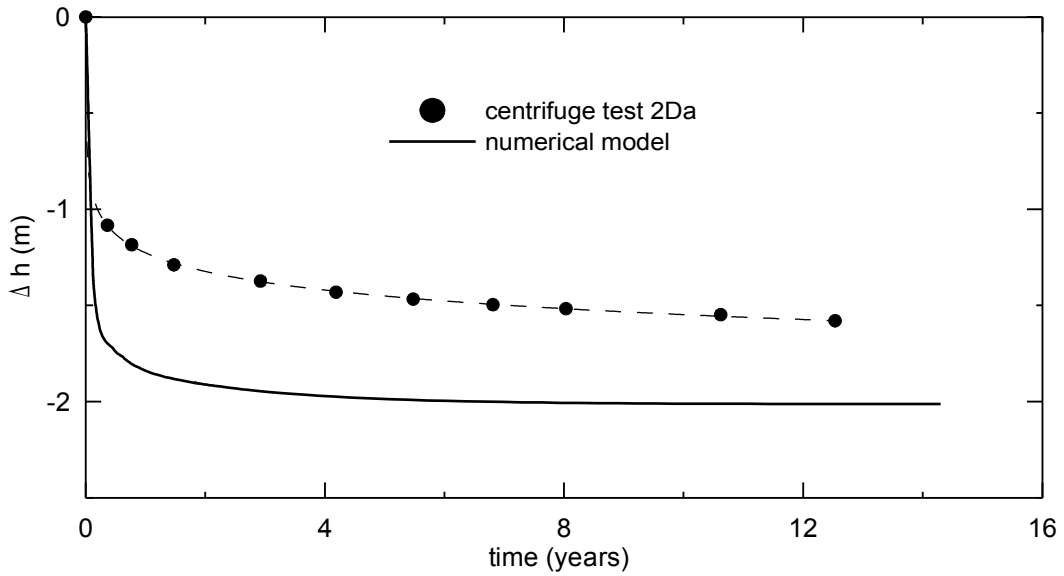

Fig. 7.25: Landfill settlement after embankment surcharge.

Figure 7.27 shows the influence of the geotextile between the embankment and the landfill modelled by truss elements without interface elements (thickness of 0.1 m, E = 25 GPa). It reveals a less uniform distribution with a higher settlement under the central axis and a smaller settlement under the embankment slope without the geotextile.

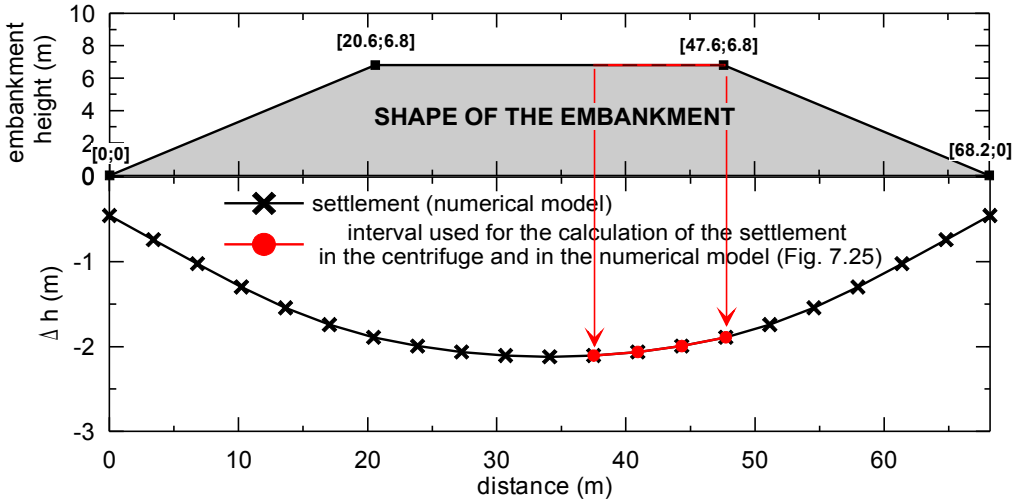

Fig. 7.26: Settlement profile under the embankment.

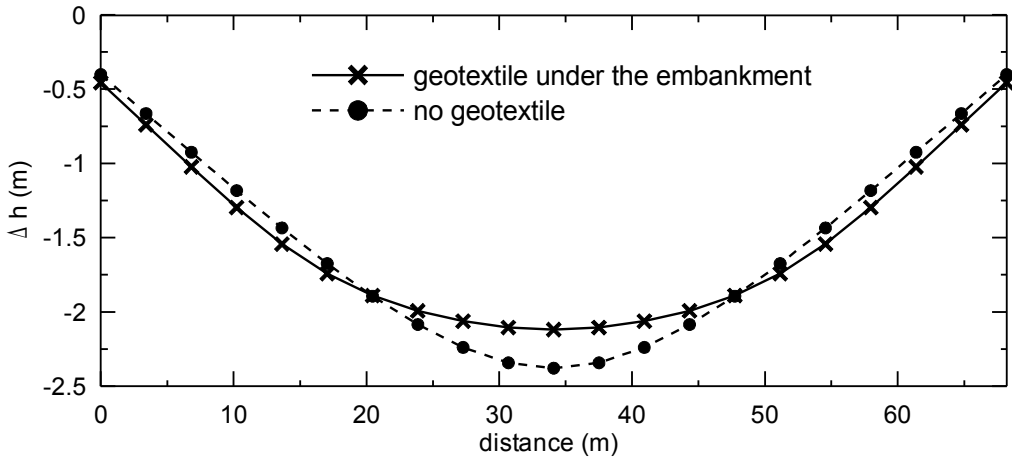

Fig. 7.27: Influence of geotextile to settlement profile under embankment.

The settlement of the landfill in the vertical profile is presented in Fig. 7.28. The position of the profile corresponds to the position of the straw system in the centrifuge model 2Da. The time of the measurement is 656 days after the embankment construction similarly to centrifuge test data presented in Fig. 6.33. The figure shows that the difference between the centrifuge and the numerical model gradually changes over the whole vertical profile. However, it may be concluded that the predictions of the centrifuge tests are in a reasonable agreement with the centrifuge test results.

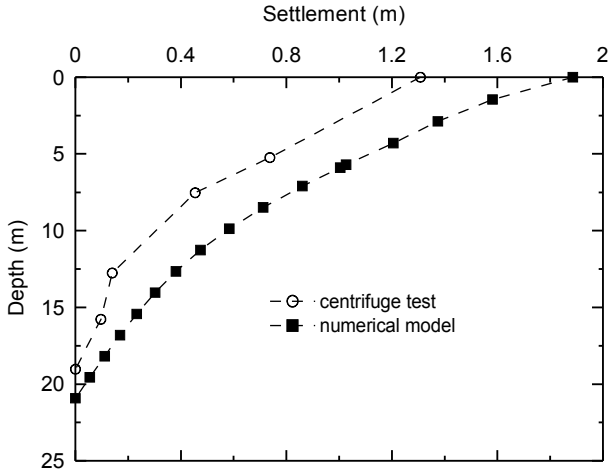

Fig. 7.28: Settlement profile in centrifuge test and numerical model.

7.5.4 Hydraulic conductivity of the landfill model

The hydraulic conductivity (k) of the landfill in all the numerical models presented in this thesis was assessed from the back analysis of the consolidation of the centrifuge model 2Da. In the back analysis, different values of hydraulic conductivity were prescribed at σ_v' = 5 kPa and σ_v' = 150 kPa. A linear interpolation and extrapolation of these values was used in the landfill profile.

First a constant value of k was assessed. The consolidation curves of the landfill and the settlement after the embankment surcharge are presented in Fig. 7.29a for seven models with k from $2*10^{-8}$ to $5*10^{-10}$ m/s. It shows that none of these values could closely represent both the self-weight consolidation and the settlement after the embankment construction. The settlement was found to be dependent on the value of k, varying from 5.8 m ($k = 2*10^{-8}$) to 6.1 m ($k = 5*10^{-10}$) in the self-weight consolidation and from 1.86 m ($k = 2*10^{-8}$) to 1.96 m ($k = 5*10^{-10}$) after the embankment surcharge. This can be attributed to the different rate of the groundwater level increase to the model surface during the self-weight consolidation and consequently the different change of the vertical effective stress profile in the model.

A linear change of the hydraulic conductivity in the vertical profile with its constant rate decrease is presented in Fig. 7.29b. It shows much better correlation with the centrifuge consolidation curves, especially for the green line ($k = 5*10^{-8}$ at σ_v' = 5 kPa and $k = 1*10^{-10}$ m/s at σ_v' = 150 kPa) and the yellow line ($k = 2*10^{-8}$ at σ_v' = 5 kPa and $k = 5*10^{-11}$ m/s at σ_v' = 150 kPa).

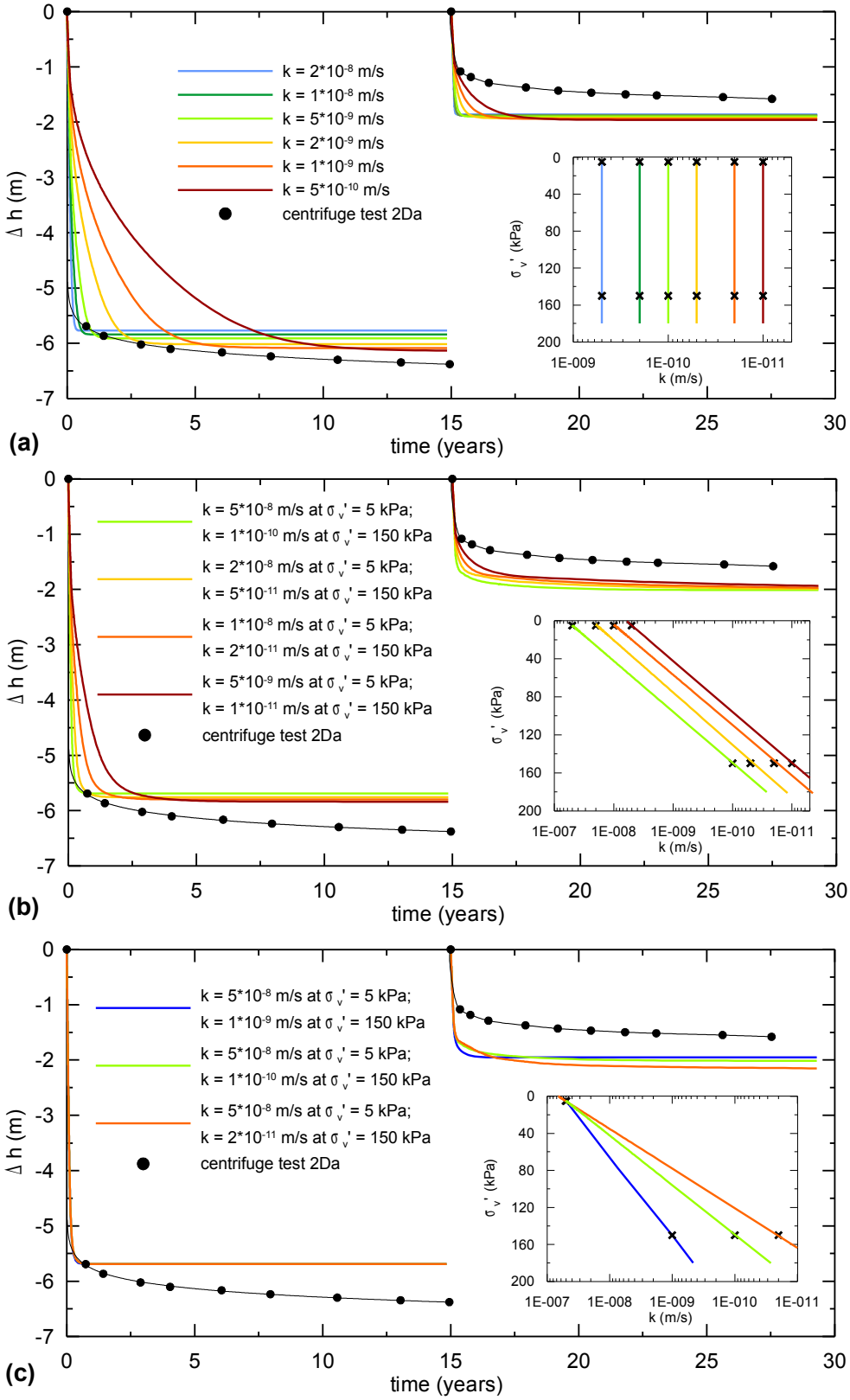

Fig. 7.29: The numerical models with the different hydraulic conductivity linearly dependent on σ_v'. The small inserted graphs represent the change of k with σ_v' within the landfill model.

Figure 7.29c shows the influence of different rates of the hydraulic conductivity decrease with the model depth (all curves are identical for the self-weight consolidation). From all the models presented, the green line in Figs. 7.29b and 7.29c (k = 5*10^{-8} at σ_v' = 5 kPa and k = 1*10^{-10} m/s at σ_v' = 150 kPa) was found to best correlate with the experimental curves and was used in all numerical models presented in the thesis.

7.5.5 Influence of landfill height

A parametric study of the depth of the active zone under the embankment was carried out. The same parameters and the same geometries were used except of the depth of the landfill. In order to keep the models simple and comparable, all the models were fully flooded from the beginning of the test and the settlement of the landfill surface under the central axis of the embankment was considered for the analysis. Nine initial landfill heights from 16.5 to 39 m were modelled. The settlements of the models are presented in Fig. 7.30. It shows gradually increasing settlements with the model height during the self-weight consolidation, while the settlements after the embankment construction were influenced by the landfill height only up to approximately 30 m. The final settlements are also presented in Fig. 7.31. It suggests that the height of the landfill model in the centrifuge test (28.5 m) may allow a realistic modelling of the embankment surcharge with respect to active zone. The numerical modelling showed a deeper active zone when compared to the *in situ* measurements of the depth reference points (active zone of approximately 22 m under Embankment 2).

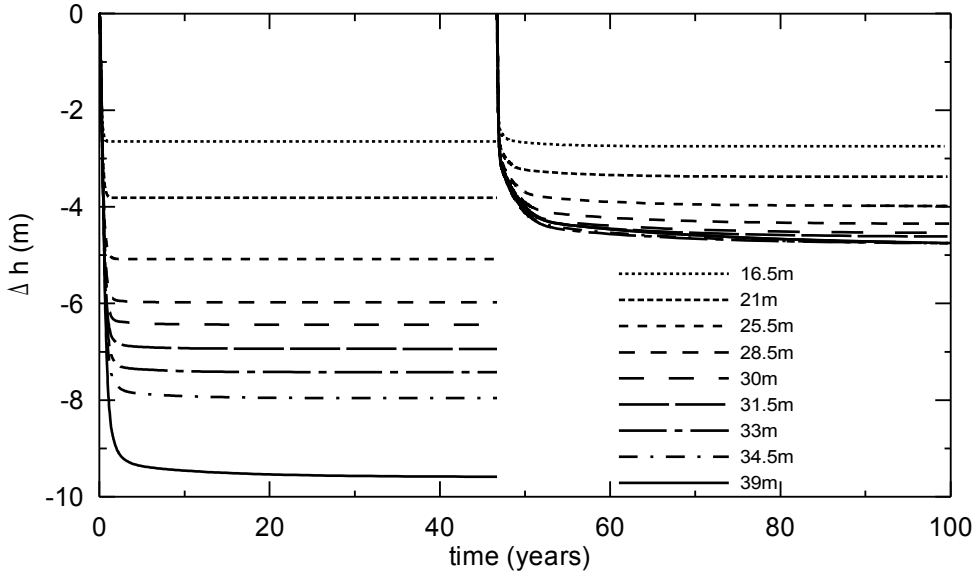

Fig. 7.30: Settlement of numerical models with different initial landfill heights.

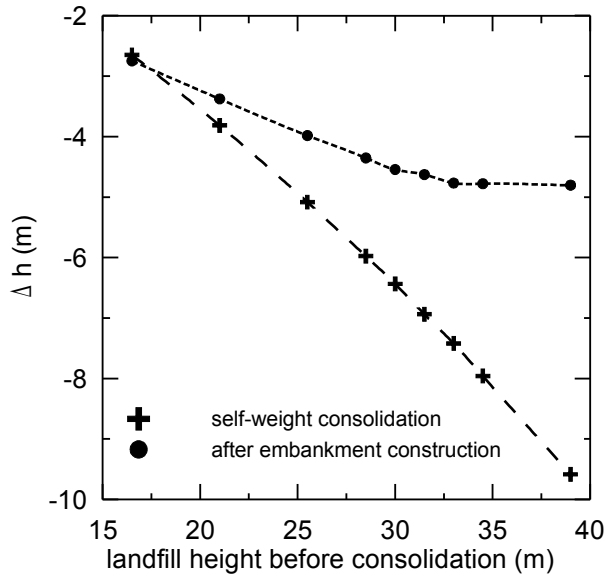

Fig. 7.31: Comparison of final settlements of numerical models.

7.6 Modelling of trial embankments

The two field trial embankments were simulated in 2D. As in the case of the modelling of the centrifuge tests, a coupled consolidation analysis was performed. The aim of the numerical modelling of the trial embankments was the simulation of the case histories starting from the placement of the landfill. *In situ*, clay lumps were poured into an exploited mine pit. The initial depth of the landfill layer in the numerical model was 40 m to represent 25-30 m deep landfill after the self-weight consolidation. During filling *in situ*, no water was present in the mine pit as a result of pumping of water during the mining. The landfill was flooded later by a gradual increase of groundwater level during the consolidation. In the numerical model, the gradual rise of the water level after placement of the landfill was simulated by a decrease of the unit weight of the landfill in 3 to 10 years after filling. Ten years after filling the groundwater level reached the landfill surface. The further steps differed for both the trial embankments and they are described in the following section.

7.6.1 Geometry of the models and input data

7.6.1.1 Embankment 1

The pluviation of the 3.5 m fly ash layer mixed with a rubble stone on the top of the landfill was simulated by a 3.5 m thick layer with the unit weight gradually increasing between 15 to 20 years after placement of the landfill. The unit weight of the landfill of γ = 16.1 kN/m^3 was used for the modelling of both the case histories based on the average density measured before the centrifuge test (no data from the field were available). The unit weight of the fly ash layer of γ = 15.9 kN/m^3 was used based on the data presented by Novotná (2002). The construction of the embankment started 25 years after filling and took 45 days. The unit weight of γ = 18 kN/m^3 was used (Křížová, 2000). The dimensions of the embankment represented the dimensions of the real embankment (Fig. 4.5). The geometry of the model and the finite element mesh are in Fig. 7.32. The vertical effective stress generated by the embankment was 108 kPa.

Both the embankment body and the fly ash layer were modelled using a Mohr-Coulomb model (the parameters are summarized in Tab. 7.6). The parameters of the hypoplastic model for structured clays used for the landfill are presented in Tab. 7.3. The initial values of void ratio e_0 = 1.78 and sensitivity s_0 = 7.54 obtained from the centrifuge model and Eq. 7.3 were used for the landfill as there were no available data about the initial porosity from the field.

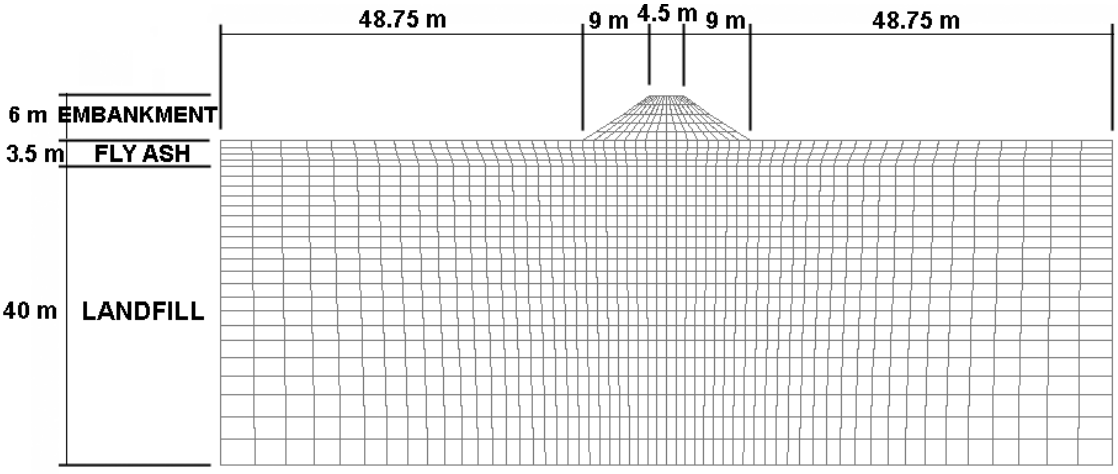

Fig. 7.32: Geometry and finite element mesh of Embankment 1.

	E (kPa)	ν (-)	φ' (°)	c' (kPa)	ψ (°)
Embankment	15 000	0.4	27	1	13.5
Fly ash	3 500	0.35	35	1	17.5

Tab. 7.6: Parameters of embankment and fly ash layer for the Mohr-Coulomb model.

7.6.1.2 Embankment 2

No fly ash was pluviated in the location of Embankment 2. After the rise of the groundwater level, the consolidation continued for another 15 years until the total time of the self-weight consolidation of 25 years was reached. Then a layer of rubble stone was placed on the top of the landfill (its thickness being 1.4 m, γ = 19 kN/m^3) and the embankment (average γ = 17.6 kN/m^3 as reported by Novotná, 2002) was constructed in 45 days. The vertical effective stress generated by the rubble stone layer was 19 kPa and σ_v' under the embankment body was 132 kPa giving the total σ_v' of 151 kPa acting on the top of the landfill. The geometry and parameters for the modelling (Mohr-Coulomb model was used for the modelling of the embankment and the rubble stone layer) are presented in Fig. 7.33 and Tab. 7.7. The parameters for the hypoplastic model of the landfill and the values of γ, e_0 and s_0 were identical to those used in the modelling of Embankment 1.

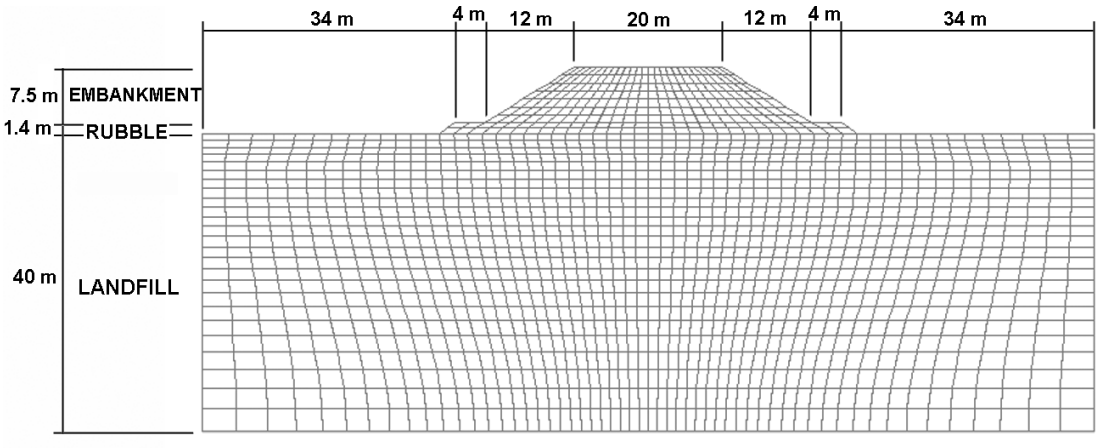

Fig. 7.33: Geometry and finite element mesh of Embankment 2.

	E (kPa)	ν (-)	φ' (°)	c' (kPa)	ψ (°)
Embankment	15 000	0.4	27	1	13.5
Rubble stone	25 000	0.25	40	1	17

Tab. 7.7: Parameters of embankment and rubble stone layer for the Mohr-Coulomb model.

7.6.2 Landfill consolidation before embankment surcharge

The settlement of the landfill surface at the site of Embankment 1 determined from the numerical modelling is presented by full line in Fig. 7.34. The end of the filling is marked by “A“ with the settlement of 8.6 m. The final settlement due to the self-weight compression was reached after approximately 2 years. The gradual increase of groundwater level in 3 to 10 years from the start of the filling (marked by “B“ and “C“) simulated by the decrease of unit weight of the landfill resulted in the heave of 0.33 m due to the decrease of σ_v'. The surcharge due to the pluviation of the fly ash (15-20 years, marked by “D“ and “E“) resulted in 0.12 m additional settlement (fly ash layer generated a surcharge of σ_v' = 21 kPa). No field measurements are available for a comparison with the numerical simulations of the self-weight consolidation.

Another numerical model was carried out to investigate the effect of filling the clay lumps into water (dashed line in Fig. 7.34). This model was fully saturated from the beginning of the self-weight consolidation, which reduced σ_v' in the model. The final settlement was 9.74 m, which was only 74% compared to the model with the gradual increase of the groundwater level (measured after 15 years of consolidation). A significant difference of the two models is presented also in Fig. 7.35 showing the void ratios in the vertical profiles of both the models. The higher compressibility of the model filled into water can be demostrated by the settlement of the landfill surface due to fly ash (0.22 m), which has almost doubled compared to the model with the gradual rise of the water level.

The position of the water level during the self-weight compression can also contribute to the different settlements under the embankment *in situ* and in the centrifuge (Fig. 6.31). While the landfill *in situ* can be represented by the gradually increasing water level (the full line in Fig. 7.34), the water level in the centrifuge models was fixed in a constant position before the acceleration to 150 g. It means that the centrifuge model except the top 7.5 m was fully flooded from the start of the self-weight consolidation, which resulted in a smaller gradient of σ_v' and a higher compressibilty after the self-weight consolidation.

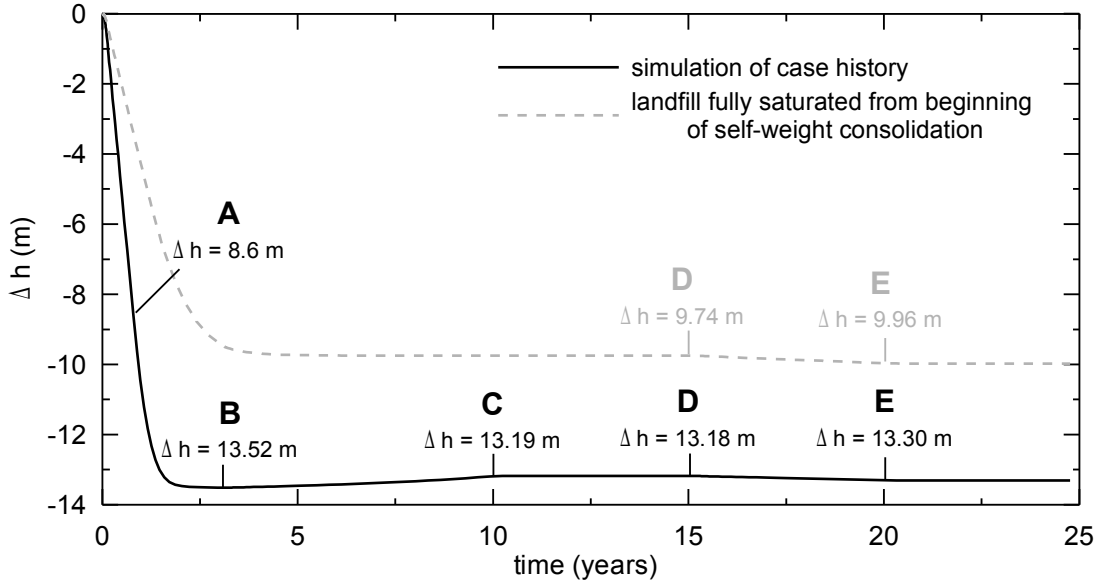

Fig. 7.34: Self-weight compression of landfill in the location of Embankment 1.

No effect of destructuration due to weathering in the top part of the landfill *in situ* was considered in the models presented in Fig. 7.34. However, weathering was likely to happen before placing the fly ash and therefore to influence the settlement of the landfill due to the fly ash layer. The absolute values of the settlement are therefore not realistic - it will be discussed in the following section that the destructuration in the top part due to weathering plays an important role *in situ* and it significantly reduces the compressibility of the landfill.

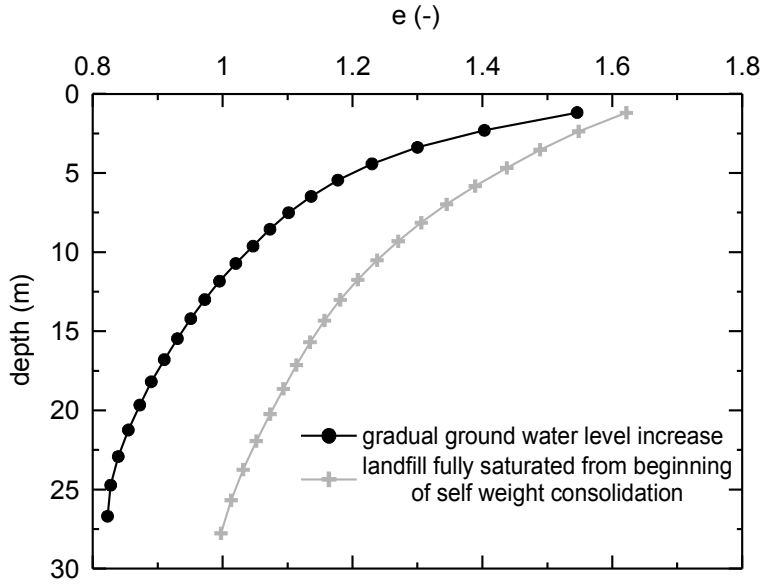

Fig. 7.35: Void ratios in landfill after self-weight consolidation.

7.6.3 Settlement after construction of embankments

After 25 years of the self-weight consolidation, the surcharge corresponding to Embankment 1 was applied on the landfill surface. Instead of fly ash layer, the numerical modelling of Embankment 2 included a 1.4 m thick rubble stone layer at the embankment foundation level, similarly to the case history.

The numerical modelling showed significantly higher settlements after the construction of the embankments compared to the field data (Fig. 7.36). The calculated settlements were 3.7 and 4.4 times higher for Embankments 1 and 2, respectively. In the case of Embankment 1, the numerical model represented the consolidation before the increase of the groundwater level (1.7 years after the embankment construction, Fig. 4.4). At this time, the last measurements of both the surface settlement and the depth reference points were carried out. The later measurements are incomplete due to the limited access to the embankment (see Chapter 4). In the case of Embankment 2, the lowering of the water level during the monitoring (Fig. 4.4) was simulated by an increase of the unit weight of the landfill in the top 5 metres in 1.6-2.2 years after the embankment construction.

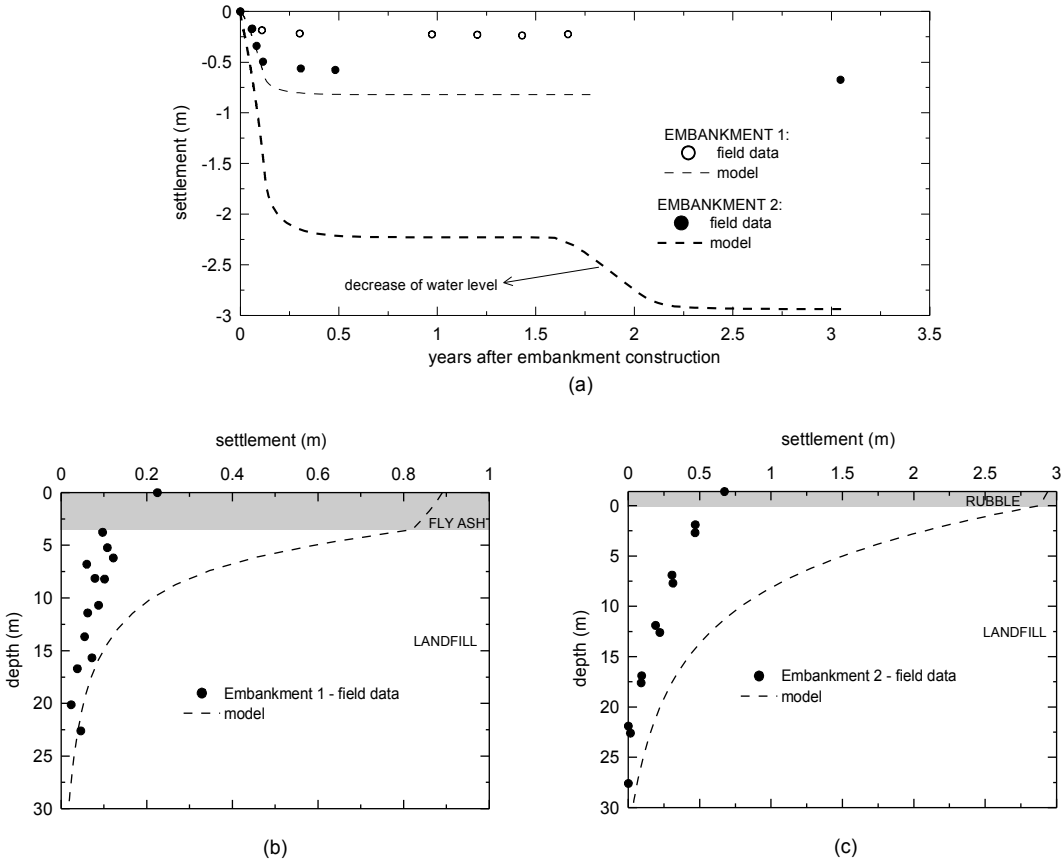

Fig. 7.36: Numerical modelling of the settlement under both embankments.

The discrepancy between the final settlements *in situ* and the numerical results is explained by the destructuration of the landfill in the shallow depth caused by weathering effects. *In situ*, the top layer is exposed to rainfall and wetting-drying cycles. The lumps get decomposed and macro voids are gradually filled with clay, which results in a lower compressibility. This hypothesis was also supported by the significantly higher settlements due to surcharge in the centrifuge than *in situ* (Figs. 6.31 and 6.33). In the centrifuge no weathering took place and the compressibility of the landfill model after the self-weight consolidation remained higher.

7.6.4 Influence of weathering destructuration

The structure degradation in the shallow depth due to weathering (termed “weathering destructuration” in the following text) was simulated by an inverse analyses of the settlement data (hydrostatic levelling profiles, depth reference points).

The calibration of the structure parameters based on the oedometer specimens with different degree of the structure degradation (Fig. 5.24) revealed that the degree of destructuration can be described by a continuous change in the void ratio, sensitivity (Fig. 7.12d, Eq. 7.3) and the model parameter κ^*, which influences the initial slope of the compression curves (Fig. 7.12a).

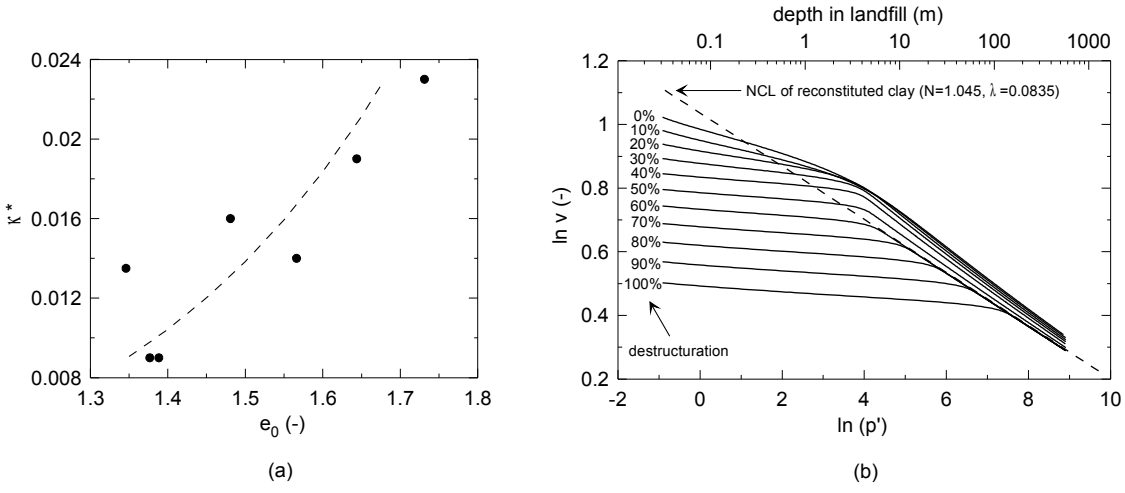

Fig. 7.37: (a) - change of κ^* with different e_0 (determined from oedometer tests); (b) - K_0 compression curves of double porosity clay with different degree of destructuration.

Weathering destructuration was included in the model by reducing the void ratio at the time of 15 years after filling. The sensitivity *s* and the parameter κ^* were calculated from the reduced *e* as follows: the value of sensitivity depends both on e_0 (Eq. 7.3) and σ_v' (it decreases with increasing σ_v' as the structure degradation proceeds). The value of *s* can thus be specified for the given void ratio and depth in the landfill. The parameter κ^* was found to decrease with the degradation of the landfill structure (Fig. 7.12a). The best fit curve within the measured range of e_0 was used to determine κ^* after weathering destructuration (Fig. 7.37a),

$$\kappa^* = \exp\left(\frac{e_0 - 3.62}{0.354}\right) \tag{7.4}$$

where e_0 is found for given *e* and *p'* in such a way that the current state lies on one of the corresponding compression curves from Fig. 7.37b. Eq. 7.4 is used to calculate κ^* in the range of e_0 = 1.73-1.35, while the values of κ^* = 0.008 (determined for the material of the clay lump by Enriquez, 2006 - Fig. 7.10b) and 0.023 (maximum κ^* determined for a double porosity specimen) were used outside this range. Figure 7.37b shows the K_0 compression curves representing the landfill with different degrees of destructuration in the whole vertical profile of the landfill with modified values of *e*, *s* and κ^*. The destructuration of 0% corresponds to the landfill with no effect of weathering, 100% destructuration represents the overconsolidated material of the lump with no intergranular porosity (K_0 compression test carried out by Enriquez, 2006, was used to define the position of its compression line, see Fig. 7.10b). The percentage of the destructuration D_s was determined from

$$D_s = \frac{e_{s100} - e}{e_{s100} - e_{s0}} \tag{7.5}$$

where e_{s100} refers to the void ratio of fully structured model and e_{s0} refers to the void ratio of the model without the double porosity structure at the corresponding depth.

The inverse analyses of the numerical models of both embankments aimed at reaching the same settlement as measured *in situ* by varying the percentage of weathering destructuration with the depth of the landfill. The results are presented by full lines in Fig. 7.38. Figures 7.38b and 7.38c show that most difference between the models with and without weathering destructuration took place in the top 10 metres of the landfill. This can be expected due to the bigger influence of the weathering near the surface.

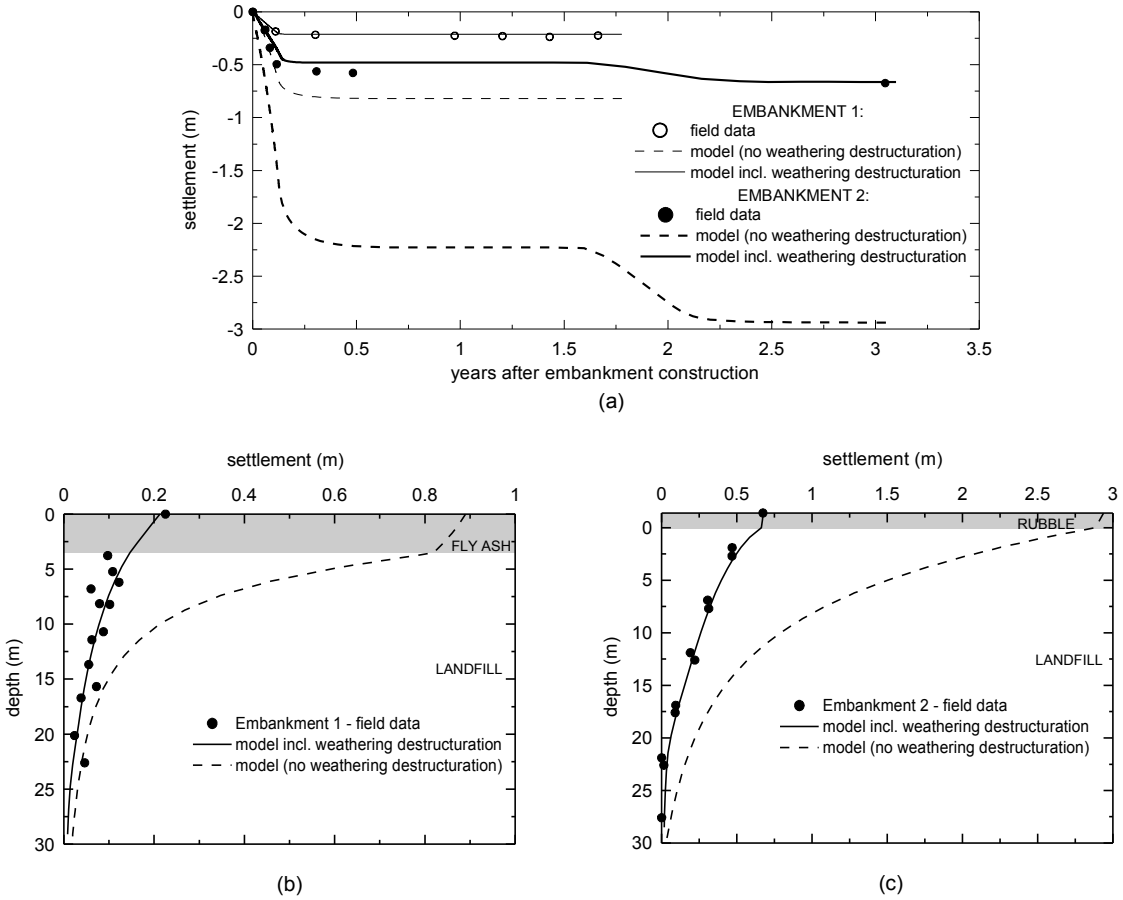

Fig. 7.38: Influence of weathering destructuration on the settlement.

The dependency of void ratio on the mean effective stress after destructuration can be seen in Fig. 7.39. It presents the profile of the landfill before weathering destructuration and the profiles of both numerical models after weathering destructuration. The compression curves from Fig. 7.37b representing 0% and 100% destructuration are added to visualize the magnitude of the destructuration used for both the case histories.

The change of destructuration with depth calculated according to Eq. 7.5 is presented in Fig. 7.40. Different values of weathering destructuration were found under both embankments. It can be assumed that the effect of weathering was similar at both sites and the difference can be attributed to a slightly different initial intergranular porosities, or other local inhomogeneities.

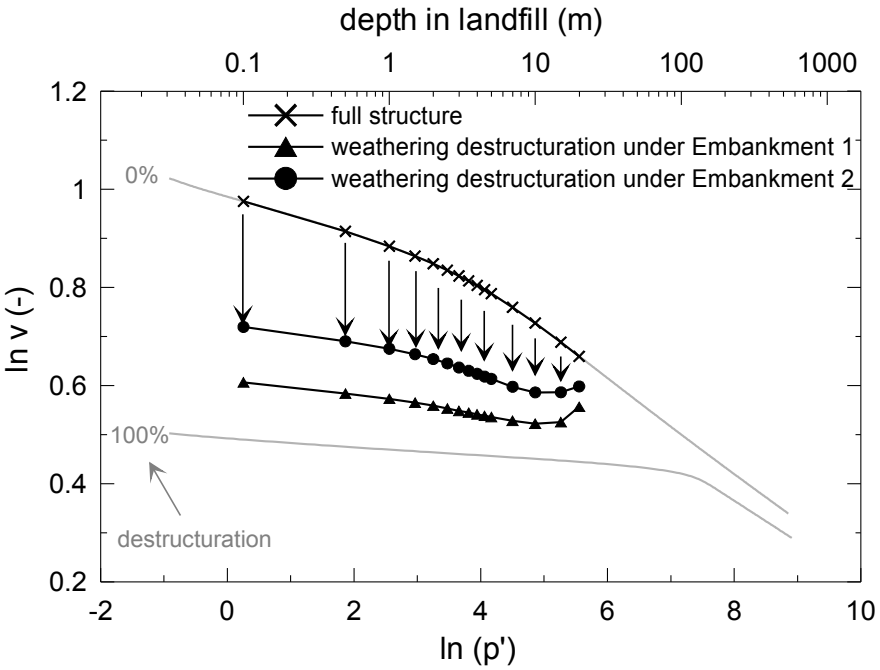

Fig. 7.39: Void ratios after weathering destructuration.

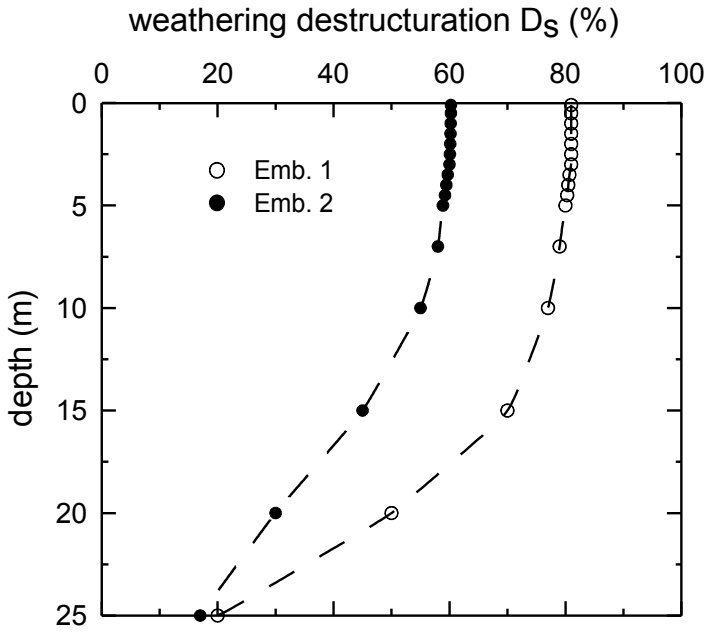

Fig. 7.40: Profile of weathering destructuration under both embankments.

7.7 Summary

The following results were obtained from the numerical modelling of the centrifuge tests and the case histories:

- The numerical modelling of the mini-centrifuge tests predicted the settlements, which were 15-20% higher compared to the results of the mini-centrifuge tests. Most of this difference (approximately 10%) can be attributed to the swelling during unloading the mini-centrifuge models.
- A simple experiment demonstrated the influence of segregation of the lumps, which is an inevitable part of landfill placement. It influences both the self-weight consolidation and the settlement after the surcharge and generates the differential settlement of the landfill.

Numerical modelling of the centrifuge tests 2Da and 2Dc:

- The position of the groundwater level (7.5 m below the surface before the self-weight consolidation) influenced the structure degradation in the upper part of the fill and reduced the compressibility of the model.
- The final settlement after the embankment construction determined by the numerical modelling (2 m) was higher compared to the centrifuge modelling result (1.6 m).

Numerical modelling of the case histories:

- The position of the water level during the self-weight consolidation *in situ* significantly influences the degradation of the landfill structure and hence the compressibility of the landfill. Dry filling followed by the rise of the water level causes a higher degradation of the structure and a less compressible landfill compared to initially saturated conditions.
- Weathering destructuration *in situ* (decomposition of the clay lumps and filling the macro voids with clay due to the rainfall and wetting-drying cycles) reduces the compressibility of the landfill. The inverse analyses of the trial embankments indicated that the weathering destructuration can lead to an approximately 4 times smaller settlement of the landfill compared to the fully structured soil.
- Modelling a structure built on the landfill requires detailed information about landfilling (filling procedure, lump size distribution and its spatial variation, groundwater level conditions) as well as a detailed description of the landfill properties before the development (groundwater level conditions, level of destructuration).

8 CONCLUSIONS AND OUTLOOK

8.1 Conclusions

The settlement of a double porosity landfill subjected to an embankment surcharge was studied by *in situ* measurements, centrifuge and numerical modelling. The comparison of the results showed significant differences. An average settlement under Embankment 1 measured *in situ* was 225 mm, while the numerical model (neglecting the influence of weathering destructuration) showed 890 mm. The settlement of Embankment 2 *in situ* was 580 mm, the centrifuge model predicted the settlement of 1.16 m and the numerical model 2.94 m. This was found to be caused by different intergranular porosities of the landfill prior to loading in the three cases. The correct determination of the intergranular porosity can be therefore considered a major problem of any modelling.

For the correct determination of intergranular porosity a detailed information about the filling process is necessary, especially lump size distribution curve and the position of the groundwater level during filling and the self-weight compression. The difference in the settlement of the fully flooded landfill (Δh = 9.7 m for 40 m high landfill) and the landfill with the gradually increasing water level (Δh = 13.2 m for 40 m high landfill) was demonstrated by the numerical modelling. In the centrifuge model, the landfill was flooded at the start of the self-weight consolidation, while *in situ* most of the settlement took place before the water level rose. It resulted in a different profile of the vertical effective stress and in the more open macro voids before the embankment construction in the centrifuge.

Closing of macro voids due to weathering destructuration significantly

reduces the compressibility of the landfill *in situ*: approximately 4 times smaller settlement was modelled numerically after considering weathering destructuration. The effect of weathering should be therefore studied *in situ* and weathering destructuration should be included in all models to reach reliable results.

The depth at which the macro voids close due to the overlying material was often discussed in the literature. The results of the oedometer testing of the double porosity specimens and the measurement of the water content in various depths of the mini-centrifuge models indicated that no clear limit can be defined in the landfill and closing of the macro voids is gradual.

The measurements by the depth reference points *in situ* and the straws in the centrifuge models did not detect any single depth separating open and closed macro voids. However, the results of the oedometer tests (Fig. 5.25) indicate that macro voids are interconnected and therefore the hydraulic conductivity high up to the vertical effective stress of approximately 50 kPa. At the vertical effective stress of 100 kPa, the macro voids seem to be closed. It corresponds to the depth of cca 12 m in the fully saturated landfill (Fig. 6.3). The centrifuge tests confirmed a very small settlement during the self-weight consolidation in the top 5-8 m (Fig. 6.23), where macro voids remained open. On the other hand a large settlement was measured after the embankment construction in the top 12 m (Fig. 6.33) as the interlump voids closed due to the surcharge. It can be concluded that for the tested material (in saturated state), the macro voids close gradually in the top 12 m. *In situ*, the same analysis would be difficult because of closing of the macro voids in the shallow depths due to weathering destructuration. It can be also expected that closing of the macro voids *in situ* is probably not only a function of the depth and depends also on other factors such as the degree of saturation.

Vaníček and Vaníček (2008) recommended to avoid the infiltration of the free water into the landfill and use all possibilities to slow down the degradation process. On the contrary, the presented study shows that dry filling followed by fast natural saturation can be recommended as the best filling method. The saturation of the landfill can be used as an effective method of landfill densification (a similar conclusion was made by Charles and Watts, 2001) and to reduce the risk of collapse on wetting after possible future development on its surface.

8.2 Outlook

This thesis studied the compression behaviour and the structure degradation of fully saturated landfills. However, most of the fresh landfills *in situ* are partially saturated and a further investigation of the behaviour of the partially saturated landfills is necessary. The investigation of the effect of S_r on the degradation of the landfill structure can be studied on the scaled-down landfill models. A radial distribution of the water inside the lumps and the resulting straining at the contacts due to the reduced strength can be investigated using neutron tomography. This approach was used for example by Carminati et al. (2007) in the study of water distribution in the aggregated soils.

A study of the preferential flow and the change of hydraulic conductivity in the landfill with various degree of structure degradation would provide a useful information about the water flow in the landfill. The preferential flow can be studied using tracers during the self-weight consolidation of the scaled-down model in the centrifuge. The hydraulic conductivity of the landfill and its change with the closing of macro voids was recently studied by Karpíšková (2009). The scaled-down models of the landfill were one dimensionally preconsolidated in the mini-centrifuge to various σ_v'. The hydraulic conductivity was investigated in the triaxial cell and in the oedometer apparatus on the specimens prepared from the preconsolidated material. However, a large scatter of the results was observed, probably due to high ratio of lump size compared to the height of the specimens. The absence of an appropriate technique for the measurement of the hydraulic conductivity of the landfill is still a major problem.

The formation of a surface crust due to cyclic changes of the water content close to the landfill surface was reported in the literature (Charles and Watts, 2001). Unfortunately there is a lack of information about the phenomenon, its extent, its influence to the porosity and compressibility and the existence of the preferential drainage paths based on dissication cracks. *In situ* measurements of these factors would provide useful information for the further investigation of the landfills.

References

Alexander, D. 1993. *Natural disasters*. Kluwer Academic Publishers.

Baudet, B.A. and Stallebrass, S.E. 2004. A constitutive model for structured clays. *Géotechnique*, **54**(4), 269–278.

Barvínek, J. 1986. Pokusné zhutňování metodou dynamické konsolidace na Ervěnickém koridoru (Dynamic compaction on Ervěnice corridor – field trial – in Czech). *Proc. Int. Conf. Zakládání Staveb*, Brno, Czech Republic, 5–13.

Boháč, J. and Škopek, J. 2000. A motorway over clayey fills of open pit coal mines. *Proc. Geoeng. 2000*, ISBN No. 1-58716-068-4, Melbourne.

Boháč, J. and Škopek, J. 2002. Autobahn über Abraumkippen. *Proc. 12th Danube-European Conf. Geotechnical Engineering*, Passau 27-28 May 2002, VGE Essen, 365–368.

Boháč, J. and Škopek, J. 2004. A spoil heap compressibility determined by trial embankments and by oedometer tests (in Czech). *Proc. 32 Int. Conf. Zakládání Staveb*, Brno, Czech Republic, 300–305.

Burland, J.B. 1990. On the compressibility and shear strength of natural clays. *Géotechnique*, **40**(3), 329-378.

Callisto, L., Gajo, A. and Muir Wood, D. 2002. Simulation of true triaxial tests on natural and reconstituted pisa clay. *Géotechnique*, **52**(9), 649–666.

Carminati, A., Kaestner, A., Ippisch, O., Koliji, A., Lehman, P., Hassanein, R., Vontobel, P., Lehmann, E., Laloui, L., Vulliet, L. and Flühler, H. 2007. Water flow between soil aggregates. *Transp. Porous Med*., **68**, 219–236.

Charles, J.A. 2002. Ground improvement: the interaction of engineering science and experinece-based technology. *Géotechnique*, **52**(7), 527–532.

Charles, J.A. 2008. The engineering behaviour of fill materials: the use, misuse and disuse of case histories. *Géotechnique*, **58**(7), 541–570.

Charles, J.A. and Watts, K.S. 2001. *Building on fill: geotechnical aspects*. 2nd edition. Construction Research Communications, London.

Cheuk, C.Y., Take, W.A, Bolton, M.D. and Oliveira, J.R.M.S. 2007. Soil restraint on buckling oil and gas pipelines buried in lumpy clay fill. *Engineering Structures*, **29**, 973–982.

Cotecchia, F. and Chandler, J. 2000. A general framework for the mechanical behaviour of clays. *Géotechnique*, **50**(4), 431–447.

Dykast, I. 1993. *Vlastnosti výsypek v SHR z hlediska jejich zástavby (Properties of landfills in SHR as foundation media).* Ph.D. thesis, Faculty of Civ. Eng., Czech Technical University, Prague.

Henriquez, H. 2006. *Sensitivity model for clayey spoil heaps – laboratory evaluation*. MSc thesis, Univ Técnica de Lisboa – PřF UK Praha.

Feda, J. 1995. Compression of unsaturated double-porosity clay. *Proc. 1st Int. Conf. on Unsaturated Soils*, Paris, Alonso and Delage Eds., 711–718.

Feda, J. 1998. Fragmentary clay – a difficult waste material. *Engineering Geology*, **51**, 77–88.

Feda, J. 2003. Behaviour of double-porosity geomaterials. *Proc. XIII ECSMGE,* Vaníček et al. (eds.), Prague, Czech Republic, 667–672.

Feda, J. 2004. Physical models of soil behaviour. *Engineering Geology*, **72**, 121–129.

Feda, J. 2006. Uniaxial creep and compression of soils. *Engineering Mechanics*, **13**(1), 49–66.

Feda, J., Boháč, J. and Herle, I. 1995. Shear resistance of fissured Neogene clays. *Engineering Geology,* **39**, 171-184.

Gerke, H.H. and van Genuchten M.Th. 1996. Macroscopic representation of structural geometry for simulating water and solute movement in dual-porosity media. *Advances in Water Resources*, **19**(6), 343–357.

Hájek, V. 2007. *Zhodnocení konstitučních modelů pro jemnozrnné zeminy o různých stupních překonsolidace (Evaluation of constitutive models for fine grained soils with different degree of overconsolidation)*. MSc thesis, PřF UK Praha.

Hájek, V., Mašín, D. and Boháč, J. 2009. Capability of constitutive models to simulate soils with different OCR using a single set of parameters. *Computers and Geotechnics*, **36**(4), 655–664.

Hartlen, J. and Ingers, C. 1981. Land reclamation using fine-grained dredged material. *Proc. 10th Int. Conf. on Soil Mech. and Found. Engrg.*, Stockholm, Vol. I, A.A. Balkema, Rotterdam, The Netherlands, 145–148.

Herbstová, V. and Herle, I. 2009. Structure transitions of clay fills in North-Western Bohemia. *Engineering Geology*, **104**, 157–166.

Herbstová, V., Mašín, D. and Boháč, J. 2005. Parameters for non-engineered colliery clayfills. In H. Bilsel and Z. Nalbantoglu (Eds.) *Proc. Int. Conf. on Problematic Soils (GEOPROB)*, Famagusta, Cyprus, Eastern Mediterrean University Press, 335–342.

Herštus, J., Šťastný, J. 1998. Vlastnosti výsypek jako základové půdy – výsledky zkoušek in situ a monitoringu (Properties of landfills for foundations – results of in situ tests and monitoring – in Czech). *Proc. 18. Mezinárodní seminář Polní geotechnické metody*, Ústí nad Labem, 34-39.

Ishihara, K, Kawijara, K., Takeda, H., Yoshino, S., Yamamoto, S., Yamazaki, S., Katagiri, M., Nishimura, M. and Terashi, M. 2006. Physical and mechanical properties of dewatered clay lump and their aggregate. *Geomechanics and geotechnics of particulate media*, Hyodo, Murata and Nakata (Eds.), Taylor and Francis Group, London, 495-500.

Kavvadas, M. and Amorosi, A. 2000. A constitutive models for structured soils. *Géotechnique*, **50**(3), 263–273.

Karpíšková, M. 2009. *Pórovitost a propustnost modelu jílovité výsypky (Porosity and permeability of a clayfill model)*. MSc thesis, PřF UK Praha.

Karthikeyan, M., Dasari, G.R. and Tan, T.S. 2004. In-situ characterization of a land reclaimed using big clay lumps. *Canadian Geotechnical Journal*, **41**, 242–256.

Koliji, A., Vulliet, L. And Laloui, L. 2008a. New basis for the constitutive modelling of aggregated soils. *Acta Geotechnica*, **3**, 61-69.

Koliji, A., Vulliet, L. And Laloui, L. 2008b. Advanced constitutive model for unsaturated structured soil with double porosity. *Proc. International Association for Computer*

Methods and Advances in Geomechanics (IACMAG), Goa, India, 709-715.

Kolymbas, D., Cambou, B. and Di-Prisco, C. (2000). Elements of hypoplasticity. Constitutive modelling of geomaterials. Revue francaise de génie civil, Vol. 4, No. 5, 85-107.

Křížová, H. 2000. *D8 – pokusný násyp (D8 - trial embankment)*. SG-Geotechnika, report.

Kurka, J. and Novotná, I. 2003. The D8 motorway over old tailing dam and spoil heaps near Ústí nad Labem. Proc. *13th ECSMGE*, Vol. 4, 131–146.

Kvaček, Z., Böhme, M., Dvořák, Z., Konzalová, M., Mach, K., Prokop, J. and Rajchl, M. 2004. Early Miocene freshwater and swamp ecosystems of the Most Basin (northern Bohemia) with particular reference to the Bílina Mine section. *Journal of Czech Geological Society*, **49**(1-2), 1–40.

Laue, J. 1996. *Zur Setzung von Flachfundamenten auf Sand unter wiederholten Lastereignissen*. PhD thesis, Schriftenreihe des Lehrstuhls für Grundbau und Bodenmechanik der Ruhr-Universität Bochum.

Laue, J. 2002. Centrifuge technology. *Proc. Workshop on Constitutive and Centrifuge Modelling: Two Extremes*, Springman (ed.), AA Balkema Publishers, 113-131.

Laue, J., Springman, S.M., Nater, P., Grämiger, E. and Ducksch, A. 2005. Creating seafloor conditions in geotechnical centrifuges. *Proc. 16th Int. Conference on Soil Mechanics and Geotechnical Engineering ICSMGE*, Millpress, Rotterdam, Netherlands, 1741–1744.

Leung, C.F., Wong, J.C., Manivanann, R. and Tan, S.A. 2001. Experimental evaluation of consolidation behaviour of stiff clay lumps in reclamation fill. *Geotechnical Testing Journal*, **24**(2), 145–156.

Lewandowska, J., Szymkiewicz, A., Burzyński, K. and Vauclin, M. 2004. Modeling of unsaturated water flow in double-porosity soils by homogenization approach. *Advances in Water Resources*, **27**, 283–296.

Manivannan, R., Wong, J.C., Leung, C.F. and Tan, S.A. 1998. Consolidation characteristics of lumpy fill, *Proc. Centrifuge 98*, Balkema, Rotterdam, The Netherlands, 889–894.

Mašín, D. 2005. A hypoplastic constitutive model for clays. *International Journal for Numerical and Analytical Methods in Geomechanics*, **28**(4), 311-336.

Mašín, D. 2007. A hypoplastic constitutive model for clays with meta-stable structure. *Canadian Geotechnical Journal*, **44**(3), 363-375.

Mašín, D. 2009. Comparison of predictive capabilities of selected elasto-plastic and hypoplastic models for structured clays. *Soils and Foundations*, **49**(3), 381–390.

Mašín, D. and Herle, I. 2005. State boundary surface of a hypoplastic model for clays. *Computers and Geotechnics*, **32**(6):400–410.

Muir Wood, D. 2004. *Geotechnical modelling*. Spon press (Taylor and Francis group), London, New York.

Najser, J. 2007a. Modelling of trial embankment on double porosity clay. *Proc. 18th European Young Geotechnical Engineers' Conference*, Ancona, Italy.

Najser, J. 2007b. Využití centrifugy při geotechnickém průzkumu pro zakládání na výsypkách (Using of centrifuge for geotechnical investigation of landfills). *Proc. Int. Conf. Foundations*, Brno, 9–14.

Najser, J. 2008. Využití centrifugy při geotechnickém průzkumu pro zakládání na výsypkách (Using of centrifuge for geotechnical investigation of landfills). *All for power,* 1, 20–26.

Najser, J. 2009. Modelling of double porosity clayfills using hypoplasticity. Proc. 4th *International Young Geotechnical Engineers' Conference*, Alexandria, Egypt, 5-8.

Najser, J., Mašín, D. and Boháč, J. 2009a. Numerical modelling of double porosity clay landfill. *International Journal for Numerical and Analytical Methods in Geomechanics*, submitted.

Najser, J., Mašín, D. and Boháč, J. 2010a. Back-analysis of weathering destructuration of a lumpy clay landfill. *Sixth International Congress on Environmental Geotechnics*, New Delhi, India, submitted.

Najser, J., Pooley, E. and Springman, S.M. 2009b. Modelling of double porosity clays in a mini-centrifuge. *International Journal of Physical Modelling in Geotechnics*, 1 (2009), 15-22.

Najser, J., Pooley, E., Springman, S. M., Laue, J. and Boháč, J. 2008. Construction of motorway on double porosity clay fill. *Proc. 6th Int. Conf. on Case Histories in Geotechnical Engineering*, Arlington, USA.

Najser, J., Pooley, E., Springman, S. M., Laue, J. and Boháč, J. 2010b. Mechanisms controlling the behaviour of double porosity clayfills – in situ and centrifuge study. *Quarterly Journal of Engineering Geology and Hydrogeology*, in print.

Nogami, T., Wang, W. and Wang, J.G. 2004. Numerical method for consolidation analysis of lumpy clay fillings with meshless method. *Soils and Foundations*, **44**(1), 125-142.

Novotná, I. 2002. *D807/I – Geotechnické výpočty násypů* (*D807/I - Geotechnical calculations of embankments)*. SG-Geotechnika, report.

Ovesen, N.K. 1979. The use of physical models in design. *VII ECSMFE*, Brighton, United Kingdom, Vol. 4, 336-339.

Pierschke, K.-J. 1995. Standfestigkeit bei der Verkippung von nicht aufbaufähigen Mischböden im rheinischen Braunkohlenrevier. *Braunkohle,* **12**, 5–12.

Pooley, E.J., Springman, S.M., Laue, J. and Najser, J. 2009. Centrifuge modelling to compare ground improvement techniques on double porosity clay landfills. *Proc. Geotechnics of Soft Soils – Focus on Ground Improvement*, Taylor and Francis Group, London.

Rajchl, M. 2006. *Tectonosedimentary evolution and fluvio-deltaic systems of the Most Basin (Tertiary, Eger Graben, Czech Republic)*. PhD thesis, Charles University in Prague.

Rajchl, M., Uličný, D. and Mach, K. 2008. Interplay between tectonics and compaction in a rift-margin, lacustrine delta system: Miocene of the Eger Graben, Czech Republic. Sedimentology, **55**, 1419–1447.

Robinson, R.G., Dasari, G.R. and Tan, T.S. 2004. Three-dimensional swelling of clay lumps. *Géotechnique*, **54**(1), 29–39.

Robinson, R.G., Tan, T.S., Dasari, G.R., Leung, C.F. and Vijayakumar, A. 2005. Experimental study of the behavior of a lumpy fill of soft clay. *International Journal of Geomechanics ASCE*, **5**(2), 125–137.

Rocchi, G., Fontana, M., and Da Prat., M. 2003. Modelling of natural soft clay destruction processes using viscoplasticity theory. *Géotechnique*, **53**(8), 729–745.

Rodemann, D. 2008. *Tochnog Professional user's manual*, http://www.feat.nl

Rouainia, M. and Muir Wood, D. 2000. A kinematic hardening constitutive model for natural clays with loss of structure. *Géotechnique*, **50**(2), 153–164.

Schofield, A.N. 1980. Cambridge Geotechnical Centrifuge Operations. *Géotechnique,* **30**(2), 227–268.

Springman, S.M., Laue, J., Boyle, R., White, J. and Zweidler, A. 2001. The ETH Zurich Geotechnical Drum Centrifuge. *International Journal of Physical Modelling in Geotechnics,* **1**(1), 59–70.

Škopek, J. 2001. Evaluation of fill compressibility by means of a trial embankment. *Proc. of Int. Conf. Insitu Measurement of Soil Properties*, Bali.

Škopek, J. and Boháč, J. 2004. Site investigation by trial embankments. *Proc. of ISC-2 on Geotechnical and Geophysical site characterization,* Porto, Vol. 2, Millpress, Rotterdam, 1571–1574.

Taylor, R.N. 1995. *Geotechnical Centrifuge Technology.* London: Blackie Academic & Professional.

Vaníček, I. and Vaníček, M. 2008. *Earth structures in transport, water and environmental engineering*. Springer.

Větrovský, M. 2006. Příspěvek k řešení problematiky zakládání staveb na báňských výsypkách Severočeského hnědouhelného revíru (Contribution to the problem of foundation on spoil heaps in North-Bohemian brown-coal basin – in Czech). Ph.D. thesis, Technical University Ostrava.

Vráblíková, J. and Vráblík, P. 2000. Vliv antropogenní činnosti na agroekosystém severních Čech (The influence of anthropogenic factors on agroecosystem in Northern Bohemia – in Czech). *Proc. 12th Regional central european conf. IUAPPA and 4th int. conf. on environmental impact assessment*, Prague, Czech Republic.

Watts, K.S. and Charles, J.A. 2003. Investigation of restored opencast mine backfill: long term settlement. *Proc. XIII ECSMGE,* Vaníček et al. (eds.), Prague, Czech Republic, 273–278.

Weber, T.M. 2007. Modellierung der Baugrundverbesserung mit Schottersäulen. Ph.D. Thesis, Institute for Geotechnical Engineering, ETH Zürich.

Weber. T.M., Laue, J. and Springman, S. 2006. Centrifuge modelling of sand compaction piles in soft clay under embankment load. *Proc 6th Int.Conf. Physical Modelling in Geotechnics*, Hong-Kong, China, 603–608.

Wheeler, S.J., Näätänen, A., Karstunen, M. and Lojander, M. 2003. An anisotropic elastoplastic model for soft clays. *Canadian Geotechnical Journal*, **40**, 403–418, 2003.

Wong, H., Leo, C.J., Pereira, J.M. And Dubujet, P. 2007. Sedimentation-consolidation of a double porosity material. *Computers and Geotechnics*, **34**, 532-538.

Yang, L.A. and Tan, T.S. 2005. One-dimensional consolidation of lumpy clay with non-linear properties. *Géotechnique,* **55**(3) 227–235.

Yang, L.A., Tan, T.S., Tan, S.A. and Leung, C.F. 2002. One-dimensional self-weight consolidation of a lumpy clay fill. *Géotechnique,* **52**(10) 713–725.

Záleský, J., Kos, J. and Salák, J. 2001. Behaviour of clay with double porosity with respect to high waste tips. *GREEN 3, The exploitation of natural resources and the consequences - Proc. 3rd int. symposium on geotechnics related to the european environment*, Sarsby and Meggyes (eds.), Berlin, Germany, 125–130.